UNIVERSITÉ DU QUÉBEC À MONTRÉAL

MODEL DEVELOPMENT AND SIMULATIONS OF NITROUS OXIDE EMISSIONS FROM GLOBAL AGRICULTURAL ECOSYSTEMS

DISSERTATION

PRESENTED IN PARTIAL

FULFILLMENT OF THE REQUIREMENT FOR

DOCTORATE IN ENVIRONMENTAL SCIENCES

BY

HANXIONG SONG

JANUARY 2025

UNIVERSITÉ DU QUÉBEC À MONTRÉAL

DÉVELOPPEMENT DE MODÈLES ET SIMULATIONS DES ÉMISSIONS D'OXYDE NITREUX PROVENANT DES ÉCOSYSTÈMES AGRICOLES MONDIAUX

THÈSE

PRÉSENTÉE

COMME EXIGENCE PARTIELLE

DU DOCTORAT EN SCIENCES DE L'ENVIRONNEMENT

PAR

HANXIONG SONG

JANVIER 2025

Dédiée à mes parents, à ma femme, à ma fille et à mes grands-parents

Dedicated to my parents, my wife, daughter, and my grandparents

献给我的父母，妻子，女儿和祖父母

ACKNOWLEDGEMENTS

This work is financially supported by the Natural Sciences and Engineering Research Council of Canada (NSERC) Discover Grant, the Fonds de recherche du Québec (FQRNT) program, and China Scholarship Council (CSC).

I would like to express my greatest acknowledgment to my supervisor, Prof. Changhui Peng, for his long-term thoughtful support in both academic and social life during my Ph.D. study at UQAM. His insightful taste and serious attitude in science will keep influence my career in the future. I also want to give great appreciation to my committee members, Prof. Zhi Chen and Prof. Jean-Pierre Blanchet, for their kind help and constructive suggestions for my research. In addition, I would like to thank my friends and colleagues, professors, and staffs in Institut des sciences de l'environnement (ISE), UQAM, for providing valuable helps and great atmosphere in discussion and science.

Importantly, I feel grateful for my parents for their support and encouragement. I would like to send great regards to my wife for her understanding and incredible dedication to my entire family, especially our first child. I also feel thankful to meet and work with my friends and lab mates during these years. Life is a journey full of challenges. Be grateful and helpful, keep sharp but clam, feel confident while stay humble and devote myself to accomplish things that supposed to whatever the outcome might be. This is not a pause, but a fresh start.

Hanxiong

Montreal, 2024, Aug

PREFACE

This dissertation is comprised of six chapters (four main articles) that present and discuss the development and application of a process-based biogeochemical model, TRIPLEX-GHGv2.0 to simulate and forecast nitrous oxide emissions from global agricultural ecosystems. All four papers involved in the dissertation are original contributions to my Ph.D. in Environmental Sciences at the Université du Québec à Montréal.

Chapters I and VI are the general introduction and general conclusion, respectively. Chapters II to V are correspondingly based on the following Four publications:

1. **Song, H.**, Peng, C., Zhang, K., & Zhu, Q. (2022). "Integrating major agricultural practices into the TRIPLEX-GHG model v2. 0 for simulating global cropland nitrous oxide emissions: Development, sensitivity analysis and site evaluation". *Science of the Total Environment*, *843*, 156945.
2. **Song, H.**, Peng, C., Zhang, K., Li, T., Yang, M., Liu, Q., & Zhu, Q. (2023). "Quantifying patterns, sources and uncertainty of nitrous oxide emissions from global grazing lands: Nitrogen forms are the determinant factors for estimation and mitigation". *Global and Planetary Change*, *223*, 104080.
3. **Song, H.**, Zhu, Q., Blanchet, J. P., Chen, Z., Zhang, K., Li, T., Zhou, F., & Peng, C. (2023). "Central role of nitrogen fertilizer relative to water management in determining direct nitrous oxide emissions from global rice-based ecosystems". *Global Biogeochemical Cycles*, 37(11), e2023GB007744.
4. **Song, H.** and Peng, C. "Projection of nitrous oxide emissions from global agricultural ecosystems under future climate change and management practices". (To be submitted)

With the guidance of my Ph.D. supervisor, Dr. Changhui Peng, I developed all hypotheses and improved the process-based biogeochemical model, TRIPLEX-GHGv2.0. I collected in-situ observations of N_2O emissions from agricultural ecosystems soils across the globe based on the published literatures. These data are used for model calibration and validation under varying environmental and management conditions. Afterwards, I conducted model simulations with different scenario designs to quantify and analyze the spatiotemporal variations of historical and future N_2O emissions from croplands, grazing-lands, and rice-based ecosystems at a global scale, respectively. My committee members, Dr. Jean-Pierre Blanchet and Dr. Zhi Chen advised and discussed with me about

my project. Dr. Qiuan Zhu and Dr. Kerou Zhang provided tutorial to early version of the TRIPLEX-GHG model and discussed programming issues. All co-authors contributed valuable suggestions to improve the quality of the published articles.

TABLE OF CONTENTS

LIST OF FIGURES

LIST OF TABLES

RÉSUMÉ

Les écosystèmes agricoles mondiaux sont une source majeure de protoxyde d'azote (N_2O), un gaz à effet de serre puissant contribuant significativement au changement climatique. Malgré les effets importants qu'on les émissions de N_2O provenant d'agroécosystèmes, beaucoup d'incertitude subsiste quant à leur ampleur, les facteurs les modulant de même qu'à leur variations potentielles à l'échelle globale. Cette thèse à pour objectifs de (1) simuler les variations spatio-temporelles des émissions de N_2O agricoles mondiales, (2) quantifier les contributions des différents facteurs déterminants et (3) projeter les tendances futures sous divers scénarios climatiques et de gestion.

Pour atteindre ces objectifs, un modèle biogéochimique basé sur les processus, TRIPLEX-GHGv2.0, a été amélioré en y incorporant des processus microbiens majeurs, des pratiques agricoles et des impacts environnementaux pour simuler la dynamique du N_2O dans les sols agricoles. La validation par rapport aux bases de données d'émissions de N_2O observées a suggéré de bonnes performances du modèle pour les terres cultivées (R^2 = 0,87), les pâturages (R^2 = 0,85) et les rizières (R^2 = 0,78) à l'échelle globale. Les simulations historiques ont révélé une tendance générale à la hausse des émissions de N_2O en terres agricoles de 1960 à 2020, avec une légère diminution au XXIe siècle. Au cours de cette période, ce sont les terres cultivées qui ont contribué le plus aux émissions totales de N_2O (3,06 ± 0,18 Tg N an^{-1}), suivies des pâturages (2,04 ± 0,02 Tg N an^{-1}), puisdes écosystèmes rizicoles (0,17 ± 0,005 Tg N an^{-1}). À l'échelle régionale, des réductions significatives des émissions de N_2O agricoles ont été observées au sein des points chauds d'émissions persistant, y compris l'Europe occidentale et l'Amérique du Nord, tandis que l'Asie de l'Est et l'Inde ont connu des augmentations rapides depuis les années 1980. Les engrais chimiques à base d'azote représentent la principale source des émissions de N_2O pour les terres cultivées (~48%) et les rizière (~25%), tandis que les excréments déposés étaient le plus grand contributeur pour les pâturages (~31%) . L'étude a également révélé que l'effet des engrais azotés sur les émissions de N_2O semble être contrôlé par la fraction de nitrate et les dépôts d'azote pour les terres cultivées à l'échelle mondiale, tandis que la quantité d'excréments de bétail et l'irrigation accrue sont les principaux facteurs modulant les réponses du N_2O à la fertilisation pour les pâturages et les écosystèmes rizicoles, respectivement. Sous trois scénarios de trajectoires communes d'évolution socio-économique (SSP1-2.6, SSP2-4.5 et

SSP5-8.5), les projections du modèle suggèrent une augmentation des émissions futures de N_2O agricoles de 27,0 à 71,0 % entre 2015 et 2100, avec les émissions les plus importantes ayant potentiellement lieu sous la trajectoire intermédiaire (SSP2-4.5) en raison de l'application excessive d'engrais azotés dans les terres cultivées. La projections a indiqué que les futures émissions de N_2O sont plus sensibles aux facteurs de gestion de l'azote qu'aux changements climatiques, ce qui représenterait 0,44 Tg N an^{-1} de l'augmentation totale. L'augmentation projetée des émissions de N_2O provenant des agroécosystèmes dans les pays en développement est susceptible de compenser les réductions réalisées dans les pays développés, rendant nécessaires des collaborations internationales pour résoudre ce déséquilibre à l'avenir.

Dans l'ensemble, cette étude fournit un outil fiable pour estimer les émissions de N_2O des agroécosystèmes à diverses échelles. Les résultats historiques modélisés quantifient l'importance des formes d'azote ainsi que de la co-gestion des engrais azotés avec le fumier, les activités de pâturage et l'irrigation dans la détermination des dynamiques spatio-temporelles des émissions agricoles mondiales de N_2O. Les projections soulignent davantage le rôle prédominant des pratiques de gestion agricole par rapport aux changements climatiques dans la formation des émissions agricoles futures de N_2O et mettent en évidence les défis de la réduction de ces émissions dans le contexte du désiquilibre du développement mondial. Cette étude améliore notre compréhension du bilan global de N_2O agricole historique et projeté de même que de ses facteurs contributifs, fournissant de nouvelles perspectives pour atténuer la contribution du secteur agricole au réchauffement climatique.

ABSTRACT

Global agricultural ecosystems are a major source of nitrous oxide (N_2O), a potent greenhouse gas contributing significantly to climate change. Despite its critical impacts, substantial uncertainties persist regarding the magnitude, driving factors, and potential changes of N_2O emissions from agricultural ecosystems globally. This dissertation aims to simulate the spatiotemporal variations of global agricultural N_2O emissions, quantifies the contributions of different driving forces, and project future trends under various climate and management scenarios.

To achieve these goals, the process-based biogeochemical model, TRIPLEX-GHGv2.0 was improved by incorporating major microbial processes, agricultural practices, and environmental impacts for simulating N_2O dynamics from agricultural soils. Validation against collected observed N_2O emissions database suggested good and consistent model performances across upland croplands ($R^2 = 0.87$, n = 68), grazing lands ($R^2 = 0.85$, n = 48), and rice-paddies ($R^2 = 0.78$, n = 50) at a global scale. Historical simulations revealed a general increasing trend of agricultural N_2O emissions from 1960 to 2020 with a slightly decline in the 21st century. During this period, upland croplands are the largest contributor to total N_2O emissions (3.06 ± 0.18 Tg N yr^{-1}) followed by grazing lands (2.04 ± 0.02 TgN yr^{-1}) and rice-based ecosystems (0.17 ± 0.005 TgN yr^{-1}). Regionally, significant reductions in agricultural N_2O emissions were found in consistent emission hotspots, including Western Europe and North America, while Eastern Asia and India experienced rapid increases since the 1980s. Chemical N fertilizer accounts for the primary source of N_2O emissions for cropland (~48%) and rice-based ecosystems (~25%) but deposited excreta were the largest contributor (~31%) for grazing lands. The study also found that the effect of N fertilizer on N_2O emissions appears to be controlled by nitrate fraction and N deposition for croplands globally, whereas the amount of livestock excreta and expanded irrigation play the dominant roles in N_2O responses to fertilization for grazing lands and rice-based ecosystems, respectively. Under three Shared Socioeconomic Pathway scenarios (SSP1-2.6, SSP2-4.5, and SSP5-8.5), model projections suggested an increase in future agricultural N_2O emissions by 27.0 – 71.0 % during 2015 – 2100, with the largest emissions potentially occurring under the intermediate pathway (SSP2-4.5) due to excessive N fertilizer application in croplands. The projections indicated that future N_2O emissions are more sensitive to N management factors than

changing climate which would account for 0.44 Tg N yr^{-1} (at least 16.7%) of the total increase. The projected enhanced N_2O emissions from agroecosystems in developing countries is likely to offset reductions achieved in developed world, which requires international collaborations to address this imbalance in the future. However, there are still existing uncertainties to be addressed including the effect of land use changes.

Overall, this study provides a reliable tool for estimating N_2O emissions from agricultural ecosystems at various scales. The modeled historical results quantitively underscore the importance of N forms and co-management of N fertilizer with manure, grazing activities, and irrigation in determining spatiotemporal dynamics of global agricultural N_2O emissions. The projections further emphasize the predominant role of agricultural management practices over climate change in shaping future agricultural N_2O emissions and highlight the challenges of mitigating these emissions in the context of imbalanced global development. This study improves our understanding of the global agricultural N_2O budget and contributing factors in both historical period and projected future, providing new insights for mitigating the agricultural sector's contribution to global warming.

CHAPTER I: GENERAL INTRODUCTION

1.1 Background

1.1.1 Climate change and greenhouse gas

Global warming effect has been recognized as one of the most significant environmental threats to human society (Hansen et al., 1981). The mean temperature of the Earth surface has increased by ~ 1.09 (0.95 – 1.20) °C from the industrial revolution in the 1850s to the present decade, with the fastest growth rate occurring since the 1960s in the past 20 centuries (Figure. 1.1 a) (IPCC, 2023). Projections suggest that between 2014 and 2100, the global mean surface temperature may continue to rise by 0.7 to 3.5 °C, under the lowest and highest forcing scenarios, respectively (Fig 1.1 b) (IPCC, 2021; O'Neill et al., 2016). Such rapid warming exacerbates extreme weather events, raises sea level, threatens biodiversity, and poses significant risks to human health and food security (Cai et al., 2014; Church & White, 2006). Human activities that lead to excessive greenhouse gas (GHG) emissions are largely responsible for this phenomenon (IPCC, 2023; Tian et al., 2016). From 1850 to 2020, atmospheric concentrations of the three major GHGs including carbon dioxide (CO_2), methane (CH_4), and nitrous oxide (N_2O) have increased substantially: CO_2 from 300 parts per million (ppm) to 410 ppm (a ~ 40% increase), CH_4 from 801 to 1866 parts per billion (ppb), and N_2O from 270 to 335 ppb by 23% during this period (IPCC, 2021; Tian et al., 2016).

Among these GHGs, nitrous oxide (N_2O) has the lowest concentration in the atmosphere but possesses the strongest radiative forcing. As a long-live trace gas (~ 120 years), N_2O has a global warming potential over a 100-year horizon that is 265 – 298 times larger than that of CO_2. More than 10% of the overall global radiative forcing in the current decade is attributed to N_2O, and there is a growing trend for its contribution to global warming to constantly increase in the future (IPCC, 2023; Tian et al., 2020). Moreover, rising atmospheric N_2O levels causes the ozone depletion in the stratosphere and the formation of acid rain, which significantly affects both environment and human health (Ravishankara et al., 2009). Currently, the mean global atmospheric N_2O concentration is experiencing an unprecedented annual growth rate of ~ 1.3 ppb yr^{-1}, necessitating effective control measures (Figure. 1.1 c) (Lan et al., 2024).

N_2O emissions from global agricultural ecosystems, largely driven by intensive management practices, are identified as the primary source of increasing atmospheric N_2O (~ 3.8 – 6.8 Tg N_2O-N yr^{-1}), accounting for more than 75% of total anthropogenic N_2O emissions in the early 21st century (Davidson & Kanter, 2014; Tian et al., 2020). However, significant uncertainties remain in existing N_2O budgets (including global, region, and country levels), particularly for agricultural ecosystems, which are hotspots for N_2O emissions (Figure. 1.1 d) (IPCC, 2023; Liang et al., 2024; Tian et al., 2024). These uncertainties arise from several factors. First, variability of N_2O fluxes from agricultural soils is difficult to accurately measure and understand on site scale because of the strong heterogeneity of biotic and abiotic factors (Rees et al., 2013; Wu et al., 2021). Second, existing models often oversimplify the biogeochemical processes involved or rely on inadequate information for their development. For example, empirical models tend to overlook the potential joint effects of other management practices and environment changes with N fertilizer (Hergoualc'h et al., 2021; Shcherbak et al., 2014), while a number of models training only focus on emissions during growing seasons, resulting in possible underestimated annual emission rates (Shang et al., 2024; Wagner-Riddle et al., 2017). Finally, inconsistent definitions of N_2O sources across models complicate the intercomparison (Tian et al., 2024). Empirical modeling results, such as those from FAOSTAT, only accounts external nitrogen inputs (e.g., N fertilizer and manure) induced N_2O as agricultural source, excluding soil background emissions.

Given the increasing demand for agricultural production, it has been reported that up to half of the global terrestrial CO_2 sink could be offset by rising N_2O emissions, significantly accelerating climate changes (Reay et al., 2012; Stocker et al., 2013). Reducing N_2O emission from agricultural soil is the central action for mitigating the agricultural carbon footprint and achieving the 1.5 (or 2.0) °C climate goal of the Paris agreement (Schleussner et al., 2016). In particular, Canada has committed to reducing its GHG emissions to 40–45% below 2005 levels by 2030 and aims to achieve net-zero emissions by 2050 while agriculture contributes ~10% of Canada's total GHG emissions. Therefore, a comprehensive understanding of trend, magnitude, and driving forces of global agricultural N_2O emissions is vital for scientists and policymakers in developing strategy of global sustainable development.

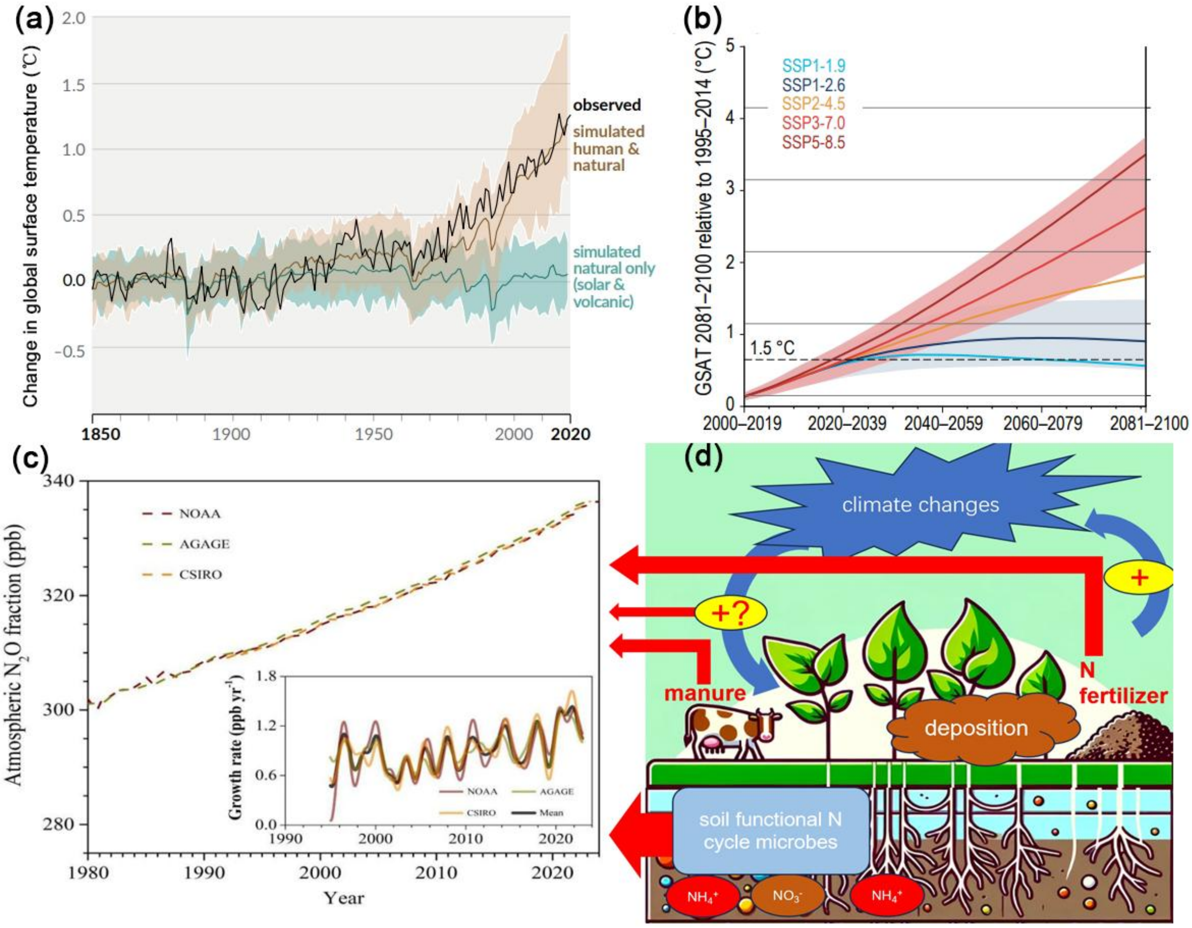

Figure 1.1 Changes in global surface temperature over the past 170 years (black line) relative to 1850–1900 and model simulated results separating anthropogenic and natural drivers (brown and blue lines and shades), derived from IPCC (2021) (a); projected future changes (after 2014) in global temperature from model ensembles of CMIP6, from IPCC (2023) (b); global mean atmospheric N_2O concentration (dry mole fraction) and growth rate estimated by AGAGE, NOAA, and CSIRO observations (c); agricultural and natural source of N_2O in atmosphere under climate changes (d).

1.1.2 Mechanisms of soil N_2O production and environmental controls

N_2O emission from natural and managed soils are predominantly controlled by biotic processes, accounting for more than 70% of global emissions, primarily through nitrification and denitrification, which are essential components of the N cycles (Figure. 1.2) (Braker & Conrad, 2011; Butterbach-Bahl et al., 2013).

Nitrification is the aerobic oxidation of ammonium (NH_4^+) or ammonia (NH_3) to nitrate (NO_3^-) via nitrite (NO_2^-). Ammonia-oxidizing bacteria (AOB) and archaea (AOA) are responsible for autotrophic ammonia oxidation, while nitrite-oxidizing bacteria (NOB) complete the subsequent conversion to NO_3^- (Daims et al., 2016; Prosser & Nicol, 2012). Both steps produce N_2O as a by-product (Wrage et al., 2001). Meanwhile, heterotrophic nitrification, mainly performed by fungi, can also contribute to N_2O emissions by oxidizing organic N compounds to NO_2^- and NO_3^- under specific conditions (Martikainen, 2022). Denitrification involves the stepwise reduction of NO_3^- to nitrogen gases (e.g., N_2O, N_2) under low soil oxygen availability by different denitrifying groups (Knowles, 1982; J. Wang et al., 2018). N_2O is a regular intermediate product during denitrification, and metabolizable organic C influencing its production as an electron donor, competing among these reduction steps (Knowles, 1982). Besides these well-known pathways, other soil biogeochemical processes also contribute to soil N_2O emissions with varying extents (Butterbach-Bahl et al., 2013). These complex interactions and the variety of microbial processes highlight the intricate nature of N_2O production in soils (Figure. 1.2). For instance, nitrifier denitrification, as a pathway of nitrification, reduce NO_2^- provided by NH_3 oxidation process to N_2O and N_2 by AOB (Wrage-Moennig et al., 2018; Zhu et al., 2013). Dissimilatory nitrate reduction to ammonium (DNRA) and anaerobic ammonia oxidation (anammox) play essential roles in soil N cycles and can potentially produce N_2O in certain ecosystem types (Nie et al., 2019; Putz et al., 2018).

These biological processes, and thus N_2O emissions, are significantly influenced by environmental factors such as soil moisture, soil temperature, and pH. Understanding these relationships is crucial for developing effective management strategies to mitigate soil N_2O emissions, especially in agroecosystems.

Soil moisture is a key driver of soil N_2O emissions, as it regulates oxygen availability to N-cycling soil microbes, and thereby affecting redox potential and microbial activities. Optimal soil moisture levels for soil N_2O production and emissions are typically within the range of 60 – 90% water-filled pore space (WFPS) due to enhanced denitrification, depending on different soil physical properties and vegetation cover (Butterbach-Bahl et al., 2013; Liu et al., 2022). It is noteworthy that N_2O emissions may decrease under extreme high soil moisture conditions because of favored reduction to N_2, although such conditions are rarely observed in upland soils (Luo et al., 2013; Wu et al., 2017). Soil temperature not only has direct impacts on denitrifier activities given the tight microbial C-N coupling in denitrification (Barnard et al., 2005; Qiu et al., 2018), but also indirectly influences N_2O production by altering soil moisture levels. In addition, soil pH, organic C content, and changes in vegetation communities are also important drivers of soil N_2O emissions (Butterbach-Bahl et al., 2013). For example, low soil pH promotes N_2O emission and its sensitivity to external N inputs by inhibiting

N_2O reductase activity (Y. Wang et al., 2018).

More importantly, agricultural practices significantly alter these environmental factors, greatly stimulating soil N_2O emissions globally (Reay et al., 2012). Synthetic N fertilizer and manure applications increase soil N supply for nitrification and denitrification, making them primary contributors to increasing atmospheric N_2O levels (Davidson, 2009; Tian et al., 2020). Urea, a commonly used fertilizer, can stimulate N_2O emission by acidifying the soil (Qiu et al., 2024). As for fertilizer rich in NO_3^-, abundant soil NO_3^- enhance denitrification and N_2O emissions because NO_3^- is a more preferred electron acceptor than N_2O (Wrage et al., 2001). Manure provides both organic C and N in various forms, favoring different soil N_2O producers (Zhou et al., 2017). Besides N management, irrigation generally increases N_2O emissions by creating more frequent anaerobic conditions, though different methods (e.g., flooding .vs. drip irrigation) can capture diverse impacts (Kuang et al., 2021). Similarly, tillage, whether conventional or reduced, appears to stimulate N_2O emissions from agricultural lands (Mei et al., 2018). However, there are strong spatiotemporal variations in the responses of N_2O emissions to changing practices across the globe due to the heterogeneity of environmental conditions and microbial activities. Furthermore, the interaction between ongoing climate changes and diverse management further complicates the dynamics of N_2O emission from agricultural soils (Barnard et al., 2005). Coupled Model Intercomparison Project (CMIP) Phase 6 (CMIP6) provides a valuable opportunity for model projection to quantitively evaluate the range and trajectories of agriculture N_2O emissions globally.

Therefore, given the necessity of balancing the mitigation of climate change and global food security, we need better understand the magnitudes of responses of N_2O emission to different agricultural practices under changing environmental conditions through both field measurements and large-scale modeling.

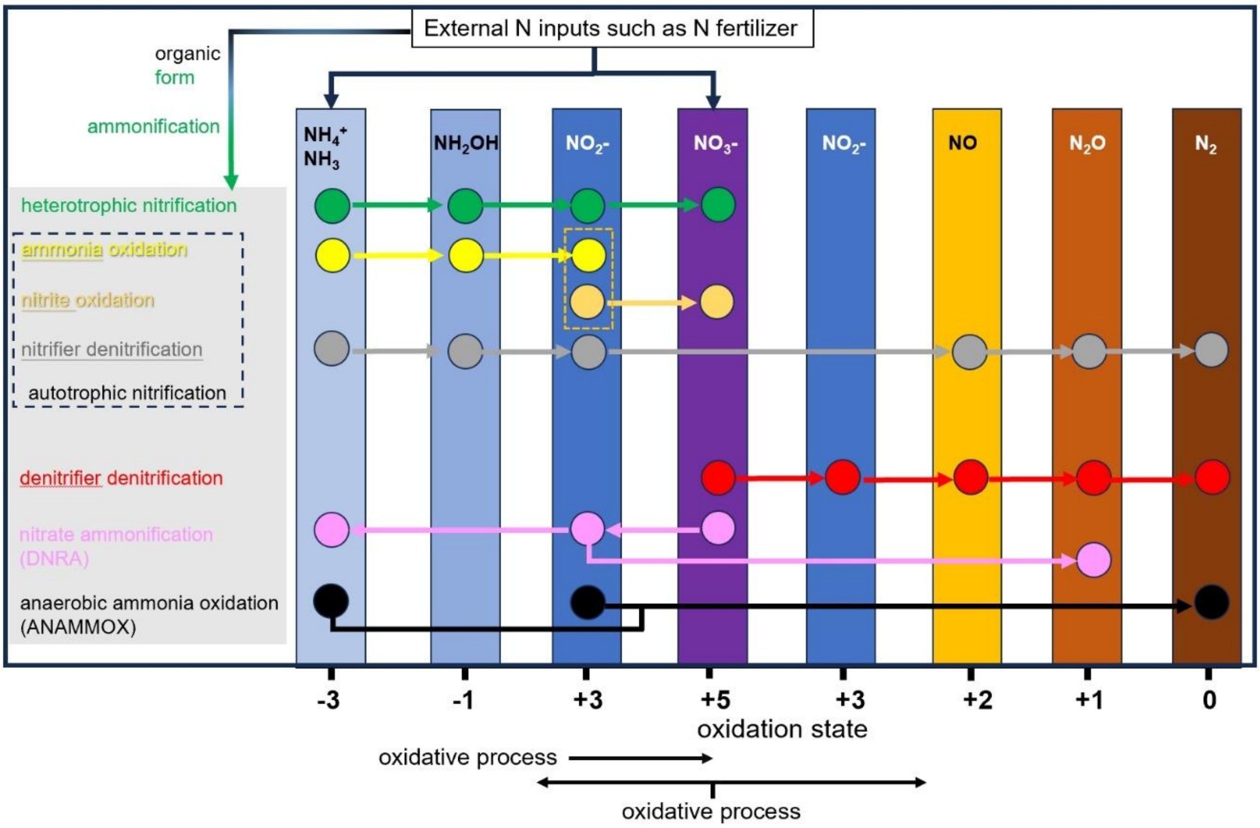

Figure 1.2 Biotic processes related to nitrous oxide (N_2O) production and consumption. Major pathways and their associated N compounds and oxidation states are shown. Revised from Butterbach-Bahl et al. 2013.

1.1.3 Measurement and modeling of soil N_2O emissions

The most widely applied method for measuring soil N_2O fluxes is the closed chamber technique (including automated versions), which covers a limited soil surface area (~1m in diameter). However, this method faces several challenges and limitations: it inadequately addresses the spatial heterogeneity of N_2O flux and has significant uncertainties related to sampling frequencies (typically weekly or bi-monthly) (Barton et al., 2015), flux calculation methods (Venterea et al., 2020), and flux values obtained through quality-controlled chamber methodology (Rochette & Eriksen-Hamel, 2008). In recent years, micrometeorological methods, eddy covariance in particular, have been used to continuously detect and quantify N_2O flux over relatively large areas (e.g., 0.5 – 2 ha) in various ecosystems (Cowan et al., 2020; Huang et al., 2014; Lognoul et al., 2019). However, uncertainties associated with gap filling approaches and complex terrain continue to limit the quality of their estimated N_2O budget (Goodrich et al., 2021).

Modelling approaches are the core to constrain and upscale existing observations to better reflect and simulate the spatial-temporal variation patterns of soil N_2O emissions, especially on large scales (i.e., landscape to global). Additionally, modelling offers opportunities to evaluate the effects of large-scale management or policy strategies on N_2O emissions and to better understand potential changes in the context of global change (Kanter et al., 2020; Shang et al., 2019). To date, empirical models, such as Emission Factors-based (EFs) models, and process-based biogeochemical models are commonly used in bottom-up approach for estimating N_2O emissions. EF-based models, like the IPCC Tier1 approach (i.e., 1.0 % of input N converted to N_2O), oversimplify the relationship between N inputs (mostly N fertilizer) and N_2O emissions across different agroecosystem types (Mancia et al., 2022; Shcherbak et al., 2014). This result in large estimated discrepancies at finer spatial or temporal scales (Gerber et al., 2016; Shang et al., 2020). Moreover, the incomplete descriptions of environmental controls and biotic interactions in these models undermine their ability to evaluate the interactive effects of combined mitigation efforts and environmental changes (Butterbach-Bahl et al., 2013).

On the other hand, process-based modelling provides a more robust framework for representing and simulating the dynamics in N_2O emissions from different ecosystem soils, underpinned by explanations of the underlying biogeochemical mechanisms (Tian et al., 2019). These models also have the potential to systematically assess the responses of N_2O and multiple ecosystem variables simultaneously to management and climate changes. Currently, a number of process-based models are developed and applied at varying scales to simulate soil N_2O fluxes (please see section 2.3). However, their inconsistent performances and inaccuracy of simulations due to parameter uncertainties, insufficient model calibration and validation at site level, and limited global datasets for model inputs cast doubt on the estimated global N_2O budget (Ehrhardt et al., 2018; Tian et al., 2019).

Machine learning-based models are emerging as an alternative to quantify N_2O emission at various scales (Hamrani et al., 2020). For example, the BP-neural network and gradient boosted regression tree were applied to explicitly build explicit denitrification models (Oehler et al., 2010). Philibert et al. (2014) demonstrated the good performance of random forest in estimating cumulative N_2O emission from croplands globally, while quantitively discussing the importance of driving factors. These models have also been successfully used for daily time-step estimation at the site level (Saha et al., 2021). However, these models are data-driven "black box" and their algorithms as well as performances are largely dependent on the training data quality and quantity, rather than a reasonable understanding of the underlying biogeochemical mechanisms (Hamrani et al., 2020).

In summary, improved soil N_2O emission modeling at various scales warrant advanced models that can address the mechanisms of N_2O emissions related biotic and abiotic processes, and undergo extensive calibrations and validations against field measurements to accurately reflect the spatiotemporal variation patterns in soil N_2O fluxes under changing environments and management conditions (Butterbach-Bahl et al., 2013; Tian et al., 2024).

1.2 Scientific questions, objectives, and dissertation structure

Given the large uncertainties and the need for systematical quantification of global terrestrial N_2O budgets to mitigate agricultural source N_2O emissions, this dissertation aims to address the following key questions:

1. What are the spatial and temporal variation patterns of historical N_2O emissions from global agricultural ecosystems?
2. What are the dominant drivers influencing the trends of historical N_2O emissions from global agricultural ecosystems?
3. How might N_2O emissions from global agricultural ecosystems respond to different scenarios of future climate and management changes?

To address the questions and fill current knowledge gaps, the overall objective of this dissertation is to develop and use an improved model to better simulate historical N_2O emissions from global agricultural ecosystems and estimate its possible trajectories under global changes.

The specific objectives are:

1. Development and improvement of the process-based biogeochemical model, TRIPLEX-GHGv2.0 to better quantify the dynamics of N_2O emissions.
2. Simulation of historical N_2O emissions from global agricultural soils and attribution to different management or environmental driving factors quantitatively.
3. Projection of future possible trends under changing climate and management scenarios (i.e., share social-economic pathways, SSPs).

Given the diversity and complexity of agricultural ecosystems and the various management practices they involve, I have categorized the agricultural ecosystems into three types: upland croplands, grazing-lands, and rice-paddies for model development and historical simulations. For future prediction, these ecosystems are addressed as a whole to provide a broad perspective.

Consequently, Chapter II, III, and IV address objectives 1 and 2 for upland croplands, grazing-lands, and rice-paddies, respectively.

These three chapters have already been published in *Science of the Total Environment* (*Song et al., "Integrating major agricultural practices into the TRIPLEX-GHG model v2. 0 for simulating global cropland nitrous oxide emissions: Development, sensitivity analysis and site evaluation." Science of the Total Environment 843 (2022): 156945.*), *Global and Planetary Change* (*Song et al., "Quantifying patterns, sources and uncertainty of nitrous oxide emissions from global grazing lands: Nitrogen forms are the determinant factors for estimation and mitigation" Global and Planetary Change. 223 (2023): 104080*), and *Global Biogeochemical Cycles* (*Song et al., "Central Role of Nitrogen Fertilizer Relative to Water Management in Determining Direct Nitrous Oxide Emissions From Global Rice-Based Ecosystems." Global Biogeochemical Cycles 37.11 (2023): e2023GB007744.*).

Chapter V addresses objective 3, in which I evaluated the possible changes in N_2O emission from global agricultural ecosystems in the future, with specific contributions from climate change and management scenarios. This Chapter will be submitted to the journal *Earth Future* shortly. Chapter I provides the general introduction, while Chapter VI offers the conclusion of the dissertation and discusses potential future directions.

1.3 References

Barnard, R., Leadley, P. W., & Hungate, B. A. (2005). Global change, nitrification, and denitrification: A review. *Global Biogeochemical Cycles*, *19*(1). https://doi.org/https://doi.org/10.1029/2004GB002282

Barton, L., Wolf, B., Rowlings, D., Scheer, C., Kiese, R., Grace, P., Stefanova, K., & Butterbach-Bahl, K. (2015). Sampling frequency affects estimates of annual nitrous oxide fluxes. *Scientific Reports*, *5*(1), 15912. https://doi.org/10.1038/srep15912

Braker, G., & Conrad, R. (2011). Chapter 2 - Diversity, Structure, and Size of N2O-Producing Microbial Communities in Soils—What Matters for Their Functioning? In A. I. Laskin, S. Sariaslani, & G. M. Gadd (Eds.), *Advances in Applied Microbiology* (Vol. 75, pp. 33-70). Academic Press. https://doi.org/https://doi.org/10.1016/B978-0-12-387046-9.00002-5

Butterbach-Bahl, K., Baggs, E. M., Dannenmann, M., Kiese, R., & Zechmeister-Boltenstern, S. (2013). Nitrous oxide emissions from soils: how well do we understand the processes and their controls? *Philosophical Transactions of the Royal Society B-Biological Sciences*, *368*(1621). https://doi.org/10.1098/rstb.2013.0122

Cai, W., Borlace, S., Lengaigne, M., van Rensch, P., Collins, M., Vecchi, G., Timmermann, A., Santoso, A., McPhaden, M. J., Wu, L., England, M. H., Wang, G., Guilyardi, E., & Jin, F.-F. (2014). Increasing frequency of extreme El Nino events due to greenhouse warming. *Nature Climate Change*, *4*(2), 111-116. https://doi.org/10.1038/nclimate2100

Church, J. A., & White, N. J. (2006). A 20th century acceleration in global sea-level rise [Article]. *Geophysical Research Letters*, *33*(1), 4, Article L01602. https://doi.org/10.1029/2005gl024826

Cowan, N., Levy, P., Maire, J., Coyle, M., Leeson, S. R., Famulari, D., Carozzi, M., Nemitz, E., & Skiba, U. (2020). An evaluation of four years of nitrous oxide fluxes after application of ammonium nitrate and urea fertilisers measured using the eddy covariance method. *Agricultural and Forest Meteorology*, *280*, 107812. https://doi.org/https://doi.org/10.1016/j.agrformet.2019.107812

Daims, H., Lücker, S., & Wagner, M. (2016). A New Perspective on Microbes Formerly Known as Nitrite-Oxidizing Bacteria. *Trends in Microbiology*, *24*(9), 699-712. https://doi.org/10.1016/j.tim.2016.05.004

Davidson, E. A. (2009). The contribution of manure and fertilizer nitrogen to atmospheric nitrous oxide since 1860. *Nature Geoscience*, *2*(9), 659-662. https://doi.org/10.1038/ngeo608

Davidson, E. A., & Kanter, D. (2014). Inventories and scenarios of nitrous oxide emissions. *Environmental Research Letters*, *9*(10), Article 105012. https://doi.org/10.1088/1748-9326/9/10/105012

Ehrhardt, F., Soussana, J.-F., Bellocchi, G., Grace, P., McAuliffe, R., Recous, S., Sandor, R., Smith, P., Snow, V., Migliorati, M. d. A., Basso, B., Bhatia, A., Brilli, L., Doltra, J., Dorich, C. D., Doro, L., Fitton, N., Giacomini, S. J., Grant, B., . . . Zhang, Q. (2018). Assessing uncertainties in crop and pasture ensemble model simulations of productivity and N2O emissions. *Global Change Biology*, *24*(2), E603-E616. https://doi.org/10.1111/gcb.13965

Gerber, J. S., Carlson, K. M., Makowski, D., Mueller, N. D., de Cortazar-Atauri, I. G., Havlik, P., Herrero, M., Launay, M., O'Connell, C. S., Smith, P., & West, P. C. (2016). Spatially explicit estimates of N2O emissions from croplands suggest climate mitigation opportunities from improved fertilizer management. *Global Change Biology*, *22*(10), 3383-3394. https://doi.org/10.1111/gcb.13341

Goodrich, J. P., Wall, A. M., Campbell, D. I., Fletcher, D., Wecking, A. R., & Schipper, L. A. (2021). Improved gap filling approach and uncertainty estimation for eddy covariance N2O fluxes. *Agricultural and Forest Meteorology*, *297*, 108280. https://doi.org/https://doi.org/10.1016/j.agrformet.2020.108280

Hansen, J., Johnson, D., Lacis, A., Lebedeff, S., Lee, P., Rind, D., & Russell, G. (1981). Climate impact of increasing atmospheric carbon dioxide. *Science*, *213*(4511), 957-966.

Hamrani, A., Akbarzadeh, A., & Madramootoo, C. A. (2020). Machine learning for predicting greenhouse gas emissions from agricultural soils. *Science of the Total Environment*, *741*, 140338.

https://doi.org/https://doi.org/10.1016/j.scitotenv.2020.140338

Hergoualc'h, K., Mueller, N., Bernoux, M., Kasimir, Ä., van der Weerden, T. J., & Ogle, S. M. (2021). Improved accuracy and reduced uncertainty in greenhouse gas inventories by refining the IPCC emission factor for direct N2O emissions from nitrogen inputs to managed soils. *Global Change Biology*, *27*(24), 6536-6550. https://doi.org/https://doi.org/10.1111/gcb.15884

Huang, H., Wang, J., Hui, D., Miller, D. R., Bhattarai, S., Dennis, S., Smart, D., Sammis, T., & Reddy, K. C. (2014). Nitrous oxide emissions from a commercial cornfield (<i>Zea mays</i>) measured using the eddy covariance technique. *Atmos. Chem. Phys.*, *14*(23), 12839-12854. https://doi.org/10.5194/acp-14-12839-2014

IPCC. (2021). *Climate Change 2021: The Physical Science Basis. Contribution of Working Group I to the Sixth Assessment Report of the Intergovernmental Panel on Climate Change* (Vol. In Press). Cambridge University Press. https://doi.org/10.1017/9781009157896

IPCC. (2023). *Climate Change 2023: Synthesis Report. Contribution of Working Groups I, II and III to the Sixth Assessment Report of the Intergovernmental Panel on Climate Change [Core Writing Team, H. Lee and J. Romero (eds.)]*. IPCC. https://doi.org/10.59327/IPCC/AR6-9789291691647

Kanter, D. R., Ogle, S. M., & Winiwarter, W. (2020). Building on Paris: integrating nitrous oxide mitigation into future climate policy. *Current Opinion in Environmental Sustainability*, *47*, 7-12. https://doi.org/https://doi.org/10.1016/j.cosust.2020.04.005

Knowles, R. (1982). Denitrification. *Microbiological reviews*, *46*(1), 43-70.

Kuang, W., Gao, X., Tenuta, M., & Zeng, F. (2021). A global meta-analysis of nitrous oxide emission from drip-irrigated cropping system. *Global Change Biology*, *27*(14), 3244-3256. https://doi.org/https://doi.org/10.1111/gcb.15636

Lan, X., K.W. Thoning, & Dlugokencky, E. J. (2024). *Trends in globally-averaged CH4, N2O, and SF6 determined from NOAA Global Monitoring Laboratory measurements.*

Liang, M., Zhou, Z., Ren, P., Xiao, H., Xu, R., Hu, Z., Piao, S., Tian, H., Tong, Q., Zhou, F., Wei, J., & Yuan, W. (2024). Four decades of full-scale nitrous oxide emission inventory in China. *National Science Review*, *11*(3), nwad285. https://doi.org/10.1093/nsr/nwad285

Liu, H., Zheng, X., Li, Y., Yu, J., Ding, H., Sveen, T. R., & Zhang, Y. (2022). Soil moisture determines nitrous oxide emission and uptake. *Science of the Total Environment*, *822*, 153566. https://doi.org/https://doi.org/10.1016/j.scitotenv.2022.153566

Lognoul, M., Debacq, A., De Ligne, A., Dumont, B., Manise, T., Bodson, B., Heinesch, B., & Aubinet, M. (2019). N2O flux short-term response to temperature and topsoil disturbance in a fertilized crop: An eddy covariance campaign. *Agricultural and Forest Meteorology*, *271*, 193-206. https://doi.org/https://doi.org/10.1016/j.agrformet.2019.02.033

Luo, G. J., Kiese, R., Wolf, B., & Butterbach-Bahl, K. (2013). Effects of soil temperature and moisture on methane uptake and nitrous oxide emissions across three different ecosystem types. *Biogeosciences*, *10*(5), 3205-3219. https://doi.org/10.5194/bg-10-3205-2013

Mancia, A., Chadwick, D. R., Waters, S. M., & Krol, D. J. (2022). Uncertainties in direct N2O emissions from grazing ruminant excreta (EF3PRP) in national greenhouse gas inventories. *Science of The Total Environment*, *803*, 149935. https://doi.org/https://doi.org/10.1016/j.scitotenv.2021.149935

Martikainen, P. J. (2022). Heterotrophic nitrification – An eternal mystery in the nitrogen cycle. *Soil Biology and Biochemistry*, *168*, 108611. https://doi.org/https://doi.org/10.1016/j.soilbio.2022.108611

Mei, K., Wang, Z., Huang, H., Zhang, C., Shang, X., Dahlgren, R. A., Zhang, M., & Xia, F. (2018). Stimulation of N2O emission by conservation tillage management in agricultural lands: A meta-analysis. *Soil & Tillage Research*, *182*, 86-93. https://doi.org/10.1016/j.still.2018.05.006

Nie, S. a., Zhu, G.-B., Singh, B., & Zhu, Y.-G. (2019). Anaerobic ammonium oxidation in agricultural soils-synthesis and prospective. *Environmental Pollution*, *244*, 127-134. https://doi.org/https://doi.org/10.1016/j.envpol.2018.10.050

O'Neill, B. C., Tebaldi, C., van Vuuren, D. P., Eyring, V., Friedlingstein, P., Hurtt, G., Knutti, R., Kriegler, E., Lamarque, J. F., Lowe, J., Meehl, G. A., Moss, R., Riahi, K., & Sanderson, B. M. (2016). The Scenario Model Intercomparison Project (ScenarioMIP) for CMIP6. *Geosci. Model Dev.*, *9*(9), 3461-3482. https://doi.org/10.5194/gmd-9-3461-2016

Oehler, F., Rutherford, J. C., & Coco, G. (2010). The use of machine learning algorithms to design a generalized simplified denitrification model. *Biogeosciences*, *7*(10), 3311-3332. https://doi.org/10.5194/bg-7-3311-2010

Prosser, J. I., & Nicol, G. W. (2012). Archaeal and bacterial ammonia-oxidisers in soil: the quest for niche specialisation and differentiation. *Trends in Microbiology*, *20*(11), 523-531. https://doi.org/10.1016/j.tim.2012.08.001

Putz, M., Schleusner, P., Rütting, T., & Hallin, S. (2018). Relative abundance of denitrifying and DNRA bacteria and their activity determine nitrogen retention or loss in agricultural soil. *Soil Biology and Biochemistry*, *123*, 97-104. https://doi.org/https://doi.org/10.1016/j.soilbio.2018.05.006

Qiu, Y., Jiang, Y., Guo, L., Burkey, K. O., Zobel, R. W., Shew, H. D., & Hu, S. (2018). Contrasting Warming and Ozone Effects on Denitrifiers Dominate Soil N2O Emissions. *Environmental Science & Technology*, *52*(19), 10956-10966. https://doi.org/10.1021/acs.est.8b01093

Qiu, Y., Zhang, Y., Zhang, K., Xu, X., Zhao, Y., Bai, T., Zhao, Y., Wang, H., Sheng, X., Bloszies, S., Gillespie, C. J., He, T., Wang, Y., Chen, H., Guo, L., Song, H., Ye, C., Wang, Y., Woodley, A., . . . Hu, S. (2024). Intermediate soil acidification induces highest nitrous oxide emissions. *Nature Communications*, *15*(1), 2695. https://doi.org/10.1038/s41467-024-46931-3

Ravishankara, A. R., Daniel, J. S., & Portmann, R. W. (2009). Nitrous Oxide (N2O): The Dominant Ozone-Depleting Substance Emitted in the 21st Century. *Science*, *326*(5949), 123-125. https://doi.org/10.1126/science.1176985

Reay, D. S., Davidson, E. A., Smith, K. A., Smith, P., Melillo, J. M., Dentener, F., & Crutzen, P. J. (2012). Global agriculture and nitrous oxide emissions. *Nature Climate Change*, *2*(6), 410-416. https://doi.org/10.1038/nclimate1458

Rees, R. M., Augustin, J., Alberti, G., Ball, B. C., Boeckx, P., Cantarel, A., Castaldi, S., Chirinda, N., Chojnicki, B., Giebels, M., Gordon, H., Grosz, B., Horvath, L., Juszczak, R., Kasimir Klemedtsson, Å., Klemedtsson, L., Medinets, S., Machon, A., Mapanda, F., . . . Wuta, M. (2013). Nitrous oxide emissions from European agriculture – an analysis of variability and drivers of emissions from field experiments. *Biogeosciences*, *10*(4), 2671-2682. https://doi.org/10.5194/bg-10-2671-2013

Rochette, P., & Eriksen-Hamel, N. S. (2008). Chamber Measurements of Soil Nitrous Oxide Flux: Are Absolute Values Reliable? *Soil Science Society of America Journal*, *72*(2), 331-342. https://doi.org/https://doi.org/10.2136/sssaj2007.0215

Saha, D., Basso, B., & Robertson, G. P. (2021). Machine learning improves predictions of agricultural nitrous oxide (N2O) emissions from intensively managed cropping systems. *Environmental Research Letters*, *16*(2), 024004. https://doi.org/10.1088/1748-9326/abd2f3

Schleussner, C.-F., Rogelj, J., Schaeffer, M., Lissner, T., Licker, R., Fischer, E. M., Knutti, R., Levermann, A., Frieler, K., & Hare, W. (2016). Science and policy characteristics of the Paris Agreement temperature goal. *Nature Climate Change*, *6*(9), 827-835.

Shang, Z., Abdalla, M., Kuhnert, M., Albanito, F., Zhou, F., Xia, L., & Smith, P. (2020). Measurement of N2O emissions over the whole year is necessary for estimating reliable emission factors. *Environmental Pollution*, *259*, 113864. https://doi.org/https://doi.org/10.1016/j.envpol.2019.113864

Shang, Z., Cui, X., van Groenigen, K. J., Kuhnert, M., Abdalla, M., Luo, J., Zhang, W., Song, Z., Jiang, Y., Smith, P., & Zhou, F. (2024). Global cropland nitrous oxide emissions in fallow period are comparable to growing-season emissions. *Global Change Biology*, *30*(2), e17165. https://doi.org/https://doi.org/10.1111/gcb.17165

Shang, Z., Zhou, F., Smith, P., Saikawa, E., Ciais, P., Chang, J., Tian, H., Del Grosso, S. J., Ito, A., Chen, M., Wang, Q., Bo, Y., Cui, X., Castaldi, S., Juszczak, R., Kasimir, A., Magliulo, V., Medinets, S., Medinets, V., . . . Sabbatini, S. (2019). Weakened growth of cropland-N2O emissions in China associated with nationwide policy interventions. *Global Change Biology*, *25*(11), 3706-3719. https://doi.org/10.1111/gcb.14741

Shcherbak, I., Millar, N., & Robertson, G. P. (2014). Global metaanalysis of the nonlinear response of soil nitrous oxide (N2O) emissions to fertilizer nitrogen. *Proceedings of the National Academy of Sciences*, *111*(25), 9199-9204. https://doi.org/10.1073/pnas.1322434111

Stocker, B. D., Roth, R., Joos, F., Spahni, R., Steinacher, M., Zaehle, S., Bouwman, L., Xu, R., & Prentice, I. C. (2013). Multiple greenhouse-gas feedbacks from the land biosphere under future climate change scenarios. *Nature Climate Change*, *3*(7), 666-672. https://doi.org/10.1038/nclimate1864

Tian, H., Lu, C., Ciais, P., Michalak, A. M., Canadell, J. G., Saikawa, E., Huntzinger, D. N., Gurney, K. R., Sitch, S., Zhang, B., Yang, J., Bousquet, P., Bruhwiler, L., Chen, G., Dlugokencky, E., Friedlingstein, P., Melillo, J., Pan, S., Poulter, B., . . . Wofsy, S. C. (2016). The terrestrial biosphere as a net source of greenhouse gases to the atmosphere. *Nature*, *531*(7593), 225-+. https://doi.org/10.1038/nature16946

Tian, H., Pan, N., Thompson, R. L., Canadell, J. G., Suntharalingam, P., Regnier, P., Davidson, E. A., Prather, M., Ciais, P., Muntean, M., Pan, S., Winiwarter, W., Zaehle, S., Zhou, F., Jackson, R. B., Bange, H. W., Berthet, S., Bian, Z., Bianchi, D., . . . Zhu, Q. (2024). Global nitrous oxide budget (1980–2020). *Earth Syst. Sci. Data*, *16*(6), 2543-2604. https://doi.org/10.5194/essd-16-2543-2024

Tian, H., Xu, R., Canadell, J. G., Thompson, R. L., Winiwarter, W., Suntharalingam, P., Davidson, E. A., Ciais, P., Jackson, R. B., Janssens-Maenhout, G., Prather, M. J., Regnier, P., Pan, N., Pan, S., Peters, G. P., Shi, H., Tubiello, F. N., Zaehle, S., Zhou, F., . . . Yao, Y. (2020). A comprehensive quantification of global nitrous oxide sources and sinks. *Nature*, *586*(7828), 248-256. https://doi.org/10.1038/s41586-020-2780-0

Tian, H., Yang, J., Xu, R., Lu, C., Canadell, J. G., Davidson, E. A., Jackson, R. B., Arneth, A., Chang, J., Ciais, P., Gerber, S., Ito, A., Joos, F., Lienert, S., Messina, P., Olin, S., Pan, S., Peng, C., Saikawa, E., . . . Zhang, B. (2019). Global soil nitrous oxide emissions since the preindustrial era estimated by an ensemble of terrestrial biosphere models: Magnitude, attribution, and uncertainty. *Global Change Biology*, *25*(2), 640-659. https://doi.org/10.1111/gcb.14514

Venterea, R. T., Petersen, S. O., de Klein, C. A. M., Pedersen, A. R., Noble, A. D. L., Rees, R. M., Gamble, J. D., & Parkin, T. B. (2020). Global Research Alliance N2O chamber methodology guidelines: Flux calculations. *J Environ Qual*, *49*(5), 1141-1155. https://doi.org/https://doi.org/10.1002/jeq2.20118

Wagner-Riddle, C., Congreves, K. A., Abalos, D., Berg, A. A., Brown, S. E., Ambadan, J. T., Gao, X., & Tenuta, M. (2017). Globally important nitrous oxide emissions from croplands induced by freeze-thaw cycles. *Nature Geoscience*, *10*(4), 279-+. https://doi.org/10.1038/ngeo2907

Wang, J., Chadwick, D. R., Cheng, Y., & Yan, X. (2018). Global analysis of agricultural soil denitrification in response to fertilizer nitrogen. *Science of the Total Environment*, *616*, 908-917. https://doi.org/10.1016/j.scitotenv.2017.10.229

Wang, Y., Guo, J., Vogt, R. D., Mulder, J., Wang, J., & Zhang, X. (2018). Soil pH as the chief modifier for regional nitrous oxide emissions: New evidence and implications for global estimates and mitigation. *Global Change Biology*, *24*(2), E617-E626. https://doi.org/10.1111/gcb.13966

Wrage-Moennig, N., Horn, M. A., Well, R., Mueller, C., Velthof, G., & Oenema, O. (2018). The role of nitrifier denitrification in the production of nitrous oxide revisited. *Soil Biology & Biochemistry*, *123*, A3-A16. https://doi.org/10.1016/j.soilbio.2018.03.020

Wrage, N., Velthof, G. L., van Beusichem, M. L., & Oenema, O. (2001). Role of nitrifier denitrification in the production of nitrous oxide. *Soil Biology & Biochemistry*, *33*(12-13), 1723-1732. https://doi.org/10.1016/s0038-0717(01)00096-7

Wu, D., Cárdenas, L. M., Calvet, S., Brüggemann, N., Loick, N., Liu, S., & Bol, R. (2017). The effect of nitrification inhibitor on N2O, NO and N2 emissions under different soil moisture levels in a permanent grassland soil. *Soil Biology and Biochemistry*, *113*, 153-160. https://doi.org/https://doi.org/10.1016/j.soilbio.2017.06.007

Wu, Y.-F., Whitaker, J., Toet, S., Bradley, A., Davies, C. A., & McNamara, N. P. (2021). Diurnal variability in soil nitrous oxide emissions is a widespread phenomenon. *Global Change Biology*, *27*(20), 4950-4966. https://doi.org/https://doi.org/10.1111/gcb.15791

Zhou, M., Zhu, B., Wang, S., Zhu, X., Vereecken, H., & Brueggemann, N. (2017). Stimulation of N2O emission by manure application to agricultural soils may largely offset carbon benefits: a global meta-analysis. *Global Change Biology*, *23*(10), 4068-4083. https://doi.org/10.1111/gcb.13648

Zhu, X., Burger, M., Doane, T. A., & Horwath, W. R. (2013). Ammonia oxidation pathways and nitrifier denitrification are significant sources of N₂O and NO under low oxygen availability. *Proceedings of the National Academy of Sciences*, *110*(16), 6328-6333. https://doi.org/10.1073/pnas.1219993110

CHAPTER II:

Integrating Major Agricultural Practices into the TRIPLEX-GHG Model v2.0 for Simulating Global Upland Cropland Nitrous Oxide Emissions: Development, Sensitivity Analysis, Site Evaluation, and Global simulation

Hanxiong Song, Changhui Peng, Kerou Zhang, and Qiuan Zhu

Article published in *Science of the Total Environment* 843 (2022): 156945.

2.1 Résumé

Les émissions de protoxyde d'azote (N_2O) provenant des terres cultivées représentent l'une des sources les plus importantes de gaz à effet de serre, tandis que l'estimation de ces émissions demeure largement incertaine à l'échelle mondiale. Pour simuler les émissions de N_2O des terres cultivées mondiales, le modèle biogéochimique basé sur les processus TRIPLEX-GHG v2.0 a été amélioré par le couplage des principales activités agricoles. Une expérience de sensibilité a été utilisée pour mesurer l'impact des processus intégrés sur les émissions de N_2O modélisées. La fertilisation azotée chimique a eu les effets relatifs les plus importants. Le coefficient de consommation de NO_3 pour la dénitrification (COE_{dNO3}), contrôlant la première étape du processus de dénitrification, a été identifié comme le paramètre le plus sensible d'après une analyse de sensibilité des paramètres du modèle. Le modèle a bien fonctionné pour simuler l'ampleur des émissions journalières de N_2O sur 39 sites de calibration (flux journaliers moyens de N_2O, R^2 = 0.87, pente = 1.07; et facteurs d'émission, EF, R^2 = 0.70, pente = 0.72) pendant les périodes expérimentales. La fiabilité du modèle a été confirmée par 68 sites de validation avec des corrélations élevées entre les résultats des émissions moyennes de N_2O modélisées et observées (R^2 = 0.86, pente = 0.82) et des FE (R^2 = 0.66, pente = 0.83). Les simulations mondiales suggèrent qu'entre 1901 et 2016, les émissions annuelles de N_2O provenant des terres cultivées mondiales ont considérablement augmenté, passant de 0.13 à 2.96 Tg N an^{-1}. L'augmentation depuis les années 1960 a été significativement plus importante, mais les émissions ont légèrement diminué depuis leur pic en 1994, principalement en raison des déclins en Europe et aux États-Unis. Les engrais azotés ont été le principal moteur de cette augmentation, avec une moyenne de 1.44 Tg N an^{-1} depuis 2000. Des améliorations supplémentaires dans des estimations plus détaillées des variations des facteurs environnementaux, des effets de gestion et des entrées de modèles précises sont nécessaires pour réduire les incertitudes dans les simulations du modèle.

2.2 Abstract

Nitrous oxide (N_2O) emissions from croplands are one of the most important greenhouse gas sources while the current estimates remain large uncertainties globally. To simulate N_2O emissions from global croplands, the process-based TRIPLEX-GHG model v2.0 was improved by coupling the major agricultural activities. Sensitivity experiment was used to measure the impact of the integrated processes to modeled N_2O emission, revealing chemical N fertilization have the highest relative effect sizes. While the coefficient of the NO_3^- consumption rate for denitrification (COE_{dNO3}), controlling the first step of the denitrification process was identified to be the most sensitive parameter based on sensitivity analysis of model parameters. The model performed well when simulating the magnitude of the daily N_2O emissions for 39 calibration sites (the means of the measured daily N_2O fluxes, R^2 = 0.87, slope = 1.07; and emission factors, EFs, R^2 = 0.70, slope = 0.72) during the experiment periods. The model reliability was further confirmed by 68 validation sites with high correlations between the results of modeled and observed mean N_2O emissions (R^2 = 0.86, slope = 0.82) and EFs (R^2 = 0.66, slope = 0.83). Global simulations suggested that from 1901 to 2016, annual N_2O emissions from global upland croplands rose significantly from 0.13 to 2.96 Tg N yr^{-1}. The increase since the 1960s was notably larger, but emissions slightly decreased after peaking in 1994 which were mainly due to decreases in Europe and the USA. N fertilizer was the primary driver of the increase, averaging 1.44 Tg N yr^{-1} since 2000. Further improvement on more detailed estimations for the variation of the environmental factors, management effects as well as accurate model input model driving data are required to reduce the uncertainties of model simulations.

2.3 Introduction

Nitrous oxide (N_2O) is a long-lived trace gas that has a global warming potential on a 100-year time horizon that is 265–298 times larger than that of carbon dioxide (CO_2), and it simultaneously results in ozone depletion in the stratosphere (Ciais et al., 2014). The atmospheric concentration of N_2O has significantly increased (i.e., by 20%) since the industrial revolution (Tian et al., 2016; Tian et al., 2020). Generally, N_2O is produced as an intermediate product of soil microbial nitrification and denitrification processes and is regulated by multiple biotic (i.e., vegetation type, microbial biomass) and abiotic factors (i.e., climate, soil temperature, humidity, nutrient content, and texture) (Bouwman et al., 2002; Butterbach-Bahl et al., 2013; Li et al., 2000; Stehfest & Bouwman, 2006; Tian et al., 2018).

Cropland is a primary source of terrestrial N_2O emissions (Reay et al., 2012; Tian et al., 2020). The current larger emission rate of cropland soil comparing with natural soil (Davidson & Kanter, 2014) results from extensive agricultural practices, including N-fertilizer input (synthetic and manure) (Davidson, 2009; Zhou et al., 2017), irrigation (Li et al., 2000; Li et al., 2010), and tillage (Mei et al., 2018; Powlson et al., 2014), because these agricultural practices directly and indirectly interfere with soil N flow and microbial activities (Cavigelli et al., 2012). Therefore, substantial observation studies have been conducted in croplands to understand the effects of different agricultural practices on N_2O emissions in order to enable sustainable agricultural production (Burney et al., 2010; Carlson et al., 2017; Snyder et al., 2009). However, because of the characteristics of the varying magnitudes across the study sites and periods (Tian et al., 2016; H. Tian et al., 2019), the emission pattern of N_2O requires models to be quantitatively investigated on large scales (Li et al., 2000; Tian et al., 2018; Wrage et al., 2001).

Modeling is an important approach for quantifying the N_2O emissions from various ecosystems, especially croplands, under changing environments and management. Linear and non-linear models based on emission factors (EF) have been widely used to estimate direct N_2O emissions on different scales (Davidson, 2009; Gerber et al., 2016; Hoben et al., 2011; Shcherbak et al., 2014). However, the EF method has been questioned due to the large uncertainty generated by its inability to depict spatial (i.e., site, regional and global) and temporal (i.e., monthly, daily) variations (Berdanier & Conant, 2012; Ehrhardt et al., 2018; H. Tian et al., 2019). Models based on machine learning algorithms such as the random forest algorithm (Philibert et al., 2013), artificial neural network (Oehler et al., 2010), and

Bayesian inversion (Berdanier & Conant, 2012) have recently been applied to cropland N_2O emission estimations, but these methods strongly depend on the quality of the training data, instead of the underlying mechanism of the N_2O-related processes.

Process-based biogeochemical models, which serve as an alternative, have been demonstrated to be an effective tool for assessing and predicting the N_2O flux by describing the nitrification, denitrification processes and N_2O dynamics at different scales (Tian et al., 2018; H. Tian et al., 2019). However, the global N_2O Model Intercomparison Project (NMIP) with ten process-based models reported that large uncertainties still exist in the current estimations of the global N_2O emissions, especially for croplands (H. Tian et al., 2019). Esemble model simulations on site scale also pointed out models showed diverse and inconsistent performances in estimating cropland N_2O (Ehrhardt et al., 2018). The differences in the model structures probably account for these uncertainties. For instance, the DAYCENT (Daily Century) model has provided adequate simulations of N_2O fluxes for a variety of agroecosystems with different scales (Alvaro-Fuentes et al., 2017; Cheng et al., 2014; Del Grosso et al., 2005; Del Grosso et al., 2009). Nevertheless, because it predominately utilizes simple functions based on soil water, inorganic nitrogen (N) concentrations, respiration, and texture (Del Grosso et al., 2000; Parton et al., 1996), the limited model descriptions for oxygen diffusion and consumption processes lead to relatively large uncertainties (Alvaro-Fuentes et al., 2017; Butterbach-Bahl et al., 2013; Song et al., 2019). Tian et al. (2010) developed a process-based biogeochemical model, i.e., the Dynamic Land Ecosystem Model (DLEM), which has been successfully used to estimate N_2O emissions at continental and global scales (Tian et al., 2010; Xu et al., 2017). However, due to the absence of the effect of soil pH, the nitrification and denitrification processes were simulated based on empirical equations (Chatskikh et al., 2005; Heinen, 2006), which might be responsible for the bias of the modeled results. In addition, insufficient parameterization schemes and the limiting model calibration could also constrain the model performance at varying scales. The Vegetation Integrative SImulator for Trace gases (VISIT) overestimated the cropland N_2O emission from eastern Asia due to limited model testing on sties level (Ito et al., 2018). The DyN-LPJ model, a dynamic global vegetation models (DGVM) coupled with N_2O-related processes, has not been extensively tested against N_2O emissions from fertilized agricultural soils before global applications, which may account for the estimated uncertainties (Xu & Prentice, 2008; Xu et al., 2012). The DeNitrification-

DeComposition (DNDC) model, a well-known process-based model, has been widely used to estimate N_2O emissions and crop production in agroecosystems on site to regional scales (Giltrap et al., 2010; Li et al., 2000; Lugato et al., 2010). However, the proper application of the DNDC requires detailed, complex input information and parameter setting, which limits its large-scale modeling ability (Perlman et al., 2014). Therefore, further improvement of the process-based N_2O emission models is critical for reducing the global modeling uncertainties and for closing the global N_2O budget in order to cope with the global change.

As a recently developed process-based model, the TRIPLEX-GHG (Zhu et al., 2014) can simulate multiple ecological processes and has been successfully applied to simulate N_2O fluxes from natural ecosystems (grasslands, forests) (K. Zhang et al., 2017). However, the impact of human disturbances (e.g., agricultural practices, land use changes, and management) have not been considered so far (Tian et al., 2018). In this study, we enhanced the TRIPLEX-GHG model's capability by addressing the impacts of major agricultural practices on the N_2O production and emission processes in order to simulate N_2O emissions from global croplands. The objectives of this study were: (1) to integrate major agricultural practices into the framework of an extant process-based model (i.e., the TRIPLEX-GHG); (2) to conduct a sensitivity experiments and sensitivity analysis of model parameters to evaluate the model response to integrated processes and identify the most sensitive parameter; and (3) to test the modeled results using field observations of various cropland sites at the global scale.

2.4 Model description

2.4.1 Overview of the original TRIPLEX-GHG model

The TRIPLEX-GHG model (K. Zhang et al., 2017; Zhu et al., 2014) is a process-based terrestrial ecosystem model, which is based on the Integrated Biosphere Simulator (IBIS) (Foley et al., 1996; Kucharik et al., 2000) and TRIPLEX (Peng et al., 2002). The basic structure of the original TRIPLEX-GHG model and the integration of agricultural management processes are shown in Figure 2.1, and are described in detail below.

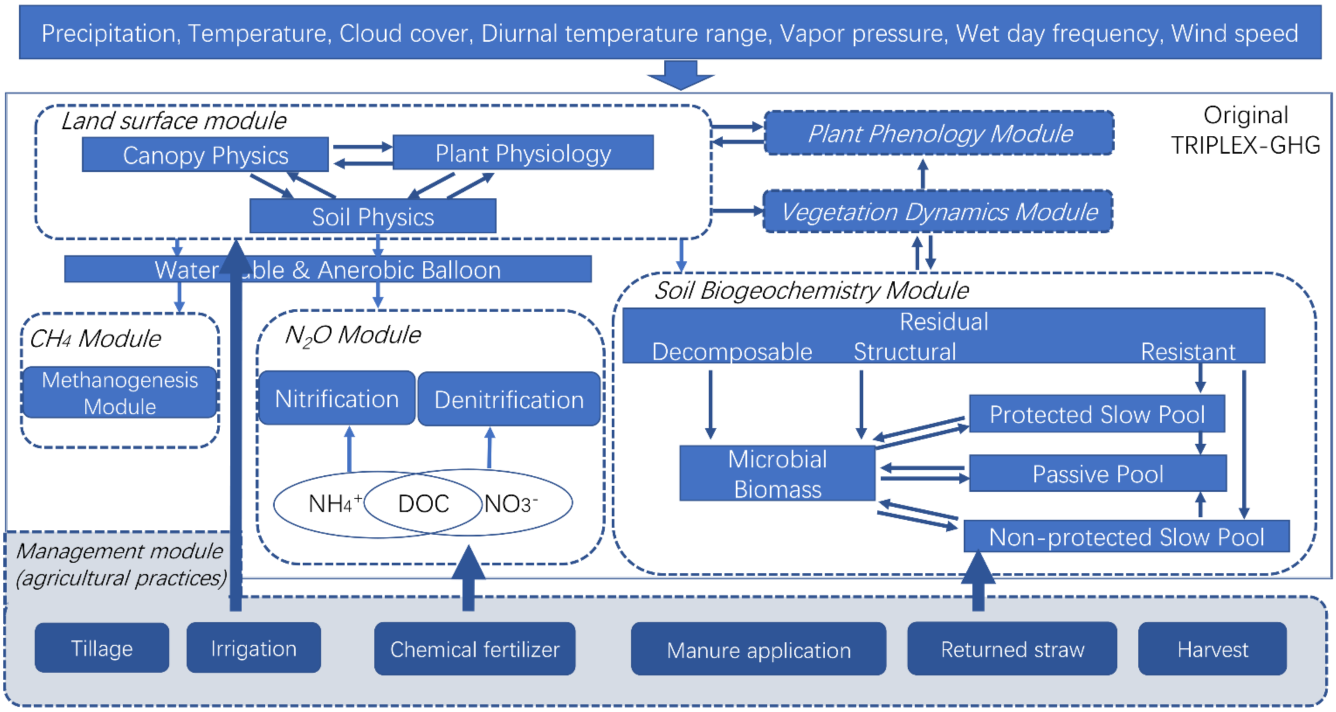

Figure 2.1 Model's structural concept and integration of agricultural practices into the TRIPLEX-GHG (revised from Zhang et al. (2017b)). The rectangular insert with the light grey background represents the different agricultural practices and how they interact with the other submodules (e.g., the land surface module).

The original TRIPLEX-GHG model consists of four key submodules: a land surface submodule for simulating the energy budget and hydrological cycle between the soil surface, vegetation canopy, and the atmosphere; a dynamic vegetation submodule that is used to determine the geographic distribution of specific plant functional types (PFTs) under climate change; a plant phenology submodule that describes the dominate phenological behavior of each PFT based on a set of phenological parameterizations (Botta et al., 2000); and a soil biogeochemical submodule that simulates the dynamics of the C and N flows and the major microbial processes, including nutrient mineralization, immobilization, and their interactions with the environment. Specifically, the biogeochemical processes mostly focus on the C cycle within three plant biomass pools (leaf, root, and wood, each of which can be further divided into the metabolic, structural, and lignin pool) and three soil organic matter pools (litter, humus, and microbial), which are comprised of non-protected, protected, and passive organic matter. However, the N cycle's scheme is coupled with the C cycle and relies on the corresponding C:N ratios of the different organic matter pools and two additional inorganic N pools (nitrite-N [NO_3^-] and ammonium-N[NH_4^+]). As a trace N gas, the N_2O emitted by nitrification and denitrification were simulated according to the anaerobic balloon concept calculated in Supporting Information Table 2.S1 (Equations (2.1–2.3)) to separate the nitrification and denitrification processes. Nitrification is an aerobic process converting ammonium (NH_4^+) into nitrate (NO_3^-) (Equations (2.4—2.7) in Table 2.S1) based on the growth and death rate of nitrifiers (Equations (2.8—2.10) in Table 2.S1) as well as the effects of soil properties (Equations (2.11—2.12) in Table 2.S1) (Li et al., 2000; Morkved et al., 2007; K. Zhang et al., 2017).

Denitrification is the process through which the nitrate is reduced stepwise into different nitrogen gases as a chain reaction process inside of the anaerobic balloon. Four independent steps of the chain reaction are linked by the competition for dissolvable organic carbon (hereafter, DOC) of the specific denitrifiers during each step (Betlach & Tiedje, 1981). The growth and mortality rates of the different denitrifiers are caliculated based on DOC and nitrogen oxides (hereafter NOx) (Equations (2.13–2.14) in Table 2.S1). The consumption of NO_X was calculated at an hourly time step as is shown in the following Eq. (2.1) (Leffelaar and Wessel, 1998; Li et al., 2000)

$$F_{ANNOX} = COE_{dNOX} \cdot B_{denit} \cdot \left(\frac{R_{NOX}}{EFF_{NOX}} + \frac{MAI_{NOX} \cdot [NO_X]}{[N]}\right) \cdot f_{NOX}(pH) \cdot f(t) \tag{2.1}$$

Here, F_{ANNOX} is the consumption rate of NO_X (kg N m^{-3} h^{-1}); COE_{dNOX} is the coefficient of NO_X consumption; B_{denit} is the biomass of the denitrifiers (kg C m^{-3}); R_{NOX} is the NO_X reduction rate (h^{-1}); EFF_{NOX} is the efficiency of the NO_X denitrifiers (kg C kg N $^{-1}$); MAI_{NOX} is the maintenance coefficient of NO_X (h^{-1}); $[NO_X]$ and $[N]$ are the NO_X and total N concentrations in the anaerobic balloon, respectively; and $f_{NOX}(pH)$ and $f(t)$ are the effects of the soil pH and soil temperature on the NO_X denitrification rate in each step, respectively (Equations (2.15–2.17) and Equation (2.18) in Table 2.S1).

In this study, the main framework for improving the TRIPLEX-GHG model was to add a new component that takes into account how agricultural practices affect the biogeochemical cycle, especially the nitrification and denitrification processes, thus modifying the pattern of the N_2O flux of croplands at the global scale.

2.4.2 Model improvements

N_2O production and emission are controlled by varying soil management practices. Understanding the direct and indirect effects of the different agricultural practices on the soil N flow (N input and output) is critical to accurately predict the N_2O fluxes in cropland ecosystems (Liu et al., 2010). We improved the model description of plant N uptake and integrated major agricultural management practices including harvest, returned residuals, chemical N fertilizer application, manure application, irrigation and tillage into original model structure as described below in detail.

2.4.2.1 N output

Plant N uptake: As a plant grows, mineral N is taken up as NO_3^--N and NH_4^+-N, which is considered to be a major pathway of soil N output. Soil mineral N is set to be first uptake by plants before the biotic processes (e.g., denitrification) in the model design (Kucharik et al., 2000; Li et al., 2000; Shcherbak et al., 2014; K. Zhang et al., 2017). In cropland soil, NO_3^--N is more easily absorbed by plants due to its higher mobility and more rapid diffusion to root systems (Chalk & Smith, 2021; Daryanto et al., 2018; Kronzucker et al., 1997; Malhi et al., 1988). Therefore, the coefficient of nitrate demand, COE_{NO3}, was introduced to the model to set a higher priority for NO_3^--N of being uptaken by plant roots in each soil layer using the following Eq (2) and Eq (3):

$$demand\_NO_{3\ i}^- = \min\left(COE_{NO3} \cdot layer_{demand_i} \cdot \frac{NO_{3\ i}^-}{(NO_{3\ i}^- + NH_{4\ i}^+)}, layer_{demand_i}\right) \qquad (2.2)$$

$$demand\_NH_{4\ i}^+ = \max\left(layer_{demand_i} - demand_{NO_{3\ i}^-}, 0.0\right) \qquad (2.3)$$

Here, $demand\_NO_{3\ i}^-$ and $demand\_NH_{4\ i}^+$ (kg N m^{-2}) are the plants' NO_3^- and NH_4^+ requirements from soil layer i; and $layer\_demand_i$ is the total plant N uptake requirement from soil layer i (kg N m^{-2}). COE_{NO3} was set to 4.0 according to the model test by comparing the mean value of the reported and simulated soil annual N_2O emission rates from unfertilized soils (Table 2.S2).

Harvest: Harvest practices significantly reduce the soil C and N inputs for cropland compared with natural soil. We systematically removed all of the litterfall from the cropland area at the end of the growing seasons to modify the harvest. 85% and 60% the total biomass carbon (aboveground and belowground calculated based on the turnover rates in the plant phenology module) was lost via harvest practices for annual and perennial crop (some crop types are perennial crop like sugarcane with diverse physiology and phenology characters compared with annual or cereal crops) respectively (Kucharik et al., 2000; Liu et al., 2010; Liu et al., 2005). The loss of nitrogen was therefore calculated based on the C:N ratios of different carbon pools of plant organs (i.e., leaf, wood and root).

2.4.2.2 N input

Returned residues: Returned residues are a significant C and N source for cropland soil and a recommended practice for improving N use efficiency. It has been reported that currently more than half of the N in crops (all of which is taken up from the soil) is removed from the ecosystem (Liu et al., 2010). Therefore, in our model, a proportion of harvested biomass is collected at the end of the growing season and is returned to soil surface as turn over to next year at daily time step (total detritus production divided by total days in a year). The returned straw is treated separately to divide their respective amounts accordingly between the three litter pool compartments based upon the C:N ratio of each residue type Eq (2.4—2.5). The cascade effect of residues on mineralization and immobilization balance is simulated by original biogeochemical submodule.

$$RS_C = \sum_{i=1}^{n} RPM_i \cdot R_{return} \cdot HV_C \quad (2.4)$$

$$RS_N = \sum_{i=1}^{n} \frac{RPM_i}{C{:}N_{pml}} \cdot R_{return} \cdot HV_C \quad (2.5)$$

Where RS_C and RS_N denote the total C and N content of returned straw (kgC m^{-2}, kgN m^{-2}); RPM_i represents the allocation ratio of plant matter type i (i.e., decomposable, structural and resistant plant matter) and $C{:}N_{pml}$ mean the C:N ratios of them; R_{return} and HV_C indicate the ratio of returned straw (in this study set as 20% following Liu et al. 2010) and total harvested biomass (kg C m^{-2}), respectively.

Chemical N fertilizer: Chemical N fertilizers were directly added to the NO_3^- and NH_4^+ pools of the top layer of soil:

$$FerNH_4{}^+ = Fr_{NH4} \cdot T_N \cdot I_{fer} \quad (2.6)$$

$$FerNO_3{}^- = (1.0 - Fr_{NH4}) \cdot T_N \cdot I_{fer} \quad (2.7)$$

Here, $FerNH_4{}^+$ and $FerNO_3{}^-$ are the amount of chemical fertilizer NH_4^+-N and NO_3^--N, respectively (kg N ha^{-1}). Fr_{NH4} is the fraction of ammonia while the T_N means the total fertilizer N applied per year (kg N ha^{-1} yr^{-1}) and the timing of application is decided by I_{fer}.

Manure N fertilizer: The manure-sourced N entered the different inorganic N and organic N pools separately. The organic portion of the manure was added to up to 3 soil organic matter (hereafter SOM) pools (the non-protected, protected, and passive organic carbon pools) separately for further decomposition (K. Zhang et al., 2017) as described in Eq (2.8—2.10):

$$ManureNH_4{}^+ = R_{NH4} \cdot Manure_N \cdot I_{man} \quad (2.8)$$

$$ManureNO_3^{\ -} = R_{NO3} \cdot Manure_N \cdot I_{man} \tag{2.9}$$

$$ManureC_{SOM} = proportion_{SOM} \cdot C{:}\,N_{SOM} \cdot Manure_N \cdot I_{man} \tag{2.10}$$

Here, $ManureNH_4^{\ +}$ and $ManureNO_3^{\ -}$ are manure-sourced NH_4^+-N and NO_3^--N, respectively (kg N m^{-2}), which are calculated using the ratio of ammonia and nitrate (i.e., R_{NH4} and R_{NO3}) to total manure N, $Manure_N$ (kg N ha^{-1}). $ManureC_{SOM}$ is the amount of manure that entered the different SOM pools (i.e., unprotected, protected and stabilized SOM pools); $proportion_{SOM}$ is the proportion of manure N added to the different SOM pools; and $C{:}\,N_{SOM}$ is the C:N ratio of a particular SOM pool. The I_{man} controls whether fertilizer application happens for the day.

2.4.2.3 Irrigation and tillage

Some agricultural practices do not directly alter the N flow in cropland soil, instead they affect N_2O by regulating the soil's physical properties.

Irrigation: The irrigation process used in this study adopted the idea of precipitation events from the DNDC (Li et al., 2000) and Agricultural Production Systems sIMulator (APSIM) (Thorburn et al., 2010). In the current model, only the flood irrigation method was included, which is similar to rainfall. During an irrigation event, exact amount of water is applied to the surface of the soil profile as 'puddle liquid' (Eq 2.11) which is designed for further infiltration, calculated by the land surface module. The information of timing and amount of irrigation was based on the reported site experiments for model calibration and validation at site-level.

$$wpud = wpud + Tw \cdot (1 - zrunf) \cdot I_{Irr} \tag{2.11}$$

$wpud$ indicates liquid content of puddles per soil area (kg H_2O m^{-2}); Tw means the total applied water per irrigation event (kg H_2O m^{-2}); $zrunf$ is the run off fraction of the applied water which is depended on the soil texture and existing amount of water to the maxim size of puddle; I_{Irr} represents the indicator of irrigation event of the day. Because land surface module is calculated in hourly time step, we designed the irrigated water was applied at 9:00 am which is a common practice during growing seasons if detailed application time is not provided.

Tillage: Tillage redistributes the soil profile and increases the availability of oxygen in each soil layer at the same time. Because of more exposure to oxygen, the anaerobic conditions and diffusion pattern also vary with the different soil moisture conditions, properties, and vegetation types (Rochette, 2008; van Kessel et al., 2013). We averaged each of the C and N pools of the top 4 soil layers (as a global conventional tillage depth) after every tillage event I_{Til} as described in the following equations 2.12—2.14.

$$SoilP_i = \frac{(SoilP_i + SoilP_{i-1})}{2} \tag{2.12}$$

$$SoilO_{2_1} = Atmos\_O_2 \tag{2.13}$$

$$SoilO_{2_i} = \frac{(SoilO_{2_i} + Atmos\_O_2)}{2} \tag{2.14}$$

i is the number of soil layer ranging from 1 to 4. $SoilP_i$ means the different organic and inorganic soil C and N pools of the soil layer i (kg C m^{-2}; kg N m^{-2}), including NH_4^+-N, NO_3^--N, NO_2^--N, DOC, non-protected, protected and stabilized SOM pools. The $SoilO_{2_i}$ represents the soil oxygen concentration of the soil layer i while $Atmos\_O_2$ means the atmospheric O_2 concentration.

2.5 Data and methods

2.5.1 Summary of model set up for simulations

Overall, 107 cropland sites were collected from published literature (section 3.2.1). Corresponding site-specific information of climate, environment, and agricultural management of these sites was obtained from either global gridded datasets (section 3.2.2) or field observation papers to drive the model. The improved TRIPLEX-GHG model v2.0 was run in a site-specific manner and model simulations were set up differently for sensitivity experiments (3.3.1), sensitivity analysis of parameters (3.3.2), calibration and, validation (3.4), especially for the management designs as listed in Table 2.

In general, the mean values of the global management datasets (e.g., N fertilizer applications) and simplest, generic practices (e.g., irrigation) were used as default constantly for sensitivity experiments. The same intensities of the management practices were applied to provide a direct evaluation of the effect sizes of integrated practices across varying environments (e.g., soil properties, climate). In contrast, to examine the relative change rate of N_2O emission induced by altering parameter values, we used site-specific management information directly obtained from global gridded datasets. Finally, for calibration and validation, the timing, intensity and property of managements of the experiment years were based on published papers. Other environmental input information was constantly obtained from grided datasets (section 3.2.2). Notably, no specific crop types (e.g., maize, wheat and soybean) were included for current model and the vegetation type was fixed as cropland for most of the simulations. Cropland was further categorized into the plant functional types (PFT) of generic C3, C4 crops for cereal crops (e.g., wheat, maize, barley, soybean) and vegetables based on the local climate as common practice for large-scale process-based models (Monfreda et al., 2008; H. Tian et al., 2019). For the experiment sites cultivated cash crops (e.g., sugarcane, litchi and grapes) which have diverse phenology and physiology characters than cereal crops, the PFTs were set as shrublands or tropical forests during the site-based simulation. Currently, the rice-paddy is not included for this model due to the different biogeochemical processes (Akiyama et al., 2005; Yan et al., 2000).

During site-level simulations, a spin-up period of about 300 years was conducted until the soil biogeochemical cycles and the compositions of the different C and N pools remained in equilibrium under stationary climate conditions, which was the multiyear mean climate data. After spin-up, the model simulation was started on January 1st, 1901, and ended on December 31st, 2016 in daily timestep.

2.5.2 Studied sites and model input information

We compiled measured N_2O emission data from croplands in published studies. 107 cropland sites were collected and the locations of which were distributed across most of the dominant terrestrial area. The detailed site information is listed in Table 3 and Table 2.S3 for calibration and validation respectively, including the geographic location, experimental period, dominate crop type, average N dose, soil properties (soil organic carbon, hereafter SOC, soil pH, soil texture), average daily N_2O emissions during the experimental period, and other agricultural practice information.

Daily climate data: We obtained daily climate data from the CRUNCEP dataset (https://www.earthsystemgrid.org/dataset/ucar.cgd.ccsm4.CRUNCEP.v4.TPHWL6Hrly.html), including the minimum, average, and maximum temperature, precipitation, specific humidity, air pressure, and wind speed, which were used to drive the model.

N fertilization data: The historical chemical fertilizer (1961–2010) and manure (1860–2014) application data for croplands were derived from the datasets produced by Nishina et al. (2017) and Zhang et al. (2017), respectively.

The synthetic N fertilization dataset is mostly based on country-specific information from the Food and Agriculture Organization statistics (FAOSTAT) after filling data gaps (Nishina et al., 2017). The dataset provided application date and monthly input N fertilizer differentiated into NH_4^+ and NO_3^-

considering the seasonal crop calendars for the dominant crops in each grid cell (Sacks et al., 2010). The synthetic N application rates in 2011–2015 were assumed to be the same as that for 2010.

The manure N dataset (B. Zhang et al., 2017) included the annual manure production and annual application, which were reconstructed using the dataset from the Global Livestock Impact Mapping System (GLIMS) in conjunction with country-specific annual livestock populations and the gridded cropland distribution map for 1860–2014 obtained from HYDE 3.2 (Goldewijk et al., 2017). The manure N production and application rates in 2015 were assumed to be the same as those in 2014.

N deposition data: We extracted the annual N deposition data based on the global maps of atmospheric nitrogen deposition (1993) (Dentener, 2006) supported by a three-dimensional global chemistry transport model (TM3) (Lelieveld & Dentener, 2000), which used N emission estimates (van Aardenne et al., 2001) and projection scenario data (Houghton, 1996; Nakicenovic et al. 2000).

Vegetation types and land use data: For the model initialization, we generated vegetation cover data by overlaying the Global Land Cover Map for 2009 (GlobCover2009) based on Medium Resolution Imaging Spectrometer (MERIS) remote sensing data (http://due.esrin.esa.int/page_globcover.php) with the ecoregions framework from the World Wildlife Fund (WWF). Then, we generated a new category of global vegetation cover types that fitted the plant functional type of the model and relied on these land cover data. The annual cropland area from 1860 to 2015 was acquired from the History Database of the Global Environment, version 3.2 (HYDE 3.2), which has reconstructed time-dependent land use using historical population and allocation algorithms with weighting maps (Goldewijk et al., 2017). Cropland can be classified into rain-fed and irrigated land, both of which were further divided into rice, generic C_3 crops (except rice, e.g., wheat), and generic C_4 crops (e.g., maize) based on the global crop distribution maps (Monfreda et al., 2008).

Soil data: The global soil properties (soil texture and soil pH) and classification were obtained from the Food and Agriculture Organization/United Nations Educational, Scientific and Cultural Organization (FAO/UNESCO) Soil Map of the World (http://www.fao.org/geonetmork/srv/en/metadata.show?id514116) and the dataset provided by Batjes (2006), respectively. The soil C and C:N ratio data used for the model initialization were generated from a global soil dataset (IGBP-DIS; 2000).

Topographic data: We used a global digital elevation model (DEM) with an approximate spatial resolution of 1 km (GTOPO30) for the topography input (http://www.temis.nl/data/gtopo30.html).

Atmospheric CO_2 concentration data: The monthly atmospheric CO_2 concentration data for the simulation period from 1860 to 2015 was obtained from the National Oceanic and Atmospheric Administration (NOAA) GLOBALVIEW-CO_2 dataset derived from atmospheric and ice core measurements (www.esrl.noaa.gov).

All of the input data were transformed into a spatial resolution of 0.5°×0.5° latitude/longitude using the ArcMap software (version 10.2).

2.5.3 Model sensitivity of processes and parameters

2.5.3.1 Sensitivity experiment of integrated agricultural practices

The critical step of the development of process-based models is to conduct a sensitivity experiment to examining the degree of model response to the integrated new processes as an indicator of improvement compared with previous versions. Therefore, we analyzed the simulated responses of N_2O emission to different agricultural treatments over 51 years (from 1960 to 2010) at 15 of the collected sites that were picked randomly from different continents. Outputs of the improved model were obtained by varying one integrated process at a time over the simulation period, while holding the other processes fixed as the same as original model (Table 2.S4) (Norton, 2015; Pappas et al., 2013). All integrated agricultural managements (including plant uptake, PU, harvest, HV, returned straw RS, chemical fertilizer application FN, manure application MN, irrigation IR and tillage TG) were designed to start from 1961 during simulation. The annual chemical fertilizer application rates and the annual manure application rate were derived from the global mean application rate of Nishina et al. (2017) and Zhang et al. (2018), respectively. While the fertilizer applied date (both chemical fertilizer and manure) is set once a year at the beginning of the growing season during model simulation. As for the irrigation and tillage practices, the amount of irrigated water is 50 mm × 1 time per year while tillage is only conducted once a year before growing seasons. Returning rate of straw is fixed at 30% of the harvested biomass and the timing of returning straw for model simulation is set at the end of growing season.

The absolute effects ($\Delta N2O_{i,j,k}$), and relative effect sizes (RES_k) of integrated processes were evaluated with Eq (2.15) and Eq (2.16) (Norton, 2015; Ogejo et al., 2010), respectively.

$$\Delta N2O_{i,j,k} = O\_N2O_{i,j} - N2O_{i,j,k} \quad (2.15)$$

$$RES_k = \frac{1}{n_i} \cdot \sum_{i=1}^{n_i} \frac{\sum_{j=1}^{n_j} |\Delta N2O_{i,j,k}|}{n_j \cdot \widehat{N2O_i}} \tag{2.16}$$

Where i denotes the random selected sites for sensitivity experiment and j represent the simulated years (i.e., 1-50). Therefore, $\Delta N2O_{i,j,k}$ means the difference between the modeled annual N_2O emissions of previous version and model with integrated process k (i.e., PU, HV, RS, FN, MN, IR, and TG) for site i and year j. $O\_N2O_{i,j}$ and $N2O_{i,j,k}$ indicated the annual N_2O emission estimated by original model and integrated model respectively. RES_k were calculated by the absolute changes of N_2O emission and the mean of N_2O emission rate for the site i during simulation as represented by $\widehat{N2O_i}$.

2.5.3.2 Sensitivity analysis of model parameters

We randomly selected 20 sites covered all continents to conduct initial sensitivity analysis of the parameters to obtain the most sensitive parameters of the production of N_2O before testing the model. According to previous N_2O modeling studies (K. Zhang et al., 2017; K. Zhang et al., 2019), the coefficient of nitrification (hereafter COE_{NR}) is the key parameter driving the amount of emitted N_2O in natural ecosystems probably because of the limited NO_3^- input. In this study, considering the increased NO_3^- input from fertilizers in cropland soil, it is conceivable for denitrification to become the dominant N_2O source as supported by increased abundance of denitrification genes under fertilized soil (Tang et al., 2016; J. Tian et al., 2019; C. Wang et al., 2018). Therefore, the sensitivities of 14 major parameters that directly control the denitrification processes, plant N uptake (COE_{NO3UP}), and the most sensitive parameter for nitrification, COE_{NR} (Table1), were compared in a site-specific manner meaning that the TRIPLEX-GHG model v2.0 was run under site-specific input climate and management information. It is notable that the parameters introduced by new integrated management practices (e.g., Fr_{NH4} in Eq.6) were excluded in the sensitivity analysis because these parameters were not directly involved in the nitrification and denitrification processes and were supposed to be controlled by model input information (i.e., published dataset or articles). We changed one parameter at a time, while holding the others fixed at default value to evaluate the response rate of the model output (i.e., in this case N_2O emission) to the changed parameter (Pappas et al., 2013) with the sensitivity index (SI) which was followed the method of Lenhart et al. (2002) using the following Eq (2.17):

$$SI = \frac{1}{n} \cdot \sum_{j=1}^{n} \left(\frac{(y_{2j} - y_{1j})/y_{0j}}{2 \cdot \Delta x / x_0} \right) \tag{2.17}$$

where n is the total number of months from 1961 to 2015 (because in our model, chemical fertilizer application started in 1961); j accounts for the number of months from 1961 to 2015; y_{0j} represents the jth monthly N_2O emissions with an initial parameter x_0; and y_{2j} and y_{1j} are the N_2O emission values produced for $+\Delta x$ and $-\Delta x$, respectively. Δx was set as 20% of x_0.

Table 2.1 List of the major parameters and their default values for processes associated with N_2O production.

Parameters	Explanation	Values	Unit	References
COE_{dNO3}	Coefficient for consumption rate of NO_3^-	0.05		(Li et al., 2000; K. Zhang et al., 2017)
COE_{NR}	Nitrification rate coefficient	0.044		(Cai et al., 2014; K. Zhang et al., 2017)
NMUEMAX	Growth coefficient for nitrifiers	0.102	d^{-1}	(Li et al., 2000)
AMAX	Mortality coefficient for nitrifiers	0.06	d^{-1}	(Li et al., 2000)
MUE_{NO3}	Maximum growth rate of NO_3^- denitrifiers	0.67	h^{-1}	(Li et al., 2000)
MUE_{NO2}	Maximum growth rate of NO_2^- denitrifiers	0.67	h^{-1}	(Li et al., 2000)
MUE_{N2O}	Maximum growth rate of N_2O denitrifiers	0.47	h^{-1}	(Li et al., 2000)
EFF_{NO3}	Efficiency parameter for NO_3^- denitrifiers	0.501	h^{-1}	(Li et al., 2000)
EFF_{NO2}	Efficiency parameter for NO_2^- Denitrifiers	0.428	h^{-1}	(Li et al., 2000)
EFF_{N2O}	Efficiency parameter for N_2O denitrifiers	0.075	h^{-1}	(Li et al., 2000)
M_{NO3}	Maintenance coefficient on NO_3^-	0.09	h^{-1}	(Li et al., 2000) Leffelaar, and Wessel 1988)

COE_{dNO2}	Coefficient for consumption rate of NO_2^-	1.0	(Norman et al., 2008; K. Zhang et al., 2017)
COE_{dNO}	Coefficient for consumption rate of NO	1.0	(Norman et al., 2008; K. Zhang et al., 2017)

2.5.4 Model calibration and validation

39 sites were used for the model calibration (Table 3), and 68 sites were used for the model validation (Table 2.S3). The model setups for model simulations were based on Table 2.3.

For model calibration, we adjusted the value of the most sensitive parameter of the N_2O emissions (obtained from sensitivity analysis of parameters) to fit the best model performance by comparing the model output of simulated daily N_2O flux data with the observed data of the 39 calibrated sites obtained from published papers via trial and error and statistical model performance indicators, site-by-site. Based on the model fitting results, we used the up-scaled fitted parameters (continental mean) to compare the modeled and measured daily mean N_2O emission rates and emission factors (EFs) during the experiment periods. Daily mean N_2O emission rate, as a function of cumulative emission during the experiment periods, is an accurate unit to evaluate the overall emission compared with using annual emission rate because existing field studies reported inconsistent measurement periods and frequencies. Emission factors represent the response level of local environment to external N input. Both factors serve as the indicators for testing the model reliability in terms of estimated emission values and understanding of underlying mechanisms.

For model validation, the calibrated COE_{dNO3} was used for model simulation. We also obtained measured daily N_2O fluxes from 15 of the validation sites with relatively long observation periods additionally to further test the performance of the model at daily time step. Finally, we tested the consistency between the simulated and observed daily mean N_2O flux across 68 validation sites to test the model performance in continent and global scale (Table 2.S3). The EFs were also examined globally.

GetData Graph Digitizer software (v2.26; getdata-graph-digitizer.com) was applied to obtain the daily N_2O fluxes data that we used for calibration and validation from figures of published literature. The index of agreement (*D*), the root mean square error (*RMSE*), and the coefficient of determination

(R^2) was used here to evaluate our model's performance when comparing the modeled and observed daily flux. The D-value and *RMSE* were calculated as follows:

$$D = 1 - \frac{\sum_{i=1}^{n}(S_i - O_i)^2}{\sum_{i=1}^{n}(|S_i - \bar{O}| + |O_i - \bar{O}|)^2}, \tag{2.18}$$

$$RMSE = \sqrt{\frac{\sum_{i=1}^{n}(S_i - O_i)^2}{n}} \tag{2.19}$$

Here, S_i is the ith simulated result corresponding to the number of observations; O_i is the ith observed value; and $\overline{O}$ is the mean of the observed values during the experimental period. D varies between 0 and 1, and is excessively sensitive to extreme values (Willmott, 1981). The model performance was considered to be perfect and unmeaningful when the D value was set to 1 and 0, respectively. The *RMSE* is the key value representing the difference between the simulated and observed values, and is significantly affected by the data units (e.g., mg N m^{-2} day^{-1} compared with kg N ha^{-1} day^{-1}).

The daily means of measured N_2O emissions for each site during experiment periods were calculated by the reported cumulative emissions and measurement periods. The emission factors (EF) of the experiment sites were calculated based on the Eq. (2.20) for both measured and simulated data.

$$EF = \sum_{i=1}^{n} \frac{(E_{Ni} - E_{0i})}{FN_i} \tag{2.20}$$

where EF denotes the mean Emission Factor (EF) of all site years; n and i represent the total number of observation years and the calculated year respectively. E_{Ni} is the cumulative emission rate of measurement period i while the E_{0i} means the simulated background emission or the emission rate of control plot or plot receive no external N applications. FN_i means the fertilizer (chemical and manure N but not for returned straw) application rate of measurement period i. Those sites without control or non-fertilizer treatment were excluded from the comparison.

2.5.5 Model simulations

The improved model is applied to simulate N_2O emission from global croplands at the spatial resolution of 0.5° covering the period of 1901—2016 (Table 2.2). We conducted three simulation experiment as shown in Table 2.4 to quantitively investigate the contribution of fertilizer and manure to changes in historical cropland N_2O emissions. S1 is the multifactor simulation, driven by all input data changed over time to obtain the 'best estimate'. While for S2 and S3, synthetic N fertilizer and both N fertilizer and manure are set at the level of 1901 throughout the simulation period. Their differences between S1 and S2, S2 and S3 reflect the effects of N fertilizer and manure, respectively.

A high-performance computer system was conducted for global simulations. Analysis of the modeled results was all processed by R software (version 4.3.1) using the packages “ncdf4”, “raster”, “terra”, and “ggplot2.”

Table 2.2 List of the model set up for simulation during sensitivity experiment, sensitivity analysis of parameters and model calibration and validation.

	Climate	Vegetation types		N fertilizer application			Manure application			Returned straw	Irrigation		Tillage	Parameters	Output information
		Before 1901	After 1901	Rate	Timing	Property	Rate	Timing	Property	Timing	Rate	Timing			
Sensitivity experiments *	CRUdata 1901-2016	Glob.veg. 2009	cropland	global mean Nishina et al. 2017	begin of growing season	global mean Nishina et al. 2017	global mean Zhang et al. 2017	365 days	global mean Li et al. 2000, 2012, 2016	365 days	50mm	Growing seasons	Growing seasons	All fixed as TRIPLEX-GHG v1.0	Annual N_2O emission from 1961-2010 (mgN m^{-2} yr^{-1})
Sensitivity analysis of model parameters	CRUdata 1901-2016	Glob.veg. 2009	cropland	Nishina et al. 2017	Nishina et al. 2017	Nishina et al. 2017	Zhang et al. 2017	365 days	global mean Li et al. 2000, 2012, 2016	365 days	50mm	Growing seasons	Growing seasons	Changing by 20% one at a time	Monthly N_2O emission from 1961-2010 (mgN m^{-2} yr^{-1})
Model calibration	CRUdata 1901-2016	Glob.veg. 2009	Dep. Papers (cropland /shrubland/forest)	Dep. papers	Dep. papers	Dep. papers	Dep. papers	Dep. papers	Dep. papers	365 days/ Dep. papers	Dep. papers	Dep. papers	Dep. papers	Changing most sensitive parameter only (model fitting)	Daily N_2O flux (mgN m^{-2} day^{-1}) Daily mean N_2O emission during experiment periods (mgN m^{-2} day^{-1}) Emission factor during the experiment periods (%)
Model validation	CRUdata 1901-2016	Glob.veg. 2009	Dep. Papers (cropland /shrubland/forest)	Dep. papers	Dep. papers	Dep. papers	Dep. papers	Dep. papers	Dep. papers	365 days/ Dep. papers	Dep. papers	Dep. papers	Dep. papers	Continent means of most sensitive parameter	Daily N_2O flux (mgN m^{-2} day^{-1}) Daily mean N_2O emission during experiment periods (mgN m^{-2} day^{-1}) Emission factor during the experiment periods (%)

***: different designs were set for sensitivity experiments of integrated processes as shown in Table S3 and here presented the default information only.**

Dep. Papers: means this information is depended on the corresponding papers of different sites

Table 2.3 Information on selected sites for model calibration.

ID	sites	lat	lon	experiment period	crop types	Nfer (kgha^{-1} yr^{-1})	return straw	irrigate	clay	silt	sand	pH	SOC (%)	soil C:N	mean N_2O (mgN m^{-2} d^{-1})	method	COE_{dNO3}	reference
NA-1	Woodslee, Ontario, CA	42.1	-82.6	2003-2005	corn	150	yes	no	52.5	27.5	20.0	6.4	12.5	4.7	0.47	closed chamber	0.05	(Drury et al., 2008)
NA-2	Rosemount, MN, USA	44.8	-93.1	2008-2009	corn	146	no	no	23.0	55.0	22.0	6.2	2.8	9.4	0.25	Stainless steel chamber	0.025	(Venterea et al., 2011)
NA-3	Marlboro, MD, USA	39.4	-77.3	2012-2014	tobacco; corn	134	yes	no	9.3	11.1	79.6	6.2	0.8	9.1	1.04	static flux chamber	0.03	(Chen et al., 2018)
NA-4	Fredericton, NB, CA	45.9	-66.6	2008-2011	potato	193	no	no	11.0	39.0	49.0	6.2	1.9	14.8	0.18	non-steady-state chamber	0.04	(Zebarth et al., 2012)
NA-5	Que´bec City, CA	46.8	-71.4	2002-2003	corn	150	no	no	48.2	40.6	11.2	6.9	3.4	14.6	1.68	non-steady-state chambers	0.03	(Rochette, Angers, Chantigny, Gagnon, et al., 2008)
NA-6	Fort Collins, Colorado, USA	40.7	-105.0	2002-2005	corn	134	yes	no	33.4	26.4	40.2	7.7	1.3	8.4	0.30	automatedgas chromatograph	0.03	(Mosier et al., 2006)
NA-7	Baton Rouge, LA, USA	30.4	-91.2	2013-2014	cotton	112	no	no	20.5	44.8	34.7	6.2	6.6	9.9	4.40	closed chamber	0.04	(Tian et al., 2015)

NA-8	Sacramento County, CA	38.3	-121.5	2010-2012	grape	38	yes	yes	23.0	27.0	50.0	6.4	11.2	10.7	1.15	closed chamber	0.029	(VERHOEVEN et al., 2014)
NA-9	British Columbia, CA	49.2	-121.8	2005-2007	corn	150	yes	no	14.0	59.0	27.0	6.1	8.0	13.6	1.04	static flux chamber	0.01	(Hunt et al., 2016)
AS-1	New Delhi, Inida	28.2	77.2	2008-2010	wheat	120	no	no	22.0	26.0	52.0	8.1	0.6	8.6	0.27	closed-chamber	0.02	(Jain et al., 2016)
AS-2	Gongzhuling, Jilin,China	43.5	124.8	2010-2012	maize	230	yes	no	23.0	38.0	39.0	6.2	2.6	9.0	0.72	static closed-chamber	0.025	(Guo et al., 2013)
AS-3	Yanting, Sichuan, China	31.3	105.5	2012-2015	wheat; maize	300	yes	no	19.6	50.3	30.1	8.1	1.2	8.3	0.80	static chamber	0.01	(Zhou et al., 2019)
AS-4	Nanjing, Jiangsu, China	32.1	119.0	2013-2014	vegetable	420	no	yes	54.5	30.4	15.2	5.5	1.5	8.8	3.52	static chamber	0.03	(Zhang et al., 2016)
AS-5	Yuncheng, Shanxi, China	34.9	110.7	2008-2010	cotton	70	no	yes	37.6	46.0	16.6	8.7	1.0	7.1	0.79	Automatic chamber	0.03	(Wang et al., 2013)
AS-6	Fengqiu, Henan, China	35.0	114.3	2002-2003	maize; wheat	150	yes	no	6.0	15.0	79.0	8.7	8.9	7.9	0.23	close-chamber	0.025	(Meng et al., 2005)
AS-7	Japan	36.0	140.1	2006-2007	komatsuna	120	no	no	21.0	47.0	32.0	5.9	10.7	8.4	0.10	automated chamber	0.025	(Hayakawa et al., 2009)

AS-8	Shandong, China	36.9	117.9	2008-2009	maize; wheat	600	yes	yes	17.1	66.1	16.8	8.3	1.8	7.9	1.10	static chamber	0.01	(Cui et al., 2012)
AS-9	Xianning, Hubei, China	29.9	114.3	2005-2007	peanut	120	yes	no	2.4	48.6	49.0	5.2	0.9	4.9	0.34	static closed chamber	0.01	(Lin et al., 2012)
AS-10	Khorezm Region, Uzbekistan	41.6	60.5	2005-2006	cotton; wheat	250	yes	yes	14.6	42.8	42.6	6.9	0.6	3.1	2.14	closed chamber	0.025	(Scheer et al., 2008)
EU-1	Potsdam Bornim, Germany	52.4	13.0	2003-2005	rape	150	no	no	4.0	8.5	87.5	6.0	0.9	14.0	1.08	static chamber	0.02	(Kavdir et al., 2008)
EU-2	Lusignan, France	46.4	0.1	2011-2014	corn; wheat	125	no	yes	17.6	69.2	13.2	6.4	13.5	10.6	0.34	Automatic chamber	0.04	(Senapati et al., 2016)
EU-3	St. Petersburg, Russia	59.6	30.1	2003-2005	potato	120	yes	no	25.5	56.5	18.0	5.8	1.5	8.8	1.22	closed chamber	0.02	(Buchkina et al., 2010)
EU-4	Bet Dagan, Israel	32.0	34.8	2006-2007	cotton	240	yes	yes	17.5	2.5	80.0	7.3	10.0	10.3	9.42	PVC sample chamber	0.02	(Heller et al., 2010)
EU-5	Skierniewice, Poland	52.6	20.3	2012-2013	barley	45	yes	no	7.0	5.0	87.0	6.6	11.0	11.1	0.44	closed chamber	0.01	(Sosulski et al., 2015)

EU-6	Wye Estate, UK	51.9	1.0	1999-2001	wheat; rye	200	yes	no	15.0	68.0	17.0	5.8	1.9	8.6	6.20	closed chamber	0.05	(Baggs et al., 2003)
EU-7	Stuttgart, Germany	48.7	9.2	2008-2010	vegetable	401	no	no	30.0	68.0	2.0	5.5	1.8	8.0	1.85	PVC-chamber	0.025	(Pfab et al., 2012)
EU-8	Naples, Italy	40.6	15.0	2007-2008	maize	130	no	no	32.9	20.1	47.0	7.5	0.8	8.4	0.10	automated closed static chambers	0.04	(Forte et al., 2017)
EU-9	Madrid, Spain	40.5	-3.3	2009-2012	maize barley	250	yes	yes	28.0	17.0	55.0	7.9	0.8	8.1	0.77	closed chamber	0.04	(Abalos et al., 2013; Sanz-Cobena et al., 2012)
AU-1	Cunderdin, Australia	-31.6	117.2	2005-2007	wheat	100;75	yes	no	18.6	4.4	77.0	6.0	0.4	10.0	0.032	automated gas chambers	0.015	(Li et al., 2012)
AU-2	Mackay, Queensland, Australia	-21.1	149.0	2006–2007	sugarcane	150	no	no	33.0	28.5	38.5	4.7	1.7	9.4	1.61	Automatic chambers	0.028	(Denmead et al., 2010)
AU-3	Brisbane, Australia	-26.0	152.0	2007-2009	lychee orchard	256	yes	no	26.0	37.0	37.0	6.0	2.7	10.1	1.22	automatic chambers	0.025	(Rowlings et al., 2013)

AU-4	Queensland, Australia	-27.5	151.8	2009-2011	cotton; wheat	200	no	yes	76.0	16.0	7.0	7.2	1.6	11.9	0.46	automated chamber	0.023	(Scheer et al., 2012, 2013; Scheer et al., 2016)
AU-5	Queensland, Australia	-28.2	152.1	2006-2009	wheat	90	yes	no	65.0	24.0	11.0	6.9	2.0	9.7	0.83	automatic gas sampling chambers	0.01	(Wang et al., 2011)
AU-6	Wagga Wagga, New South Wales, Australia	-35.4	147.5	1993-1994	ryegrass	200	no	no	15.5	10.0	74.5	5.5	8.1	9.8	0.087	automatic static chamber	0.01	(Galbally et al., 2010)
AF-1	Kaptumo, Kenya	0.12	35.5	2013-2014	vegetable	110	yes	no	27.8	9.8	62.3	6.0	4.1	12.4	0.25	static chamber	0.01	(Rosenstock et al., 2016)
AF-2	Kenya	-0.31	35.4	2015-2016	tea	150	no	no	59.0	21.0	20.0	3.9	4.0	12.4	0.34	static chamber method	0.012	(Wanyama et al., 2018)
SA-1	Ariquemes, Rondnia State, Brazil	-10.5	-52.5	2001-2002	b.brizantha	42	yes	no	23.5	5.5	71.0	5.3	6.0	9.6	0.89	recirculating chamber	0.05	(Passianoto et al., 2003)
SA-2	Santa Maria, Brazil	-29.7	-53.7	2010-2011	maize and wheat	125	no	yes	19.2	36.5	44.3	5.9	5.0	11.1	1.66	non-steady-state chambers	0.049	(Aita et al., 2015)

SA-3	Campinas, Brazil	-22.9	-47.1	2011-2013	sugarcane	120	yes	no	41.0	17.5	41.5	5.6	5.8	10.8	0.68	PVC static chambers	0.035	(Soares et al., 2015)

Table 2.4 Simulation experiment design for global simulations.

	Input variables					
	Climate	LUC	N deposition	N fertilizer	Manure	Return straw
S1	1901-2016	1901-2016	1860-2016	1961-2016	1860-2016	Yes
S2	1901-2016	1901-2016	1860-2016	1961(1901) *	1860-2016	Yes
S3	1901-2016	1901-2016	1860-2016	1961(1901) *	1901	Yes

*: N fertilizer data set starts from 1961. N fertilizer was either set at the level of 1961 or maintained at the level of 1901 throughout the period to achieve consistent results.

2.6 Results

2.6.1 Sensitivity experiment of integrated processes and sensitivity analysis of the model parameters

In general, the integrated agricultural and natural processes of the TRIPLEX-GHG model v2.0 significantly changed the emission pattern of N_2O comparing to that of previous version. However, a large divergence was found for the responses of model output to different processes. The annual N_2O emissions from selected 15 sites for sensitivity experiment produced by original model (v1.0) ranged from 3.64 to 348.46 mgN m^{-2} yr^{-1} with a mean of 99.53 (±2.76se) mgN m^{-2} yr^{-1} during 1961-2010 (Figure 2.2a). The difference between v1.0 and v2.0 simulations (Figure 2.2b) indicated that the improved description of plant uptake processes altered the model performance by reducing 3.50% of the mean annual N_2O emission and the RES value was 0.06 meaning that the integration of plant uptake module resulted in an overall 6% changes to estimated N_2O fluxes. Similar effects of harvest and returned straw were found during sensitivity experiment. The average annual N_2O emission rates were reduced by 28.48% and 40% across 15 sites for harvest and returned straw compared with original model outputs respectively (Figure 2.2c-d). Nevertheless, the impact range of returned straw was smaller than that of harvest practice as suggested by lower RES value. The model output showed consistent positive responses to application of chemical fertilizer (FN) and manure (MN) by increasing 87.66% and 24.63% of the annual N_2O emission respectively (Figure 2.2e-f). Moreover, the median of the absolute application effects of chemical fertilizer increased with growing treatment period from 10.68 mgN m^{-2} yr^{-1} in 1962 to 54.35 mgN m^{-2} yr^{-1} in 2010 whereas no tendency was detected for manure application. The impact of the timing of fertilization was minor comparing with the amount and properties of fertilizers (Figure 2.S1). Meanwhile, Figure 2.2g and 2.2h showed that the range of the annual N_2O emission response to irrigation and tillage practices were less evident in terms of the RES as 0.08 and 0.16 respectively. The absolute effect of irrigation ranged from -10.38 to 10.33 mg N m^{-2} yr^{-1} and that of tillage was larger ranging between -14.82 to 18.27 mg N m^{-2} yr^{-1}. However, the absolute and relative effects of irrigation and tillage showed increased variation in combination with fertilizer applications (Figure 2.S1).

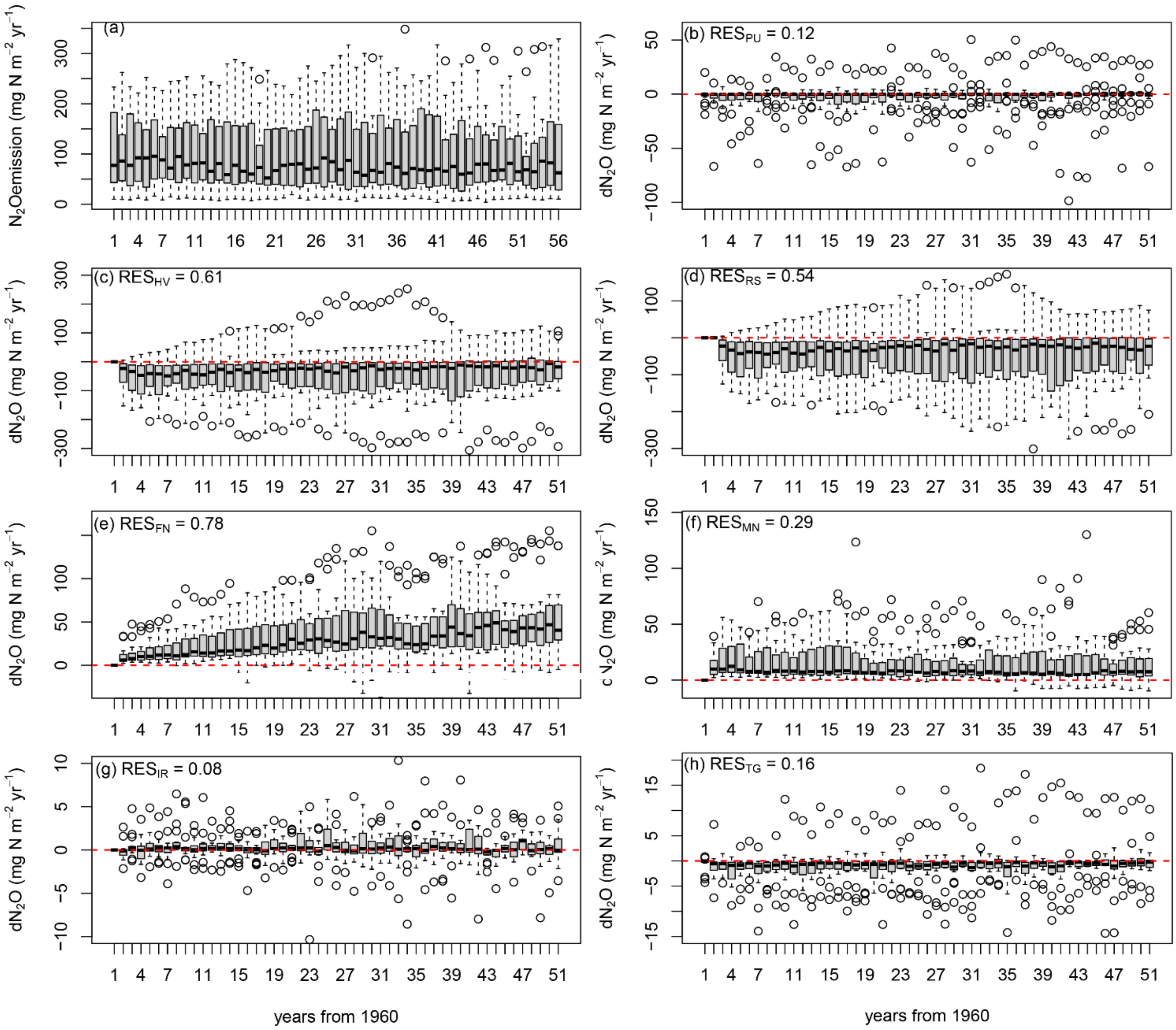

Figure 2.2 Sensitivity experiment of the newly integrated processes as indicated by the difference of annual N_2O emission between the improved model with different practices and original model . The outliers are shown as open dots. The dashed red line means the δ N_2O = 0.0. RES indicates the relative effect size of the processes (Eq. 16). (a. original model outputs; b. absolute effect of integrated PU, Plant Uptake; c. absolute effect of integrated HV, Harvest; d. absolute effect of RS, Returned Straw; e. absolute effect of integrated FN, chemical Fertilizer N application; f. absolute effect of MN, Manure N application; g. absolute effect of IR, Irrigation event; h. absolute effect of TG, Tillage event).

Large variation was observed for sensitivity analysis of model parameters. The mean sensitivity index (*SI*) varied from -0.53 (EFF_{NO2}) to 1.37 (COE_{dNO3}) for the selected 13 parameters (Figure 2.3). All of the parameters had a nonunique effect on the N_2O emissions of the different sites. COE_{dNO3}, COE_{NR}, MUE_{NO3}, M_{NO3}, EFF_{N2O}, COE_{dNO2}, and COE_{dNO} mostly had positive effects, while the remaining parameters either had negative effects (e.g., MUE_{N2O} and EFF_{NO2}) or had no evident impact (e.g., AMAX and COE_{NO3UP}) on the N_2O fluxes. The coefficient of the NO_3^- consumption rate (COE_{dNO3}) was the most sensitive parameter in the current TRIPLEX-GHG model. The *SI* ranged from -0.61 to 5.39 (with a mean of 1.37) for the current model input information. We also noticed that the *SIs* of the selected parameters were not consistent with the different input information, especially for the variations in the amount of N fertilizer applied. The COE_{dNO3} slightly increased initially and then decreased as the N dose increased; and as the most sensitive parameter, it retained a large *SI* value (Figure 2.S2).

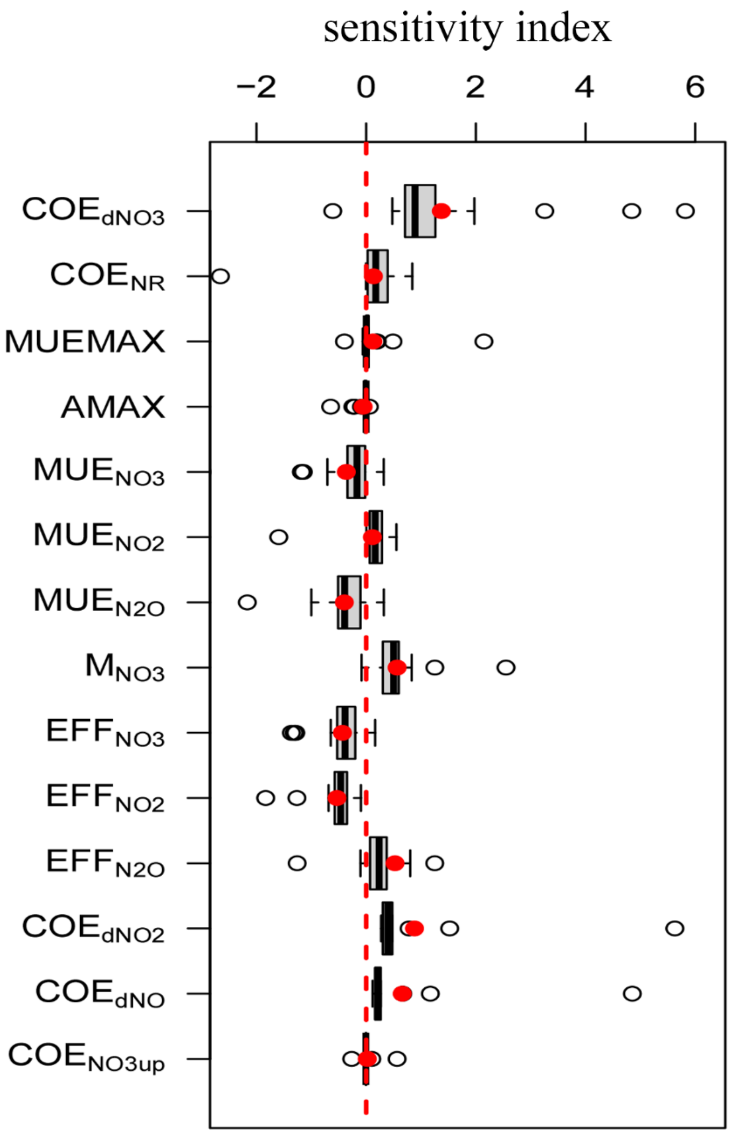

Figure 2.3 Sensitivity analysis of the different parameters. The closed red dots show the mean sensitivity index value of the parameters. The outliers are shown as open dots.

Overall, to simplify the parameter fitting processes and to evaluate the model's performance, we selected the most sensitive parameter of the model, COE_{dNO3}, as the fitting parameter for model calibration, while we set the other parameters to their original constant values as the default during model calibration (Table 2.1).

2.6.2 Model calibration

The long-term daily flux data was collected from the selected cropland sites for model calibration, including the major crop species such as corn, wheat, barley, and tomatoes (Table 2.3). These sites were categorized into six main regions according to their geographical distribution, including North America (NA), Asia (AS), Europe (EU), Australia (AU), South America (SA), and Africa (AF). Generally speaking, the model's performance was reasonably good in terms of the comparison of the site observations with the modeled results.

For the sites located in the great lakes region, North Ameirca (NA-1 and NA-2), the modeled seasonal patterns of the N_2O emission were generally consistent with the measured data (Figs. 2.4a–b), but the estimated pulses had longer durations than the observations (the model could not capture the detailed variations in the detected N_2O fluxes), which resulted in low agreement indices (D=0.65, D=0.56 for NA-1 and NA-2, respectively). For the studies carried out in the eastern Atlantic coastal region, the annual variation in the field data from site NA-3 was reproduced well by the model (Figure 2.4c), except for some underestimated peak values, which slightly reduced the level of the model evaluation indices (D=0.69, $RMSE$ = 3.6, R = 0.57). Furthermore, the modeled simulation results were well matched for the scattered detected values of sites NA-4 and NA-5 (Figs. 2.4d–e), with model agreement indices of 0.81. The model's results were also strongly correlated with the other collected observation data in the central (NA-6), southern (NA-7) USA, and western coastal regions of the continent (NA-8, NA-9). The model performed well for the long-term fertilized corn sites in Colorado (Figure 2.4f; D = 0.84, $RMSE$ = 0.90, R = 0.73). Nevertheless, the general trends of the model's results were consistent with the observation data at sites NA-7, NA-8 and NA-9 while failures to capture the timing (Figure 2.4g) and length of the intensive emission period (Figure 2.4h) led to relatively lower evaluation indices (D = 0.59, 0.61 and 0.75, respectively).

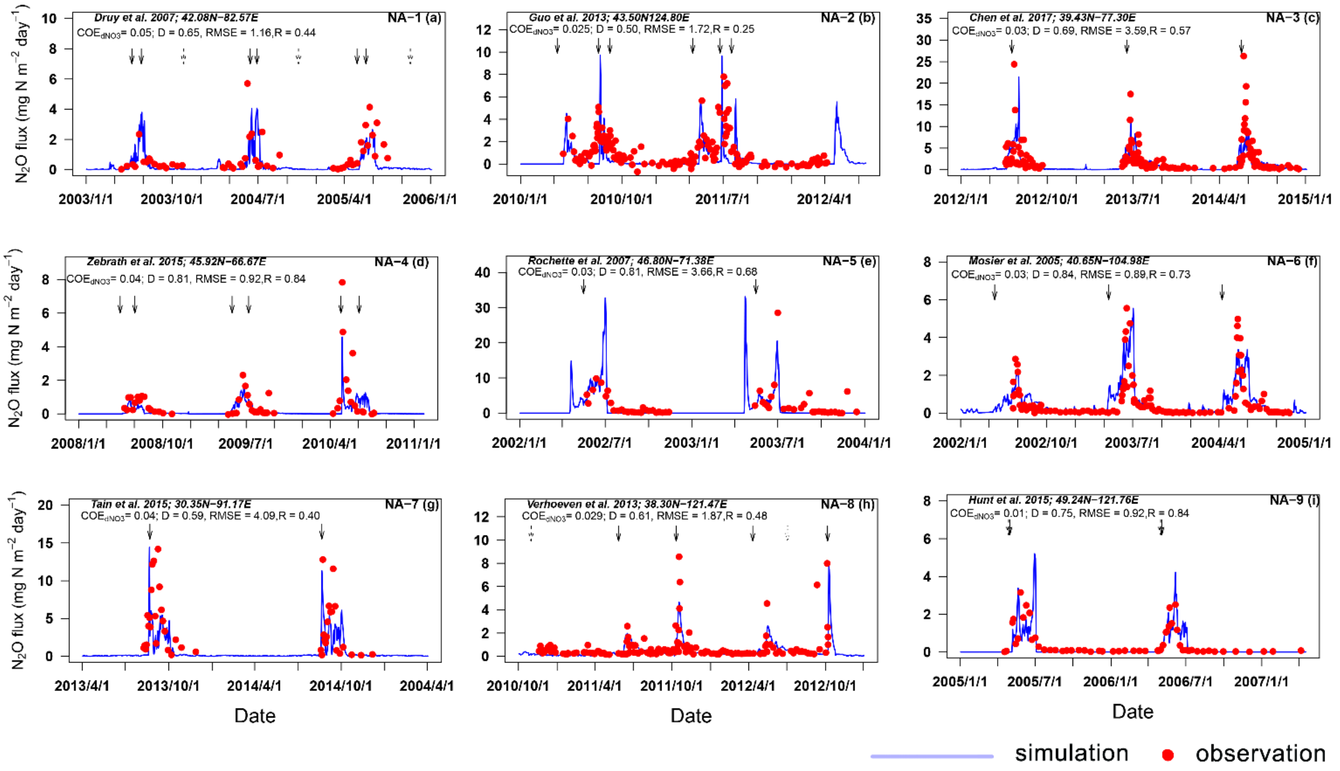

Figure 2.4 Comparison of the modeled and observed N_2O emissions during calibration for cropland sites located in North America. Site-specific COE_{dNO3} values were used for model calibration to obtain the best estimations. Solid arrows indicate the timing of fertilizer (chemical or manure) applications, dashed arrows indicate tillage while dotted arrows indicate irrigation event respectively.

In general, the model captured the main variations in the observations and agreed well with all of the daily observations for the ten upland agricultural sites located in Asia, except for conventional cropland sites AS-2. As reported by Guo et al. (2013), certain points of observation were being recorded as negative values without apparent regularity in the time series, while the model was less robust in terms of capturing the occurrence of N_2O uptake, resulting in a low index of agreement (Figure 2.5b, *D* = 0.50). In addition, the simulation exhibited reasonable N_2O flux variation patterns, especially the occurrence of emission pulses induced by fertilization, comparable to those described by Zhou et al. (2019) (Figure 2.5c) and Zhang et al. (2016) (Figure 2.5d), while the inaccurately estimated peak values suppressed the evaluation of the model's performance (AS-3, *D* = 0.67; AS-4, *D* = 0.64). The model results for sites AS-5, AS-6, AS-7, and AS-8 showed that simulated N_2O fluxes agreed well with the observed fluxes under different agricultural practices, with model agreement indices of 0.86, 0.81, 0.78, and 0.76, respectively (Figs. 2.5e–h). Scattered observation points in a peanut site located in central-subtropical China were also simulated by our model and the result showed a similar general pattern of N_2O flux with acceptable model performance indices (Figure 2.5i; *D* = 0.65, *R* = 0.49, *RMSE* = 0.31). The long-term wheat cultivation site in Uzbekistan was characterized by extremely high emission rates (>50 mg N m^{-2} day^{-1}) and the simulated N_2O emission rate matched the observations well, except for one overestimated emission pulse in 2005/7 (Figure 2.5j).

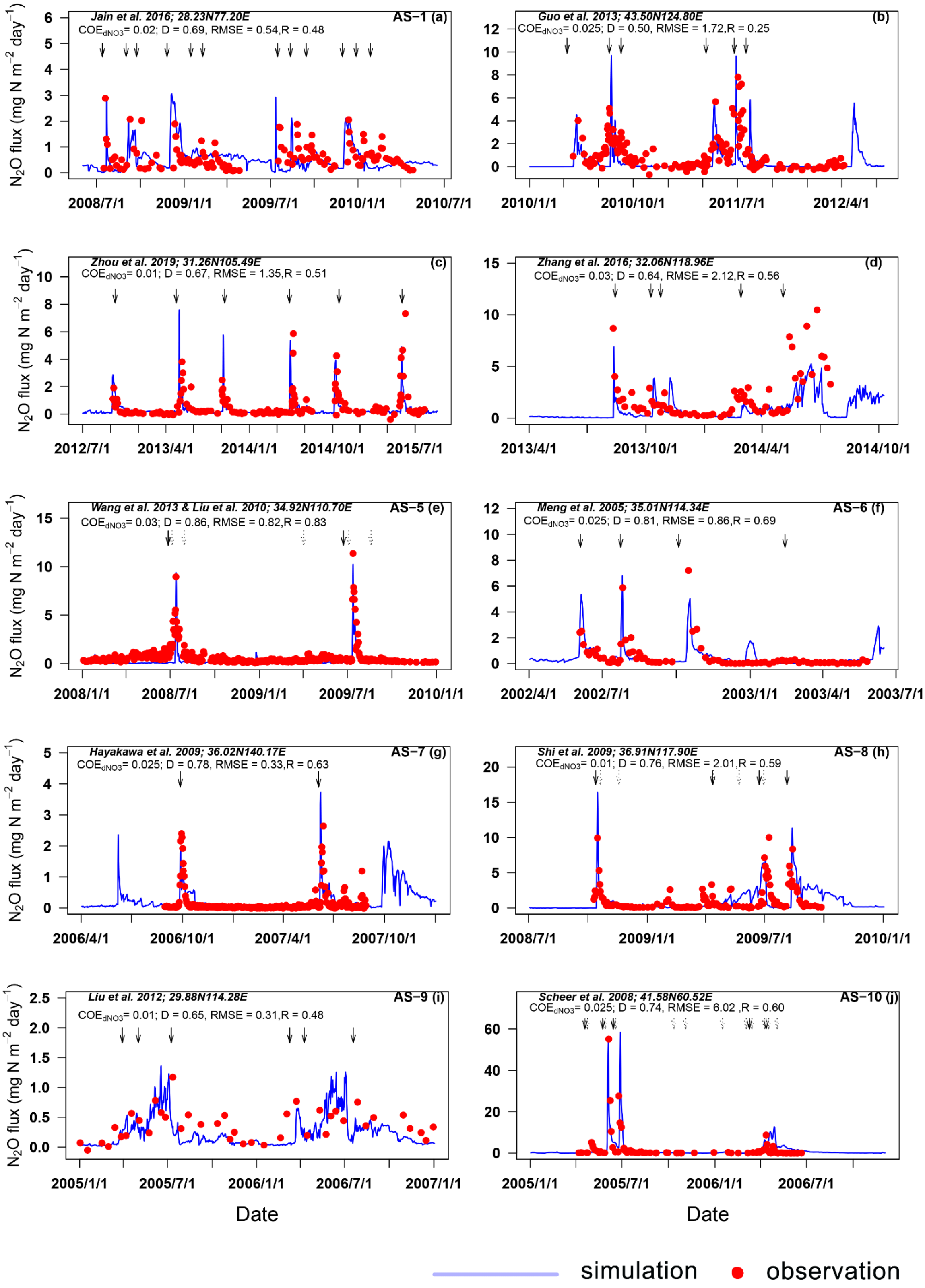

Figure 2.5 Comparison of the modeled and observed N_2O emissions during calibration for cropland sites located in Aisa. Site-specific COE_{dNO3} values were used for model calibration to obtain the best estimations. Solid arrows indicate the timing of fertilizer (chemical or manure) applications, dashed arrows indicate tillage while dotted arrows indicate irrigation event respectively.

The simulated trends and magnitudes of N_2O were generally consistent with the measured data for most of the calibrated sites in Europe. Based on the studies of Kavdir et al. (2008) and Senapati et al. (2016), the frequent failure of capturing the major emission pulses, such as the one induced by fertilizer input in 2003/1 for EU-1 (Figure 2.6a) and the one that occurred in 2013/6 for EU-2 (Figure 2.6b), accounted for the low agreement indices. Moreover, the low evaluation indices of site EU-3 (D = 0.52) are attributed to the estimation gap as the underestimation of the background emissions (Figure 2.6c). The study carried out by Hall et al. (2010) reported extremely high N_2O emission rates due to the application of large amounts of manure. The model had a low agreement index because it underestimated the major peaks and the duration (Figure 2.6d; D = 0.61). The model simulation also revealed good agreement with the scatter measured N_2O emission data for the site observations provided by Sosulski et al. (2015) and Baggs et al. (2003), the modeled emission rates the points (Figs. 2.6e–f). As for sites EU-7, EU-8 and EU-9, the modeled daily N_2O emission rates matched the general trends of the N_2O emissions in response to fertilization and irrigation practices reasonably well. However, the modeled results still mis-captured the minor emission pulses in 2009/1 at site EU-7 (Figure 2.6f; D = 0.77, $RMSE$ = 1.46, R = 0.66) and in 2007/8 at site EU-8 (Figure 2.6g; D = 0.87, $RMSE$ = 0.23, R = 0.75).

Only one rainfed continuous wheat site in western Australia, AU-1, was used in the model calibration. The low model evaluation indices (D = 0.47, $RMSE$ = 0.12, R = 0.25) was probably associated with the failure to capture the emission peaks in 2006/1, 2007/4, and 2010/3 (Figure 2.7a). For the other calibration sites located in eastern coastal regions, the general seasonal patterns of the simulated N_2O emission were consistent with the observations. The model performed reasonably well for manure dominated site AU-2, and the underestimated peak value was responsible for the slight jeopardizing of agreement index (Figure 2.7b; D = 0.88). Notably, a lychee (*Litchi chinensis*) orchard site with a high sampling frequency was included, so the PFT was considered to be subtropical forest for this site, and the model performed well (Figure 2.7c; D = 0.80) even though there was an obvious mis-capture of the emission peak in 2008/6. Sugarcane was planted at site AU-5, the PFT was set as shrub during the calibration because the C properties of sugarcane differ significantly from those of grain crops (e.g. wheat). The modeled results of the sugarcane-based crop systems agreed well with the measured data (Figure 2.7e; D = 0.73, $RMSE$ = 0.65, R = 0.55).

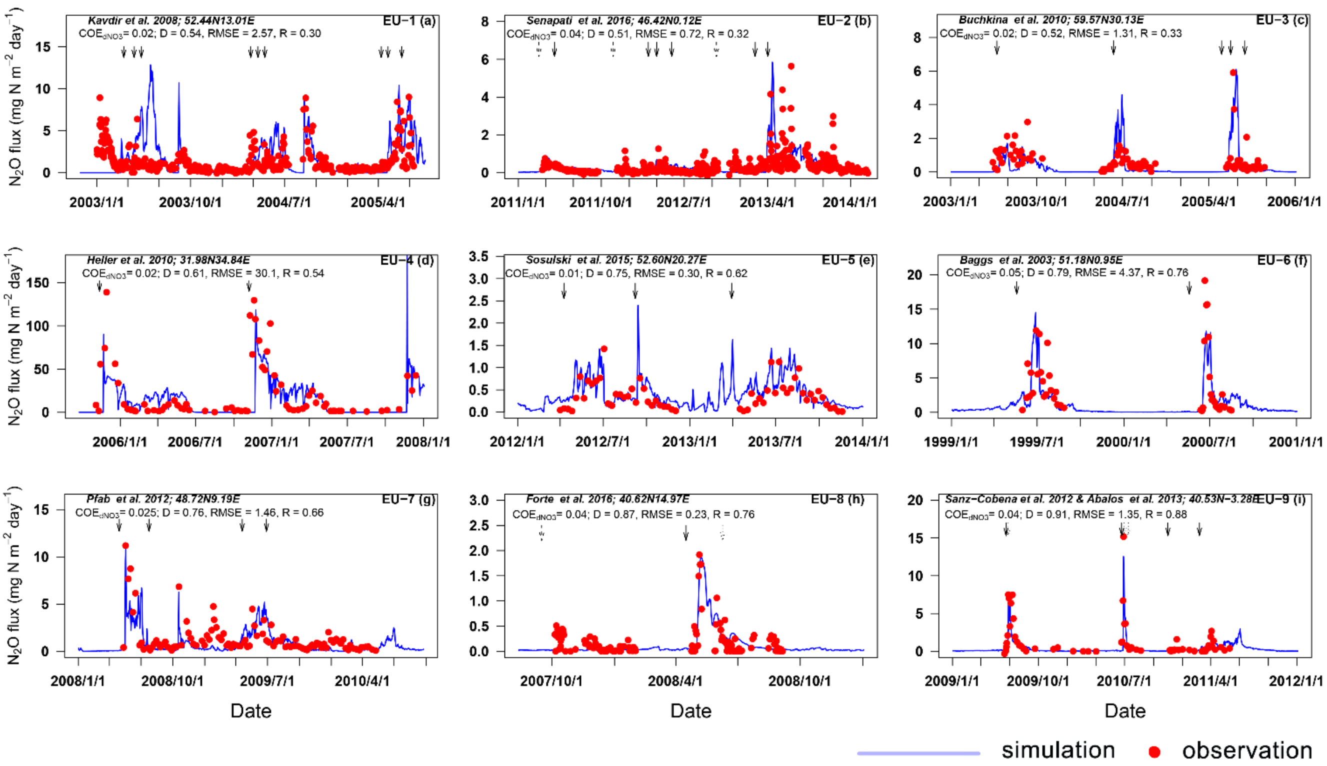

Figure 2.6 Comparison of the modeled and observed N_2O emissions during calibration for cropland sites located in Europe. Site-specific COE_{dNO3} values were used for model calibration to obtain the best estimations. Solid arrows indicate the timing of fertilizer (chemical or manure) applications, dashed arrows indicate tillage while dotted arrows indicate irrigation event respectively.

Unfortunately, there are insufficient observations of cropland N_2O emissions conducted in the agriculturally dominated regions of South America and Africa (Figure 2.8 and Table 2.3). Compared with the results of the two sites with short experimental periods in Africa (Figs. 2.8a–b), the simulated seasonal N_2O variation agreed reasonably well with the one year of observations as is indicated by model performance indices (AF-1: D = 0.92, $RMSE$ = 0.22, R = 0.94; and AF-2: D = 0.87, $RMSE$ = 0.65, R = 0.93).

In South America, both cereal and economic crop sites were included. The model results were in good agreement with the measured N_2O emission rates reported by Passianoto et al. (2003) even though the number of points were limited (Figure 2.8c; D = 0.93, $RMSE$ = 0.70, R = 0.90). Moreover, the modeled results also illustrated that the N_2O variation patterns for the model simulations and the observations are good agreement for the maize-wheat site SA-2, but the model mis-captured minor pulses, slightly reducing the evaluation index (Figure 2.8d; D = 0.81, $RMSE$ = 4.19, R = 0.67). For the sugarcane site SA-3, the vegetation type was also set as shrubland and the simulated results were generally well correlated with the measured N_2O fluxes, which are highly regulated by the agricultural practices; however, the model failed to capture the consistent relatively high-level emission rates after fertilizer application (Figure 2.8e; D = 0.74, $RMSE$ = 1.25, R = 0.65).

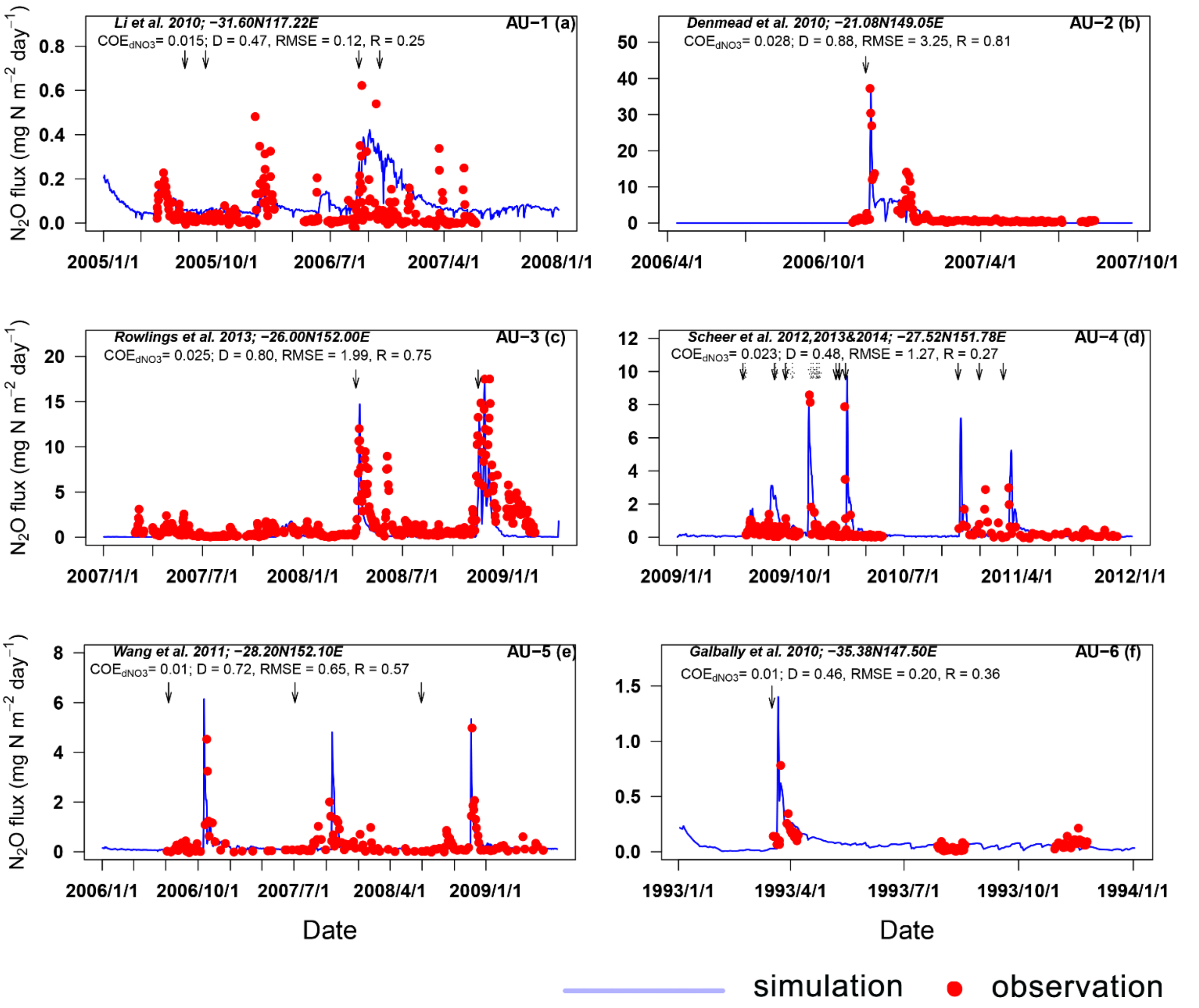

Figure 2.7 Comparison of the modeled and observed N_2O emissions during calibration for cropland sites located in Australia. Site-specific COE_{dNO3} values were used for model calibration to obtain the best estimations. Solid arrows indicate the timing of fertilizer (chemical or manure) applications, dashed arrows indicate tillage while dotted arrows indicate irrigation event respectively.

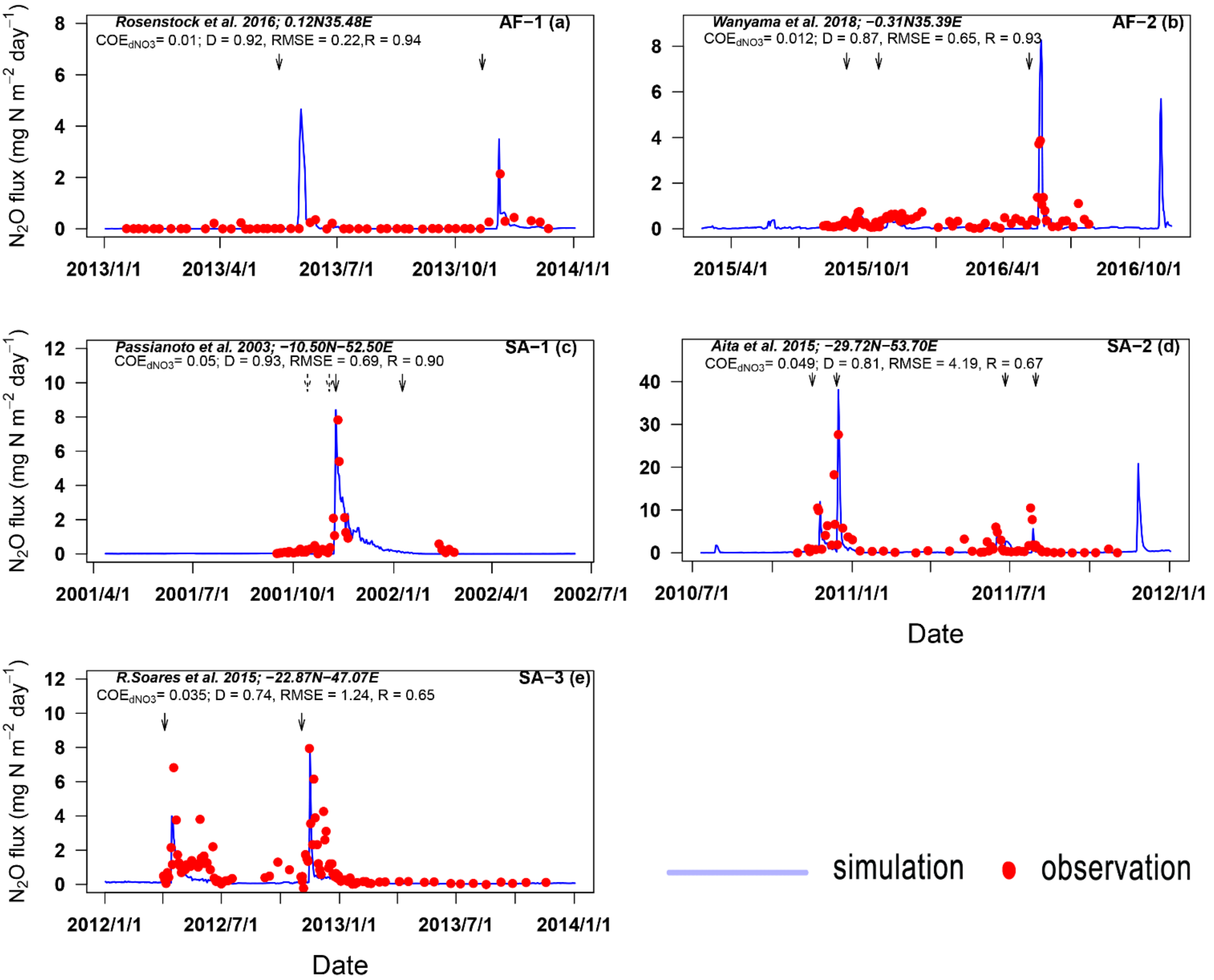

Figure 2.8 Comparison of the modeled and observed N_2O emissions during calibration for cropland sites located in Africa and South America. Site-specific COE_{dNO3} values were used for model calibration to obtain the best estimations. Solid arrows indicate the timing of fertilizer (chemical or manure) applications, dashed arrows indicate tillage while dotted arrows indicate irrigation event respectively.

2.6.3 Model accuracy in calibration in terms of emission rates and emission factors

In summary, according to the site-level calibration results, the trends and magnitudes of the simulated daily N_2O flux were generally consistent with the measured field data. As the values of COE_{dNO3} were significantly different for the six continents (p < 0.01 Table 2.S5, i.e., North America, Asia, Europe, Australia, Africa and South America), the continent mean values of the calibrated parameter COE_{dNO3}, were used for simulations to compare the estimated daily mean emission rates against the measured data of 39 calibration sites to further confirm the effectiveness of the calibrated parameters and model. The model outputs performed well as shown in Figure 2.9a, resulting in the coefficient of determination (R^2) of 0.87 with the slope of regression close to 1 (i.e., 1.07). The emission factor (EF), an evaluation of the percentage of input N emitted as N_2O, is an important indicator representing the sensitivity of the native environment to external N input. The estimated and reported mean EF were 1.19% and 1.07%, respectively. However, the regression result of estimation of EFs were less constrained compared with that of emission rates. Figure 2.9b showed that the TRIPLEX-GHG model v2.0 are able to explain 70% of the variances of the emission factors from the 35 calibrated sites with the continent mean parameters. The mean squared errors (MSEs) of simulated EFs were 0.006%, indicating a relatively low bias in the models which was probably due to a few of the simulated EFs that were found to differ significantly from observations.

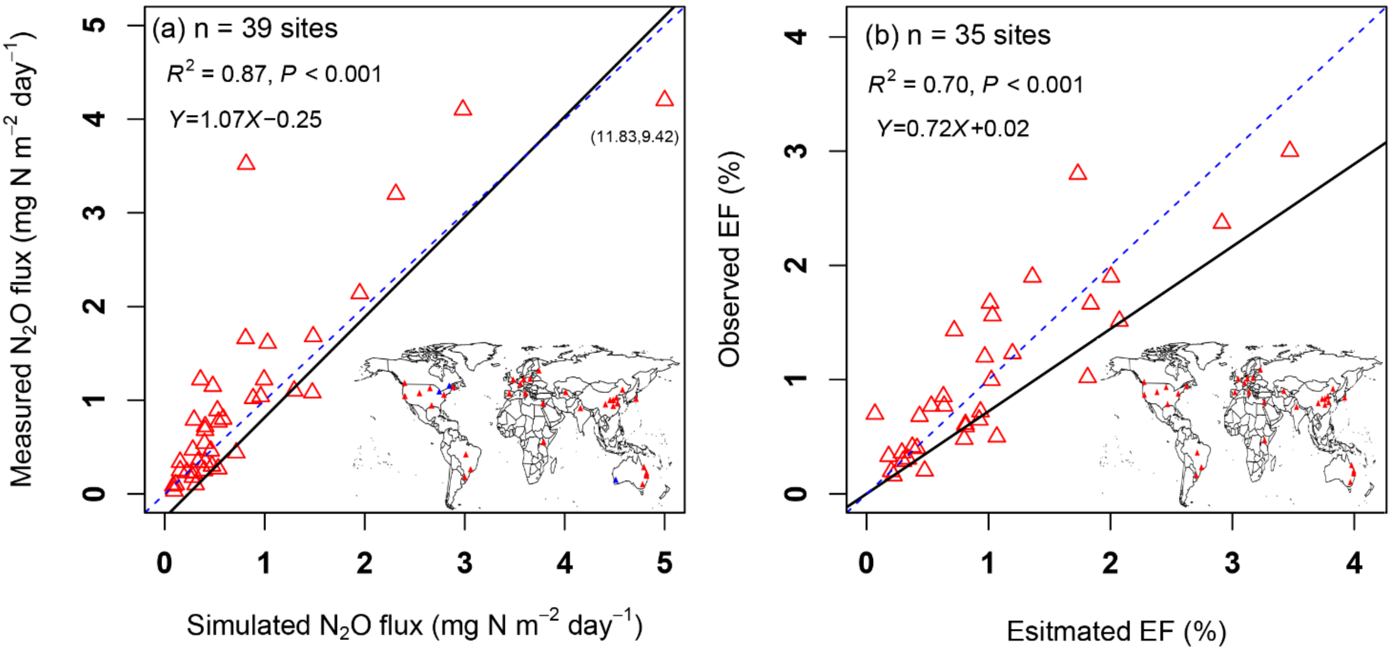

Figure 2.9. Calibration of the mean emission rates (a) and the mean emission factors (EFs) (b) for global cropland sites (39 sites) of all site years (open triangles). The value of calibrated parameter COE_{dNO3} was set as continent mean values. Closed red triangles on maps represent the location of calibrated sites while the closed blue triangles are the 4 sites that did not provide EFs information. The extremely large result (11.83, 9.42) of Figure2.9 a was moved to current position to ensure the readability.

2.6.4 Model validation

With the continent mean values of the fitted parameter, COE_{dNO3}, we first compared the continuously measured daily N_2O emissions with modeled flux results from 15 selected field experiments as shown in Figure 2.10. General trends of observed N_2O emissions from selected sites were reasonably produced by the improved model. The well-simulated timing and duration of occurred emission pulses (e.g., Figure 2.10 h, i, k, l), as well as the pattern of background fluxes (e.g., Figure 2.10 e, n) strongly illustrated the reliability of the model estimations. For example, the model captured the main variations of observations and agreed well with the mean emission rates of all observations from an intensively managed vegetable field in Northwest China (Figure 2.10h, D = 0.77) and a maize site in Tanzania (Figure 2.10o, D = 0.70). However, discrepancies between modeled and observed daily flux data still exist, including mismatched major emission pulses (e.g., Figure 2.10 h) and mis-captured frequent minor fluctuations (e.g., Figure 2.10 b, m) of N_2O fluxes. In constant with the calibration results, model showed strong sensitivity to fertilizer applications and tended to overestimate the response rate of N_2O emission to N input as indicated by the unexpected generated emission pulses (Figure 2.10 a, i, j). In the meantime, underestimated emission pulses were also observed for the validated sites such as Figure 10 d, l, n, which also accounted for the reduced model evaluation indices. By comparing with calibration results, the uncertainties of the up-scaled parameter COE_{dNO3} was probably responsible for the jeopardized the overall model performance for estimating the daily N_2O fluxes (mean of the D-value = 0.55 and 0.71 for 15 validation sites and 39 calibration sites, respectively) but, in terms of the daily mean N_2O fluxes during experiment periods, model generated comparable results to those of observations for the 15 selected sites (Table 2.S2).

Globally, we further validated the improved model by comparing the simulated and measured daily mean of the N_2O emissions for all of the 68 validated sites, and the results were presented in Figure 2.11a, Figure 2.S3 and Table 2.S2. During the validation, the simulated daily mean emission rates during the experimental periods ranged from 0.048 to 5.21 mg N m^{-2} day^{-1}, and most of the values were less than 1 mg N m^{-2} day^{-1}. The regression result was close to the 1:1 line, indicating that the modeled results were quite consistent with the observed N_2O emissions (R^2 = 0.86, slope = 0.82, n = 68, p < 0.001). When we separately investigated the model performances for six different continents, high correlation results were found indicating the universality of the model and parameter settings across the globe (Figure 2.S3). Meanwhile, the model performance for estimating EFs during experiment periods were also tested for validation sites at global scale (Figure 2.11b). We found 67% of the estimated EFs produced by the TRIPLEX-GHG v2.0 were smaller than IPCC recommended (i.e., 1%) and the mean value of which was 0.76 (±0.62) % as comparable to that of observed result (i.e., 0.68 %). The regression analysis presented a reasonable consistency between modeled with observed EFs that our improved model can provide close estimations of the reported EFs (slope = 0.83) and capture the 66% variance of the EFs across all site years at the globe. Although less agreements of the modeled and measured N_2O emissions and EFs were found for the model validation compared with those of calibration results, the model validation results still further confirmed that improved TRIPLEX-GHG model v2.0 was capable of simulating the impacts of both climate and agricultural practices on N_2O emissions across global cropland ecosystems.

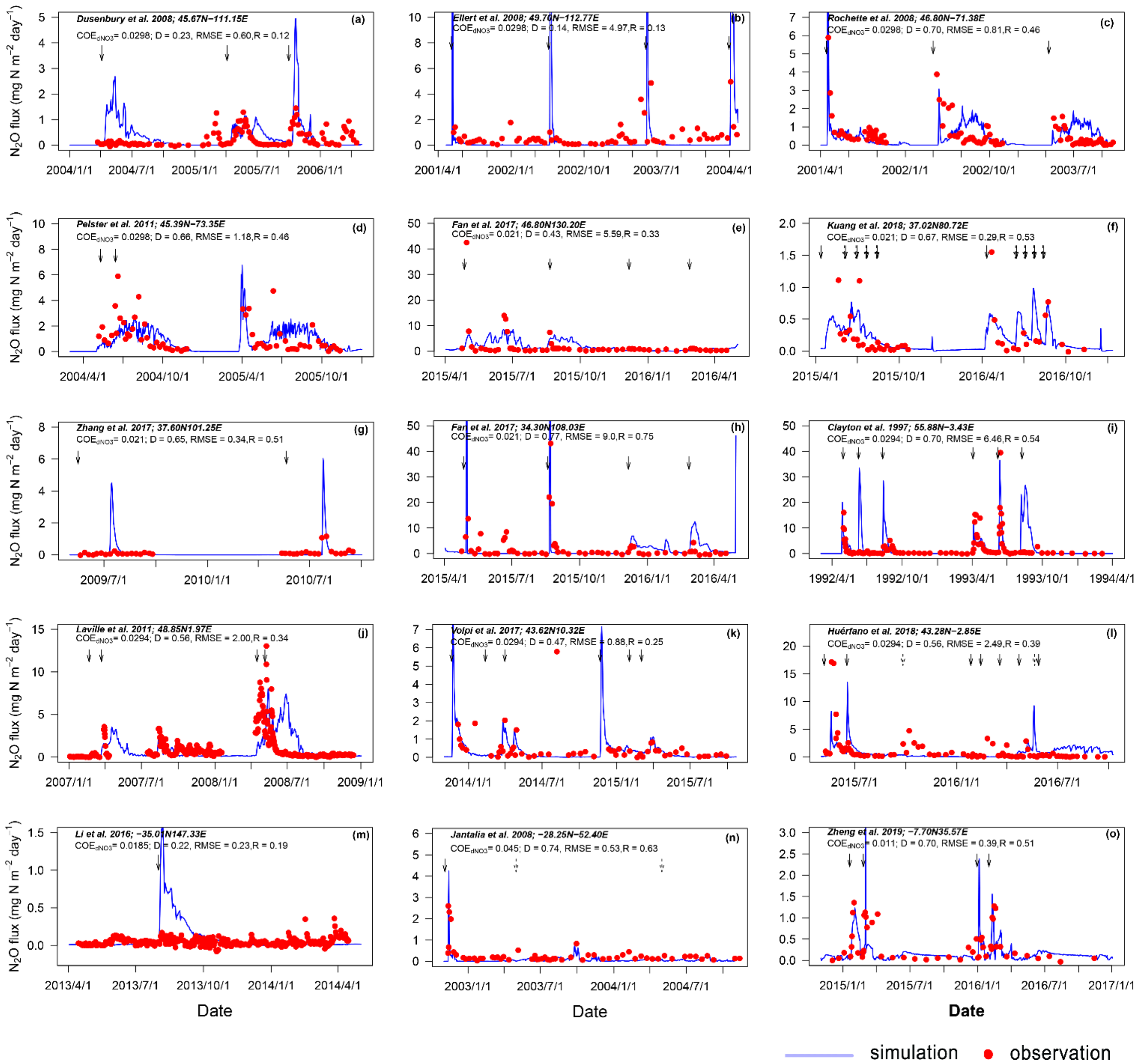

Figure 2.10 Comparison of the modeled and observed N_2O emissions for the 15 selected validation sites located in different continents. Model was driven by site-specific environment and management information. The continent mean values of COE_{dNO3} were used for validation. Solid arrows indicate the timing of fertilizer (chemical or manure) applications, dashed arrows indicate tillage while dotted arrows indicate irrigation event respectively.

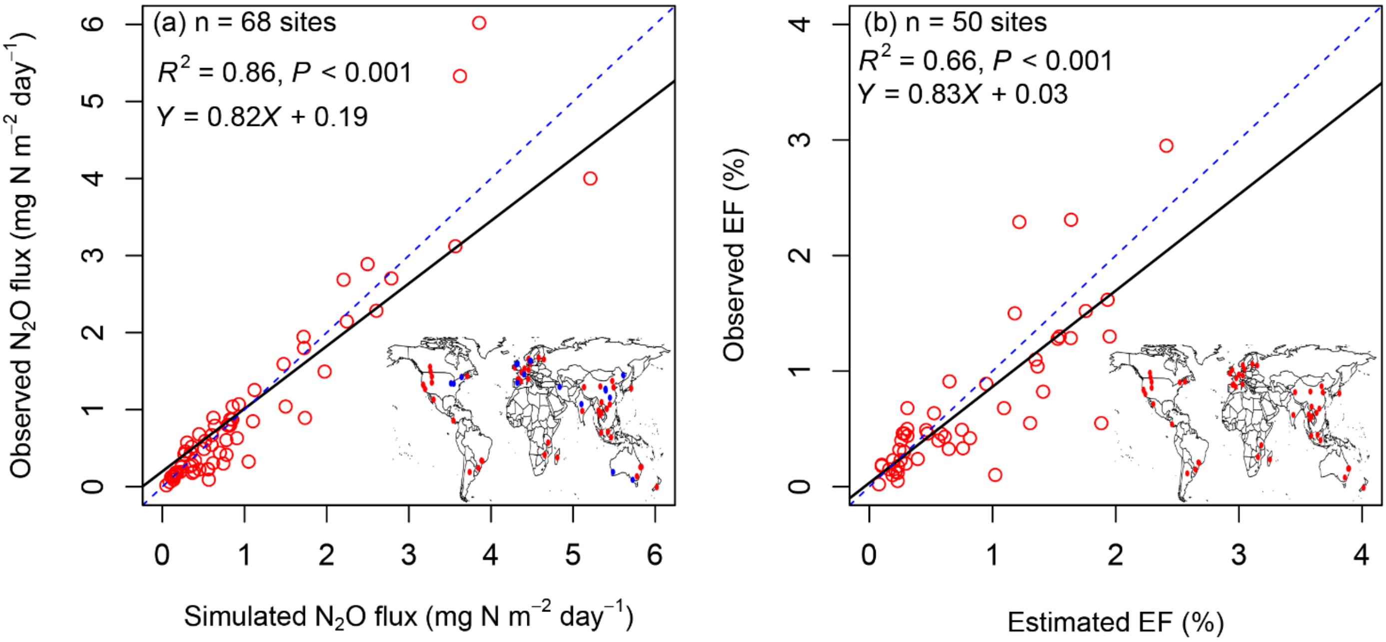

Figure 2.11 Validation of the daily mean emission rates (a) and the emission factors (EFs) (b) for global cropland sites (68 sites) during experiment periods (open circles). The value of COE_{dNO3} was set as continent mean values for validation. Closed red dots on maps represent the location of validated sites while the closed blue dots are the sites that did not provide EFs information.

2.6.5 Temporal and spatial variations of modelled cropland N_2O emissions

In general, modelled results suggested that, from 1901 to 2016, annual N_2O emission from global croplands increased from 0.13 to 2.96 Tg N yr^{-1} with a significant increasing trend ($p < 0.001$, Figure 2.12). In particular, the growth of global cropland N_2O emission since the 1960s is 8.16 times larger than the increase during 1901 to 1960. However, after a rapid increase between 1960 – 1990, a slight decreasing trend was found after the 1990s for total N_2O emission from global croplands based on SNHT for detecting the change points. The largest emission was in 1994 at 3.86 Tg N yr^{-1}. Area-weighted N_2O emission rates exhibited similar annual variation patterns with total global emissions.

Regionally, Europe, North America and Asia are the most important contributors to historical global cropland N_2O emissions (1901—2016), accounting for 41.4%, 26.7%, and 21.4%, respectively (Figure 2.12). While croplands in south America, Oceania, and Africa together are responsible for ~10% of total emission during study period. Since the 1960s, Europe and the Great Lakes region in North America are consistent hotspot for cropland N_2O emission (> 3 kgN ha^{-1} yr^{-1}, Figure 2.13). Therefore, with large upland cropland area in these regions, they became the major cropland N_2O emission sources historically.

Meanwhile, the northern China Plain and northeast China showed rapid increases in cropland N_2O fluxes after the 1980s. Similarly, south Australia and south America presented large N_2O emission rates from cropland since 21st century and the relatively limited cropland area resulted in a smaller contribution to global cumulative cropland N_2O emission.

Furthermore, I investigated changes in cropland N_2O fluxes for different regions. By comparing the pattern of N_2O emission from global croplands in 1990 against those of 1960 and 2015, reductions of cropland N_2O emission from Europe, USA, and part of India are mainly responsible for the minor decreases in global N_2O emission from cropland since the 1990s (Figure 2.14b).

By comparing the difference between simulated results of designed scenarios, we quantified the contribution of N fertilizer and manure application to global cropland N_2O emissions. Difference between S1 and S2 suggested the contribution of N fertilizer is the primary source for the increasing N_2O emissions from global croplands during study period. The effect of N fertilizer showed a similar pattern with total emission, after peaked in the 1990s, mean contribution of N fertilizer is 1.44 (± 0.19) Tg N yr^{-1} since 2000 and such positive effect is consistent across the globe (Figure 2.15a and c). Meanwhile, manure present stimulating effect on cropland N_2O emissions globally and the effect constantly increased during 1901—2016. However, divergent responses of N_2O flux to manure were found in different regions. Modelled results suggested manure application reduce N_2O flux from croplands in the Great Lake region, USA, and eastern Europe (Figure 2.15b).

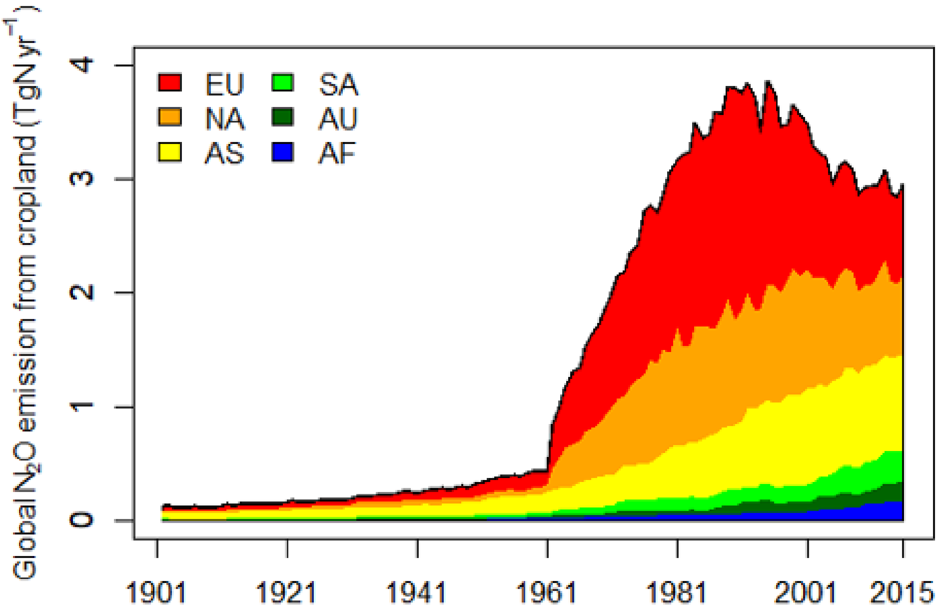

Figure 2.12 Historical N_2O emissions from global cropland ecosystems (1901 – 2016) and contributions of six different continents.

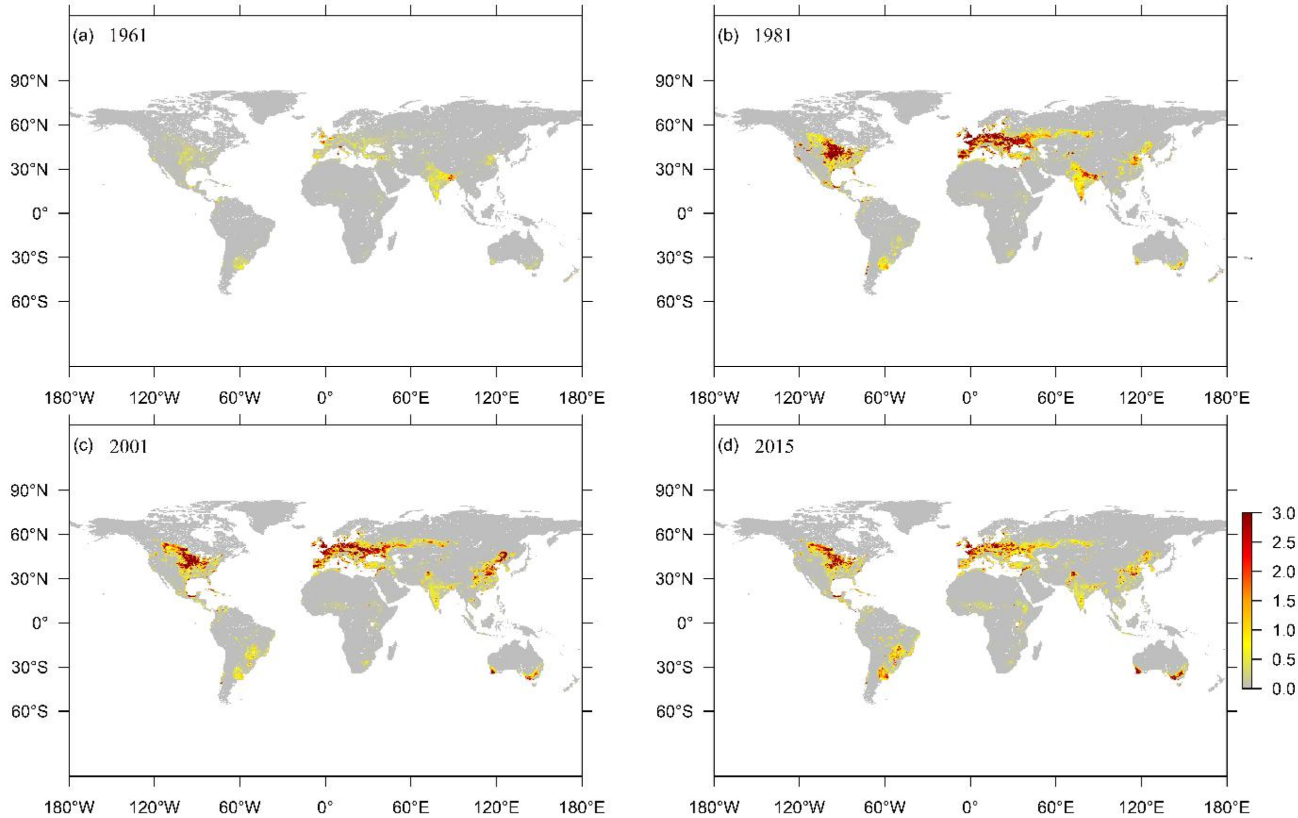

Figure 2.13 Modelled weighted mean soil N_2O emissions from cropland ecosystems in 1961 (a) 1981 (b) 2001 (c) and 2015 (d) (kg N ha^{-1} yr^{-1}).

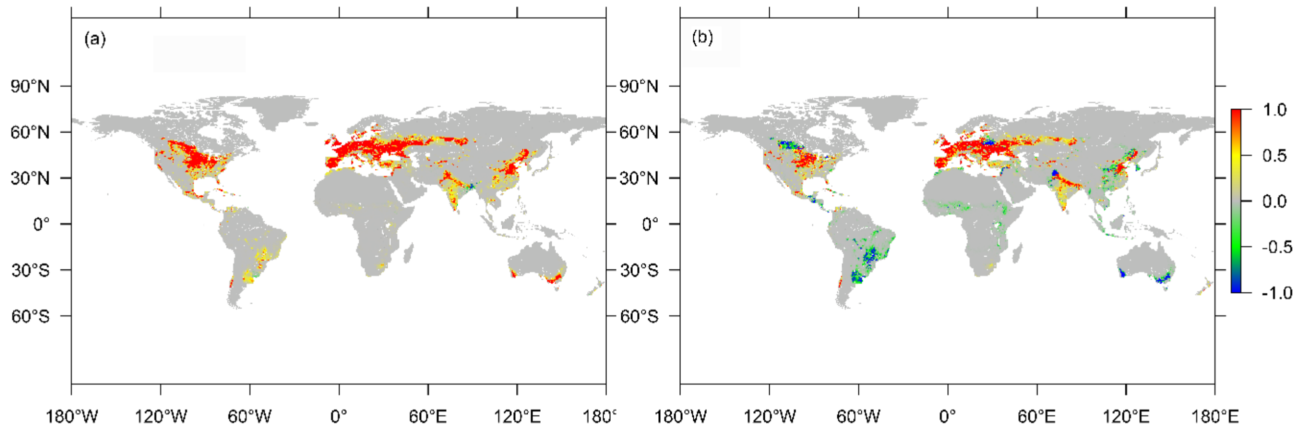

Figure 2.14 The differences of modelled N_2O emission from global cropland between the 1990 and 1961 (a), 1990 and 2016 (b) (kg N ha^{-1} yr^{-1}).

2.6.6 Driving factors of global cropland N_2O emission changes

Significant correlations between regional N_2O emissions from croplands and N synthetic fertilizer and manure suggest the predominant roles of external anthropogenic N inputs in determining dynamics in cropland N_2O emissions.

Difference between S1 and S2 quantitively demonstrated that N fertilizer application contributed more than 60% total cropland N_2O emissions during the study period. In the 21st century, mean N fertilizer effect is 1.44 (± 0.19) Tg N yr^{-1}. Meanwhile, the contribution of manure showed a consistent growth from 1901 to 2016 and it is responsible for 0.9 Tg N yr^{-1} N_2O emission from cropland since 2000 globally. Spatially, impact of N fertilizer dominates the general increasing cropland N_2O emissions in Europe, North America, and China. In contrast, cropland N_2O emissions present diverse responses to manure applications. Manure addition acts as an important cropland N_2O source for India, Australia, and South America across the study period, however, it shows negative effects on N_2O emissions from croplands in Great Lakes region and Europe (Figure 2.15).

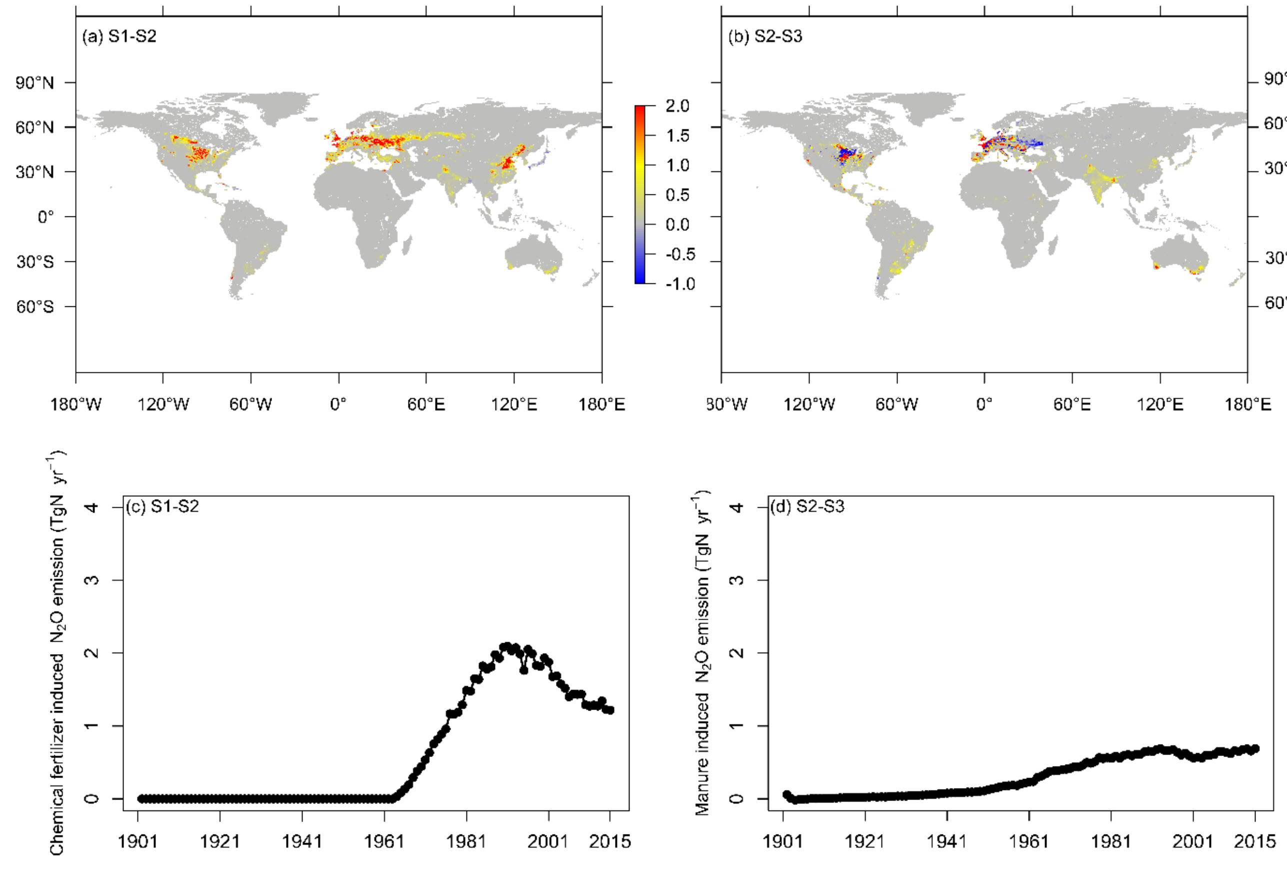

Figure 2.15 The differences of modelled N_2O emission (kg N ha^{-1} yr^{-1}) from global cropland between the 1990-1961 (a) and 1990-2016 (b).

Table 2.5 Summary of Pearson's correlation coefficients between manure induced changes of N_2O emission and major soil and environment properties.

Group	Item	Soil and environment properties

		pH	clay (%)	sand (%)	C/N ratio	SOC (%)	N deposition (kgN ha^{-1} yr^{-1})
Grids where applied manure reduce emission (S2-S3<0) Df=6855	mean	6.02[a]	23.00[a]	50.34[a]	10.63[a]	14.28[a]	241.86[a]
	r	-0.15	-0.03	0.13	0.09	0.02	-0.40
	p-value	<0.001	0.013	<0.001	<0.001	0.19	<0.001
Grids where applied manure induce emission (S2-S3>1.5) Df=8905	mean	6.65[b]	28.36[b]	41.63[b]	9.11[b]	10.62[b]	419.12[b]
	r	-0.001	-0.016	-0.03	0.03	0.15	0.19
	p-value	0.95	0.14	0.003	0.002	<0.001	<0.001

Different letters indicate significant difference between grids information ($p < 0.01$)

2.7 Discussion

Generally, the TRIPLEX-GHGv2.0 model reproduces the N_2O emissions well under different managements and environmental conditions at varying time steps. Reasonable model descriptions of agricultural practices and parameter settings ensure the overall model performance. While there are still estimated uncertainties to be improved for further studies.

2.7.1 Model features contribute to the reasonable model performances

The sensitivity experiment with newly incorporated processes and sensitivity analysis of selected key parameters are the key processes for the development of process-based models (Pappas et al., 2013; Xu et al., 2012). Sensitivity experiment provided a direct evaluation of the response rate of model outputs to the added processes in order to reflect the mechanism and effectiveness of the improved model structure while identifying the most sensitive parameter is an efficient method of improving the model performance before calibration and validation of the model (Ogejo et al., 2010; Pappas et al., 2013; Zhu & Zhuang, 2014). Agricultural activities that directly transformed the soil N input and output (via harvest, returned straw, chemical fertilizer and manure applications) showed stronger and more constant impacts on the soil N_2O emissions than others. Fertilization, especially for the chemical N fertilizer application showed the largest relative effect sizes. As a result of introducing external reactive N, surplus soil N provide excessive substrates to stimulate nitrification and denitrification processes (Liu et al., 2010; Shcherbak et al., 2014). Moreover, the relative response degree of N_2O increased with the history of fertilizer treatment (Figure 2.4e) because excessive N is retained and cumulated in fertilized soil, resulting in non-linear increased N_2O flux with further management despite of leaching, plant uptake and utilization by soil microbes (Sebilo et al., 2013). Changing processes also led to a variation in the sensitivity of parameters. The coefficient of the nitrate consumption rate, COE_{dNO3}, was found to have the highest sensitivity level for the current model instead of the coefficient of the nitrification rate, controlled the N_2O emission process as in natural soil (K. Zhang et al., 2017). Such a divergence is probably due to the introduced agricultural practices, particularly increased NO_3^- input from fertilizer. This assumption was supported by the sensitivity experiments that the growing NO_3^- input of fertilizer tend to enhance the N_2O emission in return (Figure 2.S1d). The NO_3^- consumption (from NO_3^- to NO_2^-) controls the denitrification rate and thus the N_2O production rate of N fertilized soil which is in agreement with the statement that denitrification process was the predominant contributor of cropland N_2O emission (Mosier et al., 1998; J. Wang et al., 2018). The consistency between model character and widely observed results supported the reliability of the model for further model calibration and validation.

Driven by multiple agricultural practices, the temporal and spatial variation patterns of the cropland N_2O emissions were well simulated by the TRIPLEX-GHG model v2.0. In daily time step, both model calibration and validation results showed a reasonable response to fertilizer applications in terms of the timing and duration of emission pulses. On one hand, it is common for the high emission rates of N_2O to be captured after fertilizer application, while on the other hand, field observations propose that N application alone fails to trigger the N_2O emission pulses until a substantial amount of rainfall (e.g., >25mm) to alter the soil anaerobic condition (Senapati et al., 2016; Thies et al., 2020; Wang et al., 2011). By combining the field observations and the model performance of previous studies, we conjectured that the TRIPLEX-GHG model v2.0 was capable to reproduce the immediate (e.g., Figure 2.5c and Figure 2.10i) and postponed (e.g., Figure 2.7d and Figure 2.10g) responses of fertilizer applications probably because both the soil oxygen conditions and the soil water conditions were considered. Previous studies have highlighted that the soil O_2 status is the proximal, direct, and most decisive environmental trigger of N_2O production (Song et al., 2019; Zhu et al., 2013). However, the majority of process-based models only integrated the water filled pore space (WFPS) in estimation (e.g., Tian et al., 2010; Ito et al., 2018). It was reported that although the WFPS is a critical element containing information about the soil water and gaseous status, it still requires combination with other soil structural parameters to better predict the soil O_2 concentration, microbial respiration, and subsequent gas diffusion (Farquharson & Baldock, 2008; Hall et al., 2013; Rabot et al., 2015; Song et al., 2019). Our model uses soil air-filled porosity and soil physical properties to calculate the partial pressure of oxygen representing soil O_2 status and separate the nitrification and denitrification processes allowing to capture small N_2O variations (Zhang et al., 2017b, Table 2.S1). Another particular feature of the TRIPLEX-GHG model v2.0 is to provide reasonable estimation of the manure application effect on N_2O emission. N_2O flux induced by manure input is characterized as the longer duration and higher peaks of the emitted pulses since large amount of N-substrates and DOC are mineralized and released gradually after application (e.g., EU-4). A detailed description of the manure properties and cascade decomposition processes contributed to the improved model performance (e.g., Figure 2.S4) because manure is a predominant soil organic carbon (SOC) source for croplands (Bell et al., 2015; Heller et al., 2010). The SOC serves as a key energy and carbon source for microbial growth, nitrification, and denitrification (Butterbach-Bahl et al., 2013; Snyder et al., 2009) whereas such effect is not considered by empirical models and several of the process-based models (e.g., DAYCENT, VISIT). Another advantage of our manure design is to show that the application of manure either promotes or reduces N_2O emissions (i.e., as shown in calibrated sites and sensitivity experiment) probably because the added organic C compounds support microbial growth, but stimulates completing denitrification with the further reduction of N_2O to N_2 (Abalos et al., 2021; Meijide et al., 2007; Zhou et al., 2017).

The inconsistency of the irrigation and tillage effects on cropland N_2O have been widely detected across the globe. The irrigation amount, timing as well as local management and climate determined the divergency of N_2O responses. For daily time step, modeled results found irrigation failed to trigger isolated emission pulses but had legacy effect by affecting the fertilizer induced emission peaks (e.g., Figure 2.5j and Figure 2.6i) (Mumford et al., 2019). For the cumulative effect, sensitivity experiment found higher amount of irrigated water induced larger divergence of the N_2O emissions than 50% reduced irrigation rates under fertilized soil (Figure 2.S1 i, j) due to the stronger anaerobic condition that generate denitrification (Trost et al., 2013). Field observation also revealed that lower frequency with higher amount of irrigated water increased the N_2O emission than high-frequent water-fertilizer-smart practices (e.g., sprinkle irrigation) (Kuang et al., 2021; Mumford et al., 2019; Scheer et al., 2012). On contrary, a more decisive decreasing trend of tillage effect (conventional tillage) was obtained by the sensitivity experiment. In agreement with our founding, a meta-analysis study claimed non-tillage systems have 19.2% higher N_2O emission rate than cropland under conventional tillage (Gelfand et al., 2016; Mei et al., 2018) since soil anaerobic condition is reduced following tillage activities (Angers et al., 1997; Chen et al., 2018; Forte et al., 2017). Meanwhile, in several experiment site, tillage practices stimulated short-term N_2O emission pulses (e.g., Figure 2.6b and 2.10l) which was not captured by model simulation. The limited description of soil carbon sequestration after tillage might be responsible for the underestimated small emission pulses (Luo et al., 2010) while the overall underestimation of the reduction effect of tillage might be attributed to the different soil physical properties (e.g., clay content, bulk density) and tillage intensities (e.g., tillage depth, frequency) among the selected sites of our study (Li et al., 2016; Mei et al., 2018; Rochette, 2008).

Generally, site-level simulation results of the TRIPLEX-GHG model v2.0 well reflected the varying spatial and temporal magnitudes of N_2O emission from cropland at a daily time step. On global scale, the model outputs with continent-mean parameters further demonstrated that the improved model was capable to provide reasonable estimations for both absolute daily mean emission rates (Figure 2.9a and Figure 2.11a) and emission factors (Figure 2.9b and Figure 2.11b) of different sites under diverse managements and environmental conditions during the experiment periods. Reasonably estimated daily mean N_2O fluxes provide a potential for the current model to estimate cumulative N_2O emissions across varying time scales, meanwhile the correlation between estimated and observed EFs further ensured that the modeled emission rates were derived from the understanding of the underlying mechanisms of N_2O production and emission because EFs evaluate the response level of N_2O emission to fertilizer N addition as the most important empirical indicator for cropland N_2O (Bouwman et al., 2002; Shcherbak et al., 2014).

2.7.2 N inputs drive spatiotemporal variation of N_2O emission from cropland globally

The spatiotemporal variation patterns of N_2O emission from global croplands modelled by TRIPLEX-GHGv2.0 align well with previous studies. Specifically, this study estimated the mean global cropland N_2O emission since 2000 at 3.06 ± 0.18 Tg N yr^{-1}, which falls within the range provided by IPCC (95% confidential interval 1.7 – 4.8 Tg N yr^{-1}) (IPCC, 2021). As a process-based model, our estimation is consistent with the ensemble mean of multiple process-based models (i.e., NMIP, 3.3 ± 1.2 Tg N yr^{-1}, 2007-2016) (H. Tian et al., 2019) but is larger than estimates by FAOSTAT and Syakila et al. (2011) using empirical models (i.e., 1.9 and 2.2 Tg N yr^{-1}, respectively) for the same period.

However, the high emission levels during the mid-1980s to the mid-1990s and the subsequent slightly decrease are not reported by previous modeling studies (Figure 2.12). Both model input data and model descriptions of denitrification explain this phenomenon. In general agreement with existing models, our estimate of fertilizer and manure application effects is 2.07 (± 0.15) Tg N yr-1, accounting for approximately 68.0% of total emissions during 2000—2016 (Figure 2.15) (Davidson, 2009; H. Tian et al., 2019). In this study, differentiated NH_4^+ and NO_3^- fertilizers were used to drive the model, and the declining NO_3^- application (both in absolute value and fraction to total N input) is probably responsible for the reduction in global cropland N_2O emissions, especially in Europe (Lu & Tian, 2017; Nishina et al., 2017). N_2O emissions are more sensitive to NO_3^- inputs than NH_4^+, as denitrification is the largest N_2O sources in agricultural soils (J. Wang et al., 2018). Additionally, TRIPLEX-GHGv2.0 highlights the nature of the nonlinear responses of N_2O to N additions (Shcherbak et al., 2014). Therefore, the long history of manure usage and intensive NO_3^- fertilizer application in Europe leads to the large modelled N_2O flux from croplands (Figure 2.13). Our results are well supported by documented observations. Rees et al. (2013) combined N_2O measurements from 13 long-term cropland sites in Europe and suggested that existing models such as IPCC methods significantly underestimated N_2O emission from cropland soils in this region. Moreover, emission rates over 10 kg N ha^{-1} yr^{-1} have also been extensively recorded in Europe (Regina et al., 2004; Weslien et al., 2012).

Another characteristic of our modelled results is that manure impacts N_2O emission in both directions, with possible legacy effects (Figure 2.15). This has been confirmed by site observations globally but was not fully represented in model simulations (Zhou et al., 2017). On the one hand, manure provides various N and C forms for nutrient supply of nitrification and denitrification, stimulating N_2O production to a greater extent than chemical fertilizer (i.e., EF_{manure} 1.87%, based on total manure N content). On the other hand, excessive organic C addition could enhance N_2O consumption when soil mineral N contents are limited (Dalal et al., 2010; Meijide et al., 2007). Correlation analysis suggested a significant negative relationship between annual atmospheric N deposition and the reduction in modelled N_2O due to manure inputs (Table 2.5). N deposition plays a key role in determining background N_2O emission (Aliyu et al., 2018; Yin et al., 2022). In high N deposition background with large SOC content, the accumulated mineral

N is stimulated to enhance denitrification to produce N_2O after manure additions, such as in India.

2.7.3 Uncertainty sources of model parameter, descriptions, and forcing datasets

The existing discrepancies between the observed and modeled results indicated that the possible incomplete model descriptions of the heterogeneous environmental factors and practices resulted in some uncertainties to our estimations (Butterbach-Bahl et al., 2013; Zhou et al., 2015).

First source of potential uncertainties is associated with the fitted parameter COE_{dNO3}. During validation with the continent means of COE_{dNO3}, we found overestimated N_2O emission pulses in daily variations (e.g., Figure 2.10a, b, g, h, j) and overestimated trend of EFs (i.e., Figure 2.11b, slope<1.0), suggesting a larger sensitivity level of model performance to the external N additions. The uncertainty of the continent mean COE_{dNO3} values might cause this overestimation because as the most sensitive parameter with positive effects on modeled N_2O emission (Figure 2.3), this parameter determines the consumption rate of soil NO_3^- as the controlling factor of denitrification process. Therefore, fertilizer application induced N_2O pulses can be overestimated due to the difference between sites level denitrifier NO_3^- consmpution rate and the continental mean values in our model. The uncertainties of the averaged parameters for different continents resulted from the exhibited large range of variation in the calibrated results (Figure 2.4—2.8). Such large variance can partly be reconciled by the calibration method because the NO_3^- consumption rate for denitrification is difficult to measure directly (Y. Zhang et al., 2019) which strongly discouraged the systematic adjustment of the COE_{dNO3}. However, the up-scaled parameters were found applicable for all continents when comparing the daily mean emission rates between model outputs and observations except South America (partly due to the limited number of selected sites) (Figure 2.S3). The inconsistent agricultural development and natural resources that were used by different regions may explain such phenomena. Previous studies found that long-term soil management may result in significant changes in soil microbial community and the abundance and expression of functional genes of N_2O production (Cui et al., 2016; Wang et al., 2021; Yang et al., 2017). Therefore, the varying agricultural practices, such as amounts or properties of mineral N input, probably accounted for a more important source of the variation of COE_{dNO3} compared with environmental factors. In the future, more field observations are required to refine the estimation of key parameters across the globe.

Another issue is that underestimated or mis-captured peak values of the emitted N_2O fluxes caused modeling uncertainties. The incomplete description of the processes involving the interaction between the soil pH and the external mineral N input is probably responsible for the underestimation of peak values. The soil pH is one of the most important drivers of N_2O production and acidic soils are more sensitive to N input than alkaline soils (Morkved et al., 2007; Y. Wang et al., 2018). Studies have shown that the pH values of agricultural soil tend to be significantly reduced by N additions at the global scale (Godsey et al., 2007; Guo et al., 2010; Tian & Niu, 2015). However, because the soil buffer capacity is difficult to quantify (Baron et al., 2014; Zhang et al., 2017b), the soil pH in our model was input information with a consistent pH value for each grid, and we neglected the effect of N input on soil pH such as the hydrolysis of urea (Tian & Niu, 2015; Y. Wang et al., 2018). The occasionally failure of capturing emission peaks became evident in early spring when freeze–thaw events occurred (Figs. 2.4h and 2.5g). Freeze–thaw induced N_2O emission pulses constitute a major component of the annual total N_2O emission at high latitudes (Kim et al., 2012; Wagner-Riddle et al., 2017). The increased soil temperature significantly promotes both soil physical mechanisms and microbial metabolism (Wagner-Riddle et al., 2017; Wolf et al., 2010) by releasing the accumulated trace gases (Groffman et al., 2006; Teepe et al., 2004) and triggering nitrification and denitrification processes (Sharma et al., 2006). The limited description of those processes, especially the simple empirical parameters and algorithms we used for modeling snow-melting hydrology and nutrient release, are the primary error sources (K. Zhang et al., 2017).

Furthermore, the disagreement between modeled and observed background emissions were observed in our model simulation, it is still a significant challenge for the process-based model to accurately quantify background N_2O emissions due to the following possible reasons. Our simulations used general crop classification (C_3, C_4, and rice) instead of detailed crop rotation information with different physiological parameters such as DNDC but was adopted by a majority of the large-scale process-based models (Ito et al., 2018; Monfreda et al., 2008; Saikawa et al., 2013). Generalized field observations revealed that rotation with different crop types or species might not change the N_2O fluxes pattern except for legume species (e.g., soybean) (Shcherbak et al., 2014) which have stronger N fixation ability promoting cropland soil N pools as well as background N_2O emission even without N fertilization compared with other cereal crops (Lenka et al., 2017; Liu et al., 2010; Yang & Cai, 2005). In addition, the uncertainties in the site history are also responsible for the model inaccuracy because the historical management has a tremendous effect on the soil properties and C, N dynamics (Gelfand et al., 2016; LaHue et al., 2016) with strong legacy effect on N_2O emissions (Jiang et al., 2018; Liu et al., 2014; Zhou et al., 2017). For instance, the amounts and types of residual N added in preceding years affect background emission rates in different level (Aliyu et al., 2018; Gu et al., 2009). Our model used the global mean ratio of the returned residual N to the total plant biomass for the simulation (Liu et al., 2010; Meng et al., 2005; Zhou et al., 2017) because these agricultural practices are controlled by the individual farmers and vary greatly at the local and subregional scales, without clear global distribution patterns such as those for soil and climate (Y. Wang et al., 2018). The insufficient reported site management history therefore set a barrier to the accurate estimation of the local soil nutrient conditions and thus N_2O emissions.

Other reasons for the discrepancies between the modeled results and the observations are external to the model, including the uncertainties in the field measurements and the driving data. For example, daily N_2O flux data was used to calibrate the model while the lower sampling frequency of the fieldwork (e.g., once a day) probably failed to represent the daily N_2O emission since the strong fluctuation within a day as suggested by micrometeorological methods (Jones et al., 2011; Lammirato et al., 2018; Lognoul et al., 2019). This uncertainty became even more evident during high emission rates periods (e.g., short-lived N_2O emission pulses after base fertilizer application in the fallow season), casting shadow to the estimation of cumulative emissions (Francis Clar & Anex, 2020). In the meantime, the calculated daily N_2O flux data used for model testing should also be questioned because most of the field observations used linear regression which had large uncertainties compared with other flux calculation schemes (Venterea et al., 2020). Therefore, flux measurements with high temporal resolution as well as more frequent sampling were required to reduce the uncertainties of measure N_2O flux data to ensure a more reliable estimated cumulative emissions for models (Giltrap et al., 2020). Moreover, the model's accuracy also relies on good quality input data. A 0.5°×0.5° global scale daily climate input dataset was used for the model calibration and validation, but the local environmental variables may differ significantly from that of the grid input information (Wania et al., 2010) such as precipitation and soil texture data which could cause the disagreement between the model simulations and observations (Gu et al., 2013; Philibert et al., 2013; K. Zhang et al., 2017).

2.8 Conclusion

Our study represents a successful attempt to fully integrate general agricultural activities into the framework of TRIPLEX-GHG v2.0 for simulating the magnitudes of global N_2O emissions across cropland ecosystems under varying management practices and environmental conditions. In this study, sensitivity experiments indicated that fertilizer and manure application had the highest relative effect size for estimating N_2O. The COE_{dNO3}, which controls the NO_3^- consumption rate of the denitrification process, was identified as the most sensitive parameter based on sensitivity analysis of parameters. The model was calibrated and validated against measured flux data for 39 and 68 cropland sites, respectively. We found that the TRIPLEX-GHG v2.0 can reasonably simulate N_2O variations under different conditions in daily time step and we also obtained high consistencies between estimated cumulative N_2O emissions and EFs during experiment periods with the observed data across the globe. The reliability of the improved model can be attributed to the detailed model descriptions of the fertilization effect, manure chemical properties, and soil oxygen status. Our results suggested that the interactions of agricultural practices, microbial activities, and environmental factors are important for modeling the dynamics of croplands N_2O emissions. However, uncertainties associated with the parameter settings, insufficient model description of abiotic processes, strong variations of management arrangements, as well as the driving data resulted in the model discrepancies at different time scales which limited the model's overall performance. Further development of the process-based models could contribute to sustainable agricultural development, scientific modeling, and better quantification of the global greenhouse gas budget under global change.

2.9 Supplementary Information

Table 2.S1 List of important equations for the anaerobic balloon, nitrification, denitrification, and N_2O diffusion.

No.	Equation	Definition	Reference
Anaerobic balloon			
1	$anvf = e^{-SP_{O2} \cdot P_{O2}}$	ANVF expresses the size of the anaerobic balloon	(Smith, 1980, 1990)
2	$D_{soil} = D_{air} \cdot afps^{3.33} / afps_{\max}{}^{2.0}$	oxygen diffusion coefficient in soil	(Li et al., 2000)
3	$dP_{O2} / dt = (d(D_{soil} \cdot d(P_{O2}) / dz) / dz - R) / afps$	oxygen partial pressure	(Li et al., 2000]
Nitrification			
4	$R_{nit} = B_{nit} \cdot \frac{R_{max} \cdot [NH_4]}{(6.18 + [NH_4])} \cdot pH$	nitrification rate (kg N m-2 day-1)	(Li et al., 2000; Norman et al., 2008)
5	$R_{max} = COE_{NR} \cdot N_p$	maximum nitrification rate (day-1)	(Chowdhury et al., 2017)
6	$Np = \min(4 \times 10^8 \cdot CN^{-6.311}, 96.28)$	nitrification potential	(Chowdhury et al., 2017; Lu et al., 2015)
7	$F_{NN2O} = FMAX_{N2O} \cdot R_{nit} \cdot f(t) \cdot f(m)$	maximum N2O fraction during nitrification (kg N m-2 day-1)	(Morkved et al., 2007)
8	$R_{ngrow} = NMUEMAX \cdot (\frac{[DOC]}{1.0 + [DOC]} + \frac{f(m)}{1.0 + f(m)})$	the relative growth rates of nitrifiers (kg C m-2 d-1)	(Li et al., 2000)
9	$R_{ndeath} = AMAX \cdot (\frac{B_{nit}}{(5.0 + [DOC]) + (1.0 + f(m))})$	the relative mortality rates of nitrifiers (kg C m-2 d-1)	(Li et al., 2000)
10	$B_{nnet} = B_{nit} \cdot (R_{ngrow} - R_{ndeath}) \cdot f(\mathrm{m}) \cdot f(t)$	net increase biomass of nitrifiers	(Blagodatsky and Richter, 1998; Li et al., 2000)
11	$f(t) = [(60.0 - T_{soil}) / 25.78]^{3.503} \cdot e^{[3.503 \cdot (T_{soil} - 34.22)/25.78]}$	response function of soil temperature	(Li et al., 2000)
12	$f(\mathrm{m}) = \begin{cases} 0.8 + 0.21 \cdot (1.0 - wfps) & wfps > 0.05 \\ 0.0 & wfps < 0.05 \end{cases}$	response function of soil moisture	(Li et al., 2000)
Denitrification			
13	$R_{NOX} = MUE_{NOX} \cdot \frac{[DOC]}{(K_C + [DOC])} \cdot \frac{[DOC]}{(K_N + [NO_X])}$	Relative growth rate of NOX denitrifier	(Li, 2016)

14	$R_{dgrow} = f(t) \cdot (R_{NO3} \cdot f_{NO3}(pH) + R_{NO2} \cdot f_{NO2}(pH)$ $+R_{NO} \cdot f_{NO}(pH) + R_{N2O} \cdot f_{N2O}(pH))$	relative growth rate of total denitrifiers	(Li, 2016)
15	$f_{NO3}(pH) = 1 - 1/(1 + e^{(pH-4.25)/0.5})$	function of soil pH response to NO_3^-	(Li et al., 2000)
16	$f_{NO2,NO}(pH) = 1 - 1/(1 + e^{pH-5.25})$	function of soil pH response to NO_2^- and NO consumption rate	(Li et al., 2000)
17	$f_{N2O}(pH) = 1 - 1/(1 + e^{(pH-6.25)/1.5})$	function of soil pH response to N_2O consumption rate	(Li et al., 2000)
18	$f(t) = 2^{(T_{soil}-22.5)/10}$	response function of soil temperature	(Li et al., 2000)
Diffusion			
19	$P_{N2O} = D_{N2O} \cdot \frac{\Delta F_{N2O}}{Z_l}$	the diffusion coefficient (kg m-2 h-1)	(Li, 2016)
20	$D_{N2O} = (1.0 - wfps) \cdot (0.018 + 0.124 \cdot C_{clay}$ $+(0.013 - 0.016 \cdot C_{clay}) \cdot 2^{T_{soil}/20} \cdot afps_{max})$	N_2O diffusion coefficient	(Li, 2016)

SP_{O2}: the shape parameter, following Li et al. (2000); P_{O2} : partial pressure of oxygen, calculated based on air-filled porosity; Dair: oxygen diffusion coefficient of air; afps: air-filled porosity; $afps_{max}$: maximum of air filled porosity; R: oxygen consumption rate (kg C m^{-2} h^{-1}); Z: soil layer thickness (m); D_{air}: oxygen diffusion coefficient in soil (0.07236 m^{-2} h^{-1}, (Li et al., 2000)); R_{nit}: the nitrification rate (kg N m^{-2} day^{-1}); B_{nit}: biomass concentration of nitrifying bacteria (kg C m^{-3}); $[NH_4]$: NH_4^+ concentration (kg N m^{-2}); pH: soil pH level; R_{max}: maximum nitrification rate (day^{-1}); COE_{NR}: coefficient of nitrification rate; N_p: the nitrification potential (mg N kg^{-1} day^{-1}); CN: soil C/N ratio; $FMAX_{N2O}$ the maximum N2O fraction during nitrification (kg N m-^{2} d-1), $NMUEMAX$: the growth and mortality coefficients for the nitrifiers (d^{-1}); $AMAX$: mortality coefficients for the nitrifiers (d^{-1}); T_{soil}: soil temperature (°C); *wfps*: water-filled porosity; $[DOC]$: dissolved organic carbon concentration (kg m^{-2}); MUE_{NOX}: the maximum growth rate of NOx denitrifiers (h^{-1}); Kc (kgC m^{-3}) and Kn (kg N m^{-3}): the half-saturation values of C and N oxides, respectively; $[NO_X]$: NO_X^- concentration (kg N m^{-2}; i.e. NO_3^-, NO_2^-); R_{NOx}: growth rate of NO_x denitrifiers (h^{-1}); R_{dgrow} : growth rate of total denitrifiers (h^{-1}); Z_l: the soil layer thickness (m); ΔF_{N2O}: difference in N_2O flux from two adjacent soil layers (kg N m^{-3} h^{-1}); *l*: number of layer (from top to bottom) C_{clay}: soil clay concentration.

Table 2.S2 Comparison of the variations of annual N_2O emissions (mg N m^{-2} yr^{-1}) from natural grassland sites (Zhang et al. 2017) with original model (TRIPLEX-GHG v1.0) and improved model with new integrated plant N upake process (COE_{NO3} = 4.0).

site	Lat. (N)	Lon. (E)	year	Reported emission	Original model	COE_{NO3} = 4.0	Reference
São Paulo State	-23.6	-47.5	2011	56.2	152.45	70.70	(de Urzedo et al., 2013)
Lincoln, Canterbury	-43.5	172.5	2000	25.5	24.94	24.90	(Müller and Sherlock, 2004)
Ft. Collins, Colorado	45.3	-118.1	1981-1982	12	42.31	21.97	(Parton et al., 1988)
Maseno University, Kenya	0	34.6	2012	348.7	231.44	211.43	(Arias-Navarro et al., 2013)
Inner Mongolia	43.5	116	1995	27	19.88	19.91	(Chen et al., 2000)
Inner Mongolia	43.6	116.7	2005	6.1	7.85	7.85	(Xu et al., 2003)
Wyoming	41.5	-107	1986-1987	21	31.88	19.31	(Matson et al., 1991)
					r = 0.87 ***	r = 0.98 ***	

The studied sites were selected from Zhang et al. (2017) which described the TRIPLEX-GHG v1.0 that simulated N_2O emission from natural grasslands. Those sites were used for model validation and provided in the supplementary material of Zhang et al. (2017). Pearson correlation test was used to show the model performance (***, $p < 0.001$).

Table 2.S3 **Information on the sites used for the model validation.**

Region	Lat.	Lon.	Experimental Period	Dominate Crop Type	Fertilizer Rate (kgN ha^{-1} yr^{-1})	Clay	Sand	pH	Soil C:N Ratio	Observed (mgN m^{-2} day^{-1})	Simulated (mgN m^{-2} day^{-1})	Reference
North	27.0	-109.0	2012-2014	Wheat	260	57.00	22.00	8.00	9.11	0.44	0.34	(Millar et al., 2018)
America	45.3	-73.35	2004-2005	Maize, Soybean	160	38.00	23.00	6.30	8.97	1.07	0.93	(Pelster et al., 2011)
	49.7	-112.77	2001-2004	Corn, Wheat, Barely	150	26.00	32.50	7.60	8.41	0.79	0.81	(Ellert & Janzen, 2008)
	46.8	-71.38	2001-2003	Barely	70	22.00	44.00	5.90	15.43	0.34	0.40	(Rochette, Angers, Chantigny, & Bertrand, 2008)
	39.75	-83.6	2004-2005	Corn	190	20.00	15.00	7.12	9.08	0.67	0.60	(Ussiri et al., 2009)
	35.5	-119.67	2009-2010	Almond	224	19.30	64.20	7.56	9.03	0.15	0.14	(Schellenberg et al., 2012)
	40.07	-86.93	2004-2006	Corn	250	26.00	43.50	6.00	9.19	1.80	1.72	(Omonode et al., 2011)
	38.56	-121.93	2010-2011	Tomato	237	29.00	43.00	6.35	9.24	0.87	0.85	(Kennedy et al., 2013)
	39.03	-122.05	2009-2010	Almond Orchard	235.5	29.00	43.00	6.35	9.24	0.44	0.70	(Alsina et al., 2013)
	45.15	-73.67	2004-2005	Vegetable	100	23.50	41.00	5.45	17.50	2.69	2.21	(Rochette et al., 2010)
	45.67	-111.15	2004-2006	Wheat	240	8.60	8.80	7.20	8.49	0.18	0.36	(Dusenbury et al., 2008)

	53.42	-113.37	1993-1995	Wheat	100	28.00	33.00	6.50	8.89	0.88	0.83	(Lemke et al., 1999)
	45.92	-66.6	2008-2010	Potato	190	11.00	49.00	6.20	12.70	0.59	0.52	(Snowdon et al., 2013)
	10	-84	1994-1996	Maize Taro	195	22.00	12.00	4.80	9.86	0.85	1.10	(Weitz et al., 2001)
Asia	19.5	109.48	2010-2011	Banana	519	31.00	56.00	5.53	10.00	2.70	2.79	(Zhu et al., 2015)
	18.23	99.05	1997-1998	Maize	46.9	30.00	44.50	4.70	9.72	0.16	0.16	(Watanabe et al., 2000)
	16.48	102.85	1997-1998	Maize	75	56.50	17.00	4.65	8.46	0.13	0.14	(Watanabe et al., 2000)
	14.5	100.85	1996-1997	Maize	62.4	20.50	40.00	7.40	8.76	0.12	0.13	(Watanabe et al., 2000)
	36.05	140.11	1997-1998	Vegetable	400	21.00	37.00	6.15	8.44	0.22	0.45	(Akiyama & Tsuruta, 2002)
	37.02	80.72	2015-2016	Cotton	240	6.00	90.00	8.00	3.41	0.23	0.55	(Kuang et al., 2018)
	42.04	116.3	2005-2006	Wormwood	100	15.50	55.00	7.07	10.10	0.68	0.45	(Zhang & Han, 2008)
	23.13	113.25	2013-2014	Corn	360	21.00	31.50	5.20	12.05	0.09	0.14	(Tang et al., 2015)
	46.8	130.2	2015-2016	Vegetable	770	15.60	31.60	7.60	12.70	1.95	1.81	(Fan et al., 2017)
	34.3	108.03	2015-2016	Vegetable	770	22.70	17.70	7.60	7.00	2.15	2.24	(Fan et al., 2017)
	28.53	113.38	2015-2016	Vegetable	770	12.90	47.10	5.60	6.30	5.33	3.62	(Fan et al., 2017)

	37.6	101.25	2009-2010	Pasture	150	6.00	32.00	8.20	11.00	0.20	0.21	(Z. Zhang et al., 2017)
	24.84	102.81	2005-2006	Vegetable	900	25.00	48.00	6.90	10.55	6.02	3.86	(Guo et al., 2007)
	0.33	102.3	2011-2012	Oil Palm	150	5.00	62.00	4.67	11.00	0.89	0.62	(Sakata et al., 2015)
	1.05	110.87	2010-2012	Oil Palm	113	0.03	97.00	4.78	10.50	0.42	0.27	(Sakata et al., 2015)
	35.63	107.85	2014	Alfalfa	150	22.00	22.00	8.05	7.63	0.28	0.36	(G. Wang et al., 2018)
	-3.47	114.83	2004-2005	Corn	100	9.60	66.40	4.60	17.20	0.57	0.30	(Hadi et al., 2008)
	17.85	78.48	2010-2011	Sorghum	90	51.50	26.40	8.30	8.50	0.46	0.28	(Ramu et al., 2012)
	23.3	77.4	2012-2013	Wheat, Soybean	110	56.00	15.50	7.85	9.12	0.79	0.64	(Lenka et al., 2017)
	28.67	77.2	2006-2007	Wheat	120	21.00	46.00	8.10	13.70	0.73	0.48	(Bhatia et al., 2010)
	37.2	50.02	2014-2015	Corn	500	22.00	37.00	8.10	8.80	4.00	5.21	(Sadeghi et al., 2018)
Europe	43.67	10.32	2013-2015	Wheat	110	35.00	18.50	7.85	8.62	0.41	0.78	(Volpi et al., 2018)
	43.28	-2.85	2015-2016	Maize, Ryegrass	380	15.00	33.00	7.00	8.00	1.04	0.85	(Huerfano et al., 2018)
	40.53	-3.33	2011-2013	Maize	70	11.50	50.80	7.90	8.09	0.49	0.51	(Tellez-Rio et al., 2017)
	48.85	1.97	2007-2008	Mazie, Wheat	108	31.00	6.50	8.30	12.60	0.63	0.91	(Laville et al., 2011)

55.96	-2.78	1997	Ryegrass	460	13.00	72.00	7.10	7.77	3.12	3.57	(Smith & Dobbie, 2001)
55.48	-4.56	1997	Ryegrass	320	33.50	33.50	4.45	9.37	2.28	2.60	(Smith & Dobbie, 2001)
59.82	10.78	2009-2010	Wheat, Barley	120	21.00	39.00	5.93	10.80	0.80	0.83	(Nadeem et al., 2015)
60.82	23.47	1993	Barley	103	39.00	20.00	5.80	11.00	0.80	1.79	(Simojoki & Jaakkola, 2000)
52.86	-6.54	2008-2010	Barley	135	12.50	71.50	7.30	10.00	1.04	1.50	(Abdalla et al., 2014)
59.55	30.12	2004	Barley, Potato	65	25.50	18.00	5.60	8.83	0.26	0.34	(Balashov et al., 2010)
55.88	-3.43	1992-1993	Barley, Ryegrass	360	22.00	34.00	5.50	7.77	1.49	1.97	(Clayton et al., 1997)
51.06	10.82	2011-2013	Poplar Clone, Maize	160	22.00	8.00	7.30	9.60	0.09	0.56	(Walter et al., 2015)
56.49	13	1995-1997	Wheat	120	8.00	35.00	6.80	10.38	0.79	0.82	(Klemedtsson & Smith, 2011)
58.33	12.65	2005-2006	Wheat	120	20.00	43.50	7.20	6.16	0.30	0.74	
51.99	5.67	2007-2009	Mazie	110	48.00	20.00	4.80	16.00	1.26	1.12	(Velthof & Mosquera, 2011)

	41.8	1.12	2011-2012	Barley	120	11.80	46.50	8.50	7.18	0.33	1.05	(Plaza-Bonilla et al., 2018)
	47.33	5.03	2012-2013	Wheat	140	41.10	5.30	6.90	11.50	0.89	1.74	(Vermue et al., 2016)
	43.53	-1.505	2010-2013	Soyebean, Wheat	33	4.00	87.50	7.20	13.24	0.31	0.62	(Peyrard et al., 2016)
Oceanic	-27.43	153.16	2003–2005	Sugarcane,	100	46.00	28.00	5.00	11.88	1.59	1.48	(Allen et al., 2010)
	-35.01	147.33	2013-14	Wheat	100	42.80	37.10	5.60	15.00	0.061	0.089	(Li et al., 2016)
	-27.51	151.78	2010-2011	Corn	270	76.00	6.00	7.30	11.88	0.52	0.36	(Scheer et al., 2016)
	-37.82	142.08	2013-2015	Wheat	0	17.00	71.00	5.60	14.00	0.25	0.23	(Belyaeva et al., 2016)
	-43.67	172.47	2003	Forage	800	20.00	43.00	5.70	11.80	2.89	2.50	(Thomas et al., 2008)
	-31.48	117.2	2009-2010	Wheat	75	8.50	89.00	5.10	7.73	0.018	0.047	(Barton et al., 2013)
South America	-31.5	-63.5	2009–2010	Corn, Soybean	50	17.00	24.00	6.75	8.31	0.54	0.60	(Alvarez et al., 2012)
	-28.25	-52.4	2002-2004	Mazie, Wheat	55	63.00	24.00	5.10	8.87	0.19	0.22	(Jantalia et al., 2008)
	-22.25	-48.57	2010-2011	Sugarcane	60	16.70	62.30	4.30	9.38	0.16	0.16	(do Carmo et al., 2013)
	-22.68	-47.55	2013-2015	Sugarcane	600	64.80	22.70	5.10	11.88	0.22	0.56	(Lourenco et al., 2019)

	-27.05	-65.42	2012-2015	Sugarcane	110	32.60	41.00	5.9	7.68	0.37	0.40	(Chalco Vera et al., 2017)
Africa	-7.7	35.57	2015-2017	Maize; sunflower	100	34.60	32.50	6.45	11.2	0.18	0.16	(Zheng et al., 2019)
	-19.78	47.1	2006-2007	Maize, Soybean	57	30.50	55.50	4.90	10.50	0.15	0.13	(Chapuis-Lardy et al., 2009)
	-17.58	31.23	2000-2002	Maize	0	22.00	73.00	5.10	8.03	0.13	0.11	(Chikowo et al., 2004)
	-17.7	31	2006-2009	Maize	60	11.00	81.00	6.00	8.03	0.19	0.18	(Mapanda et al., 2011)

Table 2.S4 Design of the sensitivity experiment of new integrated processes of TRIPLEX-GHG model v2.0

ID	Variables and integrated processes										
	Climate	Plan.Up.	Harv.	Ret.straw	N fertilizer application			Manure application		Irri.	Tillage
					Rate	Timing	Property	Rate	Property		
TRPLEX-GHG v1.0	1960-2010	original	N.A.	N.A.	0	N.A.	N.A.	0	N.A.	N.A.	N.A.
PU	1960-2010	new plant uptake	N.A.	N.A.	0	N.A.	N.A.	0	N.A.	N.A.	N.A.
HV	1960-2010	original	harvest	N.A.	0	N.A.	N.A.	0	N.A.	N.A.	N.A.
RS	1960-2010	original	harvest		0	N.A.	N.A.	0	N.A.	N.A.	N.A.
FN	1960-2010	original	N.A.	N.A.	def.FR	def.FT	def.FP	0	N.A.	N.A.	N.A.
FN-rate	1960-2010	original	N.A.	N.A.	120% of def.FR	def.FT	def.FP	0	N.A.	N.A.	N.A.
FN-time	1960-2010	original	N.A.	N.A.	def.FR	averaged in the year	def.FP	0	N.A.	N.A.	N.A.
FN-fra	1960-2010	original	N.A.	N.A.	def.FR	def.FT	120% of def.FP	0	N.A.	N.A.	N.A.
MN	1960-2010	original	N.A.	N.A.	0	N.A.	N.A.	def.MR	def.MP	N.A.	N.A.
MN-rate	1960-2010	original	N.A.	N.A.	0	N.A.	N.A.	120% of def.MR	def.MP	N.A.	N.A.
MN-inorg	1960-2010	original	N.A.	N.A.	0	N.A.	N.A.	def.MR	120% of def.MP (inorganic)	N.A.	N.A.
MN-organ	1960-2010	original	N.A.	N.A.	0	N.A.	N.A.	def.MR	120% if def.MP (organic)	N.A.	N.A.
IR	1960-2010	original	N.A.	N.A.	0	N.A.	N.A.	0	N.A.	def.IR	N.A.
IR-FN	1960-2010	original	N.A.	N.A.	def.FR	def.FT	def.FP	0	N.A.	def.IR	N.A.
0.5IR-FN	1960-2010	original	N.A.	N.A.	def.FR	def.FT	def.FP	0	N.A.	50% of def.IR	N.A.
TG	1960-2010	original	N.A.	def.RS	0	N.A.	N.A.	0	N.A.	N.A.	def.TG

climate input information; PU: effect of changing plant uptake design; HV: effect of harvest activity; FN: effect of chemical N fertilizer application; FN-rate: effect of changing chemical N fertilizer rate (kg N ha^{-1} yr^{-1}); FN-time: effect of changing timing of chemical N fertilizer application; FN-fra: effect of changing fertilizer properties (e.g., NH_4%); MN: effect of manure application; MN-rate: effect of changing manure application rate (kg N km^{-2} yr^{-1}); MN-inorg: effect of changing inorganic source of manure (%); MN-organ: effect of changing organic source of manure (%); IR: effect of irrigation; IR-FN: effect of irrigation with fertilizer application; 0.5IR-FN: effect of 50% irrigation rate with fertilizer application; TG: effect of tillage activity; RS: effect of returned straw activity.

def.FR: default value of chemical N fertilizer application rate is the global mean of Nishina et al. 2017; def.FT: default value of the application date of chemical N fertilizer which is the beginning of growing season for only one time; def.FP: default value of the NO_3^- :NH_4^+ ratio is set as the global mean of Nishaina et al. 2017; def.MR: default value of the manure application rate is set as the global mean of Zhang et al. 2017; def.MP: default value of the manure properties (inorganic and organic according to Eq.8-10) is set according to the average of the most widely used manure properties according the Li et al. 2000 and Li et al. 2012; def.IR: default design of the irrigation rate is set as 50mm per application *1 time for one year; def.TG: default value of the tillage depth which is the first 3 layers of soil profile for our model (Li et al. 2000; Zhang et al. 2017); def.RS: default value of the returned straw is set as the global mean ratio of returned straw according to Liu et al. (2010). N.A. means this process is not applicable (i.e., be closed) during simulation.

e.g., by comparing the difference of the annual N_2O emission between TRIPLEX-GHG v1.0 and that with PU, the effect of changing plant uptake design is obtained. The effect of changing fertilizer application rate is based on the difference between FN and FN-rate.

Table 2.S5 ANOVA and multiple comparison result of the value of calibrated parameter COE_{dNO3} across different continent.

	Df	Sum Sq	Mean Sq	F value	*P*r(>F)
Catergory	**5**	**0.002325**	**0.0004651**	**3.971**	**0.00627 ****
Residual	**33**	**0.003865**	**0.0001171**		

**** : *P* < 0.01**

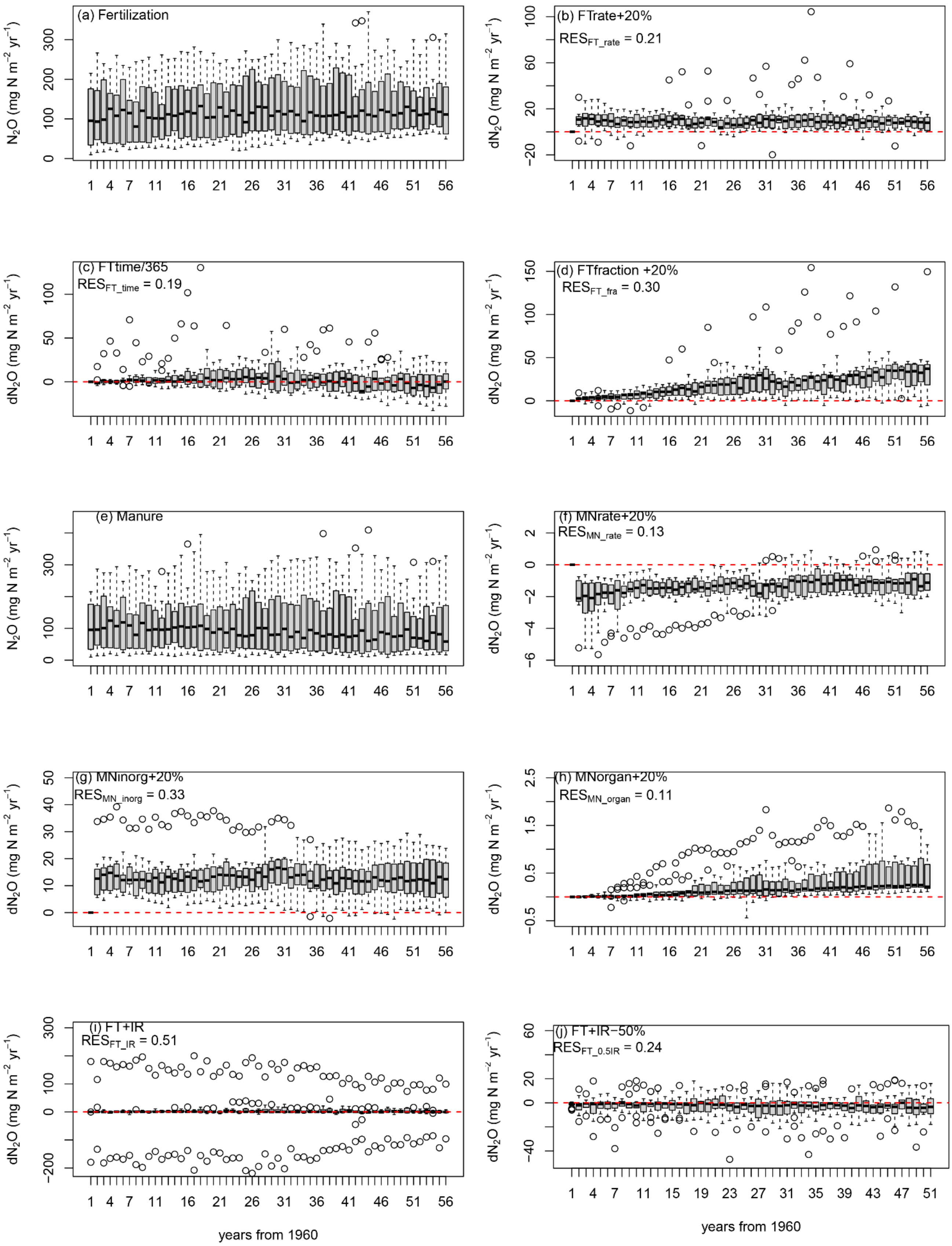

Figure 2.S1 Further sensitivity experiment of integrated processes (based on Table 2.S3). a.The

model output with default fertilization practices; b. the effect of increased fertilizer application rates (by 20%) N_2O emission compared with that of default fertilizer application rate; c. the effect of changing the time of fertilizer application (divided by 365 days) on N_2O emission compared with that of default timing of fertilizer application; d. the effect of increased nitrate fraction of fertilizer application (by 20%) on N_2O emission compared with that of default fertilizer properties; e. the model output with default manure application; f. the effect of increased manure application rates (by 20%) on N_2O emission compared with that of default manure application rate; g. the effect of increased inorganic proportion of manure (by 20%) on N_2O emission compared with that of default manure properties; h. the effect of increased organic proportion of manure (by 20%) on N_2O emission compared with that of default manure properties; i. the effect of irrigation on fertilized soil; j. the effect of reduced irrigation rates (50%) with higher frequency (3 times) on N_2O emission from fertilized soil compared with that of default irrigation-fertilized soil. The dashed red line means the δ N_2O = 0.0. RES indicates the relative effect size of the processes (Eq. 16).

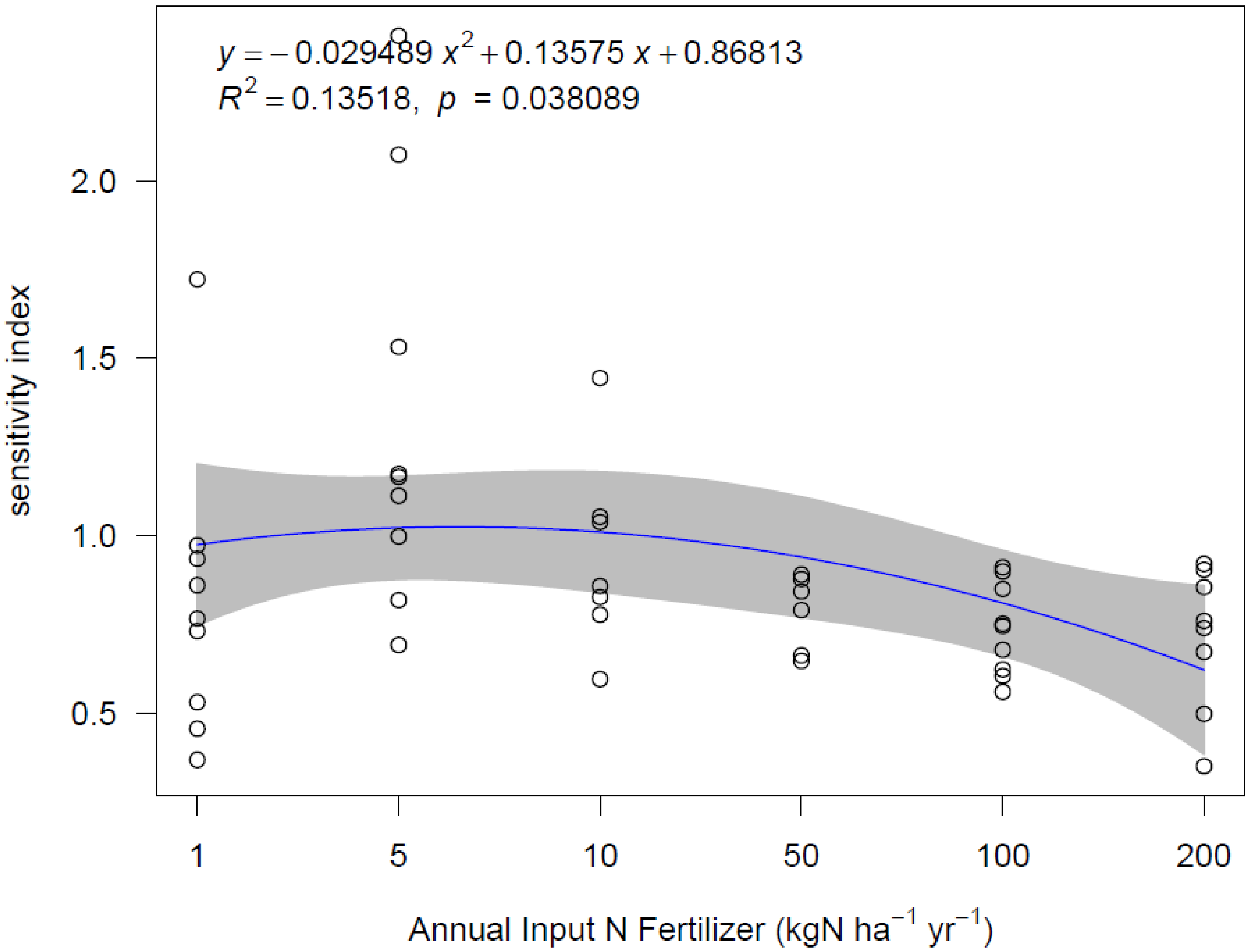

Figure 2.S2 The variation in sensitivity of the selected parameter COE_{dNO3} with varying chemical fertilizer input. The NH_4^+/NO_3^- ratio was set as 7:1 during the sensitivity analysis, which is a common ratio according to Nishina et al. (2017). The fertilization was set to start in 1961.

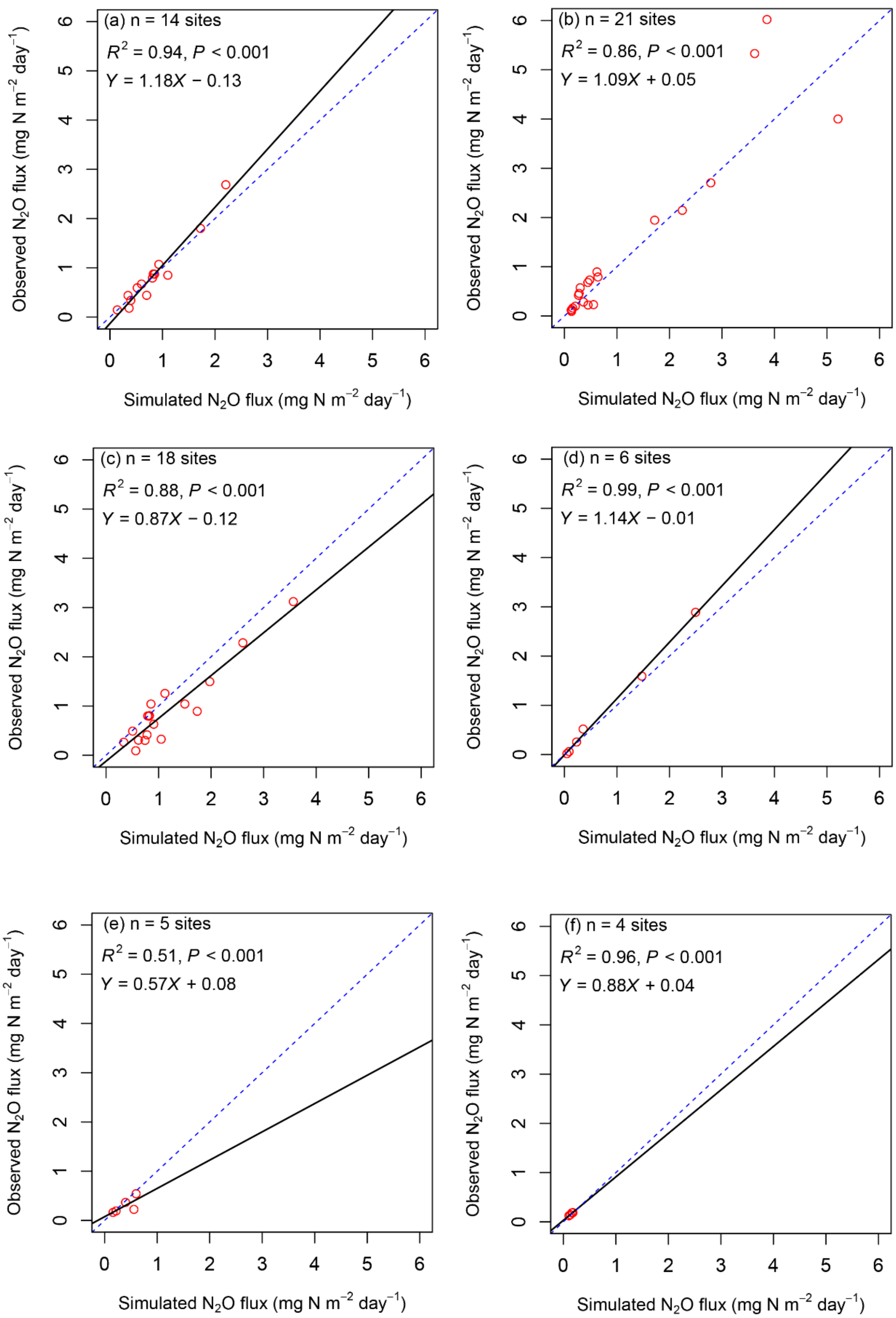

Figure 2.S3 Validation of the daily mean emission rates during experiment periods for cropland sites located in different continents (a, North America; b. Aisa; c. Europe; d. Australia; e. South America; f. Africa).

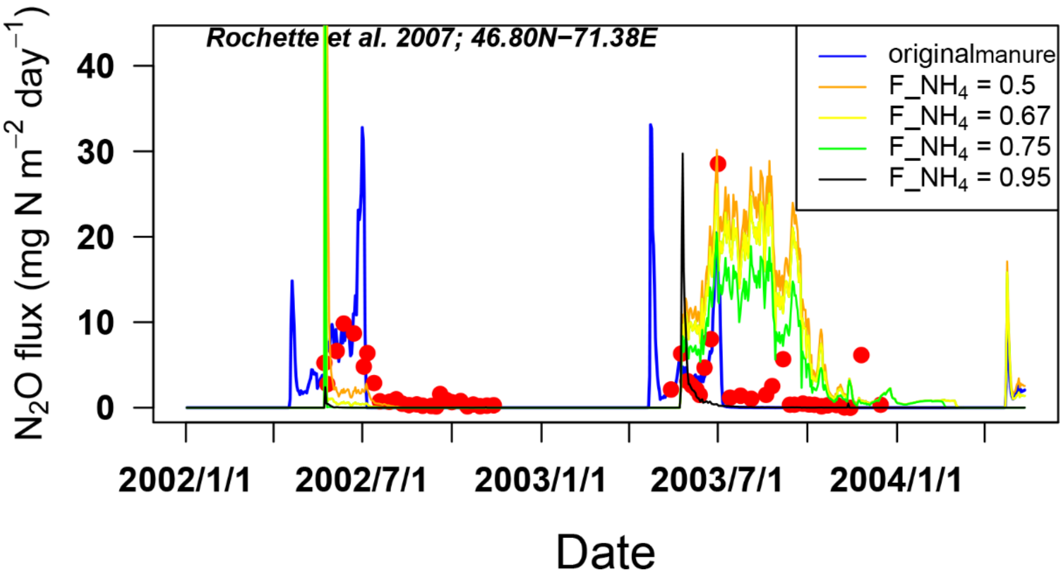

Figure 2. S4. An example for the comparison of the simulated results of the application of chemical N fertilizer with different NH_4:NO_3 ratios (Fraction of NH_4) .vs. original modeled results with of manure (blue line) at same amount of N input rate. The measured flux data is closed red dot.

2.10 References

Abalos, D., De Deyn, G. B., Philippot, L., Oram, N. J., Oudová, B., Pantelis, I., Clark, C., Fiorini, A., Bru, D., Mariscal-Sancho, I., & van Groenigen, J. W. (2021). Manipulating plant community composition to steer efficient N-cycling in intensively managed grasslands. *Journal of Applied Ecology*, *58*(1), 167-180. https://doi.org/https://doi.org/10.1111/1365-2664.13788

Abalos, D., Sanz-Cobena, A., Garcia-Torres, L., van Groenigen, J. W., & Vallejo, A. (2013). Role of maize stover incorporation on nitrogen oxide emissions in a non-irrigated Mediterranean barley field. *Plant and Soil*, *364*(1-2), 357-371. https://doi.org/10.1007/s11104-012-1367-4

Abdalla, M., Hastings, A., Helmy, M., Prescher, A., Osborne, B., Lanigan, G., Forristal, D., Killi, D., Maratha, P., Williams, M., Rueangritsarakul, K., Smith, P., Nolan, P., & Jones, M. B. (2014). Assessing the combined use of reduced tillage and cover crops for mitigating greenhouse gas emissions from arable ecosystem. *Geoderma*, *223*, 9-20. https://doi.org/10.1016/j.geoderma.2014.01.030

Aita, C., Schirmann, J., Pujol, S. B., Giacomini, S. J., Rochette, P., Angers, D. A., Chantigny, M. H., Gonzatto, R., Giacomini, D. A., & Doneda, A. (2015). Reducing nitrous oxide emissions from a maize-wheat sequence by decreasing soil nitrate concentration: effects of split application of pig slurry and dicyandiamide. *European Journal of Soil Science*, *66*(2), 359-368. https://doi.org/10.1111/ejss.12181

Akiyama, H., & Tsuruta, H. (2002). Effect of chemical fertilizer form on N2O, NO and NO2 fluxes from Andisol field. *Nutrient Cycling in Agroecosystems*, *63*(2-3), 219-230. https://doi.org/10.1023/a:1021102925159

Akiyama, H., Yagi, K., & Yan, X. (2005). Direct N2O emissions from rice paddy fields: Summary of available data. *Global Biogeochemical Cycles*, *19*(1). https://doi.org/https://doi.org/10.1029/2004GB002378

Aliyu, G., Sanz-Cobena, A., Mueller, C., Zaman, M., Luo, J., Liu, D., Yuan, J., Chen, Z., Niu, Y., Arowolo, A., & Ding, W. (2018). A meta-analysis of soil background N2O emissions from croplands in China shows variation among climatic zones. *Agriculture Ecosystems & Environment*, *267*, 63-73. https://doi.org/10.1016/j.agee.2018.08.003

Allen, D. E., Kingston, G., Rennenberg, H., Dalal, R. C., & Schmidt, S. (2010). Effect of nitrogen fertilizer management and waterlogging on nitrous oxide emission from subtropical sugarcane soils. *Agriculture Ecosystems & Environment*, *136*(3-4), 209-217. https://doi.org/10.1016/j.agee.2009.11.002

Alsina, M. M., Fanton-Borges, A. C., & Smart, D. R. (2013). Spatiotemporal variation of event related N2O and CH4 emissions during fertigation in a California almond orchard. *Ecosphere*, *4*(1), Article Unsp 1. https://doi.org/10.1890/es12-00236.1

Alvarez, C., Costantini, A., Alvarez, C. R., Alves, B. J. R., Jantalia, C. P., Martellotto, E. E., & Urquiaga, S. (2012). Soil nitrous oxide emissions under different management practices in the semiarid region of the Argentinian Pampas. *Nutrient Cycling in Agroecosystems*, *94*(2-3), 209-220. https://doi.org/10.1007/s10705-012-9534-9

Alvaro-Fuentes, J., Luis Arrue, J., Bielsa, A., Cantero-Martinez, C., Plaza-Bonilla, D., & Paustian, K. (2017). Simulating climate change and land use effects on soil nitrous oxide emissions in Mediterranean conditions using the Daycent model. *Agriculture Ecosystems & Environment*, *238*, 78-88. https://doi.org/10.1016/j.agee.2016.07.017

Angers, D. A., Bolinder, M. A., Carter, M. R., Gregorich, E. G., Drury, C. F., Liang, B. C., Voroney, R. P., Simard, R. R., Donald, R. G., Beyaert, R. P., & Martel, J. (1997). Impact of tillage practices on organic carbon and nitrogen storage in cool, humid soils of eastern Canada. *Soil & Tillage Research*, *41*(3-4), 191-201. https://doi.org/10.1016/s0167-1987(96)01100-2

Baggs, E. M., Stevenson, M., Pihlatie, M., Regar, A., Cook, H., & Cadisch, G. (2003). Nitrous oxide emissions following application of residues and fertiliser under zero and conventional tillage. *Plant and Soil*, *254*(2), 361-370. https://doi.org/10.1023/a:1025593121839

Balashov, E., Horák, J., Šiška, B., Buchkina, N., Rizhiya, E., & Pavlik, S. (2010). N2O fluxes from agricultural soils in

Slovakia and Russia - direct measurements and prediction using the DNDC model. *Folia Oecologica*, *37*(1), 8-15.

Barton, L., Murphy, D. V., & Butterbach-Bahl, K. (2013). Influence of crop rotation and liming on greenhouse gas emissions from a semi-arid soil. *Agriculture Ecosystems & Environment*, *167*, 23-32. https://doi.org/10.1016/j.agee.2013.01.003

Bell, M. J., Rees, R. M., Cloy, J. M., Topp, C. F. E., Bagnall, A., & Chadwick, D. R. (2015). Nitrous oxide emissions from cattle excreta applied to a Scottish grassland: Effects of soil and climatic conditions and a nitrification inhibitor. *Science of the Total Environment*, *508*, 343-353. https://doi.org/https://doi.org/10.1016/j.scitotenv.2014.12.008

Belyaeva, O. N., Officer, S. J., Armstrong, R. D., Harris, R. H., Wallace, A., Partington, D. L., Fogarty, K., & Phelan, A. J. (2016). Use of the agricultural practice of pasture termination in reducing soil N2O emissions in high-rainfall cropping systems of south-eastern Australia. *Soil Research*, *54*(5), 585-597. https://doi.org/10.1071/sr15307

Berdanier, A. B., & Conant, R. T. (2012). Regionally differentiated estimates of cropland N2O emissions reduce uncertainty in global calculations. *Global Change Biology*, *18*(3), 928-935. https://doi.org/10.1111/j.1365-2486.2011.02554.x

Betlach, M. R., & Tiedje, J. M. (1981). Kinetic explanation for accumulation of nitrite, nitric oxide, and nitrous oxide during bacterial denitrification. *Applied and Environmental Microbiology*, *42*(6), 1074-1084. <Go to ISI>://MEDLINE:16345900

Bhatia, A., Sasmal, S., Jain, N., Pathak, H., Kumar, R., & Singh, A. (2010). Mitigating nitrous oxide emission from soil under conventional and no-tillage in wheat using nitrification inhibitors. *Agriculture Ecosystems & Environment*, *136*(3-4), 247-253. https://doi.org/10.1016/j.agee.2010.01.004

Botta, A., Viovy, N., Ciais, P., Friedlingstein, P., & Monfray, P. (2000). A global prognostic scheme of leaf onset using satellite data. *Global Change Biology*, *6*(7), 709-725. https://doi.org/10.1046/j.1365-2486.2000.00362.x

Bouwman, A. F., Boumans, L. J. M., & Batjes, N. H. (2002). Modeling global annual N2O and NO emissions from fertilized fields. *Global Biogeochemical Cycles*, *16*(4), Article 1080. https://doi.org/10.1029/2001gb001812

Buchkina, N. P., Balashov, E. V., Rizhiya, E. Y., & Smith, K. A. (2010). Nitrous oxide emissions from a light-textured arable soil of North-Western Russia: effects of crops, fertilizers, manures and climate parameters. *Nutrient Cycling in Agroecosystems*, *87*(3), 429-442. https://doi.org/10.1007/s10705-010-9349-5

Burney, J. A., Davis, S. J., & Lobell, D. B. (2010). Greenhouse gas mitigation by agricultural intensification. *Proceedings of the National Academy of Sciences of the United States of America*, *107*(26), 12052-12057. https://doi.org/10.1073/pnas.0914216107

Butterbach-Bahl, K., Baggs, E. M., Dannenmann, M., Kiese, R., & Zechmeister-Boltenstern, S. (2013). Nitrous oxide emissions from soils: how well do we understand the processes and their controls? *Philosophical Transactions of the Royal Society B-Biological Sciences*, *368*(1621). https://doi.org/10.1098/rstb.2013.0122

Cai, Z., Wang, B., Xu, M., Zhang, H., Zhang, L., & Gao, S. (2014). Nitrification and acidification from urea application in red soil (Ferralic Cambisol) after different long-term fertilization treatments. *Journal of Soils and Sediments*, *14*(9), 1526-1536. https://doi.org/10.1007/s11368-014-0906-4

Carlson, K. M., Gerber, J. S., Mueller, N. D., Herrero, M., MacDonald, G. K., Brauman, K. A., Havlik, P., O'Connell, C. S., Johnson, J. A., Saatchi, S., & West, P. C. (2017). Greenhouse gas emissions intensity of global croplands. *Nature Climate Change*, *7*(1), 63-+. https://doi.org/10.1038/nclimate3158

Cavigelli, M. A., Del Grosso, S. J., Liebig, M. A., Snyder, C. S., Fixen, P. E., Venterea, R. T., Leytem, A. B., McLain, J. E., & Watts, D. B. (2012). US agricultural nitrous oxide emissions: context, status, and trends. *Frontiers in Ecology and the Environment*, *10*(10), 537-546. https://doi.org/10.1890/120054

Chalco Vera, J., Valeiro, A., Posse, G., & Acreche, M. M. (2017). To burn or not to burn: The question of straw burning and nitrogen fertilization effect on nitrous oxide emissions in sugarcane. *Science of the Total Environment*, *587-588*, 399-406. https://doi.org/https://doi.org/10.1016/j.scitotenv.2017.02.172

Chalk, P., & Smith, C. (2021). On inorganic N uptake by vascular plants: Can 15N tracer techniques resolve the NH4+ versus NO3− "preference" conundrum? *European Journal of Soil Science*, *72*(4), 1762-1779. https://doi.org/https://doi.org/10.1111/ejss.13069

Chapuis-Lardy, L., Metay, A., Martinet, M., Rabenarivo, M., Toucet, J., Douzet, J. M., Razafimbelo, T., Rabeharisoa, L., & Rakotoarisoa, J. (2009). Nitrous oxide fluxes from Malagasy agricultural soils. *Geoderma*, *148*(3-4), 421-427. https://doi.org/10.1016/j.geoderma.2008.11.015

Chatskikh, D., Olesen, J. E., Berntsen, J., Regina, K., & Yamulki, S. (2005). Simulation of effects of soils, climate and management on N(2)O emission from grasslands. *Biogeochemistry*, *76*(3), 395-419. https://doi.org/10.1007/s10533-005-6996-8

Chen, G., Kolb, L., Cavigelli, M. A., Weil, R. R., & Hooks, C. R. R. (2018). Can conservation tillage reduce N2O emissions on cropland transitioning to organic vegetable production? *Science of the Total Environment*, *618*, 927-940. https://doi.org/10.1016/j.scitotenv.2017.08.296

Cheng, K., Ogle, S. M., Parton, W. J., & Pan, G. (2014). Simulating greenhouse gas mitigation potentials for Chinese Croplands using the DAYCENT ecosystem model. *Global Change Biology*, *20*(3), 948-962. https://doi.org/10.1111/gcb.12368

Chikowo, R., Mapfumo, P., Nyamugafata, P., & Giller, K. E. (2004). Mineral N dynamics, leaching and nitrous oxide losses under maize following two-year improved fallows on a sandy loam soil in Zimbabwe. *Plant and Soil*, *259*(1-2), 315-330. https://doi.org/10.1023/B:PLSO.0000020977.28048.fd

Chowdhury, S., Thangarajan, R., Bolan, N., O'Reilly-Wapstra, J., Kunhikrishnan, A., & Naidu, R. (2017). Nitrification potential in the rhizosphere of Australian native vegetation. *Soil Research*, *55*(1), 58-69. https://doi.org/10.1071/sr16116

Clayton, H., McTaggart, I. P., Parker, J., Swan, L., & Smith, K. A. (1997). Nitrous oxide emissions from fertilised grassland: A 2-year study of the effects of N fertiliser form and environmental conditions. *Biology and Fertility of Soils*, *25*(3), 252-260. https://doi.org/10.1007/s003740050311

Cui, F., Yan, G., Zhou, Z., Zheng, X., & Deng, J. (2012). Annual emissions of nitrous oxide and nitric oxide from a wheat-maize cropping system on a silt loam calcareous soil in the North China Plain. *Soil Biology & Biochemistry*, *48*, 10-19. https://doi.org/10.1016/j.soilbio.2012.01.007

Cui, P., Fan, F., Yin, C., Song, A., Huang, P., Tang, Y., Zhu, P., Peng, C., Li, T., Wakelin, S. A., & Liang, Y. (2016). Long-term organic and inorganic fertilization alters temperature sensitivity of potential N2O emissions and associated microbes. *Soil Biology and Biochemistry*, *93*, 131-141. https://doi.org/https://doi.org/10.1016/j.soilbio.2015.11.005

Dalal, R. C., Gibson, I., Allen, D. E., & Menzies, N. W. (2010). Green waste compost reduces nitrous oxide emissions from feedlot manure applied to soil. *Agriculture, Ecosystems & Environment*, *136*(3), 273-281. https://doi.org/https://doi.org/10.1016/j.agee.2009.06.010

Daryanto, S., Wang, L., Gilhooly, W. P., III, & Jacinthe, P.-A. (2018). Nitrogen preference across generations under changing ammonium nitrate ratios. *Journal of Plant Ecology*, *12*(2), 235-244. https://doi.org/10.1093/jpe/rty014

Davidson, E. A. (2009). The contribution of manure and fertilizer nitrogen to atmospheric nitrous oxide since 1860. *Nature Geoscience*, *2*(9), 659-662. https://doi.org/10.1038/ngeo608

Davidson, E. A., & Kanter, D. (2014). Inventories and scenarios of nitrous oxide emissions. *Environmental Research Letters*, *9*(10), Article 105012. https://doi.org/10.1088/1748-9326/9/10/105012

Del Grosso, S. J., Mosier, A. R., Parton, W. J., & Ojima, D. S. (2005). DAYCENT model analysis of past and contemporary soil N(2)O and net greenhouse gas flux for major crops in the USA. *Soil & Tillage Research*, *83*(1), 9-24. https://doi.org/10.1016/j.still.2005.02.007

Del Grosso, S. J., Ojima, D. S., Parton, W. J., Stehfest, E., Heistermann, M., DeAngelo, B., & Rose, S. (2009). Global scale

DAYCENT model analysis of greenhouse gas emissions and mitigation strategies for cropped soils. *Global and Planetary Change*, *67*(1-2), 44-50. https://doi.org/10.1016/j.gloplacha.2008.12.006

Del Grosso, S. J., Parton, W. J., Mosier, A. R., Ojima, D. S., Kulmala, A. E., & Phongpan, S. (2000). General model for N2O and N-2 gas emissions from soils due to dentrification. *Global Biogeochemical Cycles*, *14*(4), 1045-1060. https://doi.org/10.1029/1999gb001225

Denmead, O. T., Macdonald, B. C. T., Bryant, G., Naylor, T., Wilson, S., Griffith, D. W. T., Wang, W. J., Salter, B., White, I., & Moody, P. W. (2010). Emissions of methane and nitrous oxide from Australian sugarcane soils. *Agricultural and Forest Meteorology*, *150*(6), 748-756. https://doi.org/10.1016/j.agrformet.2009.06.018

do Carmo, J. B., Filoso, S., Zotelli, L. C., de Sousa Neto, E. R., Pitombo, L. M., Duarte-Neto, P. J., Vargas, V. P., Andrade, C. A., Gava, G. J. C., Rossetto, R., Cantarella, H., Neto, A. E., & Martinelli, L. A. (2013). Infield greenhouse gas emissions from sugarcane soils in Brazil: effects from synthetic and organic fertilizer application and crop trash accumulation. *Global Change Biology Bioenergy*, *5*(3), 267-280. https://doi.org/10.1111/j.1757-1707.2012.01199.x

Drury, C. F., Yang, X. M., Reynolds, W. D., & McLaughlin, N. B. (2008). Nitrous oxide and carbon dioxide emissions from monoculture and rotational cropping of corn, soybean and winter wheat. *Canadian Journal of Soil Science*, *88*(2), 163-174. https://doi.org/10.4141/cjss06015

Dusenbury, M. P., Engel, R. E., Miller, P. R., Lemke, R. L., & Wallander, R. (2008). Nitrous oxide emissions from a northern great plains soil as influenced by nitrogen management and cropping systems. *Journal of Environmental Quality*, *37*(2), 542-550. https://doi.org/10.2134/jeq2006.0395

Ehrhardt, F., Soussana, J.-F., Bellocchi, G., Grace, P., McAuliffe, R., Recous, S., Sandor, R., Smith, P., Snow, V., Migliorati, M. d. A., Basso, B., Bhatia, A., Brilli, L., Doltra, J., Dorich, C. D., Doro, L., Fitton, N., Giacomini, S. J., Grant, B., . . . Zhang, Q. (2018). Assessing uncertainties in crop and pasture ensemble model simulations of productivity and N2O emissions. *Global Change Biology*, *24*(2), E603-E616. https://doi.org/10.1111/gcb.13965

Ellert, B. H., & Janzen, H. H. (2008). Nitrous oxide, carbon dioxide and methane emissions from irrigated cropping systems as influenced by legumes, manure and fertilizer. *Canadian Journal of Soil Science*, *88*(2), 207-217. https://doi.org/10.4141/cjss06036

Fan, C., Chen, H., Li, B., & Xiong, Z. (2017). Biochar reduces yield-scaled emissions of reactive nitrogen gases from vegetable soils across China. *Biogeosciences*, *14*(11), 2851-2863. https://doi.org/10.5194/bg-14-2851-2017

Farquharson, R., & Baldock, J. (2008). Concepts in modelling N2O emissions from land use. *Plant and Soil*, *309*(1-2), 147-167. https://doi.org/10.1007/s11104-007-9485-0

Forte, A., Fiorentino, N., Fagnano, M., & Fierro, A. (2017). Mitigation impact of minimum tillage on CO2 and N2O emissions from a Mediterranean maize cropped soil under low-water input management. *Soil & Tillage Research*, *166*, 167-178. https://doi.org/10.1016/j.still.2016.09.014

Francis Clar, J. T., & Anex, R. P. (2020). Flux intensity and diurnal variability of soil N2O emissions in a highly fertilized cropping system. *Soil Science Society of America Journal*, *84*(6), 1983-1994. https://doi.org/https://doi.org/10.1002/saj2.20132

Galbally, I. E., Meyer, M. C. P., Wang, Y.-P., Smith, C. J., & Weeks, I. A. (2010). Nitrous oxide emissions from a legume pasture and the influences of liming and urine addition. *Agriculture Ecosystems & Environment*, *136*(3-4), 262-272. https://doi.org/10.1016/j.agee.2009.10.013

Gelfand, I., Shcherbak, I. I., Millar, N., Kravchenko, A. N., & Robertson, G. P. (2016). Long-term nitrous oxide fluxes in annual and perennial agricultural and unmanaged ecosystems in the upper Midwest USA. *Global Change Biology*, *22*(11), 3594-3607. https://doi.org/10.1111/gcb.13426

Gerber, J. S., Carlson, K. M., Makowski, D., Mueller, N. D., de Cortazar-Atauri, I. G., Havlik, P., Herrero, M., Launay, M., O'Connell, C. S., Smith, P., & West, P. C. (2016). Spatially explicit estimates of N2O emissions from croplands suggest climate mitigation opportunities from improved fertilizer management. *Global Change Biology*, *22*(10), 3383-3394. https://doi.org/10.1111/gcb.13341

Giltrap, D., Yeluripati, J., Smith, P., Fitton, N., Smith, W., Grant, B., Dorich, C. D., Deng, J., Topp, C. F., Abdalla, M., Liáng, L. L., & Snow, V. (2020). Global Research Alliance N2O chamber methodology guidelines: Summary of modeling approaches. *J Environ Qual*, *49*(5), 1168-1185. https://doi.org/https://doi.org/10.1002/jeq2.20119

Giltrap, D. L., Li, C., & Saggar, S. (2010). DNDC: A process-based model of greenhouse gas fluxes from agricultural soils. *Agriculture Ecosystems & Environment*, *136*(3-4), 292-300. https://doi.org/10.1016/j.agee.2009.06.014

Godsey, C. B., Pierzynski, G. M., Mengel, D. B., & Lamond, R. E. (2007). Changes in soil pH, organic carbon, and extractable aluminum from crop rotation and tillage. *Soil Science Society of America Journal*, *71*(3), 1038-1044. https://doi.org/10.2136/sssaj2006.0170

Goldewijk, K. K., Beusen, A., Doelman, J., & Stehfest, E. (2017). Anthropogenic land use estimates for the Holocene - HYDE 3.2. *Earth System Science Data*, *9*(2), 927-953. https://doi.org/10.5194/essd-9-927-2017

Groffman, P. M., Hardy, J. P., Driscoll, C. T., & Fahey, T. J. (2006). Snow depth, soil freezing, and fluxes of carbon dioxide, nitrous oxide and methane in a northern hardwood forest. *Global Change Biology*, *12*(9), 1748-1760. https://doi.org/10.1111/j.1365-2486.2006.01194.x

Gu, J., Nicoullaud, B., Rochette, P., Grossel, A., Henault, C., Cellier, P., & Richard, G. (2013). A regional experiment suggests that soil texture is a major control of N2O emissions from tile-drained winter wheat fields during the fertilization period. *Soil Biology & Biochemistry*, *60*, 134-141. https://doi.org/10.1016/j.soilbio.2013.01.029

Gu, J., Zheng, X., & Zhang, W. (2009). Background nitrous oxide emissions from croplands in China in the year 2000. *Plant and Soil*, *320*(1-2), 307-320. https://doi.org/10.1007/s11104-009-9896-1

Guo, H., Li, G., Zhang, D., Zhang, X., & Lu, C. a. (2007). Nitrogen balance and dynamics as affected by water table and fertilization management in celery (Apium graveolens) cropping system of southwestern China. *African Journal of Agricultural Research*, *2*(4), 139-149. <Go to ISI>://WOS:000259903800003

Guo, J. H., Liu, X. J., Zhang, Y., Shen, J. L., Han, W. X., Zhang, W. F., Christie, P., Goulding, K. W. T., Vitousek, P. M., & Zhang, F. S. (2010). Significant Acidification in Major Chinese Croplands. *Science*, *327*(5968), 1008-1010. https://doi.org/10.1126/science.1182570

Guo, Y., Luo, L., Chen, G., Kou, Y., & Xu, H. (2013). Mitigating nitrous oxide emissions from a maize-cropping black soil in northeast China by a combination of reducing chemical N fertilizer application and applying manure in autumn. *Soil Science and Plant Nutrition*, *59*(3), 392-402. https://doi.org/10.1080/00380768.2013.775006

Hadi, A., Jumadi, O., Inubushi, K., & Yagi, K. (2008). Mitigation options for N2O emission from a corn field in Kalimantan, Indonesia. *Soil Science and Plant Nutrition*, *54*(4), 644-649. https://doi.org/10.1111/j.1747-0765.2008.00280.x

Hall, S. J., McDowell, W. H., & Silver, W. L. (2013). When Wet Gets Wetter: Decoupling of Moisture, Redox Biogeochemistry, and Greenhouse Gas Fluxes in a Humid Tropical Forest Soil. *Ecosystems*, *16*(4), 576-589. https://doi.org/10.1007/s10021-012-9631-2

Hayakawa, A., Akiyama, H., Sudo, S., & Yagi, K. (2009). N2O and NO emissions from an Andisol field as influenced by pelleted poultry manure. *Soil Biology & Biochemistry*, *41*(3), 521-529. https://doi.org/10.1016/j.soilbio.2008.12.011

Heinen, M. (2006). Simplified denitrification models: Overview and properties. *Geoderma*, *133*(3-4), 444-463. https://doi.org/10.1016/j.geoderma.2005.06.010

Heller, H., Bar-Tal, A., Tamir, G., Bloom, P., Venterea, R. T., Chen, D., Zhang, Y., Clapp, C. E., & Fine, P. (2010). Effects of Manure and Cultivation on Carbon Dioxide and Nitrous Oxide Emissions from a Corn Field under Mediterranean Conditions. *Journal of Environmental Quality*, *39*(2), 437-448. https://doi.org/10.2134/jeq2009.0027

Hoben, J. P., Gehl, R. J., Millar, N., Grace, P. R., & Robertson, G. P. (2011). Nonlinear nitrous oxide (N2O) response to nitrogen fertilizer in on-farm corn crops of the US Midwest. *Global Change Biology*, *17*(2), 1140-1152. https://doi.org/10.1111/j.1365-2486.2010.02349.x

Huerfano, X., Maria Estavillo, J., Fuertes-Mendizabal, T., Torralbo, F., Gonzalez-Murua, C., & Menendez, S. (2018). DMPSA and DMPP equally reduce N2O emissions from a maize-ryegrass forage rotation under Atlantic climate conditions. *Atmospheric Environment*, *187*, 255-265. https://doi.org/10.1016/j.atmosenv.2018.05.065

Hunt, D. E., Bittman, S., Zhang, H., Bhandral, R., Grant, C. A., & Lemke, R. (2016). Effect of polymer-coated urea on nitrous oxide emission in zero-till and conventionally tilled silage corn. *Canadian Journal of Soil Science*, *96*(1), 12-22. https://doi.org/10.1139/cjss-2015-0071

IPCC. (2021). *Climate Change 2021: The Physical Science Basis. Contribution of Working Group I to the Sixth Assessment Report of the Intergovernmental Panel on Climate Change* (Vol. In Press). Cambridge University Press. https://doi.org/10.1017/9781009157896

Ito, A., Nishina, K., Ishijima, K., Hashimoto, S., & Inatomi, M. (2018). Emissions of nitrous oxide (N2O) from soil surfaces and their historical changes in East Asia: a model-based assessment. *Progress in Earth and Planetary Science*, *5*. https://doi.org/10.1186/s40645-018-0215-4

Jain, N., Arora, P., Tomer, R., Mishra, S. V., Bhatia, A., Pathak, H., Chakraborty, D., Kumar, V., Dubey, D. S., Harit, R. C., & Singha, J. P. (2016). Greenhouse gases emission from soils under major crops in Northwest India. *Science of the Total Environment*, *542*, 551-561. https://doi.org/10.1016/j.scitotenv.2015.10.073

Jantalia, C. P., dos Santos, H. P., Urquiaga, S., Boddey, R. M., & Alves, B. J. R. (2008). Fluxes of nitrous oxide from soil under different crop rotations and tillage systems in the South of Brazil. *Nutrient Cycling in Agroecosystems*, *82*(2), 161-173. https://doi.org/10.1007/s10705-008-9178-y

Jiang, G., Zhang, W., Xu, M., Kuzyakov, Y., Zhang, X., Wang, J., Di, J., & Murphy, D. V. (2018). Manure and Mineral Fertilizer Effects on Crop Yield and Soil Carbon Sequestration: A Meta-Analysis and Modeling Across China. *Global Biogeochemical Cycles*, *32*(11), 1659-1672. https://doi.org/10.1029/2018gb005960

Jones, S. K., Famulari, D., Di Marco, C. F., Nemitz, E., Skiba, U. M., Rees, R. M., & Sutton, M. A. (2011). Nitrous oxide emissions from managed grassland: a comparison of eddy covariance and static chamber measurements. *Atmos. Meas. Tech.*, *4*(10), 2179-2194. https://doi.org/10.5194/amt-4-2179-2011

Kavdir, Y., Hellebrand, H. J., & Kern, J. (2008). Seasonal variations of nitrous oxide emission in relation to nitrogen fertilization and energy crop types in sandy soil. *Soil & Tillage Research*, *98*(2), 175-186. https://doi.org/10.1016/j.still.2007.11.002

Kennedy, T. L., Suddick, E. C., & Six, J. (2013). Reduced nitrous oxide emissions and increased yields in California tomato cropping systems under drip irrigation and fertigation. *Agriculture Ecosystems & Environment*, *170*, 16-27. https://doi.org/10.1016/j.agee.2013.02.002

Kim, D. G., Vargas, R., Bond-Lamberty, B., & Turetsky, M. R. (2012). Effects of soil rewetting and thawing on soil gas fluxes: a review of current literature and suggestions for future research. *Biogeosciences*, *9*(7), 2459-2483. https://doi.org/10.5194/bg-9-2459-2012

Klemedtsson, A. K., & Smith, K. A. (2011). The significance of nitrous oxide emission due to cropping of grain for biofuel production: a Swedish perspective. *Biogeosciences*, *8*(12), 3581-3591. https://doi.org/10.5194/bg-8-3581-2011

Kronzucker, H. J., Siddiqi, M. Y., & Glass, A. D. M. (1997). Conifer root discrimination against soil nitrate and the ecology of forest succession. *Nature*, *385*(6611), 59-61. https://doi.org/10.1038/385059a0

Kuang, W., Gao, X., Gui, D., Tenuta, M., Flaten, D. N., Yin, M., & Zeng, F. (2018). Effects of fertilizer and irrigation management on nitrous oxide emission from cotton fields in an extremely arid region of northwestern China. *Field Crops Research*, *229*, 17-26. https://doi.org/10.1016/j.fcr.2018.09.010

Kuang, W., Gao, X., Tenuta, M., & Zeng, F. (2021). A global meta-analysis of nitrous oxide emission from drip-irrigated cropping system. *Global Change Biology*, *27*(14), 3244-3256. https://doi.org/https://doi.org/10.1111/gcb.15636

Kucharik, C. J., Foley, J. A., Delire, C., Fisher, V. A., Coe, M. T., Lenters, J. D., Young-Molling, C., Ramankutty, N., Norman, J. M., & Gower, S. T. (2000). Testing the performance of a Dynamic Global Ecosystem Model: Water balance, carbon balance, and vegetation structure. *Global Biogeochemical Cycles*, *14*(3), 795-825. https://doi.org/10.1029/1999gb001138

LaHue, G. T., van Kessel, C., Linquist, B. A., Adviento-Borbe, M. A., & Fonte, S. J. (2016). Residual Effects of Fertilization History Increase Nitrous Oxide Emissions from Zero-N Controls: Implications for Estimating Fertilizer-Induced Emission Factors. *J Environ Qual*, *45*(5), 1501-1508. https://doi.org/10.2134/jeq2015.07.0409

Lammirato, C., Lebender, U., Tierling, J., & Lammel, J. (2018). Analysis of uncertainty for N2O fluxes measured with the closed-chamber method under field conditions: Calculation method, detection limit, and spatial variability. *Journal of Plant Nutrition and Soil Science*, *181*(1), 78-89. https://doi.org/10.1002/jpln.201600499

Laville, P., Lehuger, S., Loubet, B., Chaumartin, F., & Cellier, P. (2011). Effect of management, climate and soil conditions on N2O and NO emissions from an arable crop rotation using high temporal resolution measurements. *Agricultural and Forest Meteorology*, *151*(2), 228-240. https://doi.org/10.1016/j.agrformet.2010.10.008

Lelieveld, J., & Dentener, F. J. (2000). What controls tropospheric ozone? *Journal of Geophysical Research-Atmospheres*, *105*(D3), 3531-3551. https://doi.org/10.1029/1999jd901011

Lemke, R. L., Izaurralde, R. C., Nyborg, M., & Solberg, E. D. (1999). Tillage and N source influence soil-emitted nitrous oxide in the Alberta Parkland region. *Canadian Journal of Soil Science*, *79*(1), 15-24. https://doi.org/10.4141/s98-013

Lenka, S., Lenka, N. K., Singh, A. B., Singh, B., & Raghuwanshi, J. (2017). Global warming potential and greenhouse gas emission under different soil nutrient management practices in soybean- wheat system of central India. *Environmental Science and Pollution Research*, *24*(5), 4603-4612. https://doi.org/10.1007/s11356-016-8189-5

Li, C. S., Aber, J., Stange, F., Butterbach-Bahl, K., & Papen, H. (2000). A process-oriented model of N2O and NO emissions from forest soils: 1. Model development. *Journal of Geophysical Research-Atmospheres*, *105*(D4), 4369-4384. https://doi.org/10.1029/1999jd900949

Li, G., Conyers, M., Schwenke, G., Hayes, R., Liu, D. L., Lowrie, A., Poile, G., Oates, A., & Lowrie, R. (2016). Tillage does not increase nitrous oxide emissions under dryland canola (Brassica napus L.) in a semi-arid environment of south-eastern Australia. *Soil Research*, *54*(5), In press.

Li, H., Qiu, J., Wang, L., Tang, H., Li, C., & Van Ranst, E. (2010). Modelling impacts of alternative farming management practices on greenhouse gas emissions from a winter wheat-maize rotation system in China. *Agriculture Ecosystems & Environment*, *135*(1-2), 24-33. https://doi.org/10.1016/j.agee.2009.08.003

Li, Y., Barton, L., & Chen, D. (2012). Simulating response of N2O emissions to fertiliser N application and climatic variability from a rain-fed and wheat-cropped soil in Western Australia. *Journal of the Science of Food and Agriculture*, *92*(5), 1130-1143. https://doi.org/10.1002/jsfa.4643

Lin, S., Iqbal, J., Hu, R., Ruan, L., Wu, J., Zhao, J., & Wang, P. (2012). Differences in nitrous oxide fluxes from red soil under different land uses in mid-subtropical China. *Agriculture Ecosystems & Environment*, *146*(1), 168-178. https://doi.org/10.1016/j.agee.2011.10.024

Liu, C., Lu, M., Cui, J., Li, B., & Fang, C. (2014). Effects of straw carbon input on carbon dynamics in agricultural soils: a meta-analysis. *Global Change Biology*, *20*(5), 1366-1381. https://doi.org/10.1111/gcb.12517

Liu, J., You, L., Amini, M., Obersteiner, M., Herrero, M., Zehnder, A. J. B., & Yang, H. (2010). A high-resolution assessment on global nitrogen flows in cropland. *Proceedings of the National Academy of Sciences*, *107*(17), 8035-8040. https://doi.org/10.1073/pnas.0913658107

Liu, J. X., Price, D. T., & Chen, J. A. (2005). Nitrogen controls on ecosystem carbon sequestration: a model implementation and application to Saskatchewan, Canada. *Ecological Modelling*, *186*(2), 178-195. https://doi.org/10.1016/j.ecolmodel.2005.01.036

Lognoul, M., Debacq, A., De Ligne, A., Dumont, B., Manise, T., Bodson, B., Heinesch, B., & Aubinet, M. (2019). N2O flux short-term response to temperature and topsoil disturbance in a fertilized crop: An eddy covariance campaign. *Agricultural and Forest Meteorology*, *271*, 193-206. https://doi.org/10.1016/j.agrformet.2019.02.033

Lourenco, K. S., Rossetto, R., Vitti, A. C., Montezano, Z. F., Soares, J. R., Sousa, R. d. M., do Carmo, J. B., Kuramae, E. E., & Cantarella, H. (2019). Strategies to mitigate the nitrous oxide emissions from nitrogen fertilizer applied with organic fertilizers in sugarcane. *Science of the Total Environment*, *650*, 1476-1486. https://doi.org/10.1016/j.scitotenv.2018.09.037

Lu, C., & Tian, H. (2017). Global nitrogen and phosphorus fertilizer use for agriculture production in the past half century: shifted hot spots and nutrient imbalance. *Earth System Science Data*, *9*(1), 181-192. https://doi.org/10.5194/essd-9-181-2017

Lugato, E., Zuliani, M., Alberti, G., Delle Vedove, G., Gioli, B., Miglietta, F., & Peressotti, A. (2010). Application of DNDC biogeochemistry model to estimate greenhouse gas emissions from Italian agricultural areas at high spatial resolution. *Agriculture Ecosystems & Environment*, *139*(4), 546-556. https://doi.org/10.1016/j.agee.2010.09.015

Luo, Z., Wang, E., & Sun, O. J. (2010). Can no-tillage stimulate carbon sequestration in agricultural soils? A meta-analysis of paired experiments. *Agriculture Ecosystems & Environment*, *139*(1-2), 224-231. https://doi.org/10.1016/j.agee.2010.08.006

Malhi, S. S., Nyborg, M., Jahn, H. G., & Penney, D. C. (1988). Yield and nitrogen uptake of rapessed (Brassica campestris L.) with ammonium and nitrate. *Plant and Soil*, *105*(2), 231-239. https://doi.org/10.1007/BF02376787

Mapanda, F., Wuta, M., Nyamangara, J., & Rees, R. M. (2011). Effects of organic and mineral fertilizer nitrogen on greenhouse gas emissions and plant-captured carbon under maize cropping in Zimbabwe. *Plant and Soil*, *343*(1-2), 67-81. https://doi.org/10.1007/s11104-011-0753-7

Mei, K., Wang, Z., Huang, H., Zhang, C., Shang, X., Dahlgren, R. A., Zhang, M., & Xia, F. (2018). Stimulation of N2O emission by conservation tillage management in agricultural lands: A meta-analysis. *Soil & Tillage Research*, *182*, 86-93. https://doi.org/10.1016/j.still.2018.05.006

Meijide, A., Díez, J. A., Sánchez-Martín, L., López-Fernández, S., & Vallejo, A. (2007). Nitrogen oxide emissions from an irrigated maize crop amended with treated pig slurries and composts in a Mediterranean climate. *Agriculture Ecosystems & Environment*, *121*(4), 383-394.

Meng, L., Ding, W. X., & Cai, Z. C. (2005). Long-term application of organic manure and nitrogen fertilizer on N2O emissions, soil quality and crop production in a sandy loam soil. *Soil Biology & Biochemistry*, *37*(11), 2037-2045. https://doi.org/10.1016/j.soilbio.2005.03.007

Millar, N., Urrea, A., Kahmark, K., Shcherbak, I., Robertson, G. P., & Ortiz-Monasterio, I. (2018). Nitrous oxide (N2O) flux responds exponentially to nitrogen fertilizer in irrigated wheat in the Yaqui Valley, Mexico. *Agriculture Ecosystems & Environment*, *261*, 125-132. https://doi.org/10.1016/j.agee.2018.04.003

Monfreda, C., Ramankutty, N., & Foley, J. A. (2008). Farming the planet: 2. Geographic distribution of crop areas, yields, physiological types, and net primary production in the year 2000. *Global Biogeochemical Cycles*, *22*(1), Article Gb1022. https://doi.org/10.1029/2007gb002947

Morkved, P. T., Dorsch, P., & Bakken, L. R. (2007). The N2O product ratio of nitrification and its dependence on long-term changes in soil pH. *Soil Biology & Biochemistry*, *39*(8), 2048-2057. https://doi.org/10.1016/j.soilbio.2007.03.006

Mosier, A., Kroeze, C., Nevison, C., Oenema, O., Seitzinger, S., & Cleemput, O. (1998). Closing the Global N2O Budget: Nitrous Oxide Emissions through the Agricultural Nitrogen Cycle. *Nutrient Cycling in Agroecosystems*, *52*, 225–248. https://doi.org/10.1023/A:1009740530221

Mosier, A. R., Halvorson, A. D., Reule, C. A., & Liu, X. J. (2006). Net global warming potential and greenhouse gas intensity in irrigated cropping systems in northeastern Colorado. *Journal of Environmental Quality*, *35*(4), 1584-

1598. https://doi.org/10.2134/jeq2005.0232

Mumford, M. T., Rowlings, D. W., Scheer, C., De Rosa, D., & Grace, P. R. (2019). Effect of irrigation scheduling on nitrous oxide emissions in intensively managed pastures. *Agriculture, Ecosystems & Environment*, *272*, 126-134. https://doi.org/https://doi.org/10.1016/j.agee.2018.11.011

Nadeem, S., Borresen, T., & Dorsch, P. (2015). Effect of fertilization rate and ploughing time on nitrous oxide emissions in a long-term cereal trail in south east Norway. *Biology and Fertility of Soils*, *51*(3), 353-365. https://doi.org/10.1007/s00374-014-0979-7

Nishina, K., Ito, A., Hanasaki, N., & Hayashi, S. (2017). Reconstruction of spatially detailed global map of NH4+ and NO3- application in synthetic nitrogen fertilizer. *Earth System Science Data*, *9*(1), 149-162. https://doi.org/10.1594/pangaea.861203

Norman, J., Jansson, P.-E., Farahbakhshazad, N., Butterbach-Bahl, K., Li, C., & Klemedtsson, L. (2008). Simulation of NO and N2O emissions from a spruce forest during a freeze/thaw event using an N-flux submodel from the PnET-N-DNDC model integrated to CoupModel. *Ecological Modelling*, *216*(1), 18-30. https://doi.org/10.1016/j.ecolmodel.2008.04.012

Norton, J. (2015). An introduction to sensitivity assessment of simulation models. *Environmental Modelling & Software*, *69*, 166-174. https://doi.org/10.1016/j.envsoft.2015.03.020

Oehler, F., Rutherford, J. C., & Coco, G. (2010). The use of machine learning algorithms to design a generalized simplified denitrification model. *Biogeosciences*, *7*(10), 3311-3332. https://doi.org/10.5194/bg-7-3311-2010

Ogejo, J. A., Senger, R. S., & Zhang, R. H. (2010). Global sensitivity analysis of a process-based model for ammonia emissions from manure storage and treatment structures. *Atmospheric Environment*, *44*(30), 3621-3629. https://doi.org/https://doi.org/10.1016/j.atmosenv.2010.06.053

Omonode, R. A., Smith, D. R., Gal, A., & Vyn, T. J. (2011). Soil Nitrous Oxide Emissions in Corn following Three Decades of Tillage and Rotation Treatments. *Soil Science Society of America Journal*, *75*(1), 152-163. https://doi.org/10.2136/sssaj2009.0147

Pappas, C., Fatichi, S., Leuzinger, S., Wolf, A., & Burlando, P. (2013). Sensitivity analysis of a process-based ecosystem model: Pinpointing parameterization and structural issues [https://doi.org/10.1002/jgrg.20035]. *Journal of Geophysical Research: Biogeosciences*, *118*(2), 505-528. https://doi.org/https://doi.org/10.1002/jgrg.20035

Parton, W. J., Mosier, A. R., Ojima, D. S., Valentine, D. W., & Kulmala, A. E. (1996). Generalized model for N2 and N2O production from nitrification and denitrification. *Global Biogeochemical Cycles*, *10*(3), 401-412.

Passianoto, C. C., Ahrens, T., Feigl, B. J., Steudler, P. A., do Carmo, J. B., & Melillo, J. M. (2003). Emissions of CO(2), N(2)O, and NO in conventional and no-till management practices in Rondonia, Brazil. *Biology and Fertility of Soils*, *38*(4), 200-208. https://doi.org/10.1007/s00374-003-0653-y

Pelster, D. E., Larouche, F., Rochette, P., Chantigny, M. H., Allaire, S., & Angers, D. A. (2011). Nitrogen fertilization but not soil tillage affects nitrous oxide emissions from a clay loam soil under a maize–soybean rotation. *Soil & Tillage Research*, *115*(5), 16-26.

Perlman, J., Hijmans, R. J., & Horwath, W. R. (2014). A metamodelling approach to estimate global N2O emissions from agricultural soils. *Global Ecology and Biogeography*, *23*(8), 912-924. https://doi.org/10.1111/geb.12166

Peyrard, C., Mary, B., Perrin, P., Vericel, G., Grehan, E., Justes, E., & Leonard, J. (2016). N2O emissions of low input cropping systems as affected by legume and cover crops use. *Agriculture Ecosystems & Environment*, *224*, 145-156. https://doi.org/10.1016/j.agee.2016.03.028

Pfab, H., Palmer, I., Buegger, F., Fiedler, S., Mueller, T., & Ruser, R. (2012). Influence of a nitrification inhibitor and of placed N-fertilization on N2O fluxes from a vegetable cropped loamy soil. *Agriculture Ecosystems & Environment*, *150*, 91-101. https://doi.org/10.1016/j.agee.2012.01.001

Philibert, A., Loyce, C., & Makowski, D. (2013). Prediction of N2O emission from local information with Random Forest.

Environmental Pollution, *177*, 156-163. https://doi.org/10.1016/j.envpol.2013.02.019

Plaza-Bonilla, D., Alvaro-Fuentes, J., Bareche, J., Pareja-Sanchez, E., Justes, E., & Cantero-Martinez, C. (2018). No-tillage reduces long-term yield-scaled soil nitrous oxide emissions in rainfed Mediterranean agroecosystems: A field and modelling approach. *Agriculture Ecosystems & Environment*, *262*, 36-47. https://doi.org/10.1016/j.agee.2018.04.007

Powlson, D. S., Stirling, C. M., Jat, M. L., Gerard, B. G., Palm, C. A., Sanchez, P. A., & Cassman, K. G. (2014). Limited potential of no-till agriculture for climate change mitigation. *Nature Climate Change*, *4*(8), 678-683. https://doi.org/10.1038/nclimate2292

Rabot, E., Cousin, I., & Henault, C. (2015). A modeling approach of the relationship between nitrous oxide fluxes from soils and the water-filled pore space. *Biogeochemistry*, *122*(2-3), 395-408. https://doi.org/10.1007/s10533-014-0048-1

Ramu, K., Watanabe, T., Uchino, H., Sahrawat, K. L., Wani, S. P., & Ito, O. (2012). Fertilizer induced nitrous oxide emissions from Vertisols and Alfisols during sweet sorghum cultivation in the Indian semi-arid tropics. *Science of the Total Environment*, *438*, 9-14. https://doi.org/10.1016/j.scitotenv.2012.08.005

Reay, D. S., Davidson, E. A., Smith, K. A., Smith, P., Melillo, J. M., Dentener, F., & Crutzen, P. J. (2012). Global agriculture and nitrous oxide emissions. *Nature Climate Change*, *2*(6), 410-416. https://doi.org/10.1038/nclimate1458

Regina, K., Syväsalo, E., Hannukkala, A., & Esala, M. (2004). Fluxes of N2O from farmed peat soils in Finland. *European Journal of Soil Science*, *55*(3), 591-599. https://doi.org/10.1111/j.1365-2389.2004.00622.x

Rochette, P. (2008). No-till only increases N2O emissions in poorly-aerated soils. *Soil & Tillage Research*, *101*(1-2), 97-100. https://doi.org/10.1016/j.still.2008.07.011

Rochette, P., Angers, D. A., Chantigny, M. H., & Bertrand, N. (2008). Nitrous oxide emissions respond differently to no-till in a loam and a heavy clay soil. *Soil Science Society of America Journal*, *72*(5), 1363-1369. https://doi.org/10.2136/sssaj2007.0371

Rochette, P., Angers, D. A., Chantigny, M. H., Gagnon, B., & Bertrand, N. (2008). N2O fluxes in soils of contrasting textures fertilized with liquid and solid dairy cattle manures. *Canadian Journal of Soil Science*, *88*(2), 175-187. https://doi.org/10.4141/cjss06016

Rochette, P., Tremblay, N., Fallon, E., Angers, D. A., Chantigny, M. H., MacDonald, J. D., Bertrand, N., & Parent, L. E. (2010). N2O emissions from an irrigated and non-irrigated organic soil in eastern Canada as influenced by N fertilizer addition. *European Journal of Soil Science*, *61*(2), 186-196. https://doi.org/10.1111/j.1365-2389.2009.01222.x

Rosenstock, T. S., Mpanda, M., Pelster, D. E., Butterbach-Bahl, K., Rufino, M. C., Thiong'o, M., Mutuo, P., Abwanda, S., Rioux, J., Kimaro, A. A., & Neufeldt, H. (2016). Greenhouse gas fluxes from agricultural soils of Kenya and Tanzania. *Journal of Geophysical Research-Biogeosciences*, *121*(6), 1568-1580. https://doi.org/10.1002/2016jg003341

Rowlings, D. W., Grace, P. R., Scheer, C., & Kiese, R. (2013). Influence of nitrogen fertiliser application and timing on greenhouse gas emissions from a lychee (Litchi chinensis) orchard in humid subtropical Australia. *Agriculture Ecosystems & Environment*, *179*, 168-178. https://doi.org/10.1016/j.agee.2013.08.013

Sacks, W. J., Deryng, D., Foley, J. A., & Ramankutty, N. (2010). Crop planting dates: an analysis of global patterns. *Global Ecology and Biogeography*, *19*(5), 607-620. https://doi.org/10.1111/j.1466-8238.2010.00551.x

Sadeghi, S. M., Noorhosseini, S. A., & Damalas, C. A. (2018). Environmental sustainability of corn (Zea mays L.) production on the basis of nitrogen fertilizer application: The case of Lahijan, Iran. *Renewable & Sustainable Energy Reviews*, *95*, 48-55. https://doi.org/10.1016/j.rser.2018.07.005

Saikawa, E., Schlosser, C. A., & Prinn, R. G. (2013). Global modeling of soil nitrous oxide emissions from natural processes. *Global Biogeochemical Cycles*, *27*(3), 972-989. https://doi.org/10.1002/gbc.20087

Sakata, R., Shimada, S., Arai, H., Yoshioka, N., Yoshioka, R., Aoki, H., Kimoto, N., Sakamoto, A., Melling, L., & Inubushi, K. (2015). Effect of soil types and nitrogen fertilizer on nitrous oxide and carbon dioxide emissions in oil palm plantations. *Soil Science and Plant Nutrition*, *61*(1), 48-60. https://doi.org/10.1080/00380768.2014.960355

Sanz-Cobena, A., Sanchez-Martin, L., Garcia-Torres, L., & Vallejo, A. (2012). Gaseous emissions of N2O and NO and NO3- leaching from urea applied with urease and nitrification inhibitors to a maize (Zea mays) crop. *Agriculture Ecosystems & Environment*, *149*, 64-73. https://doi.org/10.1016/j.agee.2011.12.016

Scheer, C., Grace, P. R., Rowlings, D. W., & Payero, J. (2012). Nitrous oxide emissions from irrigated wheat in Australia: impact of irrigation management. *Plant and Soil*, *359*(1-2), 351-362. https://doi.org/10.1007/s11104-012-1197-4

Scheer, C., Grace, P. R., Rowlings, D. W., & Payero, J. (2013). Soil N2O and CO2 emissions from cotton in Australia under varying irrigation management. *Nutrient Cycling in Agroecosystems*, *95*(1), 43-56. https://doi.org/10.1007/s10705-012-9547-4

Scheer, C., Rowlings, D. W., & Grace, P. R. (2016). Non-linear response of soil N2O emissions to nitrogen fertiliser in a cotton-fallow rotation in sub-tropical Australia. *Soil Research*, *54*(5), 494-499. https://doi.org/10.1071/sr14328

Scheer, C., Wassmann, R., Kienzler, K., Ibragimov, N., Lamers, J. P. A., & Martius, C. (2008). Methane and nitrous oxide fluxes in annual and perennial land-use systems of the irrigated areas in the Aral Sea Basin. *Global Change Biology*, *14*(10), 2454-2468. https://doi.org/10.1111/j.1365-2486.2008.01631.x

Schellenberg, D. L., Alsina, M. M., Muhammad, S., Stockert, C. M., Wolff, M. W., Sanden, B. L., Brown, P. H., & Smart, D. R. (2012). Yield-scaled global warming potential from N2O emissions and CH4 oxidation for almond (Prunus dulcis) irrigated with nitrogen fertilizers on arid land. *Agriculture Ecosystems & Environment*, *155*, 7-15. https://doi.org/10.1016/j.agee.2012.03.008

Sebilo, M., Mayer, B., Nicolardot, B., Pinay, G., & Mariotti, A. (2013). Long-term fate of nitrate fertilizer in agricultural soils. *Proceedings of the National Academy of Sciences of the United States of America*, *110*(45), 18185-18189. https://doi.org/10.1073/pnas.1305372110

Senapati, N., Chabbi, A., Giostri, A. F., Yeluripati, J. B., & Smith, P. (2016). Modelling nitrous oxide emissions from mown-grass and grain-cropping systems: Testing and sensitivity analysis of DailyDayCent using high frequency measurements. *Science of the Total Environment*, *572*, 955-977. https://doi.org/10.1016/j.scitotenv.2016.07.226

Sharma, S., Szele, Z., Schilling, R., Munch, J. C., & Schloter, M. (2006). Influence of freeze-thaw stress on the structure and function of microbial communities and denitrifying populations in soil. *Applied and Environmental Microbiology*, *72*(3), 2148-2154. https://doi.org/10.1128/aem.72.3.2148-2154.2006

Shcherbak, I., Millar, N., & Robertson, G. P. (2014). Global metaanalysis of the nonlinear response of soil nitrous oxide (N2O) emissions to fertilizer nitrogen. *Proceedings of the National Academy of Sciences of the United States of America*, *111*(25), 9199-9204. https://doi.org/10.1073/pnas.1322434111

Simojoki, A., & Jaakkola, A. (2000). Effect of nitrogen fertilization, cropping and irrigation on soil air composition and nitrous oxide emission in a loamy clay. *European Journal of Soil Science*, *51*(3), 413-424. https://doi.org/10.1046/j.1365-2389.2000.00308.x

Smith, K. A., & Dobbie, K. E. (2001). The impact of sampling frequency and sampling times on chamber-based measurements of N2O emissions from fertilized soils. *Global Change Biology*, *7*(8), 933-945. https://doi.org/10.1046/j.1354-1013.2001.00450.x

Snowdon, E., Zebarth, B. J., Burton, D. L., Goyer, C., & Rochette, P. (2013). Growing season N2O emissions from two-year potato rotations in a humid environment in New Brunswick, Canada. *Canadian Journal of Soil Science*, *93*(3), 279-294. https://doi.org/10.4141/cjss2012-115

Snyder, C. S., Bruulsema, T. W., Jensen, T. L., & Fixen, P. E. (2009). Review of greenhouse gas emissions from crop production systems and fertilizer management effects. *Agriculture Ecosystems & Environment*, *133*(3-4), 247-266. https://doi.org/10.1016/j.agee.2009.04.021

Soares, J. R., Cantarella, H., Vargas, V. P., Carmo, J. B., Martins, A. A., Sousa, R. M., & Andrade, C. A. (2015). Enhanced-Efficiency Fertilizers in Nitrous Oxide Emissions from Urea Applied to Sugarcane. *Journal of Environmental Quality*, *44*(2), 423-430. https://doi.org/10.2134/jeq2014.02.0096

Song, X., Ju, X., Topp, C. F. E., & Rees, R. M. (2019). Oxygen Regulates Nitrous Oxide Production Directly in Agricultural Soils. *Environmental Science & Technology*, *53*(21), 12539-12547. https://doi.org/10.1021/acs.est.9b03089

Sosulski, T., Szara, E., Stepien, W., & Rutkowska, B. (2015). The influence of mineral fertilization and legumes cultivation on the N2O soil emissions. *Plant Soil and Environment*, *61*(12), 529-536. https://doi.org/10.17221/229/2015-pse

Stehfest, E., & Bouwman, L. (2006). N2O and NO emission from agricultural fields and soils under natural vegetation: summarizing available measurement data and modeling of global annual emissions. *Nutrient Cycling in Agroecosystems*, *74*(3), 207-228. https://doi.org/10.1007/s10705-006-9000-7

Tang, Y., Zhang, X., Li, D., Wang, H., Chen, F., Fu, X., Fang, X., Sun, X., & Yu, G. (2016). Impacts of nitrogen and phosphorus additions on the abundance and community structure of ammonia oxidizers and denitrifying bacteria in Chinese fir plantations. *Soil Biology and Biochemistry*, *103*, 284-293. https://doi.org/https://doi.org/10.1016/j.soilbio.2016.09.001

Teepe, R., Vor, A., Beese, F., & Ludwig, B. (2004). Emissions of N2O from soils during cycles of freezing and thawing and the effects of soil water, texture and duration of freezing. *European Journal of Soil Science*, *55*(2), 357-365. https://doi.org/10.1111/j.1365-2389.2004.00602.x

Tellez-Rio, A., Vallejo, A., Garcia-Marco, S., Martin-Lammerding, D., Luis Tenorio, J., Martin Rees, R., & Guardia, G. (2017). Conservation Agriculture practices reduce the global warming potential of rainfed low N input semi-arid agriculture. *European Journal of Agronomy*, *84*, 95-104. https://doi.org/10.1016/j.eja.2016.12.013

Thies, S., Joshi, D. R., Bruggeman, S. A., Clay, S. A., Mishra, U., Morile-Miller, J., & Clay, D. E. (2020). Fertilizer timing affects nitrous oxide, carbon dioxide, and ammonia emissions from soil [https://doi.org/10.1002/saj2.20010]. *Soil Science Society of America Journal*, *84*(1), 115-130. https://doi.org/https://doi.org/10.1002/saj2.20010

Thomas, S. M., Beare, M. H., Francis, G. S., Barlow, H. E., & Hedderley, D. I. (2008). Effects of tillage, simulated cattle grazing and soil moisture on N(2)O emissions from a winter forage crop. *Plant and Soil*, *309*(1-2), 131-145. https://doi.org/10.1007/s11104-008-9586-4

Thorburn, P. J., Biggs, J. S., Collins, K., & Probert, M. E. (2010). Using the APSIM model to estimate nitrous oxide emissions from diverse Australian sugarcane production systems. *Agriculture Ecosystems & Environment*, *136*(3-4), 343-350. https://doi.org/10.1016/j.agee.2009.12.014

Tian, D., & Niu, S. (2015). A global analysis of soil acidification caused by nitrogen addition. *Environmental Research Letters*, *10*(2), Article 024019. https://doi.org/10.1088/1748-9326/10/2/024019

Tian, H., Chen, G., Lu, C., Xu, X., Hayes, D. J., Ren, W., Pan, S., Huntzinger, D. N., & Wofsy, S. C. (2015). North American terrestrial CO2 uptake largely offset by CH4 and N2O emissions: toward a full accounting of the greenhouse gas budget. *Climatic Change*, *129*(3-4), 413-426. https://doi.org/10.1007/s10584-014-1072-9

Tian, H., Lu, C., Ciais, P., Michalak, A. M., Canadell, J. G., Saikawa, E., Huntzinger, D. N., Gurney, K. R., Sitch, S., Zhang, B., Yang, J., Bousquet, P., Bruhwiler, L., Chen, G., Dlugokencky, E., Friedlingstein, P., Melillo, J., Pan, S., Poulter, B., . . . Wofsy, S. C. (2016). The terrestrial biosphere as a net source of greenhouse gases to the atmosphere. *Nature*, *531*(7593), 225-+. https://doi.org/10.1038/nature16946

Tian, H., Xu, R., Canadell, J. G., Thompson, R. L., Winiwarter, W., Suntharalingam, P., Davidson, E. A., Ciais, P., Jackson, R. B., Janssens-Maenhout, G., Prather, M. J., Regnier, P., Pan, N., Pan, S., Peters, G. P., Shi, H., Tubiello, F. N., Zaehle, S., Zhou, F., . . . Yao, Y. (2020). A comprehensive quantification of global nitrous oxide sources and sinks. *Nature*, *586*(7828), 248-256. https://doi.org/10.1038/s41586-020-2780-0

Tian, H., Xu, X., Liu, M., Ren, W., Zhang, C., Chen, G., & Lu, C. (2010). Spatial and temporal patterns of CH4 and N2O fluxes in terrestrial ecosystems of North America during 1979-2008: application of a global biogeochemistry model. *Biogeosciences*, *7*(9), 2673-2694. https://doi.org/10.5194/bg-7-2673-2010

Tian, H., Yang, J., Lu, C., Xu, R., Canadell, J. G., Jackson, R. B., Arneth, A., Chang, J., Chen, G., Ciais, P., Gerber, S., Ito, A., Huang, Y., Joos, F., Lienert, S., Messina, P., Olin, S., Pan, S., Peng, C., . . . Zhu, Q. (2018). The Global N2O Model Intercomparison Project. *Bulletin of the American Meteorological Society*, *99*(6), 1231-1251. https://doi.org/10.1175/bams-d-17-0212.1

Tian, H., Yang, J., Xu, R., Lu, C., Canadell, J. G., Davidson, E. A., Jackson, R. B., Arneth, A., Chang, J., Ciais, P., Gerber, S., Ito, A., Joos, F., Lienert, S., Messina, P., Olin, S., Pan, S., Peng, C., Saikawa, E., . . . Zhang, B. (2019). Global soil nitrous oxide emissions since the preindustrial era estimated by an ensemble of terrestrial biosphere models: Magnitude, attribution, and uncertainty. *Global Change Biology*, *25*(2), 640-659. https://doi.org/10.1111/gcb.14514

Tian, J., Dungait, J. A. J., Lu, X., Yang, Y., Hartley, I. P., Zhang, W., Mo, J., Yu, G., Zhou, J., & Kuzyakov, Y. (2019). Long-term nitrogen addition modifies microbial composition and functions for slow carbon cycling and increased sequestration in tropical forest soil. *Global Change Biology*, *25*(10), 3267-3281. https://doi.org/https://doi.org/10.1111/gcb.14750

Trost, B., Prochnow, A., Drastig, K., Meyer-Aurich, A., Ellmer, F., & Baumecker, M. (2013). Irrigation, soil organic carbon and N2O emissions. A review. *Agronomy for Sustainable Development*, *33*(4), 733-749. https://doi.org/10.1007/s13593-013-0134-0

Ussiri, D. A. N., Lal, R., & Jarecki, M. K. (2009). Nitrous oxide and methane emissions from long-term tillage under a continuous corn cropping system in Ohio. *Soil & Tillage Research*, *104*(2), 247-255. https://doi.org/10.1016/j.still.2009.03.001

van Aardenne, J. A., Dentener, F. J., Olivier, J. G. J., Goldewijk, C., & Lelieveld, J. (2001). A 1 degrees x 1 degrees resolution data set of historical anthropogenic trace gas emissions for the period 1890-1990. *Global Biogeochemical Cycles*, *15*(4), 909-928. https://doi.org/10.1029/2000gb001265

van Kessel, C., Venterea, R., Six, J., Adviento-Borbe, M. A., Linquist, B., & van Groenigen, K. J. (2013). Climate, duration, and N placement determine N2O emissions in reduced tillage systems: a meta-analysis. *Global Change Biology*, *19*(1), 33-44. https://doi.org/10.1111/j.1365-2486.2012.02779.x

Velthof, G. L., & Mosquera, J. (2011). The impact of slurry application technique on nitrous oxide emission from agricultural soils. *Agriculture Ecosystems & Environment*, *140*(1-2), 298-308. https://doi.org/10.1016/j.agee.2010.12.017

Venterea, R. T., Maharjan, B., & Dolan, M. S. (2011). Fertilizer Source and Tillage Effects on Yield-Scaled Nitrous Oxide Emissions in a Corn Cropping System. *Journal of Environmental Quality*, *40*(5), 1521-1531. https://doi.org/10.2134/jeq2011.0039

Venterea, R. T., Petersen, S. O., de Klein, C. A. M., Pedersen, A. R., Noble, A. D. L., Rees, R. M., Gamble, J. D., & Parkin, T. B. (2020). Global Research Alliance N2O chamber methodology guidelines: Flux calculations. *J Environ Qual*, *49*(5), 1141-1155. https://doi.org/https://doi.org/10.1002/jeq2.20118

VERHOEVEN, Elizabeth, & Johan. (2014). Biochar does not mitigate field-scale N2O emissions in a Northern California vineyard: An assessment across two years. *Agriculture Ecosystems & Environment*, *191*(15), 27-38.

Vermue, A., Nicolardot, B., & Henault, C. (2016). High N2O variations induced by agricultural practices in integrated weed management systems. *Agronomy for Sustainable Development*, *36*(3), Article 45. https://doi.org/10.1007/s13593-016-0381-y

Volpi, I., Laville, P., Bonari, E., Nassi o Di Nasso, N., & Bosco, S. (2018). Nitrous oxide mitigation potential of reduced tillage and N input in durum wheat in the Mediterranean. *Nutrient Cycling in Agroecosystems*, *111*(2-3), 189-201. https://doi.org/10.1007/s10705-018-9922-x

Wagner-Riddle, C., Congreves, K. A., Abalos, D., Berg, A. A., Brown, S. E., Ambadan, J. T., Gao, X., & Tenuta, M. (2017).

Globally important nitrous oxide emissions from croplands induced by freeze-thaw cycles. *Nature Geoscience*, *10*(4), 279-+. https://doi.org/10.1038/ngeo2907

Walter, K., Don, A., & Flessa, H. (2015). Net N2O and CH4 soil fluxes of annual and perennial bioenergy crops in two central German regions. *Biomass & Bioenergy*, *81*, 556-567. https://doi.org/10.1016/j.biombioe.2015.08.011

Wang, C., Liu, D., & Bai, E. (2018). Decreasing soil microbial diversity is associated with decreasing microbial biomass under nitrogen addition. *Soil Biology and Biochemistry*, *120*, 126-133. https://doi.org/https://doi.org/10.1016/j.soilbio.2018.02.003

Wang, G., Yang, X., Li, Y., Ding, X., & Shen, Y. (2018). Characteristics of N2O emission from Medicago sativa stands and its response to nitrogen fertilizers in the Longdong dryland Plateau. *Chinese Journal of Applied and Environmental Biology*, *24*(3), 450-456. https://doi.org/10.19675/j.cnki.1006-687x.2017.06039

Wang, J., Chadwick, D. R., Cheng, Y., & Yan, X. (2018). Global analysis of agricultural soil denitrification in response to fertilizer nitrogen. *Science of the Total Environment*, *616*, 908-917. https://doi.org/10.1016/j.scitotenv.2017.10.229

Wang, K., Zheng, X., Pihlatie, M., Vesala, T., Liu, C., Haapanala, S., Mammarella, I., Rannik, U., & Liu, H. (2013). Comparison between static chamber and tunable diode laser-based eddy covariance techniques for measuring nitrous oxide fluxes from a cotton field. *Agricultural and Forest Meteorology*, *171*, 9-19. https://doi.org/10.1016/j.agrformet.2012.11.009

Wang, W., Dalal, R. C., Reeves, S. H., Butterbach-Bahl, K., & Kiese, R. (2011). Greenhouse gas fluxes from an Australian subtropical cropland under long-term contrasting management regimes. *Global Change Biology*, *17*(10), 3089-3101. https://doi.org/10.1111/j.1365-2486.2011.02458.x

Wang, W., Hou, Y., Pan, W., Vinay, N., Mo, F., Liao, Y., & Wen, X. (2021). Continuous application of conservation tillage affects in situ N2O emissions and nitrogen cycling gene abundances following nitrogen fertilization. *Soil Biology and Biochemistry*, *157*, 108239. https://doi.org/https://doi.org/10.1016/j.soilbio.2021.108239

Wang, Y., Guo, J., Vogt, R. D., Mulder, J., Wang, J., & Zhang, X. (2018). Soil pH as the chief modifier for regional nitrous oxide emissions: New evidence and implications for global estimates and mitigation. *Global Change Biology*, *24*(2), E617-E626. https://doi.org/10.1111/gcb.13966

Wania, R., Ross, I., & Prentice, I. C. (2010). Implementation and evaluation of a new methane model within a dynamic global vegetation model: LPJ-WHyMe v1.3.1. *Geoscientific Model Development*, *3*(2), 565-584. https://doi.org/10.5194/gmd-3-565-2010

Wanyama, I., Pelster, D. E., Arias-Navarro, C., Butterbach-Bahl, K., Verchot, L. V., & Rufino, M. C. (2018). Management intensity controls soil N2O fluxes in an Afromontane ecosystem. *Science of the Total Environment*, *624*, 769-780. https://doi.org/10.1016/j.scitotenv.2017.12.081

Watanabe, T., Chairoj, P., Tsuruta, H., Masarngsan, W., Wongwiwatchai, C., Wonprasaid, S., Cholitkul, W., & Minami, K. (2000). Nitrous oxide emissions from fertilized upland fields in Thailand. *Nutrient Cycling in Agroecosystems*, *57*(1), 55-65. https://doi.org/10.1023/a:1009764421174

Weitz, A. M., Linder, E., Frolking, S., Crill, P. M., & Keller, M. (2001). N(2)O emissions from humid tropical agricultural soils: effects of soil moisture, texture and nitrogen availability. *Soil Biology & Biochemistry*, *33*(7-8), 1077-1093. https://doi.org/10.1016/s0038-0717(01)00013-x

Weslien, P., Rütting, T., Kasimir-Klemedtsson, Å., & Klemedtsson, L. (2012). Carrot cropping on organic soil is a hotspot for nitrous oxide emissions. *Nutrient Cycling in Agroecosystems*, *94*(2), 249-253. https://doi.org/10.1007/s10705-012-9538-5

Willmott, C. J. (1981). On the Validation of Model. *Physical Geography*, *2*(2), 219-232.

Wolf, B., Zheng, X., Brüggemann, N., Chen, W., Dannenmann, M., Han, X., Sutton, M. A., Wu, H., Yao, Z., & Butterbach-Bahl, K. (2010). Grazing-induced reduction of natural nitrous oxide release from continental steppe. *Nature*, *464*(7290), 881-884. https://doi.org/10.1038/nature08931

Wrage, N., Velthof, G. L., van Beusichem, M. L., & Oenema, O. (2001). Role of nitrifier denitrification in the production of nitrous oxide. *Soil Biology & Biochemistry*, *33*(12-13), 1723-1732. https://doi.org/10.1016/s0038-0717(01)00096-7

Xu, R., & Prentice, I. C. (2008). Terrestrial nitrogen cycle simulation with a dynamic global vegetation model. *Global Change Biology*, *14*(8), 1745-1764. https://doi.org/10.1111/j.1365-2486.2008.01625.x

Xu, R., Prentice, I. C., Spahni, R., & Niu, H. S. (2012). Modelling terrestrial nitrous oxide emissions and implications for climate feedback. *New Phytologist*, *196*(2), 472-488. https://doi.org/10.1111/j.1469-8137.2012.04269.x

Xu, R., Tian, H., Lu, C., Pan, S., Chen, J., Yang, J., & Zhang, B. (2017). Preindustrial nitrous oxide emissions from the land biosphere estimated by using a global biogeochemistry model. *Climate of the Past*, *13*(7), 977-990. https://doi.org/10.5194/cp-13-977-2017

Yan, X., Shi, S., Du, L., & Xing, G. (2000). Pathways of N2O emission from rice paddy soil. *Soil Biology and Biochemistry*, *32*(3), 437-440. https://doi.org/https://doi.org/10.1016/S0038-0717(99)00175-3

Yang, L., Zhang, X., & Ju, X. (2017). Linkage between N2O emission and functional gene abundance in an intensively managed calcareous fluvo-aquic soil. *Scientific Reports*, *7*(1), 43283. https://doi.org/10.1038/srep43283

Yang, L. F., & Cai, Z. C. (2005). The effect of growing soybean (Glycine max. L.) on N2O emission from soil. *Soil Biology & Biochemistry*, *37*(6), 1205-1209. https://doi.org/10.1016/j.soilbio.2004.08.027

Yin, Y., Wang, Z., Tian, X., Wang, Y., Cong, J., & Cui, Z. (2022). Evaluation of variation in background nitrous oxide emissions: A new global synthesis integrating the impacts of climate, soil, and management conditions. *Global Change Biology*, *28*(2), 480-492. https://doi.org/https://doi.org/10.1111/gcb.15860

Zebarth, B. J., Snowdon, E., Burton, D. L., Goyer, C., & Dowbenko, R. (2012). Controlled release fertilizer product effects on potato crop response and nitrous oxide emissions under rain-fed production on a medium-textured soil. *Canadian Journal of Soil Science*, *92*(5), 759-769. https://doi.org/10.4141/cjss2012-008

Zhang, B., Tian, H., Lu, C., Dangal, S. R. S., Yang, J., & Pan, S. (2017). Global manure nitrogen production and application in cropland during 1860-2014: a 5 arcmin gridded global dataset for Earth system modeling. *Earth System Science Data*, *9*(2), 667-678. https://doi.org/10.5194/essd-9-667-2017

Zhang, J., & Han, X. (2008). N2O emission from the semi-arid ecosystem under mineral fertilizer (urea and superphosphate) and increased precipitation in northern China. *Atmospheric Environment*, *42*(2), 291-302. https://doi.org/10.1016/j.atmosenv.2007.09.036

Zhang, K., Peng, C., Wang, M., Zhou, X., Li, M., Wang, K., Ding, J., & Zhu, Q. (2017). Process-based TRIPLEX-GHG model for simulating N2O emissions from global forests and grasslands: Model development and evaluation. *Journal of Advances in Modeling Earth Systems*, *9*(5), 2079-2102. https://doi.org/https://doi.org/10.1002/2017MS000934

Zhang, K., Zhu, Q., Liu, J., Wang, M., Zhou, X., Li, M., Wang, K., Ding, J., & Peng, C. (2019). Spatial and temporal variations of N2O emissions from global forest and grassland ecosystems. *Agricultural and Forest Meteorology*, *266*, 129-139. https://doi.org/10.1016/j.agrformet.2018.12.011

Zhang, Y., Lin, F., Jin, Y., Wang, X., Liu, S., & Zou, J. (2016). Response of nitric and nitrous oxide fluxes to N fertilizer application in greenhouse vegetable cropping systems in southeast China. *Scientific Reports*, *6*, Article 20700. https://doi.org/10.1038/srep20700

Zhang, Y., Zheng, X., Ren, X., Zhang, J., Misselbrook, T., Cardenas, L., Carswell, A., Müller, C., & Ding, H. (2019). Land-use type affects nitrate production and consumption pathways in subtropical acidic soils. *Geoderma*, *337*, 22-31. https://doi.org/https://doi.org/10.1016/j.geoderma.2018.09.012

Zhang, Z., Zhu, X., Wang, S., Duan, J., Chang, X., Luo, C., He, J.-S., & Wilkes, A. (2017). Nitrous oxide emissions from different land uses affected by managements on the Qinghai-Tibetan Plateau. *Agricultural and Forest Meteorology*, *246*, 133-141. https://doi.org/10.1016/j.agrformet.2017.06.013

Zheng, J., Qu, Y., Kilasara, M. M., Mmari, W. N., & Funakawa, S. (2019). Soil-atmosphere exchange of nitrous oxide in two Tanzanian croplands: Effects of nitrogen and stover management. *Agricultural and Forest Meteorology*, *275*, 24-36. https://doi.org/https://doi.org/10.1016/j.agrformet.2019.05.009

Zhou, F., Shang, Z., Zeng, Z., Piao, S., Ciais, P., Raymond, P. A., Wang, X., Wang, R., Chen, M., Yang, C., Tao, S., Zhao, Y., Meng, Q., Gao, S., & Mao, Q. (2015). New model for capturing the variations of fertilizer-induced emission factors of N2O. *Global Biogeochemical Cycles*, *29*(6), 885-897. https://doi.org/10.1002/2014gb005046

Zhou, M., Wang, X., Ke, Y., & Zhu, B. (2019). Effects of afforestation on soil nitrous oxide emissions in a subtropical montane agricultural landscape: A 3-year field experiment. *Agricultural and Forest Meteorology*, *266*, 221-230. https://doi.org/10.1016/j.agrformet.2019.01.003

Zhou, M., Zhu, B., Wang, S., Zhu, X., Vereecken, H., & Brueggemann, N. (2017). Stimulation of N2O emission by manure application to agricultural soils may largely offset carbon benefits: a global meta-analysis. *Global Change Biology*, *23*(10), 4068-4083. https://doi.org/10.1111/gcb.13648

Zhu, Q., Liu, J., Peng, C., Chen, H., Fang, X., Jiang, H., Yang, G., Zhu, D., Wang, W., & Zhou, X. (2014). Modelling methane emissions from natural wetlands by development and application of the TRIPLEX-GHG model. *Geoscientific Model Development*, *7*(3), 981-999. https://doi.org/10.5194/gmd-7-981-2014

Zhu, Q., & Zhuang, Q. (2014). Parameterization and sensitivity analysis of a process-based terrestrial ecosystem model using adjoint method. *Journal of Advances in Modeling Earth Systems*, *6*(2), 315-331. https://doi.org/https://doi.org/10.1002/2013MS000241

Zhu, T., Zhang, J., Huang, P., Suo, L., Wang, C., Ding, W., Meng, L., Zhou, K., & Hu, Z. (2015). N2O emissions from banana plantations in tropical China as affected by the application rates of urea and a urease/nitrification inhibitor. *Biology and Fertility of Soils*, *51*(6), 673-683. https://doi.org/10.1007/s00374-015-1018-z

Zhu, X., Burger, M., Doane, T. A., & Horwath, W. R. (2013). Ammonia oxidation pathways and nitrifier denitrification are significant sources of N₂O and NO under low oxygen availability. *Proceedings of the National Academy of Sciences*, *110*(16), 6328-6333. https://doi.org/10.1073/pnas.1219993110

CHAPTER III:

Quantifying patterns, sources and uncertainty of nitrous oxide emissions from global grazing lands: Nitrogen forms are the determinant factors for estimation and mitigation

Hanxiong Song, Changhui Peng, Kerou Zhang, Tong Li, Mingxia Yang, Qiuyu Liu, and Qiuan Zhu

Article published in *Global and Planetary Change* 223 (2023): 104080.

3.1 Résumé

Les émissions de protoxyde d'azote (N_2O) provenant des terres de pâturage (c'est-à-dire des pâturages et des prairies) constituent une source importante du réchauffement climatique mondial, bien que les estimations actuelles présentent encore de grandes incertitudes. Cette étude a amélioré et appliqué le modèle biogéochimique basé sur les processus, TRIPLEX-GHG v2.0, pour estimer l'ampleur des émissions de N_2O des terres de pâturage à l'échelle mondiale. Nous avons utilisé 60 observations de sites indépendants pour la calibration et la validation du modèle, et les résultats ont montré une grande cohérence entre les émissions de N_2O modélisées et mesurées à travers le monde. Les simulations mondiales ont été effectuées à une résolution spatiale de 0.5°×0.5°. Après une augmentation significative entre 1961 et 1990, les émissions de N_2O modélisées provenant des terres de pâturage mondiales ont montré une tendance légèrement décroissante, passant de 2.34 ± 0.04 TgN an^{-1} dans les années 1990 à 2.04 ± 0.02 TgN an^{-1} dans les années 2010. Spatialement, l'Europe, l'Amérique du Nord et l'Asie du Sud étaient les principaux points chauds d'émissions au cours de la période étudiée. En utilisant différentes simulations de scénarios, les excréments de bétail déposés ont été identifiés comme le principal contributeur, représentant 30.76 % des émissions historiques de N_2O, bien que cette contribution ait probablement été surestimée par les études précédentes en raison d'un manque de descriptions des propriétés chimiques des excréments et de l'effet des cycles gel-dégel. Les différentes formes d'apports en azote jouent un rôle déterminant dans les variations spatio-temporelles des émissions de N_2O des terres de pâturage à l'échelle mondiale. Nous suggérons que les différentes formes d'apports en azote aux terres de pâturage devraient être prises en compte pour les estimations des modèles, ce qui pourrait également constituer une méthode possible d'atténuation des émissions de N_2O.

3.2 Abstract

Nitrous oxide (N_2O) emissions from grazing lands (i.e., pasturelands and rangelands) are an important source of global warming while current estimations remain large uncertainties. This study has improved and applied the biogeochemical process-based model, TRIPLEX-GHG modelv2.0, to estimate the magnitude of the N_2O emissions from global grazing lands. We used 60 independent site observations for model calibration and validation and the results suggested a high consistency between modelled and measured N_2O emissions across the globe. Global simulations were conducted at 0.5°×0.5° spatial resolution. After the significant increase between 1961 – 1990, modeled N_2O emissions from global grazing lands exhibited a slightly decreasing trend from 2.34 ± 0.04 TgN yr^{-1} in the 1990s to 2.04 ± 0.02 TgN yr^{-1} in the 2010s. Spatially, Europe, North America, and southern Asia were major emission hotspots over study period. Using different scenario simulations, the deposited livestock excreta were identified as the predominant contributor, accounting for 30.76% of historical N_2O emissions, while such contribution was probably overestimated by previous studies due to a lack of descriptions of the chemical properties of excreta and the effect of freeze-thaw cycles. N chemical fertilizer application was identified as the primary source for the overall increase in N_2O emissions during study period. The different chemical forms of all types of anthropogenic N inputs have a determinant role in spatial-temporal variations patterns of N_2O emissions from grazing lands on a global scale. We suggest the different forms of N input to grazing lands should be addressed for model estimations and implies a possible mitigation method for mitigating N_2O emissions.

3.3 Introduction

Nitrous oxide (N_2O) is a powerful greenhouse gas and has a major role in the destruction of stratospheric ozone (Canadell, 2021). It is mainly produced via microbially mediated nitrification and denitrification processes, which are directly and indirectly controlled by multiple variables (Butterbach-Bahl *et al.*, 2013; Davidson, 2009; Reay *et al.*, 2012). The growing anthropogenic activities have led to a significant increase of the atmospheric N_2O concentration from 270.1 to 333.0 ppb (parts per billion) since pre-industry (Canadell, 2021) and agricultural management explains more than 60% of such growth (Davidson et Kanter, 2014). As an essential component of agriculture, grazing land ecosystems are considered as the second largest contributor to the total terrestrial N_2O emissions (Chang *et al.*, 2021; Dangal *et al.*, 2019; Klein Goldewijk *et al.*, 2017; Tian *et al.*, 2020). Both agricultural management and environmental factors regulate the grazing lands N_2O emissions. Field observations have revealed that increasing stocking and fertilizing intensities are the key drivers of the growth in grazing lands N_2O emissions, particularly during the growing seasons (Yan *et al.*, 2016; Yin, M. *et al.*, 2020). In addition, the rising temperature and changes in precipitation also affect N_2O emission patterns by altering the soil physical properties and nutrient dynamics (Gong *et al.*, 2021; Xu, R. *et al.*, 2012). However, the inconsistent measured grazing lands N_2O patterns were detected across the globe, casting doubt on the total N_2O budget (Tian *et al.*, 2020). Additionally, the contributions of the different driving factors are still poorly quantified at large scales because of the high geographic variability of the environmental parameters and the complicated distribution of management practices (Dangal *et al.*, 2019; Du *et al.*, 2021; Flechard *et al.*, 2007).

Different models have been developed for quantifying the dynamics of N_2O emissions from grazing lands at different scales. The Intergovernmental Panel on Climate Change (IPCC) recommended an empirical emission factors model (EFs, the percentage of direct N lost as N_2O gas from N inputs). While numerous field measurements reported large uncertainties with this approach because of ignoring the variations of soil (Yin, M. *et al.*, 2020), climate (Cardoso *et al.*, 2017; Flechard *et al.*, 2007), topography factors (Marsden *et al.*, 2019; Zhong *et al.*, 2016). The background N_2O emissions (i.e., natural emissions) were also poorly quantified (Aliyu *et al.*, 2018; Yin, Y. *et al.*, 2021). In contrast, process-based models can provide more comprehensive descriptions of the N_2O-related processes and attribute the variations to different driving forces (Tian *et al.*, 2020). However, current process-based models still have substantial challenges in simulating grazing induced N_2O emissions due to limited model representations and validation of nitrification and denitrification responses to grazing activities (Giltrap *et al.*, 2020; Tian *et al.*, 2019). For instance, the water and nitrogen management model (WNMM) showed inconstant performances in simulating pastureland N_2O with diverse fertilizer application rates at a single site (Chen *et al.*, 2010). The N_2O emissions from grasslands in China determined by the denitrification and decomposition (DNDC) model were probably underestimated because they neglected the impact of freeze-thaw cycles (Zhang, F. *et al.*, 2010). Dangal et al. (2019) obtained a reasonable N_2O budget for global grazing ecosystems using the dynamic land ecosystem model (DLEM). Nevertheless, only integrating it with the animal excreta deposit module, their results may underestimate the contribution of the changes in the plant environment to the total N_2O emissions. Therefore, further improvement and application of reliable models are required to constrain the current inconsistent observations and extrapolate to the global scale for scientific basis of sustainable management.

The objectives of this study were to: 1) improve a process-based biogeochemical model, the TRIPLEX-GHG v2.0 by integrating grazing-related biogeochemical and management processes; 2) estimate the magnitude of the historical N_2O emissions from global grazing lands; 3) use different scenarios to attribute the changes in grazing lands N_2O emission to different driving forces; and 4) quantify the importance of different N input forms in estimating N_2O emissions. We hypothesized that: first, the magnitude of the N_2O emissions from global grazing lands exhibit strong temporal and spatial variations during the historical time period; second, deposited livestock excreta associated with grazing activities is the most important contributor to N_2O emissions from global grazing lands; and third, the changing chemical forms of N inputs are the major source of the uncertainty of the estimated N_2O emissions.

3.4 Materials and methods

3.4.1 Model description and improvements

TRIPLEX-GHG model v2.0 is a process-based biogeochemical model based on the TRIPLEX model (Peng, C. H. *et al.*, 2002), the integrated biosphere simulator (Foley *et al.*, 1996), and the DNDC model (Li, C. S. *et al.*, 2000). Generally, the TRIPLEX-GHG modelv2.0 simulate dynamic vegetation, water movement, and C and N cycling in various ecosystems (Peng, C. *et al.*, 2013; Song *et al.*, 2022) (Figure 3.S1; Supplementary material 3.8.1).

In this study, we improved the model by introducing detailed descriptions of natural and management practices for grazing lands. The livestock excreta production and deposition, trampling as well as freeze-thaw effects were integrated into the model structure. The deposited excreta of grazing livestock, including urine and dung are important nutrient (e.g., C and N) sources to grazed soil. Urine is considered directly as 'fertigation' which adds inorganic N and water simultaneously. However, the dung is further separated into inorganic and organic portion with different C:N ratios as soil organic matter pools (Velthof, Gerard L *et al.*, 2015; Zhang, B. *et al.*, 2017) (Eq. S1-S4). Meanwhile, the impact of grazer trampling was also included (Wolf *et al.*, 2012) (Eq. S5). The freeze-thaw induced N_2O emission pulse was modeled by describing the soil temperature triggered microbial mortality and recovery, soil moisture movement and substrate availabilities (Eq. S6-12) (Kariyapperuma *et al.*, 2011; Risk *et al.*, 2013). Details were given in Supplementary material 3.8.2 and Table 3.S1.

Grazing lands were divided into two categories as pasturelands (intensively managed) and rangelands (extensively managed or un-disturbed), respectively. Pasturelands were designed to receive intensive management practices including chemical fertilizer and manure application, grazing activities with deposited excreta and irrigation. In contrast, rangelands only experienced grazing activities or stayed un-disturbed temporarily (Dangal *et al.*, 2019; Goldewijk *et al.*, 2017).

3.4.2 Model calibration and validation

Observed N_2O emissions data from 60 published studies with 62 grazing land sites worldwide were collected to evaluate the model's performance. Fourteen sites from different continents were randomly selected for the model calibration, and the remaining were used for the model validation. The related environmental and management information used for the calibration and validation are summarized in Tables 3.S2 and 3.S3, respectively. Based on previous studies, the coefficient of the nitrate consumption rate of denitrification (COE_{dNO3}) has the highest sensitivity level for N_2O emissions from managed soils (Song *et al.*, 2022). Therefore, the model calibration was conducted by adjusting COE_{dNO3} to fit the best model performance through trial and error while other parameters were set as the default values. We also used the agreement index (D), root mean square error (RMSE), and correlation efficient (R) to quantify the agreement between the modeled and observed daily N_2O emissions (Supplementary material 3.8.3). For the model validation, we compared the modeled and observed average daily N_2O fluxes during the measurement period to further test the reliability of the model at the global scale. Site-specific information was used to drive the model in the calibration and validation stages.

3.4.3 Simulation scenarios designs

First, the model simulation went through an initial 300-year spin-up procedure driven by the multi-year averaged historical meteorological data to reach a state of relative equilibrium in the soil carbon and nitrogen pools before the analysis. After the spin-up, the model was run at a spatial resolution of 0.5°×0.5° from 1860 to 2016 with a daily time step.

Overall, six different scenarios for the model simulations were performed to investigate the magnitude of the N_2O emissions from global grazing lands (S1), and attribute emission patterns to different driving factors (S2-S5) (Table 3.1). The baseline simulation, S0, only considered the variations in the climate factors and the fixed N input information at the beginning of the simulation. As a multifactor simulation, S1 aimed to provide an estimation of the magnitude of the global N_2O emissions from grazing lands using all of the driving data, including transient N fertilizer and manure application, excreta deposition, climate, and N deposition data. Simulations S2 and S3 were conducted with manure and fertilizer application constant at the level in 1961 to quantify their contributions by comparing the results of simulations S2 and S3 with the results of S1. For S4, the excreta N deposition was fixed to estimate the amount of N_2O emitted from livestock excreta input. In addition, the background emissions (N_2O emissions without the addition of external anthropogenic N) were simulated using S5, and the difference between S5 and S0 indicated the contribution of atmospheric N deposition to the total N_2O emissions from grazing lands. To investigate the possible uncertainties and ranges of the estimated global N_2O emissions from grazing lands, we conducted six additional scenarios based on S1 by changing the key and sensitive N input information associated with the management information and datasets one at a time. The chemical fertilizer properties (i.e., the NH_4^+-N fraction) and excreta properties (i.e., the inorganic fraction and soil organic carbon composition) were varied by 20% to evaluate the possible range of uncertainties. All of these simulations are described in Table 3.1.

Table 3.1 Model simulation experiment designs with different scenarios used to evaluate the contributions of the different factors (mostly different N inputs) to the global N_2O emissions from grazing lands and the possible uncertainties of the estimates due to changing N input forms.

No.	Input Variables							
	Clim.	AtmoN.dep	Fer.app		Man.app		Exc.dep	
			Amount	Properties	Amount	Properties	Amount	Properties
S0	1901–2016	1901	1961	NA	1901	NA	1901	NA
S1	1901–2016	1860–2016	1961–2016	Default	1901–2016	Default	1901–2016	Default
S2	1901–2016	1860–2016	1961	Default	1901–2016	Default	1901–2016	Default
S3	1901–2016	1860–2016	1961–2016	Default	1901	Default	1901–2016	Default
S4	1901–2016	1860–2016	1961–2016	Default	1901–2016	Default	1901	Default
S5	1901–2016	1860–2016	1961	Default	1901	Default	1901	Default
S6	1901–1920	1860–2016	1961–2016	Default	1860–2016	Default	1901–2016	Default
F_p1	1901–2016	1860–2016	1961–2016	Fr_{NH4}(120%)	1901–2016	Default	1901–2016	Default
F_p2	1901–2016	1901–2016	1961–2016	Fr_{NH4}(80%)	1901–2016	Default	1901–2016	Default
E_ip1	1901–2016	1901–2016	1961–2016	Default	1901–2016	Default	1901–2016	Fr_{inorg} (120%)
E_ip2	1901–2016	1901–2016	1961–2016	Default	1901–2016	Default	1901–2016	Fr_{inorg} (80%)
E_op1	1901–2016	1901–2016	1961–2016	Default	1901–2016	Default	1901–2016	Fr_{org_com} (120%)
E_op2	1901–2016	1901–2016	1961–2016	Default	1901–2016	Default	1901–2016	Fr_{org_com} (80%)

Clim: climate data; AtmoN.dep: atmospheric N deposition; Fer.app: chemical N fertilizer application; Man.app: manure application; and Exc.dep: livestock excreta N deposition. The data sources and descriptions are listed in the supplementary material 3.8.4. Default indicates that the information used for S0 simulation was used. The default property of the chemical N fertilizer was derived from Naishia et al. (2017) while that for the excreta N was based on data reported by Li et al. (2012, 2016) and Song et al. (2022). F_p1 and F_p2 denote the two scenarios that controlled the properties of the chemical fertilizer (i.e., Fr_{NH4}(120% or 80%): fertilizer NH_4 fraction is set to be 20% larger or 20% smaller than default values). E_ip and E_op denote the scenarios that vary the inorganic fraction of the excreta (Fr_{inorg}) and the composition of the organic matter deposited in the excreta (i.e., $Fr_{org_com}$the proportion of passive organic matter of total organic matter).

3.4.4 Input datasets

Daily climatological datasets (precipitation, max, min and mean air temperature etc.) from 1901-2016 were obtained from CRUNCEP website to drive the model. Soil properties, vegetation cover, and atmospheric N deposition data, were directly downloaded from available datasets. Anthropogenic management information, such as the fertilizer, manure application rates, and N deposited in excreta from livestock, was based on datasets provided by Lu et al. (2019). The changes in N forms of chemical fertilizer were adopted from Nishina et al. (2017). While the chemical properties of manure and deposited excreta were extracted from previous modeling and synthetic studies (Li, C. *et al.*, 2012; Wolf *et al.*, 2010). Particularly, the global distribution maps of pastureland and rangelands were acquired from the History Database of the Global Environment, version 3.2 (HYDE 3.2). Detailed descriptions are presented in Supplementary material 3.8.4.

3.4.5 Statistical analysis

The total N_2O emissions (T) were calculated as follows:

$$T = \sum_{i=1}^{n1} \sum_{j=1}^{n2} F_{i,j} \cdot A_{i,j} \quad (1)$$

Where n1 and n2 are the number of different grazing land types and the total number of grids of grazing lands, respectively. $F_{i,j}$ and $A_{i,j}$ denote the N_2O flux (kgN-N_2O ha^{-1}) and the area of the biome type i in the grid j. The former was produced by model simulations while the latter was based on HYDE3.2 datasets.

The trends of the annual N_2O emissions from grazing lands in different regions and types of biomes were identified using the Mann-Kendall test (Kendall, 1948; Zhang, K. *et al.*, 2019). In addition, Spearman correlation analysis was conducted to measure the strength of the correlations between the emission factors (EFs) and the model-driven datasets for each grid cell for controlling factors over 1961–2016 (Supplementary material 3.8.3) (Wang, Q. *et al.*, 2019). For current study, the EF_1 (EF for chemical fertilizer) and EF_{3PRP} (EF for deposited livestock excreta) were calculated based on the difference between scenarios as follows:

$$EF_1 = \left(\frac{N_2O_{S1} - N_2O_{S2}}{Fertilizer\ N}\right) \cdot 100\% \quad (2)$$

$$EF_{3PRP} = \left(\frac{N_2O_{S1} - N_2O_{S4}}{Excreta\ N}\right) \cdot 100\% \qquad (3)$$

Where N_2O_{S1}, N_2O_{S2} and N_2O_{S3} denote the N_2O emission results from scenario S1, S2 and S3 respectively. $Fertilizer\ N$ represents the fertilizer application rate on pasturelands while $Excreta\ N$ means the deposited excreta N on both pasturelands and rangelands.

All of the statistical analyses were performed using the R software (version 4.3.1) and the ncdf4, map, raster, lmodel2, and trend packages.

3.5 Results

3.5.1 Evaluation of model performance at the site scale

The calibrated model performed well for estimating N_2O dynamics from both the rangeland and pastureland sites (Figure 3.1and 3.S2). The model accurately estimated the timing and magnitude of the major N_2O emission pulses induced by freeze-thaw events from temporarily undisturbed rangelands (e.g., Figure 3.1a). In the meantime, the modeled daily N_2O emissions were generally consistent with the trends of measured data for the grazed rangeland sites under different grazing activities and environmental conditions (e.g., Figure 3.1b). As for pasturelands which received intensive managements, the model could provide good estimations of the dynamics of N_2O under fertilization, grazing and mowing (Figure 3.1c and d). We further tested the model performance for estimating cumulative N_2O emissions and a high correlation was found between the observed and simulated results during the experimental periods from the 14 calibrated sites (R^2=0.97, n=14; Figure 3.1e).

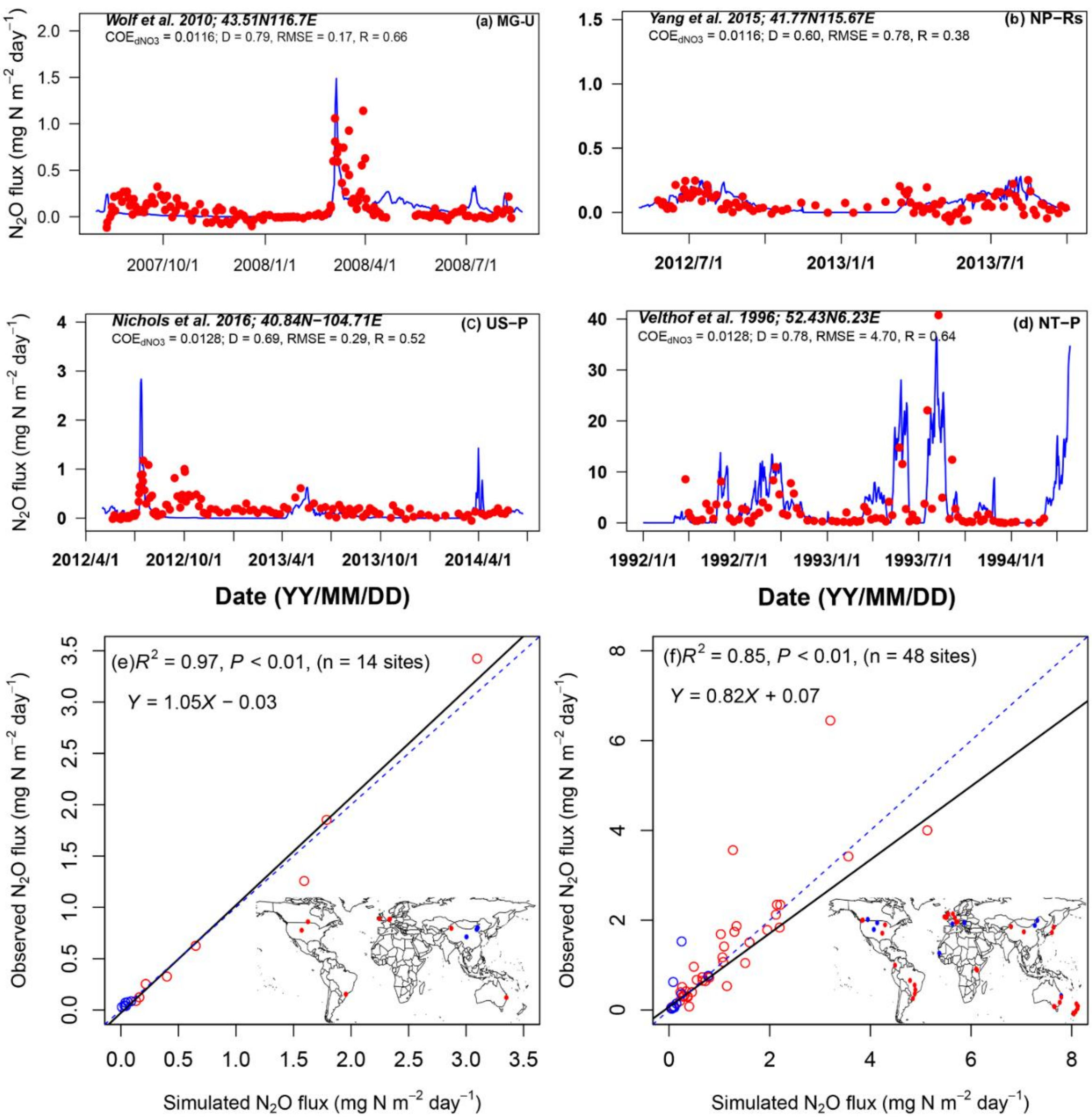

Figure 3.1 Comparison of the modeled and measured N_2O emission from grazing lands under different management and environmental conditions during model calibration (a-e) and validation (f). The blue and red dots represent averaged N_2O emissions during experiment periods for rangeland sites and pastureland sites, respectively.

Model validation suggested the TRIPLEX-GHG model v2.0 can explain 85% of the variance of the observed N_2O emission rates from the 48 experimental sites across the different types of grazing lands and management intensities, with a reasonable agreement between the measured and modeled daily mean N_2O emissions during the experimental periods (R^2=0.85, slope=0.82, n=48; Figure 3.1f). The mean squared error (MSE) of the simulated emission rates was 0.46, indicating a low bias for the model.

3.5.2 Temporal and spatial variations in N_2O emissions from global grazing lands

Globally, based on the S1 scenario simulation, there was an overall significant increasing trend in the annual N_2O emissions from grazing lands from 1.20 in 1961 to 2.02 TgN yr^{-1} in 2016, with a mean value of 1.80 (± 0.19) TgN yr^{-1}. Specifically, the rate of increase slowed down from 0.030 TgN yr^{-2} before 1990 ($p < 0.001$, $R^2 = 0.91$) to 0.005 TgN yr^{-2} during 1990 – 2010 ($p < 0.05$, $R^2 = 0.27$) based on Pettitt's test (Pettitt, 1979). Finally, the N_2O emissions exhibited a slightly decreasing trend from 2.34 TgN yr^{-1} in the 1990s to 2.04 (± 0.02) TgN yr^{-1} in the 2010s (Figure 2a). In addition, the pastureland N_2O emissions significantly increased during study period with a peak value of 1.38 TgN yr^{-1} in 2000. No significant trend in the rangelands N_2O emissions was detected (0.85 ± 0.02 TgN yr^{-1}). Although the pasturelands and rangelands contributed comparably to the historical N_2O emissions (52.0 % and 48.0 %, respectively), the pasturelands contribution was doubled to approximately 60 %, dominating the overall temporal changes in the global grazing lands N_2O emissions. For the seasonal variations, large monthly emission rates occurred in the growing seasons for pasturelands while the N_2O emissions in April and May contributed more for rangelands (Figure 3.S3)

Strong spatial variations in the simulated global grazing land N_2O emissions were obtained. At the continent scale, the grazing lands in Europe (EU) and North America (NA) accounted for 21.2 % and 16.5 % of the total historical emissions, respectively, followed by southern Asia (AS), Africa (AF), South America (SA), northern Asia (NAS), and Oceania (AU) (Figure 3.2b). Pasturelands were consistently the major source in the regional N_2O budgets for EU, NA, and AF while the rangelands emissions played more important roles for the other continents because of the larger rangelands area (Figure 3.S5). Notably, an evident decreasing trend was observed for the N_2O emissions in EU since the 1990s as driven by the decreased NO_3^-, manure applications and the reducing pastureland area (Figures S5b, S6b). The seasonal patterns of the N_2O emissions from pasturelands and rangelands vary greatly among the different continents. It is noteworthy that for the rangelands, the spring thaw induced large variations in the N_2O emissions for the semi-arid cool climate regions (e.g., NAS, Figure 3.S3). Moreover, the N_2O emissions from the temperate regions in the Northern Hemisphere (55–30°N) dominated the global N_2O emission from grazing lands for approximately 65% (Figure 3.3a). The total N_2O emissions and the mean N_2O flux from the grazing lands in this region increased from 0.01 TgN yr^{-1} and 0.12 kgN ha^{-1} yr^{-1} in the 1960s to 0.046 TgN yr^{-1} and 0.59 kgN ha^{-1} yr^{-1} in the 2010s, respectively. While in the tropical and sub-tropical Southern Hemisphere, the annual N_2O emissions and flux rates from the grazing lands were found to be relatively consistent (i.e., 0.01 TgN yr^{-1} and 0.13 kgN ha^{-1} yr^{-1}). Specifically, western EU, southeastern NA, and southern SA were constant hotspots of grazing lands N_2O emissions (>6.0 kgN ha^{-1} yr^{-1}), especially after 1990 since the pasturelands received more anthropogenic N input in these regions (Figure 3.S4a). Whereas the rangeland soil exhibited overall smaller N_2O emission rates except the rangelands in central Asia and Australia with annual N_2O emissions of approximately 3 kgN ha^{-1} yr^{-1} (Figure 3.S4b).

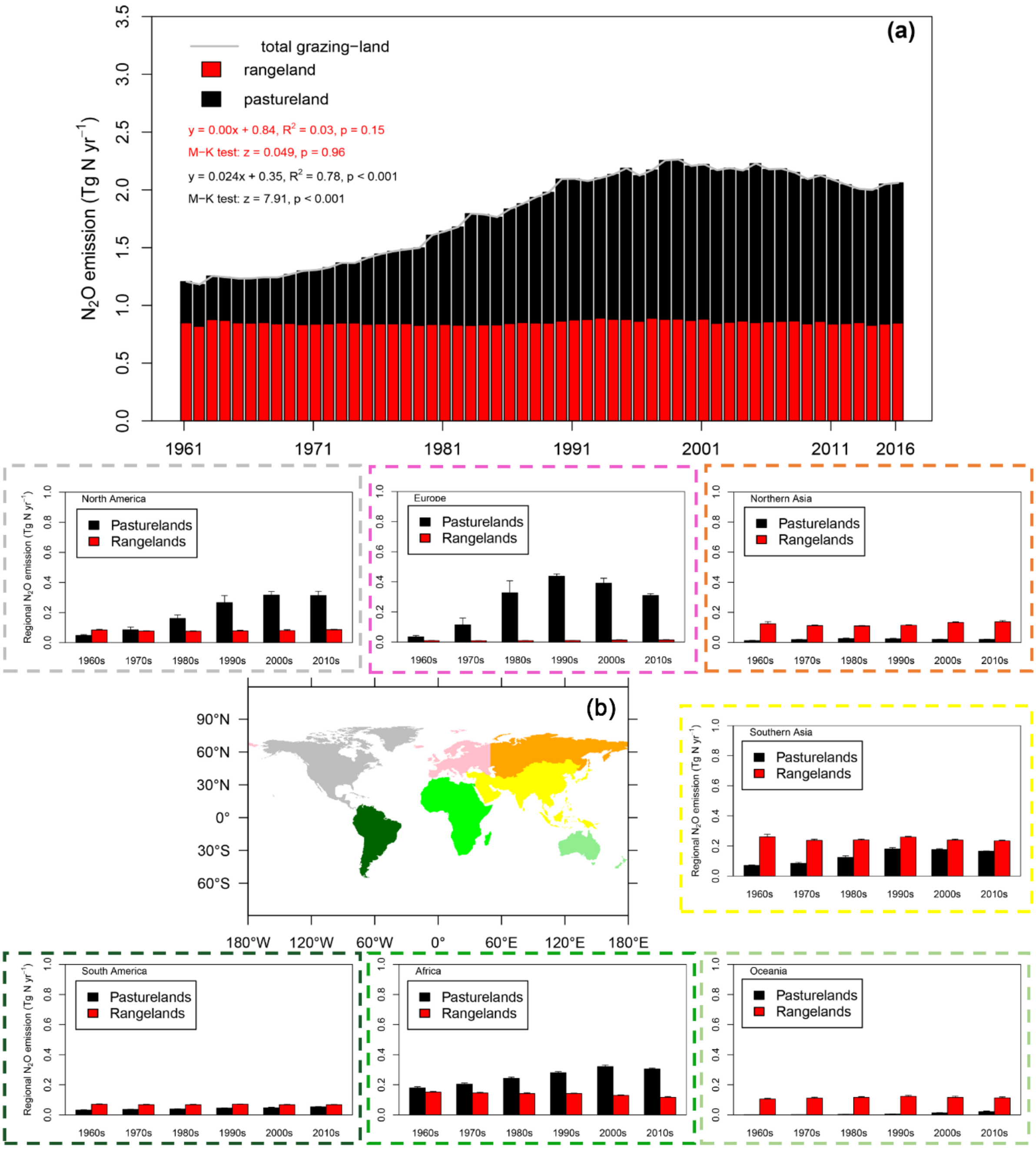

Figure 3.2 Temporal changes in the N_2O emissions from global grazing lands (a) and seven major continents (b) during 1961–2016.

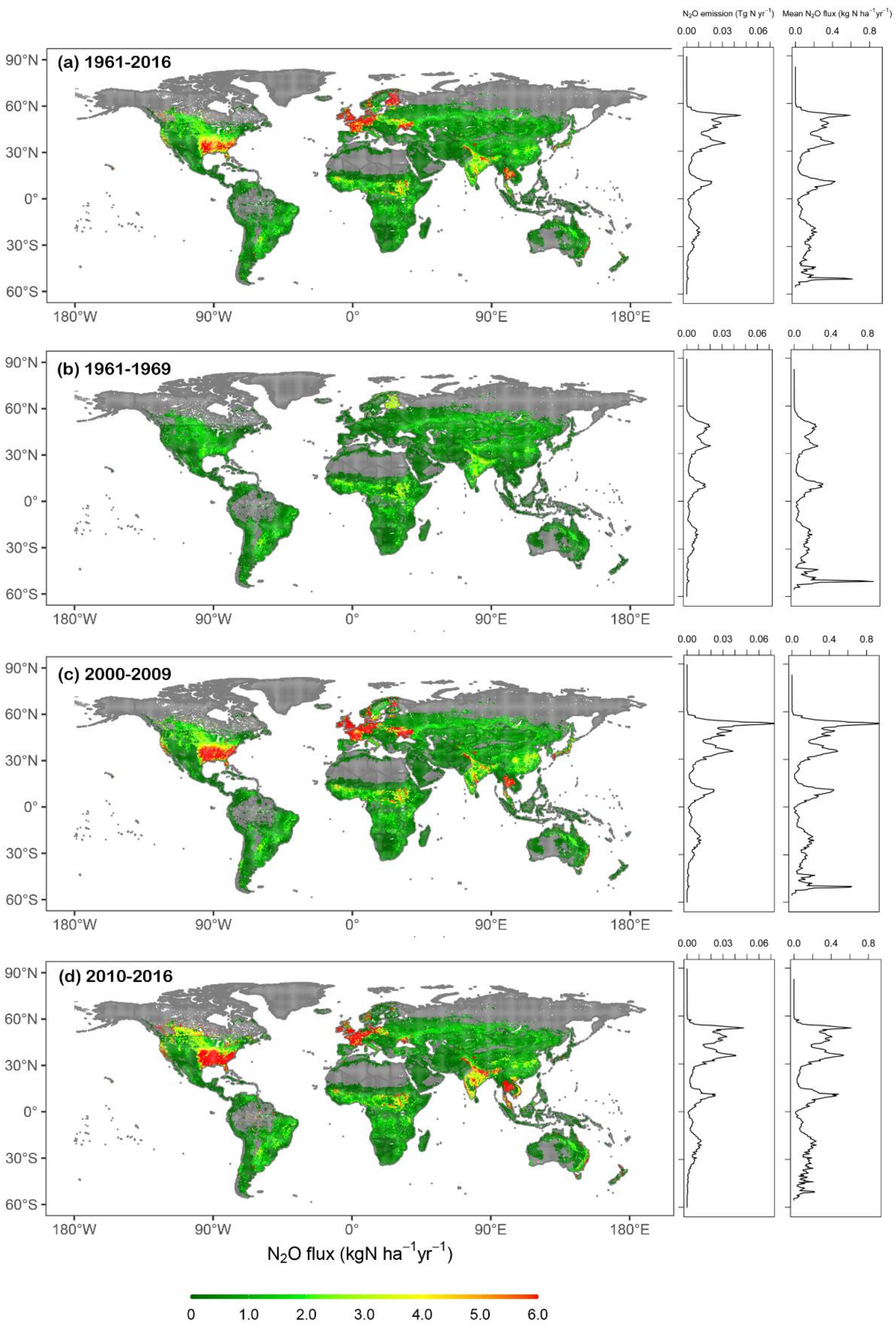

Figure 3.3 Spatial patterns of the mean N_2O emissions from grazing lands during the whole study period (1961–2016, a), and three representative decades (the 1960s, b; the 2000s, c; and the 2010s, d) as a result of multiple environmental and management changes based on the multifactor simulation (S1).

3.5.3 Contribution of different driving factors to the total N2O emission from the grazing lands

From 1961 to 2016, the N deposited in livestock excreta (DE) was the predominant contributor to N_2O emissions from grazing lands. The induced N_2O was consistent at 0.54 (± 0.03) TgN yr^{-1} accounting for 30.76 (± 2.7)% of the total emissions. Regarding the types of biomes, the influence of the livestock excreta deposition on the pastureland N_2O emissions was 19.24% after 1980s, whereas it accounted the majority of the total emissions from the rangelands, i.e., 35.15 (± 4.25)% during the entire study period (Figure 3.4). The chemical fertilizer (FN) and manure (MN) applications together were identified as the most important source that drove the overall increase in the global N_2O emissions from the grazing lands, especially after the 1980s (Figure 3.4). Applied to pastureland soil only, the combined contribution of the external fertilizer and manure to the total N_2O emissions from the grazing lands increased from 1.48% to 36.6%. During the study period, FN accounted for 0.38 (±0.11) TgN yr^{-1} by 19.53 (±0.10)% of the total N_2O emission and MN was responsible for approximately 5.3% of the net emissions. The environmental factors that determine the background emissions had less impact on the changes in the total N_2O emissions. For instance, the total N_2O emissions from grazing lands attributed to AD declined from 28.5% in the 1960s to 16.0% in the 21st century (Figure 3.4). Moreover, in the absence of all of the external N inputs, we found that the residual N_2O emissions (RS), i.e., those controlled by litter decomposition, soil mineralization, and climate variables, also took 23.23% of the grazing lands N_2O emission on the global scale.

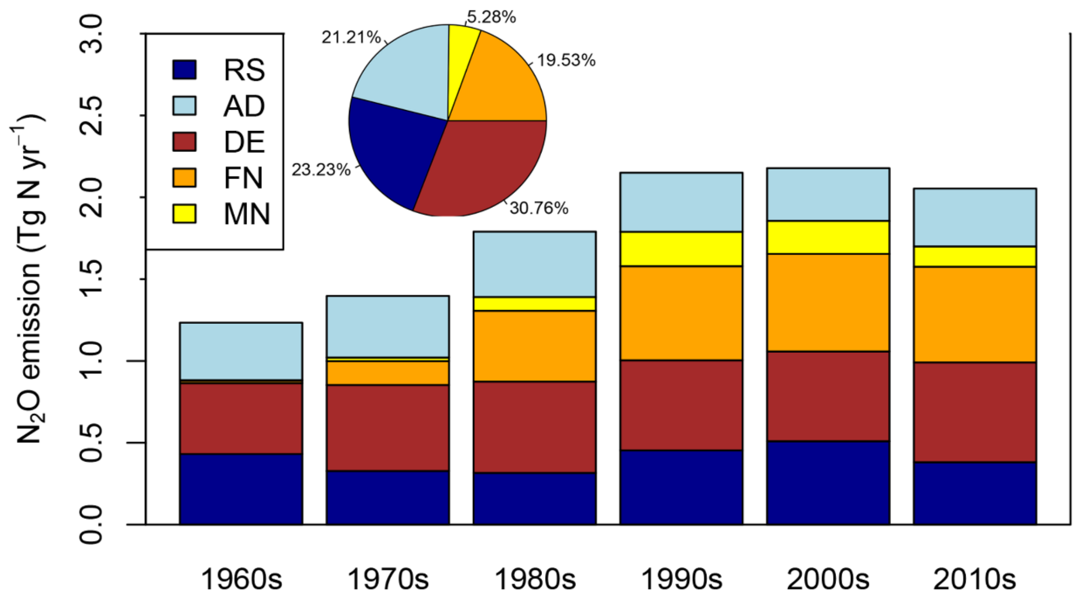

Figure 3.4 Attribution of the decadal average N_2O emissions from global grazing lands to

different driving factors. The pie plot covers the whole study period. RS: residual emissions; AD: atmospheric N deposition induced emissions; DE: N deposited in livestock excreta induced emissions; FN: fertilizer application induced emissions (pastureland only); MN: manure application induced emissions (pastureland only).

3.5.4 Variations in emission factors of fertilizer and deposited excreta

N_2O Emission factors (EFs) are a pragmatic approach to evaluate the sensitivity of ecosystem to external N inputs on different scales. Identifying the controlling factors of EF is helpful for specific management. Based on the difference between S1 and S5, the mean EF for anthropogenic N for the grazing lands was 0.85% during the study period. For the different biome types, the mean EFs were 1.59% and 0.60% for the pasturelands (DE, FN, MN) and rangelands (DE), respectively. For the forms of anthropogenic N inputs, the globally averaged EF_1 was larger (2.49%) than that of the deposited livestock excreta (EF_{3PRP}) for both the pasturelands and rangelands (0.82%). Modeled EF_1 and EF_{3PRP} exhibited strong spatial variation patterns globally. The EF_1 was consistent with the emission hotspots (Figure 3.3 and 5a), in which the pastoral N_2O emissions were largely sensitive to the addition of reactive N (EF_1 > 5%). As the most important factor controlling EF_1 among multiple variables (Table 3.S4), the NO_3^- fraction exhibited a positive correlation with EF_1 in most of the pastureland areas, but it had a negative effect on the increase in the NO_3 fraction in the eastern NA and western EU (e.g., France) (Figure 3.5b). EF_{3PRP} was less than 0.5% in most of the world's grazing lands but large values were still found in the Qinghai-Tibetan region, AF, and NA (Figure 3.5c). The changes in EF_{3PRP} in all of the grazing lands showed an overall significant negative correlation with the excreta deposition (Table 3.S4). However, the relationship was not consistent across the globe since the EF_{3PRP} was positively correlated with the amount of excreta N in pasturelands, whereas it was negatively or not correlated for the rangelands (Figure 3.5d).

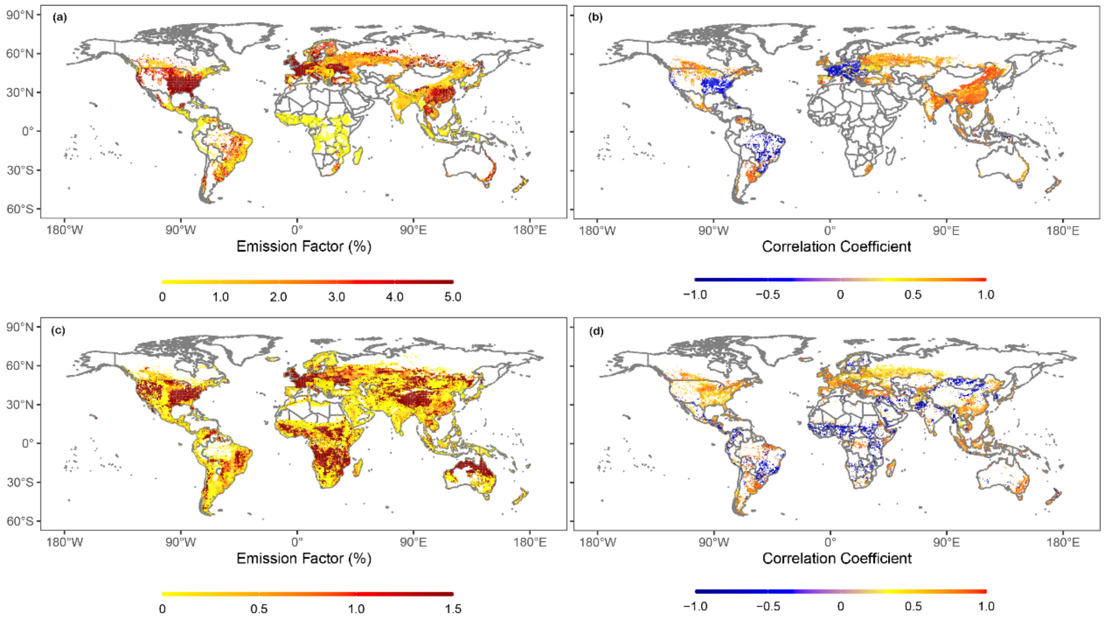

Figure 3.5 Spatial patterns of the mean emission factors (EFs) and the correlation coefficients of the major control variables during 1961–2016. (a, c) Mean values of EF_1 and EF_{3PRP}, respectively. (b, d) Correlation coefficients between EF_1 and the fraction of applied NO_3^- and between EF_{3PRP} and excreta deposition. Notably, only the significant correlated grid cells (*p* < 0.01) over the study period were presented.

3.5.5 Variations of estimated N_2O emission in response to changing N input forms

By varying the forms of the applied chemical fertilizer on the pasturelands and the excreta deposited on all of the grazing lands, the estimated magnitudes of the N_2O emissions exhibit large variations (Figure 3.6). During the study period, a 20% decrease in the NH_4 fraction of the fertilizer (i.e., 20% increase in the NO_3^- fraction) resulted in an overall 41.24(±19.38)% increase in the total N_2O emissions, while a 20% increase reduced the N_2O emissions by 16.8%. Notably, for the higher fertilizer NO_3^- input under scenario F_p2, a constant increasing trend was obtained for the estimated N_2O emissions, reaching 3.64 TgN yr^{-1} in the 2010s. As for the forms of the deposited livestock excreta, a higher proportion of inorganic matter in the deposited excreta led to a constantly increase in the N_2O emissions from the grazing lands at a rate of 0.76 TgN yr^{-1}, while a 20% decrease in the inorganic fraction of the excreta resulted in a reduction of the total N_2O emissions by 11.93%. However, the changing composition of the organic matter in the deposited excreta (e.g., larger C:N ratios of organic substance) caused less variations in the N_2O emissions from the grazing lands.

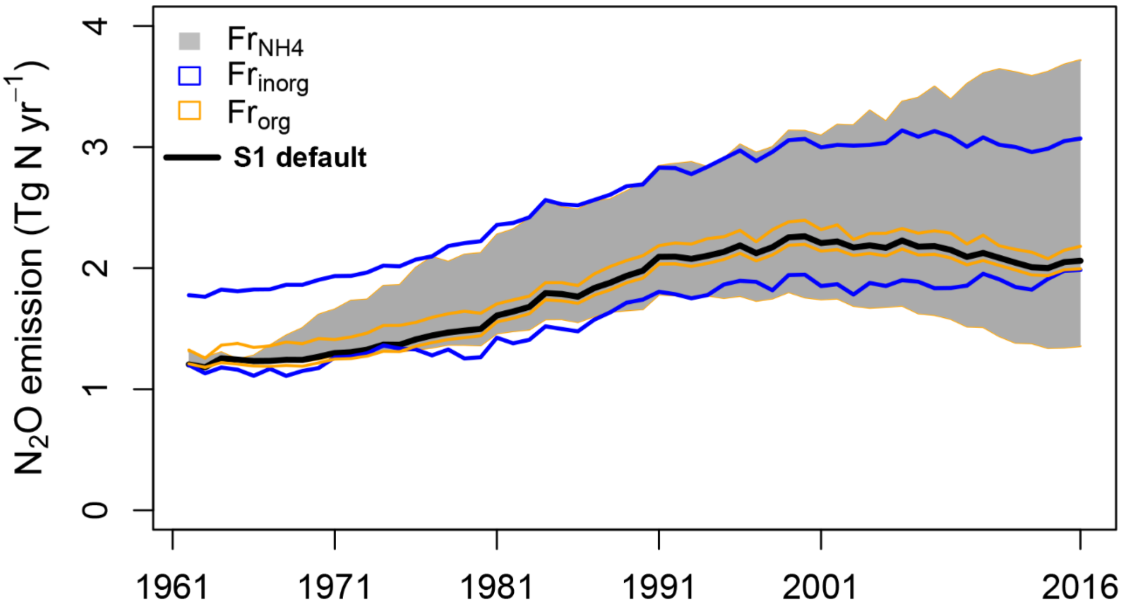

Figure 3.6 Range of the uncertainty of the global N_2O emissions from the grazing lands during 1961–2016 due to varying the properties of the chemical N fertilizer (grey) and deposited excreta (blue and orange). Fr_{NH4}, Fr_{inorg}, and Fr_{org} denote the fixed fraction of NH_4^+ in chemical fertilizer, fixed inorganic and organic proportions of deposited excreta N, respectively.

3.6 Discussion

3.6.1 Simulated spatiotemporal patterns compared with previous estimations

At the site scale, the consistency between the modeled and observed results suggests that TRIPLEX-GHG model v2.0 is capable of producing a reasonable estimation of the N_2O emissions from grazing lands under diverse climatic and management conditions. In agreement with our first hypothesis, globally, the estimated magnitude of the global N_2O emissions from pasturelands and rangelands exhibited large temporal and spatial variations, which were generally consistent with the ranges of previous modeling studies and the field observations.

Using the process-based ORCHIDEE-GM model, Chang et al. (2021) provided an estimation of the total emission rate (1.78 TgN yr^{-1}) from global grasslands in 2010, which is comparable with our result (2.04±0.02 TgN yr^{-1} in the 2010s; Figure 3.2a). The slight difference is probably due to the different model input information, such as fertilizer application and wild grazer activities (Chang *et al.*, 2021). In another modeling study, the DLEM determined that the grazing lands produced a net N_2O flux of 2.4 TgN_2O-N yr^{-1} during 1961–2014 (Dangal *et al.*, 2019). Given the use of the same grassland N input forcing data for the simulation, our lower N_2O estimation (1.8 TgN yr^{-1} 1961-2016; Figure 3.2a) may result from the application of NO_3:NH_4 ratio data (Nishina *et al.*, 2017) and the description of the organic N input properties. We further compared our results with the estimate obtained by an artificial neural network, i.e., a grassland N_2O emission rate of 1.31 TgN yr^{-1} in 2000 (Zhuang *et al.*, 2012). Their underestimation (compared to 2.20 TgN yr^{-1} in this study) was probably attributed to the limited training data used for the developing regions, such as Africa, which have extensive grazing activities (Butterbach-Bahl *et al.*, 2020). Previous studies using TRIPLEX-GHG v1.0 reported the N_2O emissions from global grasslands were 1.40 ± 0.03 TgN yr^{-1} during 1992–2016 (Zhang, K. *et al.*, 2019). The different modeled result (2.13±0.04 TgN yr^{-1}; Figure 3.2a) highlighted the effective model improvement in estimating the effect of grazing management on N_2O emissions. As for the spatial patterns of the global N_2O emissions from grazing lands during the study period, including distribution of emission hotspots and magnitudes of N_2O fluxes under varying conditions, this study was also generally in line with existing literatures (Figure 3.2) (Chang *et al.*, 2021; Dangal *et al.*, 2019). For instance, our estimated grazing lands N_2O emission in Europe and North America are consistent with DLEM but we found a smaller contribution of grazing lands in China (Figure 3.3), which may result from the different descriptions of excreta decomposition.

3.6.2 Deposited excreta alone was a minor contributor to N_2O emissions without fertilizer

Our simulated results partially supported the second hypothesis. Although the constantly increasing amount of livestock excreta N, which is a major indicator of grazing activities, was the largest historical N_2O emission source, the estimated contribution was minor (~31.67% at 0.54 TgN yr^{-1}) compared to previous modeling results (Figure 3.4). For instance, the widely adopted IPCC 2006 default models and the process-based DLEM model obtained similar results that the deposited excreta produced 1.55 and 1.31 TgN_2O-N yr^{-1}, respectively (Dangal *et al.*, 2019; Oenema *et al.*, 1997). The difference suggested the impact of grazing activity alone to the global N_2O emissions from grazing lands has probably been overestimated.

A growing number of observations and synthetic studies across large areas supported this finding with significantly smaller field excretal emission factors (EF_{3PRP}) than that of IPCC 2006 and other modelled results (Cai *et al.*, 2017; Chadwick *et al.*, 2018; van der Weerden *et al.*, 2020; Zhu, Y. *et al.*, 2021). Studies conducted in European grasslands reported that the effect of grazing on N_2O emissions was primarily observed at fertilized sites only and was by no means systematic (Flechard *et al.*, 2007). A global meta-analysis further proposed that in the absence of fertilization and other management, the effect of isolated grazing on the N_2O flux was not consistent and tended to reduce the year-round cumulative N_2O emissions, especially under heavy grazing intensities (Tang *et al.*, 2019). Our simulated results prevented the possible overestimation as suggested by addressing the insensitivity of rangelands to excreta depositions (i.e., smaller EF_{3PRP}, Figure 3.5c-d). As a support, our estimated mean EF_{3PRP} for animal wastes falls within the estimated range of the recent 2019 refinement to the IPCC Guidelines report (i.e., 0.77% and 0.39% for cattle and sheep, respectively) (Mancia *et al.*, 2022). The good agreement with the detected grazing effects is favored by three model features and mechanisms. First, the excreta are not exact external nutrient sources like chemical fertilizers (Zhang, B. *et al.*, 2017) because although deposited excreta is a more accessible form to soil microbes, grazing activity reduces the vegetation litter input for the N_2O production compared with undisturbed soil (López-Aizpún et Horrocks, 2020; Tang *et al.*, 2019; Yan *et al.*, 2016). Next, the legacy effects of organic input also account for the low N_2O emissions from excreta since the decomposition is required before being utilized for nitrification and denitrification in the model structure (Gerber *et al.*, 2013; Li, C. *et al.*, 2012). Additionally, grazing activities reduce the freeze-thaw cycles induced N_2O pulses from rangelands in cool-climate meadow regions as consistent with our results (Figure 3.S9b) (Wolf *et al.*, 2010). Meanwhile grazing also limit the potential N_2O production by affecting soil microbial activities (Zhong *et al.*, 2017).

Although the different chemical compositions of livestock excreta result in diverse response levels of N_2O to N additions (Lopez-Aizpun *et al.*, 2020; Mancia *et al.*, 2022), our results suggest the grazing activity could become a less concern without other agricultural management (e.g., fertilization) to changing climate. Existing models directly estimated the effect of the N contained in excreta based on application experiments within the chambers which might result in overestimations because excreta deposition occurs in inconstant amounts and the patches are unevenly disturbed over a large area (David, 2013; O'Neill *et al.*, 2021; Voglmeier *et al.*, 2019). Therefore, it is necessary for model communities to reassess and update the contribution of the grazing activity to N_2O emissions. More large scale observations (e.g., eddy covariance) are also required to systematically investigate the response of N_2O emissions to different grazing intensities in absence of fertilization for model testing (Liang, L. L. *et al.*, 2018; Murphy *et al.*, 2022; Voglmeier *et al.*, 2019).

3.6.3 Different forms of N inputs regulate the variations in N_2O emissions from grazing lands

Consistent with our third hypothesis, our results highlighted the fact that the estimated N_2O emissions showed significant changes with the varying N forms of the fertilizer, manure and excreta input to the grazing lands. However, previous large-scale modeling studies have only paid attention to the estimation based on amount of the N input rate (Chang *et al.*, 2021; Dangal *et al.*, 2019; Liu *et al.*, 2020). Their neglected effects of the variations and differentiation in the forms of the input N resulted in the difference with our modelled patterns and introduced major uncertainties to estimations.

We found slowly decreasing trends in the N_2O emissions from global grazing lands since the end of the 1990s. The decreased pasturelands emissions, especially in EU (by -0.20 TgN yr^{-1}, Figure 3.2b), were responsible for this reduction because of the decreased NO_3^- ratio of applied fertilizer (Nishina *et al.*, 2017) and reducing manure application rates, although the total pasturelands area and N input rates consistently increased during the same period. Additional simulations (i.e., with the NO_3^- and manure application rate held constant after 1990) confirmed that the decreased NO_3^- application had larger impacts on the declined total emissions (Figure 3.S3b, S6) (Smith *et al.*, 2012). The wet soil condition created by large water content of livestock excreta favors denitrification while inhibits nitrification, accelerating the production of N_2O. Next, we obtained a lower contribution of N_2O emissions from the pasturelands in southern AS (e.g., China) than previous estimations but the modelled emission rates agreed well with the measured data for this region, ranging from 0.5 to about 3.0 kgN ha^{-1} yr^{-1} (Peng, Q. *et al.*, 2011; Yang *et al.*, 2015; Zhang, L. *et al.*, 2017). This discrepancy may result from the lower fraction of applied fertilizer NO_3^- (Figure 3.S3) and the degraded soil properties (Nishina *et al.*, 2017), supporting the determinant role of chemical forms of input N.

The different effects of fertilizers and livestock excreta on N_2O emissions were detected across the globe, suggesting a strong impact for estimation (Cai et Akiyama, 2016; Shcherbak *et al.*, 2014). In this study, the response level of N_2O to fertilizer application was higher overall than the most wide-spread empirical results (i.e., IPCC 2006, $EF_1 = 1.0\%$), but it was in agreement with the range of recent field observations (Liu *et al.*, 2017). Our modeled N_2O emissions confirmed the stronger sensitivity to the NO_3^- addition than other forms of N (Table 3.S4) because denitrification processes are the most important source of N_2O production in managed soils (Harty *et al.*, 2016; Liang, D. et Robertson, 2021; Smith *et al.*, 2012; Wang, J. *et al.*, 2018). We also found the combination of different forms of N (i.e., inorganic and organic) can change the response level of the N_2O emissions. As a common feature of grazing lands, interactions between fertilizer N and manure and excreta create significant N_2O emission hotspots (Luo *et al.*, 2017) but related studies are limited (Maire *et al.*, 2020; Murphy *et al.*, 2022). When manure and excreta are applied (organic N), the sensitivity of N_2O to the addition of N may increase due to the increase in the soil organic matter content (Pärn *et al.*, 2018), microbial abundance (e.g., denitrifiers) and activity (e.g., enzymatic) compared with single N loading (Wang, C. *et al.*, 2021; Zhang, Y. *et al.*, 2022). The forms of livestock excreta N is another factor affecting the responses of estimated N_2O emissions (Du *et al.*, 2021; Mancia *et al.*, 2022). In line with field experiments, the simulated results were more sensitive to urine N (inorganic) than dung addition (organic, Figure 3.6) (de Bastos *et al.*, 2020; van der Weerden *et al.*, 2020; Zhu, Y. *et al.*, 2021). Furthermore, on the global scale, N_2O emissions showed diverse responses to the additions of urine and dung from different animal species because of the varying chemical compositions (Cai *et al.*, 2017; Dijkstra *et al.*, 2013; López-Aizpún et Horrocks, 2020).

By summarizing the contribution of different drivers to total N_2O emissions and the relationships between EFs and various factors, our study demonstrated N inputs have more important role in determining spatiotemporal variations in grazing lands N_2O emissions than environmental factors, which contradicts with other agricultural lands globally (Cui *et al.*, 2021). In particular, we quantitively emphasized the significance of different responses of N_2O emissions to changes in input N forms for grazing lands. Therefore, except reducing overall N input amounts, it is possible to use fertilizer with low NO_3^- fraction and apply excreta (or manure) with high organic matter content as environment-friendly practices to mitigate N_2O emissions from global grazing lands.

3.6.4 Other sources of modeling uncertainties and future improvements

Land use and vegetation maps may also generate uncertainties in the estimation of N_2O emission. The underlying grazing lands datasets are fairly different in terms of the methodology and thus the spatial extent of the grazing land areas (Goldewijk *et al.*, 2017; Ramankutty *et al.*, 2008). A more inclusive definition of grazing land causes less N surplus overall and discrepancies in the N indicators (Kaltenegger *et al.*, 2021) (Figure 3.S10). The detailed timing of the fertilizer and manure applications and global distribution maps of grazers density are helpful for accurate estimation (Sordi, André *et al.*, 2014; Thies *et al.*, 2020). Further model incorporation of additional biological N fixation processes

(Fuchs *et al.*, 2020), destabilization on the N substrates and the death of fine roots (Ruan et Robertson, 2017) are helpful in improving the estimation. It is noteworthy that climate factors also change the magnitude of grazing lands N_2O emissions. But inconsistent effects of changing climate were obtained for field experiments and model estimated results due to the heterogeneity and complexity of climate factors that affects N_2O emissions in both directions as reflected by our simulations (Chatskikh *et al.*, 2005; Dangal *et al.*, 2019; Flechard *et al.*, 2007). Therefore, higher quality global climate and management datasets are required to reduce the current uncertainties of estimations of N_2O emissions from grazing lands and to support sustainable development (Tian *et al.*, 2019).

3.7 Conclusion

Our study provided a reliable estimation of the magnitude, source, and uncertainty of global grazing lands N_2O emissions. The results demonstrated the strong spatiotemporal variation patterns of N_2O emission from grazing lands are largely determined by management practices, including chemical fertilizer application and grazing activities. Scenario simulations suggested N fertilizer is responsible for the overall increase in historical N_2O emissions from global grazing lands. The contribution of the deposited excreta accounts for the largest source of total grazing lands N_2O emissions but such effect was overestimated by previous oversimplified modeling studies. The exclusive effect of grazing activity may act as a less concern in emitting N_2O. We further noticed the different descriptions of the forms of anthropogenic N inputs to grazing lands have major impacts on the estimated N_2O emission patterns because the strong sensitivity to nitrate fraction of chemical fertilizer and inorganic proportion of deposited excreta N. This study has important implications for enhancing our understanding of the forms of external N additions in model estimations and mitigation strategy of grazing lands N_2O emissions.

3.8 Supplementary information

3.8.1 Model description of production of N_2O as well as manure allocation

The TRIPLEX-GHG model used the concept anerobic balloon to separate the nitrification and denitrification processes.

The anaerobic volumetric fraction (ANVF) was the key parameter, which represents the soil oxygen status and regulates the allocation rates of the substrates (e.g., dissolved soil organic carbon (DOC), NH_4^+, and NO_3^-) for nitrification and denitrification. It was calculated using the oxygen partial pressure and the air-filled porosity (S1):

$$anvf = e^{-SP_{O2} \cdot P_{O2}} \qquad \text{(s1)}$$

where SP_{O2} is the shape parameter, and P_{O2} is calculated based on air-filled porosity, which can be substituted for missing aggregated soil data for O_2 calculations.

In the TRIPLEX-GHG model, nitrification is an aerobic process that occurs outside of the anaerobic balloon, converting ammonium (NH_4^+) into nitrate (NO_3^-) driven by nitrifying bacteria with N_2O as a by-product (Li, C. S. *et al.*, 2000; Morkved *et al.*, 2007; Zhang, K. *et al.*, 2017). The nitrification rate was calculated using the Michaelis–Menten function based on the concentration of NH_4^+ and the microbial activity of the nitrifying bacteria which is defined by nitrifier growth and death rates. The effects of the soil properties were also simulated.

$$R_{nit} = B_{nit} \cdot \frac{R_{max} \cdot [NH_4]}{(6.18 + [NH_4])} \cdot pH \qquad \text{(s2)}$$

Where R_{nit} is the nitrification rate (kg N m^{-2} d-1); R_{max} is the maximum nitrification rate (d-1); [NH4] represents the NH4+ concentration (kg N m^{-2}); Bnit is the biomass concentration of nitrifiers (kg C m^{-2}); and pH is the soil pH level.

Denitrification is the process through which the nitrate is reduced stepwise into different nitrogen gases as a chain reaction process inside of the anaerobic balloon. Denitrification can be divided into 4 independent steps, which are linked by the competition for DOC by the specific denitrifiers during each step (Betlach et Tiedje, 1981). Similarly, the growth and mortality rates of the different denitrifiers utilized a double substrate based (DOC and NOx) Michaelis–Menten equation. The consumption of NO_X for the growth of the different denitrifiers was calculated at an hourly time step according to previous studies as is shown in the following Eq s3. (1) (Leffelaar and Wessel, 1998; (Li, C. S. *et al.*, 2000):

$$F_{ANNOX} = COE_{dNOX} \cdot B_{denit} \cdot \left(\frac{R_{NOX}}{EFF_{NOX}} + \frac{MAI_{NOX} \cdot [NO_X]}{[N]}\right) \cdot f_{NOX}(pH) \cdot f(t). \qquad \text{(s3)}$$

Here, F_{ANNOX} is the consumption rate of NO_X (kg N m^{-3} h^{-1}); COE_{dNOX} is the coefficient of NO_X consumption; B_{denit} is the biomass of the denitrifiers (kg C m^{-3}); R_{NOX} is the NO_X reduction rate (h^{-1}); EFF_{NOX} is the efficiency of the NO_X denitrifiers (kg C kg N $^{-1}$); MAI_{NOX} is the maintenance coefficient of NO_X (h^{-1}); $[NO_X]$ and $[N]$ are the NO_X and total N concentrations in the anaerobic balloon, respectively; and

$f_{NOX}(pH)$ and $f(t)$ are the effects of the soil pH and soil temperature on the NO_X denitrification rate in each step, respectively.

The manure-sourced N entered the different inorganic N and organic N pools separately. The organic portion of the manure was added to up to 3 soil organic matter pools (the non-protected, protected, and passive organic carbon pools) separately for further decomposition.

$$ManureNH_4{}^+ = R_{NH4} \cdot Manure_N. \tag{s4}$$

$$ManureNO_3{}^- = R_{NO3} \cdot Manure_N. \tag{s5}$$

$$ManureC_{SOM} = proportion_{SOM} \cdot C{:}N_{SOM} \cdot Manure_N. \tag{s6}$$

Here, $ManureNH_4{}^+$ and $ManureNO_3{}^-$ are manure-sourced NH_4^+-N and NO_3^--N, respectively, which are calculated using the ratio of ammonia and nitrate (i.e., R_{NH4} and R_{NO3}) to total manure N. $ManureC_{SOM}$ is the amount of manure that entered the different SOM pools; $proportion_{SOM}$ is the proportion of manure N added to the different SOM pools; and $C{:}N_{SOM}$ is the C:N ratio of a particular SOM pool.

For more detailed process descriptions of the model, please check the Zhang et al. (2017) and Song et al. (2021).

3.8.2 Model descriptions of integrated processes related with grazing lands

Livestock grazing effects

Any change in grazing practices mostly affects the quantity and quality of the animal waste input and grass litter incorporation, which eventually redefines the soil C and N balance with the local climate and soil conditions. The deposited excreta of grazing livestock, including urine and dung are important nutrient (e.g., C and N) sources to grazed soil.

Urine is considered directly as the practice named 'fertigation' which adds inorganic N substrates and water to soil surface simultaneously. However, the chemical composition of dung includes both inorganic and organic N which is further separated in respect of different C:N ratios of soil organic matter pools for further decomposition. Based on previous modeling and field experiments, the amounts and properties of input dung and urine were calculated by the following equations accordingly (Reed *et al.*, 2015; Velthof, Gerard L *et al.*, 2015; Zhang, B. *et al.*, 2017) (Eq.1-4):

$$N_{dung} = (1.0 - R_{collect}) \cdot RDN_i \cdot \min\left(\sum_{i=1}^{n} head_i \cdot adN_{coni} \cdot (1.0 - NUE_i), ExNrate_i\right) \tag{S1}$$

$$C_{dung} = proportion_{SOM} \cdot C{:}N_{SOM} \cdot N_{dung} \tag{S2}$$

$$N_{urine} = (1.0 - R_{collect}) \cdot RUN_i \cdot \min\left(\sum_{i=1}^{n} head_i \cdot adN_{coni} \cdot (1.0 - NUE_i), ExNrate_i\right) \tag{S3}$$

$$w_{urine} = N_{urine} \cdot RN_{uine} \quad \text{(S4)}$$

where i=1-n correspond to different major livestock species, dairy cow, beef cattle, swine, sheep and other species respectively. While only one livestock species was involved for most of the reported field experiments which were included in calibration and validation. N_{dung} and C_{dung} denote the N and C content of dung left on the soil surface for each grazing day and N_{urine} represents the N concentration of animal deposited urine, respectively. $R_{collect}$ means the recollected ratio for dung and the value is set based on the information 'ratio for manure left on grassland' provided by Zhang et al. (2017). RDN_i and RUN_i are used for representing the ratios that deposited nitrogen in feces is split into urine and dung for species i, respectively. NUE_i indicate the nutrient use efficiency for nitrogen (from consumed vegetation) of species i and the values were taken from IPCC (2019) (Table 10.20) which described the fraction of daily N intake that is retained by different grazing animals while $ExNrate_i$ is the default N excretion rate for livestock category i based on Zhang et al. (2017). $head_i$ means the number (density, head ha^{-1}) of the livestock species i. In the meantime, the adN_{coni} denote the daily N consumption rate from vegetation for species i per animal (based on the consumed C and vegetation C:N ratios). $C:N_{SOM}$ represents the C:N ratios of different SOM pools. w_{urine} and RN_{uine} indicated the volume of urine water and urine N concentration, respectively. The values of associated parameters were listed in Table 3.S1.

Meanwhile, grazing activity directly consumes aboveground plant biomass but trampling may also damage plant tissues which lead to a reduction in aboveground net primary productivity (NPP) as described with Eq.5. Meanwhile, trampling also induces soil compaction, which changes the soil physical properties (i.e., soil prosperity and oxygen diffusion rate) and thereby affecting the subsequent processes of production and release of gases. Such effect is mostly observed for top layer of the soil profile.

$$f_g = I_{graz} \cdot (-0.0072 + COE_{tramp} \cdot head_i) \quad \text{(S5)}$$

Where f_g (%) means the reduction rate of plant growth with existence of grazers at one time step (daily); I_{graz} is the indicator of grazing activity and COE_{tramp} donates the coefficient of animal trampling effect.

Freeze-thaw cycle

For natural grasslands and those with minor management practices, freeze-thaw induced N_2O emission pulse dominate the annual total N_2O budget. The denser and higher vegetation cover supports higher snow-pack which further promotes microbial activities and provides more moisture supply with rising temperature in early spring compared with intensively grazed grasslands. For current model, soil temperature is designed to trigger the freeze-thaw cycle. When soil temperature is below 0 °C, a fraction of microbial biomass dies followed by further decomposition and released dissolved organic C (DOC) as well as N-substrate from dead microbial biomass. A proportion of these nutrient are trapped within frozen soil aggregates. As soil temperature recover to 0°C, the trapped DOC, NH_4^+, and NO_3^- are mobilized gradually with free water and stimulates denitrification process. Equation 4 to 9 describe the process in detail.

$$Fdmic_{frost} = COE_{frost} \cdot e^{(Temp_{min} - Tsoil_i)} \tag{S6}$$

$$DOC_{dmic} = B_{mic} \cdot Fdmic_{frost} \tag{S7}$$

$$St\_NO3_{dmic} = Immob \cdot B_{mic} \cdot Fdmic_{frost} \cdot Rcn_{mic} \tag{S8}$$

$$St\_NH4_{dmic} = Immob \cdot B_{mic} \cdot Fdmic_{frost} \cdot Rcn_{mic} \tag{S9}$$

$$Rl\_NO3_{dmic} = WFPS \cdot St\_NO3_{dmic} \tag{S10}$$

$$Rl\_NH4_{dmic} = WFPS \cdot St\_NH4_{dmic} \tag{S11}$$

Where $Fdmic_{frost}$ indicates the fraction of dead soil microbial biomass induced by freezing temperature. $Temp_{min}$ and $Tsoil_i$ is the minimum air temperature of the reference year (monthly mean of 1901-1920) and soil temperature for layer i respectively while COE_{frost} is the coefficient of frost induced death. DOC_{dmic} represents the DOC concentration from dead microbes. The variable $Immob$ means the ice-induced immobilization ratios which is a related with soil texture, ice-content, and free water concentration. St_DOC_{dmic}, St_NH4_{dmic}, and St_NO3_{dmic} mean the DOC, NH_4^+, and NO_3^- immobilized by soil ice-parcels while Rl_DOC_{dmic}, Rl_NH4_{dmic}, and Rl_NO3_{dmic} represent the released part of the immobilized nutrients, which could be utilized for plant growth, microbial regrowth, and N-trace gas production. B_{mic} is the soil micro-biomass (g C m^{-2}) and Rcn_{mic} is the C:N ratio of soil microbes as calculated within model, respectively.

Moreover, we improved the simulation of snow melting, soil freezing point depression and soil hydraulic conductivity. Soil water never freezes completely as new ice formation is calculated based on a ratio of the available liquid water, so that the process that the freezing point of soil moisture decreases linearly with increasing soil ice content was described in Eq.12.

$$T\_Freeze_i = T_{melt} - COE_{iceform} \cdot Isoil_i \qquad \text{(S12)}$$

Here, T_Freeze_i denotes the freezing point of soil layer i, T_{melt} means the ice-melting point (0°C) while $Isoil_i$ is the soil ice content (%) of layer i. $COE_{iceform}$ indicates the coefficient of ice-formation.

3.8.3 Evaluation of model performances on site level

For model calibration, we adjusted value of the most sensitive parameter of the N_2O emissions (obtained from sensitivity analysis of parameters) in order to fit the best model performance by comparing the output of daily N_2O flux data with the observed data obtained from published papers via trial and error and statistical model performance indicators.

The index of agreement (*D*), the root mean square error (*RMSE*), and the coefficient of determination (R^2) were used to evaluate our model's performance in daily time step, and the D-value and *RMSE* were calculated as follows:

$$D = 1 - \frac{\sum_{i=1}^{n}(S_i - O_i)^2}{\sum_{i=1}^{n}(|S_i - {}^{-}O| + |O_i - \overline{O}|)^2}, \qquad \text{(s7)}$$

$$RMSE = \sqrt{\frac{\sum_{i=1}^{n}(S_i - O_i)^2}{n}}. \qquad \text{(s8)}$$

Here, S_i is the ith simulated result corresponding to the number of observations; O_i is the ith observed value; and $\overline{O}$ is the mean of the observed values during the experimental period. D varies between 0 and 1, and is excessively sensitive to extreme values (Willmott, 1981). The model performance was considered to be perfect and unmeaningful when the D value was set to 1 and 0, respectively. The *RMSE* is the key value representing the difference between the simulated and observed values, and is significantly affected by the data units (e.g., mg N m^{-2} day^{-1} compared with kg N ha^{-1} day^{-1}).

All the observed N_2O flux data was obtained from published literatures with GetData software (Digitize graphs and plots - GetData Graph Digitizer - graph digitizing software (getdata-graph-digitizer.com)))

3.8.4 Description of model input dataset

Climate data: we obtained daily climate data from reconstructed climate dataset in daily time step from 1901-2015 provided by Climatic Research Unit–National Centers for Environmental Prediction (CRU–NCEP) climate version 7 which is a fusion of the CRU and NCEP–NCAR reanalysis climate datasets (https://www.earthsystemgrid.org/dataset/ucar.cgd.ccsm4.CRUNCEP.v4.TPHWL6Hrly.html). Major variables include minimum, average and maximum air temperature (K), precipitation (mm/6h), specific humidity (%), air pressure (kp) and wind speed (m/s) to drive the model.

N deposition data: The monthly atmospheric N depositions (NHx-N and NOy-N) during 1860–2014 were primarily based on the International Global Atmospheric Chemistry (IGAC)/Stratospheric Processes and Their Role in Climate (SPARC) Chemistry–Climate Model Initiative (CCMI) N deposition fields. CCMI models explicitly considered N emissions from natural biogenic sources, lightning, anthropogenic and biofuel sources as well as biomass burning (Eyring et al. 2013). The transport of N gases was simulated by the chemical transport module in CCMI models. These data were recommended by the Coupled Model Intercomparison Project (CMIP) and used as the official products for CMIP6 models that lack interactive chemistry components (https://blogs.reading.ac.uk/ccmi/forcing-databases-in-support-of-cmip6/).

Vegetation cover data: For model initialization, we generated vegetation cover data by overlaying the Global Land Cover Map for 2009 (GlobCover2009) based on Medium Resolution Imaging Spectrometer (MERIS) remote sensing data (http://due.esrin.esa.int/page_globcover.php) with the ecoregions framework from the World Wildlife Fund (WWF). For model calibration and validation, the input information of land cover data is based on the corresponding published literatures (e.g., savanna; grassland / steppe; dense shrubland; open shrubland). Relying on these land cover data as input information, an overall 14 plant functional types (PFTs) are provided within the model structure and a set of climatic criteria determines which PFTs are allowed to exist in each grid cell.

During model simulation, the annual vegetation maps were aggregated from the Climate Change Initiative land cover project led by the European Space Agency (ESA−CCI−LC), which span cover a period of 24 years from 1992 to 2015 at a spatial resolution of 300m (ESA, 2017, http://maps.elie.ucl.ac.be/CCI/viewer/). These maps describe the terrestrial surface of the Earth in 37 original land cover (LC) classes based on the United Nations Land Cover Classification System (UN-LCCS) (Di Gregorio, 2005). These data were developed by combining the global daily surface reflectance of 5 different observation systems, and the data accuracy was evaluated at a global scale

(ESA, 2017).

Land use data: Annual grassland area and relative fraction of grid cell from 1860 to 2016 was acquired from the History Database of the Global Environment, version 3.2 (HYDE 3.2), datasets (ftp://ftp.pbl.nl/hyde/), which reconstructed time-dependent land use by historical population and allocation algorithms with weighting maps (Goldewijk et al. 2017). In support of the calculation of arid index, population density, grazing lands were further divided into pasture and rangeland which referred to extensively managed and intensively managed grassland respectively. Pasture receives chemical fertilizer and manure application during growing seasons to produce high level of grass/forage production, meanwhile, more intense grazing rate (density of livestock and duration days) often take place in pasture land. In comparison, rangeland only experience grazing activity and the only soil N input is animal excreta N. Pasture and rangeland were also categorized into C3 and C4 grass referring to local climate characteristics. Such category approach was also accepted by Dangal et al. (2019) and Tian et al. (2018) for process-based driven global simulation assessments.

In order to assess how discrepancies in land maps translate to differences in patterns and magnitude of grassland N2O emissions, another 2 land use maps were utilized.

Soil data: Global soil information of properties (soil texture and soil pH) and classification were obtained from the FAO/UNESCO Soil Map of the World (http://www.fao.org/geonetmork/srv/en/metadata.show?id514116) and data set provided by Batjes (2006) respectively. Meanwhile soil C and C:N ratio data for model initialization were generated from a global soil data set (IGBP-DIS; 2000).

Topographic data: We used a global digital elevation model (DEM) with an approximate spatial resolution of 1 km (GTOPO30) for topography input (http://www.temis.nl/data/gtopo30.html).

Atmospheric CO2 concentration data: Monthly atmospheric CO2 concentration data for the simulation period from 1860 to 2015 was obtained from the NOAA GLOBALVIEW-CO2 dataset derived from atmospheric and ice core measurements (www.esrl.noaa.gov).

Grassland N management data: For the site-level model calibration and validation processes, the amount and property (e.g., NH_4^+:NO_3^-, C:N ratios) of N input rates (chemical fertilizer, manure application) were based on the published literatures while if the corresponding information was not provided, we obtained the input data used for global simulation instead.

For the global simulation, the datasets associated with grassland management of nitrogen were provided by Lu et al. (2019), including annual manure N deposition (by grazing animals) rate, synthetic N fertilizer and N manure application rates at a resolution of 0.5°× 0.5°. Synthetic N fertilizer applied to pastureland only and it started from 1961 same as described by Nishina et al. (2017) and Lassaletta et al. (2014) while the applied manure on pastureland and deposited excreta N were for the period from 1860 to 2016 based on FAO dataset (2018) and Zhang et al. (2017). The properties of applied N fertilizer and manure were generated from Nishina et al. (2017) and Li et al. (2012), Song et al. (2021), respectively. Meanwhile, the deposited excreta properties were based on Wolf et al. (2012) and Li et al. (2012). The annual N input rates were separated into daily application due to the varying timing of application on pasture and rangeland area.

All of the input information was transformed to a spatial resolution of 0.5°×0.5° (about 50×50 km) using the ArcMap software (version 10.2) before the simulation.

3.8.5 Supplementary Figures

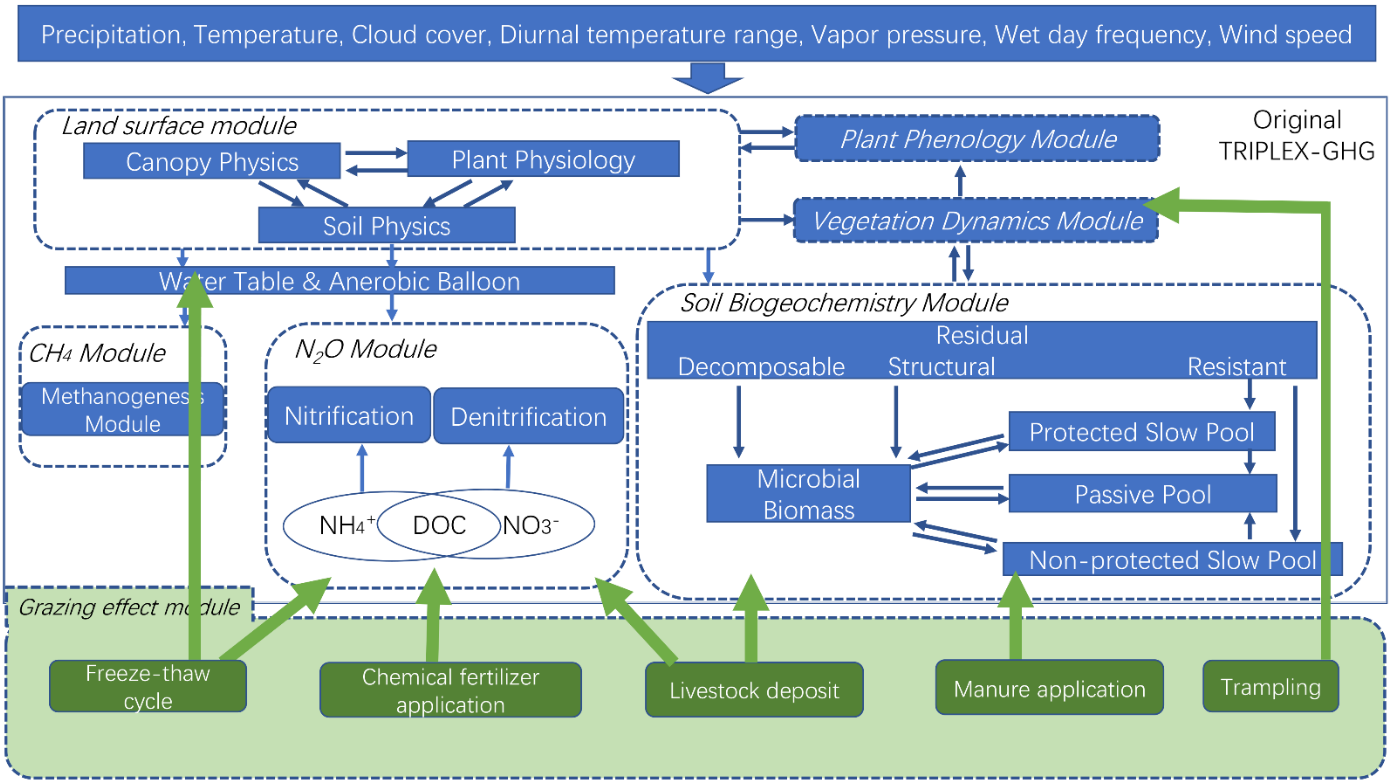

Figure 3.S1 Model's structural concept and the integration of the effects of grazing management into the TRIPLEX-GHG model v2.0 (revised with permission from Zhang et al. (2017)). The rectangular inset with the light green background represents the different management and natural processes and how they interact with the other submodules (e.g., the land surface module).

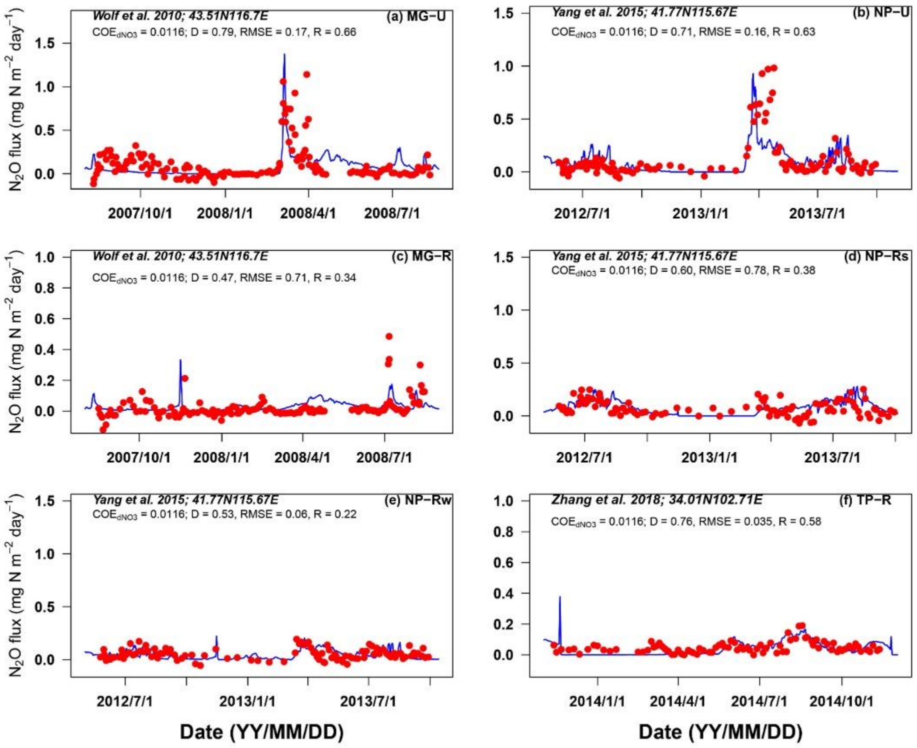
Wolf et al. 2010; 43.51N116.7E (a) MG−U
COEdNO3 = 0.0116; D = 0.79, RMSE = 0.17, R = 0.66
Yang et al. 2015; 41.77N115.67E (b) NP−U
COEdNO3 = 0.0116; D = 0.71, RMSE = 0.16, R = 0.63
Wolf et al. 2010; 43.51N116.7E (c) MG−R
COEdNO3 = 0.0116; D = 0.47, RMSE = 0.71, R = 0.34
Yang et al. 2015; 41.77N115.67E (d) NP−Rs
COEdNO3 = 0.0116; D = 0.60, RMSE = 0.78, R = 0.38
Yang et al. 2015; 41.77N115.67E (e) NP−Rw
COEdNO3 = 0.0116; D = 0.53, RMSE = 0.06, R = 0.22
Zhang et al. 2018; 34.01N102.71E (f) TP−R
COEdNO3 = 0.0116; D = 0.76, RMSE = 0.035, R = 0.58
N2O flux (mg N m−2 day−1)
Date (YY/MM/DD)

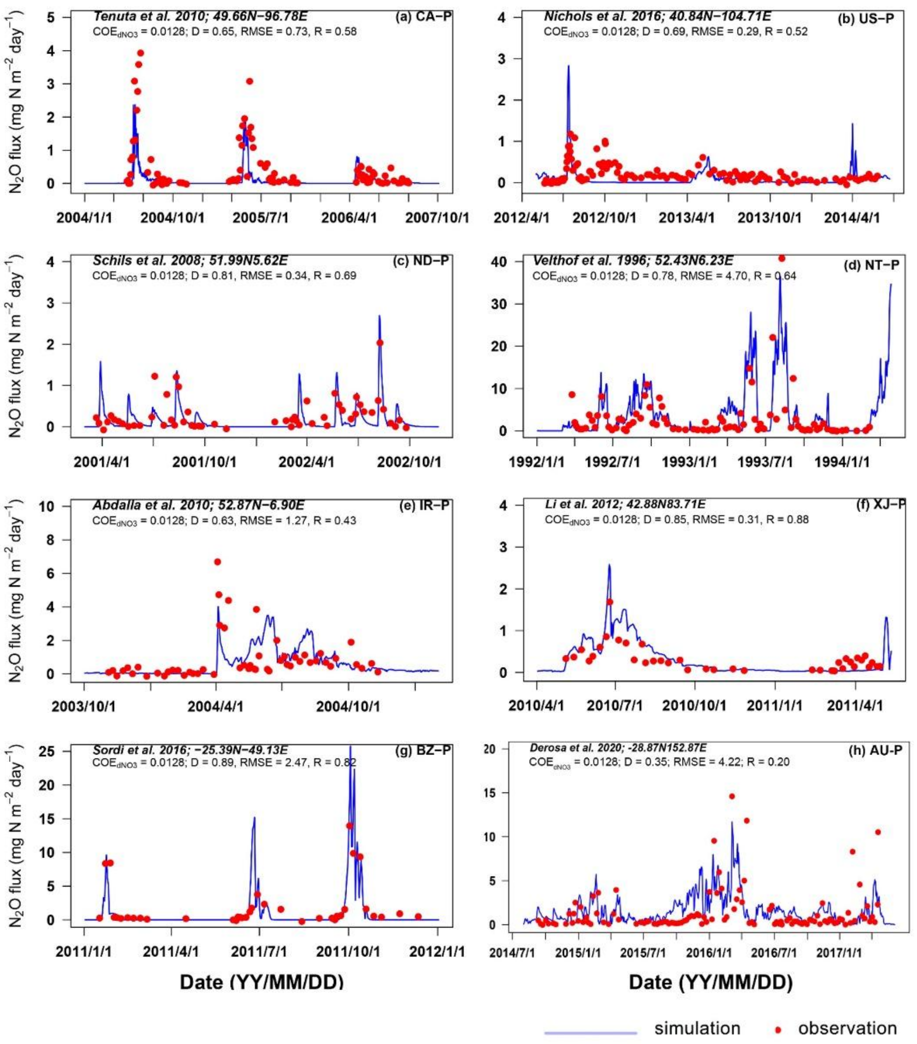
Tenuta et al. 2010; 49.66N−96.78E (a) CA−P
COEdNO3 = 0.0128; D = 0.65, RMSE = 0.73, R = 0.58
Nichols et al. 2016; 40.84N−104.71E (b) US−P
COEdNO3 = 0.0128; D = 0.69, RMSE = 0.29, R = 0.52
Schils et al. 2008; 51.99N5.62E (c) ND−P
COEdNO3 = 0.0128; D = 0.81, RMSE = 0.34, R = 0.69
Velthof et al. 1996; 52.43N6.23E (d) NT−P
COEdNO3 = 0.0128; D = 0.78, RMSE = 4.70, R = 0.64
Abdalla et al. 2010; 52.87N−6.90E (e) IR−P
COEdNO3 = 0.0128; D = 0.63, RMSE = 1.27, R = 0.43
Li et al. 2012; 42.88N83.71E (f) XJ−P
COEdNO3 = 0.0128; D = 0.85, RMSE = 0.31, R = 0.88
Sordi et al. 2016; −25.39N−49.13E (g) BZ−P
COEdNO3 = 0.0128; D = 0.89, RMSE = 2.47, R = 0.82
Derosa et al. 2020; -28.87N152.87E (h) AU−P
COEdNO3 = 0.0128; D = 0.35, RMSE = 4.22; R = 0.20
N2O flux (mg N m−2 day−1)
Date (YY/MM/DD)
simulation
observation

Figure 3.S2 Comparison of the modeled and measured N_2O emissions from the rangeland (unmanaged or sites with grazing activity only) and pastureland (intensively managed) sites with a daily time step.
MG-U and NP-U: unmanaged sites in Mongolia and North China Plain, respectively. MG-R: rangeland in Mongolia; NP-Rs: summer grazed rangeland in North China Plain; NP-Rw: winter grazed rangeland in North China Plain; TP-R: rangeland in Tibetan Plateau.
Comparison of the modeled and measured daily N2O fluxes from pastureland sites (intensively managed) with a daily time step. CA-P: pastureland in Canada; US-P: pastureland in the United States; NDP and NT-P: pasturelands in the Netherlands; IR-P: pastureland in Ireland; XJ-P: pastureland in Xinjiang; BZ-P: pastureland in Brazil; AU-P: pastureland in Australia

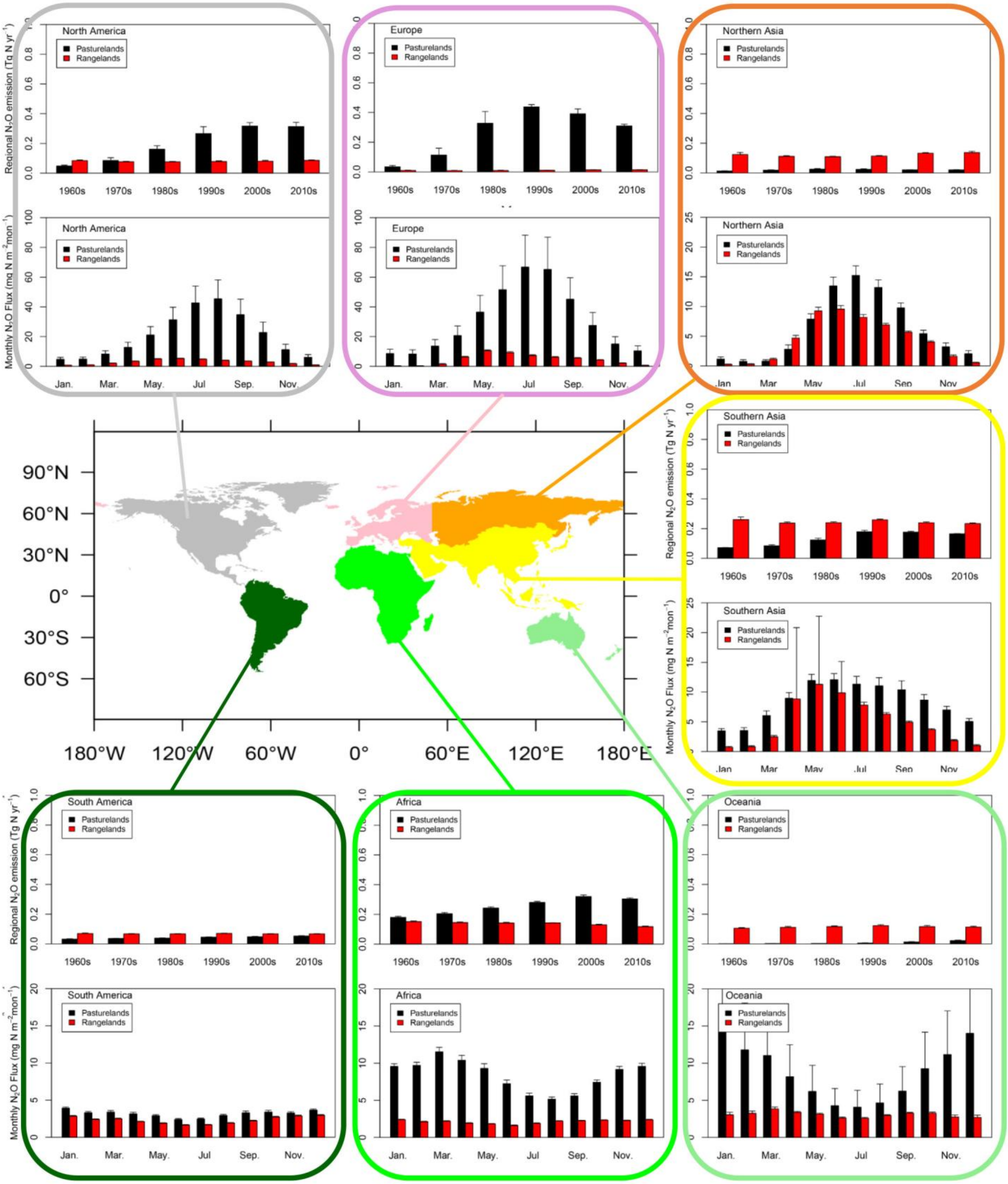

Figure 3.S3 Annual and seasonal variations of N_2O emissions from global grazing-lands and from pasturelands and rangelands of different continents

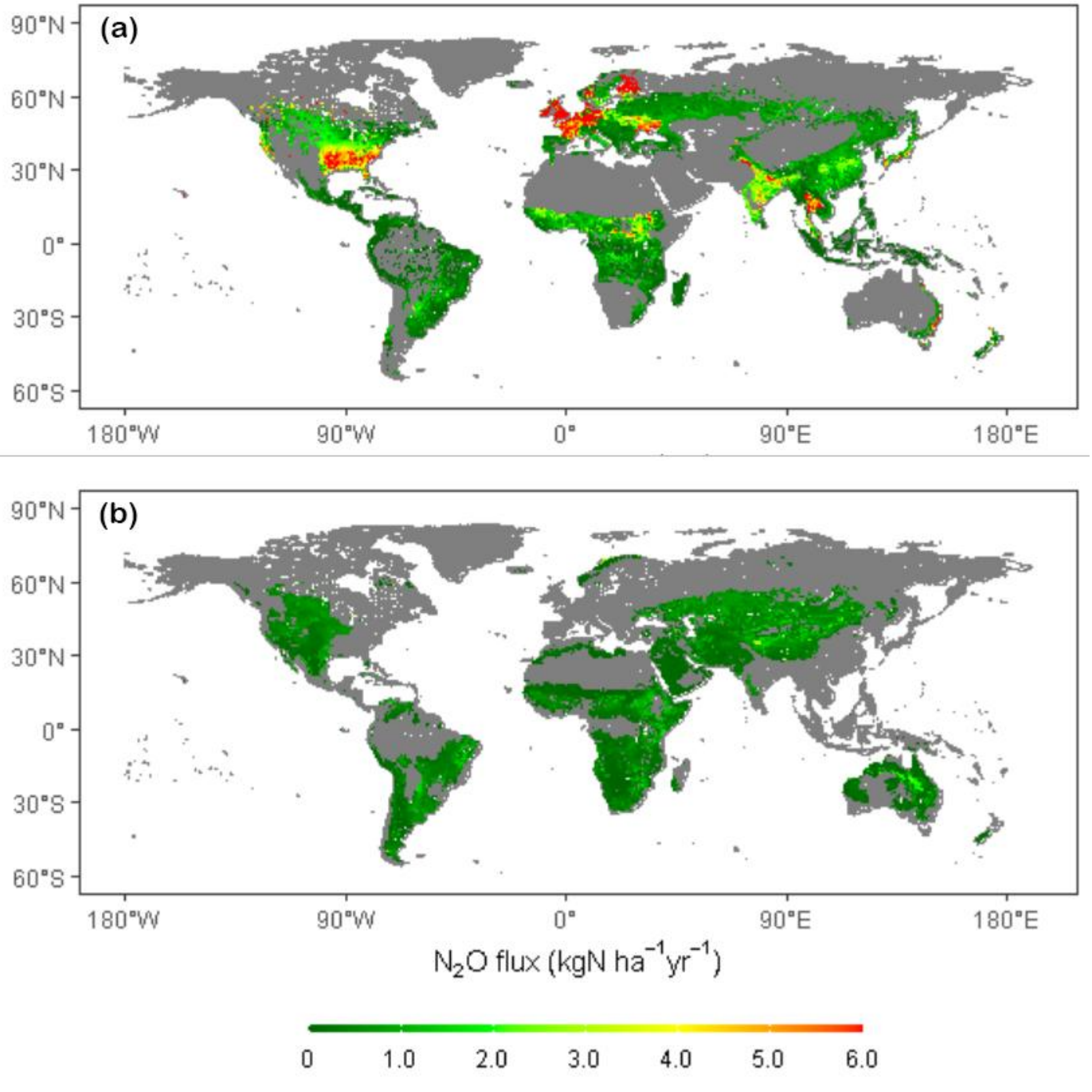

Figure 3.S4 Spatial variations of annual mean N_2O emissions from global pasturelands (a) and rangelands (b) during 1961 – 2016.

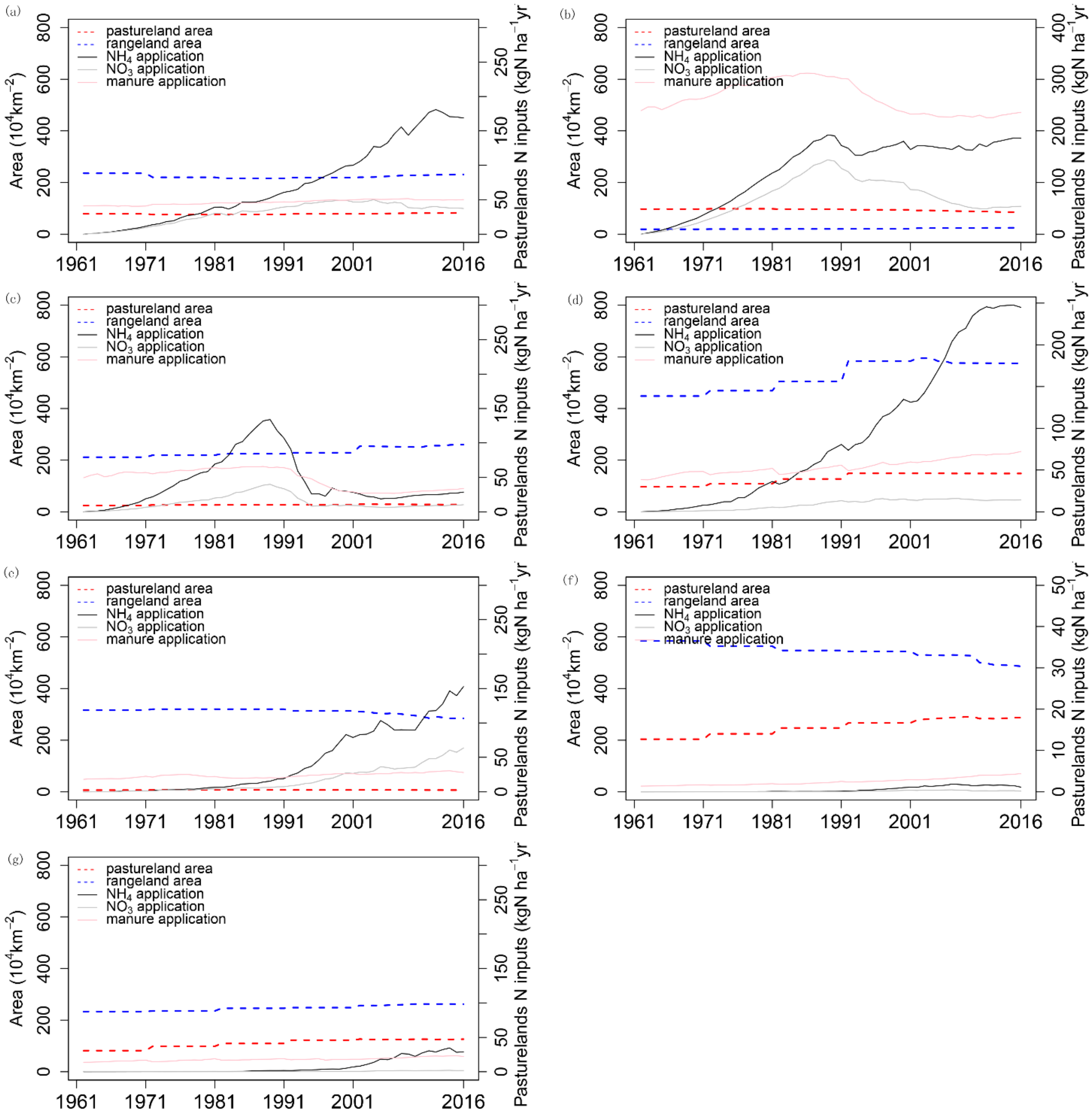

Figure 3.S5 Historical changes in total area of pastureland and rangeland, and fertilizer, manure application rates in pasturelands for (a) North America, (b) Europe, (c) Northern Asia, (d) Southern Asia, (e) Oceania, (f) Africa and (g) South America, respectively.

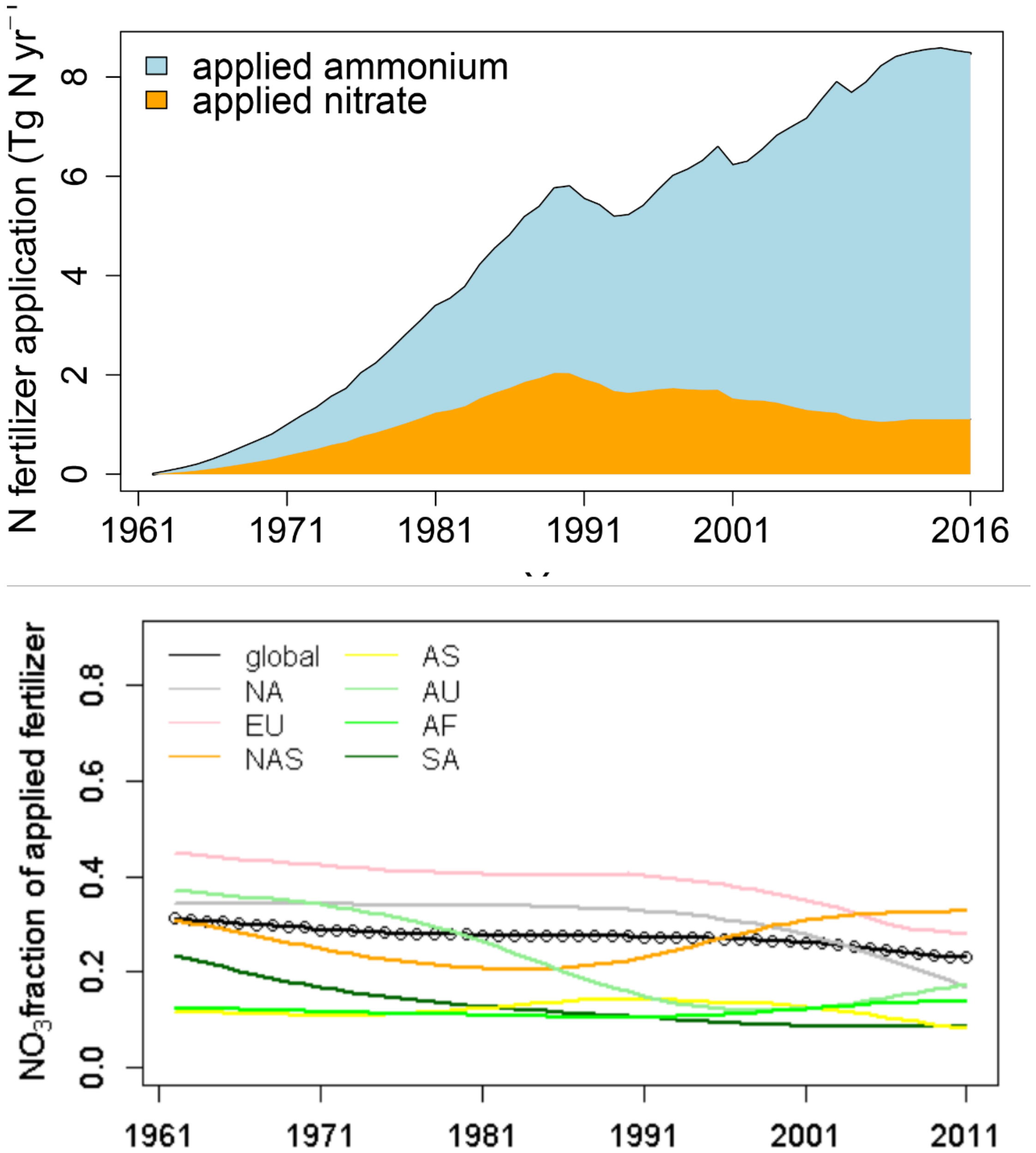

Figure 3.S6 Historical changes in total applied NH_4^+ and NO_3^- fertilizer to global pasturelands (a) and the variation of NO_3^- fraction of applied fertilizer at the globe and each continent (b) respectively. NA: North America, EU: Europe, NAS: Northern Asia, AS: Southern Asia, AU: Oceanic, AF: Africa, SA: South America.

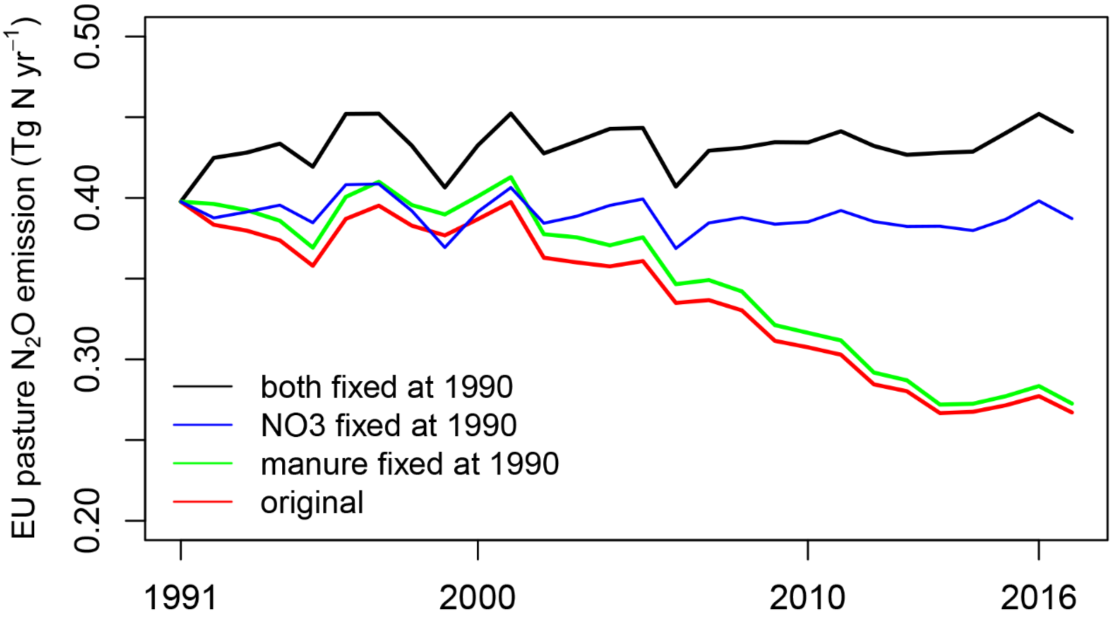

Figure 3.S7 Different scenario simulations (fraction of chemical fertilizer NO_3^-, manure application rate fixed at the level of 1990 from 1990-2016) for European pastureland N_2O emissions

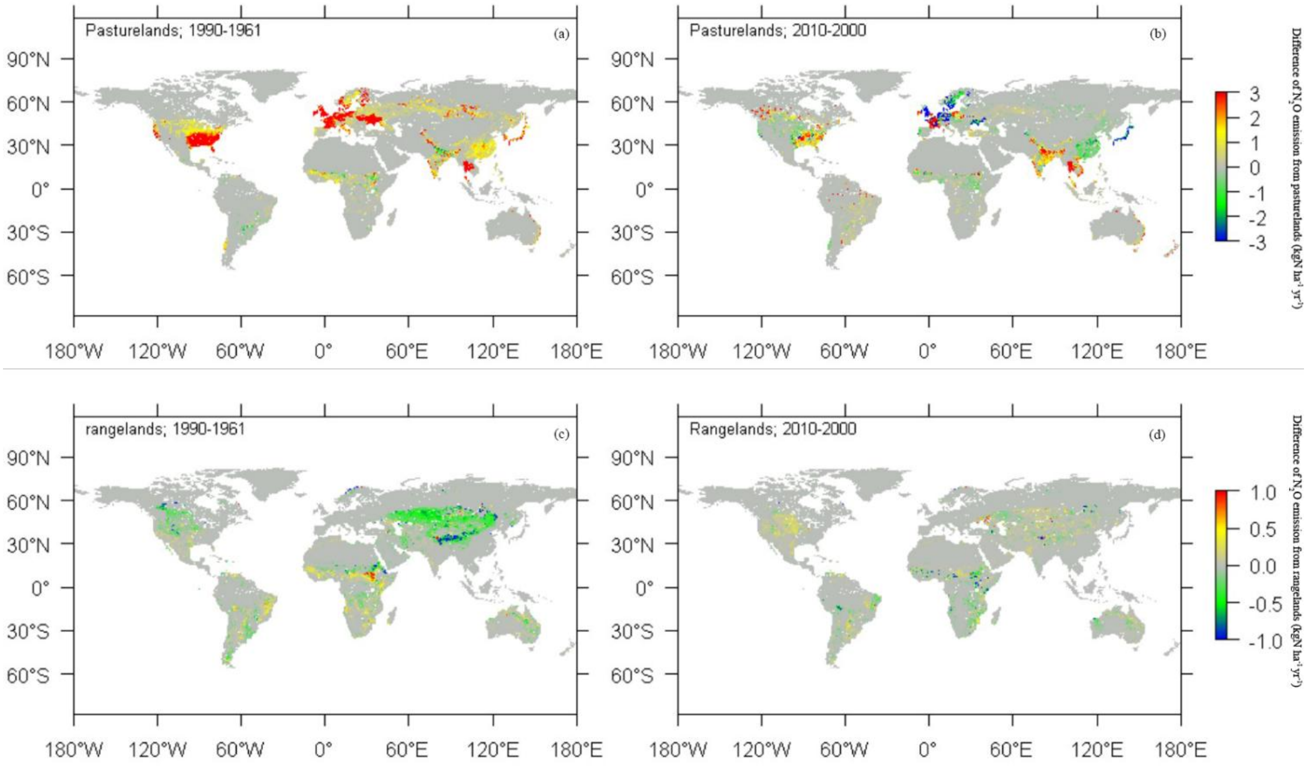

Figure 3. S8 Spatial variation patterns of the modelled N_2O emission difference between two time periods. (a) the difference of N_2O emission from pastureland between 1990 and 1961; (b) the difference of N_2O emission from pastureland between 2010 and 2000; (c) the difference of N_2O emission from rangeland between 1990 and 1961 and (d) the difference of N_2O emission from rangeland between 2010 and 2000.

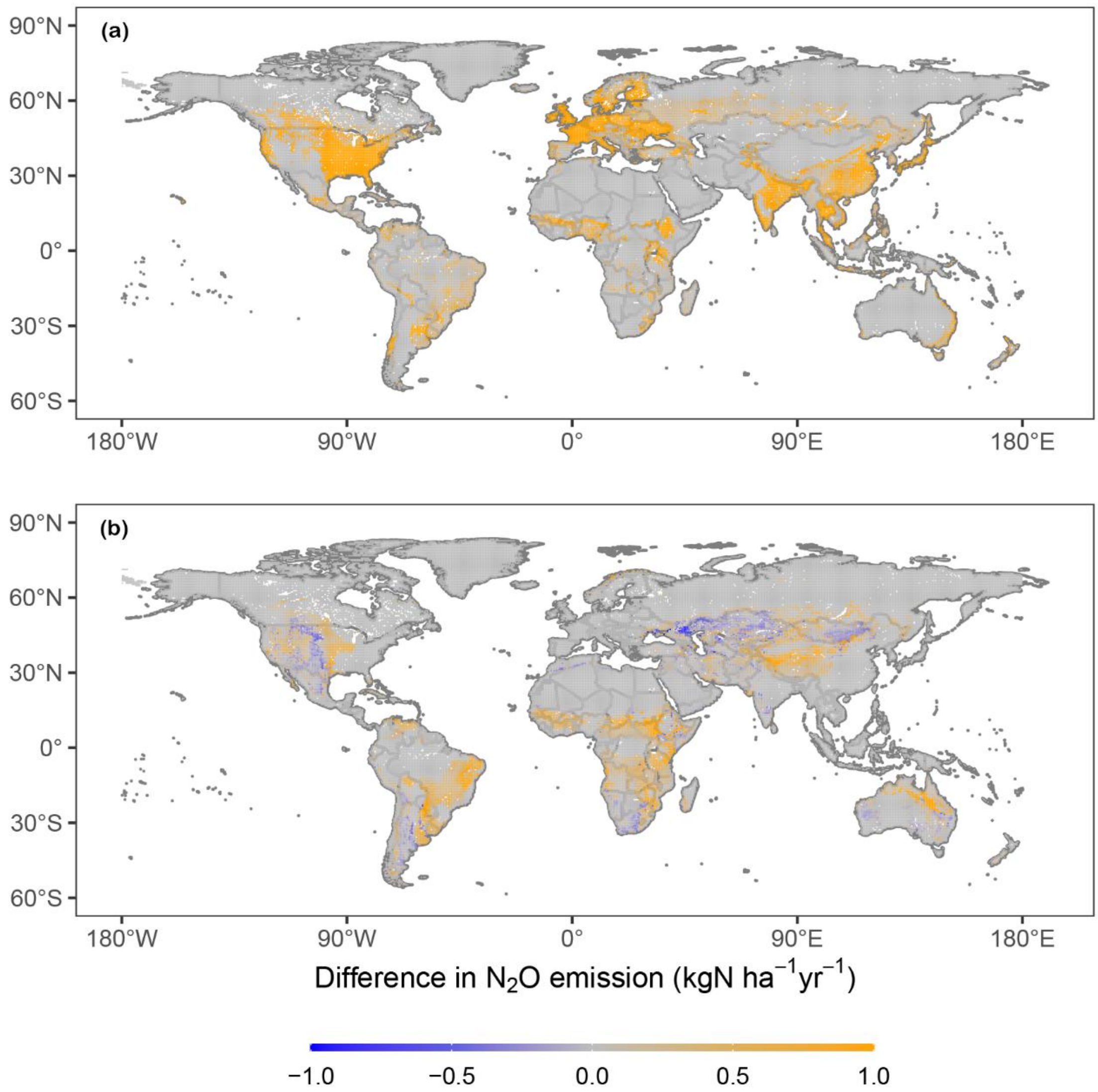

Figure 3. S9 N_2O emission difference generated by excluding livestock deposited excreta for (a) pasturelands and (b) rangelands, respectively.

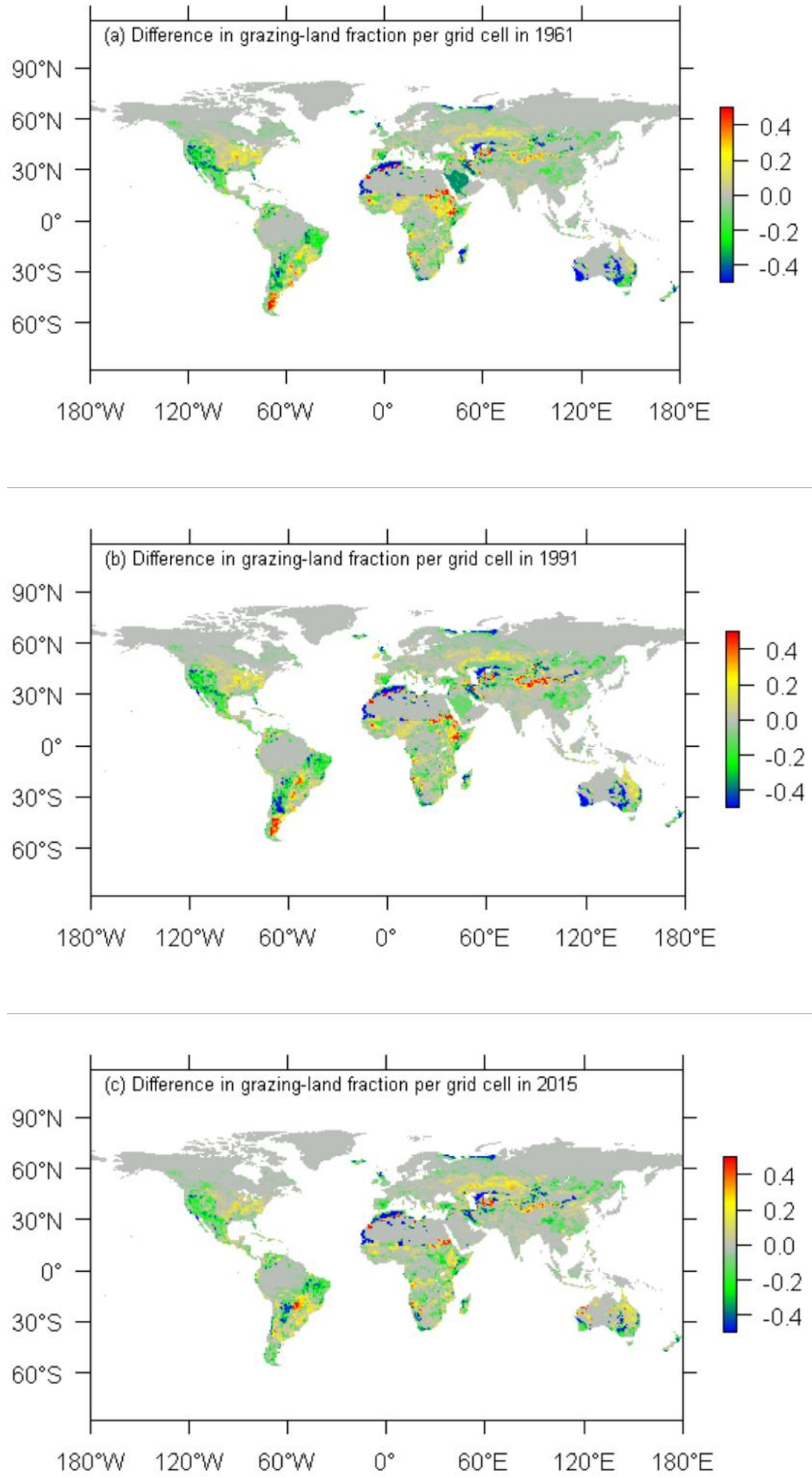

Figure 3. S10 The difference of spatial distribution of global grazing-lands between two widely recommended global land use and land cover datasets: HYDE3.2 and LUH2_V2, respectively.

3.8.6 Supplementary Tables

Table 3. S1. List of the major parameters and their default values for the new added processes and the key parameters.

parameter	description	value	biome type stock species	range	unit	reference
COE_{dNO3}	Coefficient of nitrate consumption of denitrification	0.0128	Pastureland	0.00-0.05		(Song *et al.*, 2022)
		0.0116	Rangeland			
COE_{NR}	Coefficient of nitrification	0.03	Pastureland and Rangeland	0.00-0.08		(Zhang, K. *et al.*, 2017)
adN_{con}	the daily N consumption rate of one livestock unit (LSU)	Cows will voluntarily consume 2 percent of body weight or 24 pounds per day(10.8kg)	Livestock unit	0.18-0.67	kgN per livestock unit day^{-1}	(Chang *et al.*, 2016; Sheldrick *et al.*, 2003)
NUE_i	nitrogen use efficiency of species i	0.31	dairy cow	0.05-0.70	NA	(Giese *et al.*, 2013; Li, C. *et al.*, 2012; Marsden *et al.*, 2020; Stojanovic *et al.*, 2019; Van der Hoek, 1998; Velthof, Gerard L *et al.*, 2015; Wolf *et al.*, 2012)
		0.27	beef cattle			
		0.18	swine			
		0.25	sheep/goat			
		0.1	others			
RDN_i	ratios that deposited nitrogen in feces is split into dung for species i	0.5	cow	0.0-0.60	NA	(Beltran *et al.*, 2022; Li, C. *et al.*, 2012; Reed *et al.*, 2015; Wolf *et al.*, 2012)
		0.5	cattle			
		0.21	swine			
		0.2	sheep/goat			
		0.1	others			
RUN_i	ratios that deposited nitrogen in feces is split into urine for species i	0.5	dairy cow	0.4-1.0	NA	
		0.5	beef cattle			
		0.79	swine			
		0.8	sheep/goat			
		0.4	others			
$ExNrate_i$	default N excretion rate for livestock category i	0.22	dairy cow	0.01-0.48	kgN head^{-1} day^{-1}	(Sheldrick *et al.*, 2003; Zhang, B. *et al.*, 2017)
		0.14	beef cattle			
		0.05	swine			
		0.04	sheep/goat			
		0.02	others			
RN_{uine}	urine N concentration	5.2	cow & cattle	3.0-21.6	gN L^{-1}	

		6.1	swine			(Bristow *et al.*, 1992; Marsden *et al.*, 2020; Powell et Rotz, 2015)
		8.0	sheep			
COE_{tramp}	coefficient of animal trampling effect	0.05	NA	0.04-0.08	NA	(Bhandral *et al.*, 2007; Wolf *et al.*, 2012)
$COE_{iceform}$	coefficient of ice-formation	0.25	NA	0.2-0.3	NA	(Wolf *et al.*, 2012)

1 LSU indicates a mature dairy cow, while beef cattle was considered at 0.5, sheep and goats at 0.1, pigs at 0.35, other poultry at 0.018 LSU) based on Liu et al. 2015 and Li et al. 2012, www.agupdate.com/agriview/news/livestock.

Table 3. S2. Environment and management data for the experimental sites used for the model calibration.

Site ID	Lat.	Lon.	Exp. period	N fertilizer (kgN ha^{-1} yr^{-1})	Stocking rate (head ha^{-1} yr^{-1})	Soil properties				Performance indices	Measured daily mean N_2O flux (mgN m^{-2} day^{-1})	Modeled daily mean N_2O flux (mgN m^{-2} day^{-1})	Reference
						pH	Sand (%)	Clay (%)	C:N ratio	D, RMSE, R			
MG-R	43.51	116.7	2008–2009	0	0	7.55	33	25	9.39	0.79, 0.17, 0.66	0.060	0.076	(Wolf *et al.*, 2010)
NP-R	41.76	115.67	2012–2013	0	0	7.63	71.9	10.4	8.89	0.71, 0.16, 0.63	0.088	0.085	(Yang *et al.*, 2015)
MG-R	43.51	116.7	2008–2009	0	1.03 (sheep)	7.55	33	25	9.39	0.47, 0.71, 0.34	0.008	0.029	(Wolf *et al.*, 2010)
NP-Rw	41.77	115.68	2012–2013	0	1.5 (sheep)	7.7	50.6	21.8	8.63	0.60, 0.75, 0.36	0.039	0.071	(Yang *et al.*, 2015)
NP-Rs	41.78	115.69	2012–2013	0	2.1 (sheep)	8.07	45.3	18.8	8.86	0.53, 0.06, 0.22	0.031	0.043	(Yang *et al.*, 2015)
TP-R	34.01	102.71	2013–2014	0	6.8 (sheep)	7.1	25	15	13.4	0.76, 0.035, 0.58	0.043	0.039	(Zhang, H. *et al.*, 2018)
CA-P	49.66	−96.78	2004–2006	M148	0	7	12	40.5	9.37	0.65, 0.73, 0.58	0.131	0.088	(Tenuta *et al.*, 2010)
US-P	40.84	−104.71	2012–2014	M430	0	7.6	32.5	26	8.89	0.69, 0.29, 0.52	0.160	0.123	(Nichols *et al.*, 2016)
ND-P	51.99	5.62	2001–2002	M410	0	6.5	20	48	12.28	0.81, 0.34, 0.69	0.215	0.253	(Schils *et al.*, 2008)
NT-P	52.43	6.23	1992–1994	F305	1.2 (cow)	4.65	85.5	4.5	14.53	0.78, 4.70, 0.64	3.096	3.424	(Velthof, G. L. *et al.*, 1996)
IR-P	52.86	−6.90	2003–2004	F200	0.9 (cattle)	6.6	39	25.5	9.15	0.63, 1.27, 0.43	0.650	0.625	(Abdalla *et al.*, 2010)

XJ-P	42.88	83.71	2010–2011	F100	0	6.65	46	20	9.34	0.85, 0.31, 0.88	0.400	0.326	(Li, K. *et al.*, 2012)
BZ-P	−25.39	−49.13	2011–2012	M220	0	4.8	33.5	45	11.51	0.89, 2.47, 0.82	1.593	1.257	(Sordi, André *et al.*, 2014)
AU-P	−28.87	152.87	2014–2017	F380	2.5 (cow)	6.0	25.0	45.0	12.0	0.35, 4.22, 0.20	1.788	1.852	(De Rosa *et al.*, 2020)

The site ID letters R and P indicate rangeland and pastureland, respectively. For the N applications, M and F indicate the application of manure and chemical fertilizer, respectively.

Table 3. S3. Information on the sites used for the model validation.

Veg. type	Lat.	Lon.	Per.	N fer. app. (kgN ha^{-1} yr^{-1})	manure N app. (kgN ha^{-1} yr^{-1})	grazing density (LU ha^{-1} yr^{-1})	cutting	Measured daily mean N_2O (mgN m^{-2} day^{-1})	Modeled daily mean N_2O (mgN m^{-2} day^{-1})	Reference
rangeland	40.01	-105.55	2007	NA	NA	NA	NA	0.36	0.25	(Filippa *et al.*, 2009)
rangeland	49.33	119.91	2001-2012	NA	NA	NA	Yes	0.76	0.78	(Xu, L. *et al.*, 2018)
rangeland	15.95	-15.32	2014-2015	NA	NA	0.96	NA	1.53	0.25	(Assouma *et al.*, 2017)
rangeland	-27.33	152.88	2013-2015	NA	NA	NA	Yes	0.08	0.10	(van Delden *et al.*, 2018)
rangeland	46.69	19.60	2006-2007	NA	NA	0.65	NA	0.04	0.04	(Horvath *et al.*, 2008)
rangeland	45.61	2.75	2002-2005	NA	NA	0.5	NA	0.04	0.06	(Flechard *et al.*, 2005)
rangeland	46.77	-100.90	2016-2019	NA	NA	1.47	NA	0.62	0.08	(Liebig *et al.*, 2020)
rangeland	50.21	-113.91	2013-2015	NA	NA	13.2	NA	0.03	0.05	(Gao *et al.*, 2018)
rangeland	44.17	116.37	2013-2014	NA	NA	NA	NA	0.14	0.15	(Bai *et al.*, 2018)
rangeland	3.62	-76.31	2014-2015	NA	NA	1.3	NA	0.96	0.49	(Rivera *et al.*, 2019)
pastureland	-1.26	36.72	2014	NA	M403	NA	NA	0.41	0.34	(Pelster *et al.*, 2016)
pastureland	-21.43	-48.39	2012-2013	170	NA	5.75	NA	0.20	0.22	(Cardoso *et al.*, 2017)
pastureland	-34.10	150.70	2012-2014	460	NA	NA	Yes	0.65	0.67	(Dougherty *et al.*, 2016)
pastureland	-21.25	-48.3	2013-2014	80	NA	Na	Yes	1.84	2.20	(Cardoso *et al.*, 2019)
pastureland	36.24	-93.91	2000-2001	NA	D144	Yes	NA	0.40	0.46	(Sauer *et al.*, 2009)
pastureland	-30.09	-51.67	2013-2014	NA	U1325+D861	NA	Yes	0.31	0.37	(Schirmann *et al.*, 2020)
pastureland	-0.10	35.49	2013-2014	NA	U1066+D240	NA	Yes	0.72	0.80	(Tully *et al.*, 2017)
pastureland	47.90	9.99	1996-1998	NA	M167.5	NA	Yes	0.08	0.09	(Glatzel et Stahr, 2001)

Veg. type	Lat.	Lon.	Per.	N fer. app. (kgN ha^{-1} yr^{-1})	manure N app. (kgN ha^{-1} yr^{-1})	grazing density (LU ha^{-1} yr^{-1})	cutting	Measured daily mean N_2O (mgN m^{-2} day^{-1})	Modeled daily mean N_2O (mgN m^{-2} day^{-1})	Reference
pastureland	53.36	-4.52	2018	NA	U925	NA	Yes	0.31	0.30	(Marsden *et al.*, 2019)
pastureland	55.87	-3.00	2002-2003	200	NA	NA	NA	1.51	1.60	(Flechard *et al.*, 2007)
pastureland	55.89	3.43	2002-2004	300	NA	Na	Na	0.64	0.72	(Jones *et al.*, 2005)
pastureland	47.29	7.72	2002-2004	30	M150	NA	NA	0.53	1.15	(Flechard *et al.*, 2005)
pastureland	52.85	-8.35	2009-2010	57.5	M31	0.8	Yes	1.74	1.30	(Li, D. *et al.*, 2011)
pastureland	51.86	6.14	2010-2012	265	NA	NA	Yes	2.34	2.21	(Helfrich *et al.*, 2020)
pastureland	49.23	-121.76	2001-2002	105	M22.5	NA	NA	0.30	0.27	(Bhandral *et al.*, 2008)
pastureland	-40.38	175.30	2002-2004	40	NA	1.7	NA	0.74	0.77	(Saggar *et al.*, 2007)
pastureland	-43.68	172.61	2014	NA	U600	NA	Yes	1.87	1.34	(Di *et al.*, 2016)
pastureland	-45.8	170.3	2018-2019	NA	U560	NA	NA	2.34	2.14	(Simon *et al.*, 2019)
pastureland	-28.80	152.90	2015-2016	381	NA	NA	Yes	0.73	0.66	(Mumford *et al.*, 2019)
pastureland	-38.43	143.78	2010-2011	240	NA	NA	Yes	0.07	0.06	(Suter *et al.*, 2016)
pastureland	-25.38	-49.12	2011	NA	U3300	NA	Yes	4.00	5.13	(Sordi, Andre *et al.*, 2014)
pastureland	42.35	142.49	2001-2004	80.75	NA	NA	Yes	0.67	0.55	(Katayanagi *et al.*, 2008)
pastureland	37.61	101.20	2010-2012	40	NA	NA	Yes	0.29	0.37	(Zhu, X. *et al.*, 2015)
pastureland	42.43	142.46	2013-2016	63	M181	NA	Yes	1.69	1.03	(Nagatake *et al.*, 2018)
pastureland	-11.84	-55.62	2016	80	NA	NA	NA	0.40	0.23	(do Nascimento *et al.*, 2021)
pastureland	-37.78	175.30	2013-2014	NA	U492	NA	NA	2.12	2.12	(Li, J. *et al.*, 2016)

Veg. type	Lat.	Lon.	Per.	N fer. app. (kgN ha^{-1} yr^{-1})	manure N app. (kgN ha^{-1} yr^{-1})	grazing density (LU ha^{-1} yr^{-1})	cutting	Measured daily mean N_2O (mgN m^{-2} day^{-1})	Modeled daily mean N_2O (mgN m^{-2} day^{-1})	Reference
pastureland	-37.78	175.80	2016-2017	37	NA	2.9	NA	1.78	1.95	(Liang, L. L. *et al.*, 2018)
pastureland	52.00	-6.00	2001-2003	225	NA	14	NA	3.42	3.56	(Hyde *et al.*, 2006)
pastureland	-44.83	169.63	2016-2017	NA	U371	NA	NA	1.41	1.09	(Luo *et al.*, 2019)
pastureland	-35.58	173.76	2016-2017	NA	U310	NA	NA	6.45	3.20	(Luo *et al.*, 2019)
pastureland	-16.48	-49.31	2009-2010	NA	U60	NA	Yes	9.35	8.72	(Lessa *et al.*, 2014)
pastureland	49.69	-120.76	2014-2015	NA	U247.58	NA	NA	3.56	1.27	(Thomas *et al.*, 2017)
pastureland	-30.08	-51.65	2009-2013	NA	U251.33	NA	NA	1.17	1.06	(de Bastos *et al.*, 2020)
pastureland	42.87	83.7	2013-2016	30	NA	NA	NA	0.08	0.40	(Geng *et al.*, 2019)
pastureland	36.9	139.97	2010-2011	NA	U696	2.5	NA	1.05	1.51	(Mori et Hojito, 2015)
pastureland	-38.23	142.92	2013-2014	NA	D448	NA	NA	1.07	1.08	(Ward *et al.*, 2018)
pastureland	44.76	-90.09	2014-2016	NA	U146	NA	Yes	0.51	0.26	

LU : live stock unit. One live stock unit represents one mature dairy cattle. Other livestock species was calculated accordingly based on Liu et al. (2016). M, U and D indicate the application of manure, urine and dung, respectively.

Table 3. S4 The global correlation results between Emission Factors (EF_1 and EF_{3PRP}) and related management, environmental factors. All the data was log transformed before processing.

	Variables	t	df	cor	*p*-value
EF_1	Fraction NO_3^-	66.621	15983	0.47**	<0.001
	Total fer app	25.259	19057	0.18**	<0.001
	Soil pH	-2.1253	19057	-0.01	0.034
	Soil clay content	-3.2401	19057	-0.02*	<0.01
	Soil C:N ratio	-1.1589	19006	-0.008	0.2465
	Soil organic carbon content	7.535	19057	0.054**	<0.001
	Atmospheric N deposition	35.881	19057	0.25**	<0.001
EF_{3PRP}	Amount of excreta	-115.11	27568	-0.57**	<0.001
	Soil pH	-0.70235	28243	-0.00	0.48
	Soil clay content	-10.575	28243	-0.06*	<0.01
	Soil C:N ratio	2.097	28164	0.012	0.036
	Soil organic carbon content	-3.4858	28243	-0.021*	<0.01
	Atmospheric N deposition	-17.699	28243	-0.10**	<0.001

The correlation is considered significant when $p < 0.01$ * and $p < 0.001$ **.

3.9 References

Abdalla, M., Jones, M., Yeluripati, J., Smith, P., Burke, J. et Williams, M. (2010, 2010/08/01/). Testing DayCent and DNDC model simulations of N2O fluxes and assessing the impacts of climate change on the gas flux and biomass production from a humid pasture. *Atmospheric Environment*, *44*(25), 2961-2970. https://doi.org/https://doi.org/10.1016/j.atmosenv.2010.05.018

Aliyu, G., Sanz-Cobena, A., Müller, C., Zaman, M., Luo, J., Liu, D., Yuan, J., Chen, Z., Niu, Y., Arowolo, A. et Ding, W. (2018, 2018/11/15/). A meta-analysis of soil background N2O emissions from croplands in China shows variation among climatic zones. *Agriculture, Ecosystems & Environment*, *267*, 63-73. https://doi.org/https://doi.org/10.1016/j.agee.2018.08.003

Assouma, M. H., Serca, D., Guerin, F., Blanfort, V., Lecomte, P., Toure, I., Ickowicz, A., Manlay, R. J., Bernoux, M. et Vayssieres, J. (2017, Apr). Livestock induces strong spatial heterogeneity of soil CO2, N2O and CH4 emissions within a semi-arid sylvo-pastoral landscape in West Africa. *Journal of Arid Land*, *9*(2), 210-221. https://doi.org/10.1007/s40333-017-0001-y

Bai, Y., Li, X., Wen, W., Mi, X., Li, R., Huang, Q. et Zhang, M. (2018, Jun). CO2, CH4 and N2O flux changes in degraded grassland soil of Inner Mongolia, China. *Journal of Arid Land*, *10*(3), 347-361. https://doi.org/10.1007/s40333-018-0101-3

Beltran, I. E., Calvache, I., Cofre, R., Salazar, F., Keim, J. P., Morales, A., Pulido, R. G. et Alfaro, M. (2022). Nitrogen Intake and Its Partition on Urine, Dung and Products of Dairy and Beef Cattle in Chile. *Agronomy*, *12*(1). https://doi.org/10.3390/agronomy12010015

Betlach, M. R. et Tiedje, J. M. (1981, 1981-Dec). Kinetic explanation for accumulation of nitrite, nitric oxide, and nitrous oxide during bacterial denitrification. *Applied and Environmental Microbiology*, *42*(6), 1074-1084. <Go to ISI>://MEDLINE:16345900

Bhandral, R., Bittman, S., Kowalenko, C. G., Friesen, A. et Hunt, D. E. (2008, Aug). Emissions of nitrous oxide after application of dairy slurry on bare soil and perennial grass in a maritime climate. *Canadian Journal of Soil Science*, *88*(4), 517-527. https://doi.org/10.4141/cjss07103

Bhandral, R., Saggar, S., Bolan, N. S. et Hedley, M. J. (2007, 2007/06/01/). Transformation of nitrogen and nitrous oxide emission from grassland soils as affected by compaction. *Soil and Tillage Research*, *94*(2), 482-492. https://doi.org/https://doi.org/10.1016/j.still.2006.10.006

Bristow, A. W., Whitehead, D. C. et Cockburn, J. E. (1992, 1992/01/01). Nitrogenous constituents in the urine of cattle, sheep and goats [https://doi.org/10.1002/jsfa.2740590316]. *Journal of the Science of Food and Agriculture*, *59*(3), 387-394. https://doi.org/https://doi.org/10.1002/jsfa.2740590316

Butterbach-Bahl, K., Baggs, E. M., Dannenmann, M., Kiese, R. et Zechmeister-Boltenstern, S. (2013, Jul 5). Nitrous oxide emissions from soils: how well do we understand the processes and their controls? *Philosophical Transactions of the Royal Society B-Biological Sciences*, *368*(1621). https://doi.org/10.1098/rstb.2013.0122

Butterbach-Bahl, K., Gettel, G., Kiese, R., Fuchs, K., Werner, C., Rahimi, J., Barthel, M. et Merbold, L. (2020, 2020/09/15). Livestock enclosures in drylands of Sub-Saharan Africa are overlooked hotspots of N2O emissions. *Nature communications*, *11*(1), 4644. https://doi.org/10.1038/s41467-020-18359-y

Cai, Y. et Akiyama, H. (2016, 2016/12/01/). Nitrogen loss factors of nitrogen trace gas emissions and leaching from excreta patches in grassland ecosystems: A summary of available data. *Science of the Total Environment*, *572*, 185-195. https://doi.org/https://doi.org/10.1016/j.scitotenv.2016.07.222

Cai, Y., Chang, S. X. et Cheng, Y. (2017, 2017/08/01/). Greenhouse gas emissions from excreta patches of grazing animals and their mitigation strategies. *Earth-Science Reviews*, *171*, 44-57. https://doi.org/https://doi.org/10.1016/j.earscirev.2017.05.013

Canadell, J. G., Monteiro, P. M. S., Costa, M. H., Cotrim da Cunha, L., Cox, P. M., Eliseev, A. V., Henson, S., Ishii, M., Jaccard, S., Koven, C., Lohila, A., Patra, P. K., Piao, S., Rogelj, J., Syampungani, S., Zaehle, S., & Zickfeld, K. (2021). . (2021). Global carbon and other biogeochemical cycles and feedbacks. *Climate change 2021: The physical science basis. Contribution of Working Group I to the Sixth Assessment Report of the Intergovernmental Panel on Climate Change. Cambridge University Press, in press.*

.

Cardoso, A. d. S., Brito, L. d. F., Janusckiewicz, E. R., Morgado, E. d. S., Barbero, R. P., Werner Koscheck, J. F., Reis, R. A. et Ruggieri, A. C. (2017, Jun). Impact of Grazing Intensity and Seasons on Greenhouse Gas Emissions in Tropical Grassland. *Ecosystems*, *20*(4), 845-859. https://doi.org/10.1007/s10021-016-0065-0

Cardoso, A. d. S., Oliveira, S. C., Janusckiewicz, E. R., Brito, L. F., Morgado, E. d. S., Reis, R. A. et Ruggieri, A. C. (2019, Nov). Seasonal effects on ammonia, nitrous oxide, and methane emissions for beef cattle excreta and urea fertilizer applied to a tropical pasture. *Soil & Tillage Research*, *194*, Article 104341. https://doi.org/10.1016/j.still.2019.104341

Chadwick, D. R., Cardenas, L. M., Dhanoa, M. S., Donovan, N., Misselbrook, T., Williams, J. R., Thorman, R. E., McGeough, K. L., Watson, C. J., Bell, M., Anthony, S. G. et Rees, R. M. (2018, 2018/09/01/). The contribution of cattle urine and dung to nitrous oxide emissions: Quantification of country specific emission factors and implications for national inventories. *Science of the Total Environment*, *635*, 607-617. https://doi.org/https://doi.org/10.1016/j.scitotenv.2018.04.152

Chang, J., Ciais, P., Gasser, T., Smith, P., Herrero, M., Havlik, P., Obersteiner, M., Guenet, B., Goll, D. S., Li, W., Naipal, V., Peng, S., Qiu, C., Tian, H., Viovy, N., Yue, C. et Zhu, D. (2021, 2021 Jan). Climate warming from managed grasslands cancels the cooling effect of carbon sinks in sparsely grazed and natural grasslands. *Nature communications*, *12*(1), 118-118. https://doi.org/10.1038/s41467-020-20406-7

Chang, J., Ciais, P., Herrero, M., Havlik, P., Campioli, M., Zhang, X., Bai, Y., Viovy, N., Joiner, J., Wang, X., Peng, S., Yue, C., Piao, S., Wang, T., Hauglustaine, D. A., Soussana, J.-F., Peregon, A., Kosykh, N. et Mironycheva-Tokareva, N. (2016, 2016). Combining livestock production information in a process-based vegetation model to reconstruct the history of grassland management. *Biogeosciences*, *13*(12), 3757-3776. https://doi.org/10.5194/bg-13-3757-2016

Chatskikh, D., Olesen, J. E., Berntsen, J., Regina, K. et Yamulki, S. (2005). Simulation of effects of soils, climate and management on N2O emission from grasslands. *Biogeochemistry*, *76*(3), 395-419.

Chen, D., Li, Y., Kelly, K. et Eckard, R. (2010, Mar 15). Simulation of N2O emissions from an irrigated dairy pasture treated with urea and urine in Southeastern Australia. *Agriculture Ecosystems & Environment*, *136*(3-4), 333-342. https://doi.org/10.1016/j.agee.2009.12.007

Cui, X., Zhou, F., Ciais, P., Davidson, E. A., Tubiello, F. N., Niu, X., Ju, X., Canadell, J. G., Bouwman, A. F., Jackson, R. B., Mueller, N. D., Zheng, X., Kanter, D. R., Tian, H., Adalibieke, W., Bo, Y., Wang, Q., Zhan, X. et Zhu, D. (2021, 2021/11/01). Global mapping of crop-specific emission factors highlights hotspots of nitrous oxide mitigation. *Nature Food*, *2*(11), 886-893. https://doi.org/10.1038/s43016-021-00384-9

Dangal, S. R. S., Tian, H., Xu, R., Chang, J., Canadell, J. G., Ciais, P., Pan, S., Yang, J. et Zhang, B. (2019, Feb). Global Nitrous Oxide Emissions From Pasturelands and Rangelands: Magnitude, Spatiotemporal Patterns, and Attribution. *Global Biogeochemical Cycles*, *33*(2), 200-222. https://doi.org/10.1029/2018gb006091

David, J. A. (2013, 2013-01). Spatial Redistribution of Nitrogen by Cattle in Semiarid Rangeland. *Rangeland Ecology & Management*, *v. 66*(no. 1), pp. 56-62-2013 v.2066 no.2011. https://doi.org/10.2111/REM-D-11-00228.1

Davidson, E. A. (2009, Sep). The contribution of manure and fertilizer nitrogen to atmospheric nitrous oxide since 1860. *Nature Geoscience*, *2*(9), 659-662. https://doi.org/10.1038/ngeo608

Davidson, E. A. et Kanter, D. (2014, Oct). Inventories and scenarios of nitrous oxide emissions. *Environmental Research*

Letters, *9*(10), Article 105012. https://doi.org/10.1088/1748-9326/9/10/105012

de Bastos, D. F., Magiero, E. C., Tomazi, M., Schirmann, J., Veloso, M. G., de Faccio Carvalho, P. C. et Bayer, C. (2020, 2020/02/01). A 3-year assessment of nitrous oxide emission factors for urine and dung of grazing sheep in a subtropical ecosystem. *Journal of Soils and Sediments*, *20*(2), 982-991. https://doi.org/10.1007/s11368-019-02456-7

De Rosa, D., Rowlings, D. W., Fulkerson, B., Scheer, C., Friedl, J., Labadz, M. et Grace, P. R. (2020, 2020/07/01). Field-scale management and environmental drivers of N2O emissions from pasture-based dairy systems. *Nutrient Cycling in Agroecosystems*, *117*(3), 299-315. https://doi.org/10.1007/s10705-020-10069-7

Di, H. J., Cameron, K. C., Podolyan, A., Edwards, G. R., de Klein, C. A. M., Dynes, R. et Woods, R. (2016, Sep). The potential of using alternative pastures, forage crops and gibberellic acid to mitigate nitrous oxide emissions. *Journal of Soils and Sediments*, *16*(9), 2252-2262. https://doi.org/10.1007/s11368-016-1442-1

Dijkstra, J., Oenema, O., van Groenigen, J. W., Spek, J. W., van Vuuren, A. M. et Bannink, A. (2013, 2013/01/01/). Diet effects on urine composition of cattle and N2O emissions. *Animal*, *7*, 292-302. https://doi.org/https://doi.org/10.1017/S1751731113000578

do Nascimento, A. F., de Oliveira, C. M., Pedreira, B. C., Pereira, D. H. et de Aragao Rodrigues, R. R. (2021, Jan). Nitrous oxide emissions and forage accumulation in the Brazilian Amazon forage-livestock systems submitted to N input strategies. *Grassland Science*, *67*(1), 63-72. https://doi.org/10.1111/grs.12287

Dougherty, W. J., Collins, D., Van Zwieten, L. et Rowlings, D. W. (2016, 2016). Nitrification (DMPP) and urease (NBPT) inhibitors had no effect on pasture yield, nitrous oxide emissions, or nitrate leaching under irrigation in a hot-dry climate. *Soil Research*, *54*(5), 675-683. https://doi.org/10.1071/sr15330

Du, Y., Ke, X., Li, J., Wang, Y., Cao, G., Guo, X. et Chen, K. (2021, 2021/04/01/). Nitrogen deposition increases global grassland N2O emission rates steeply: A meta-analysis. *CATENA*, *199*, 105105. https://doi.org/https://doi.org/10.1016/j.catena.2020.105105

Filippa, G., Freppaz, M., Williams, M. W., Helmig, D., Liptzin, D., Seok, B., Hall, B. et Chowanski, K. (2009, Aug). Winter and summer nitrous oxide and nitrogen oxides fluxes from a seasonally snow-covered subalpine meadow at Niwot Ridge, Colorado. *Biogeochemistry*, *95*(1), 131-149. https://doi.org/10.1007/s10533-009-9304-1

Flechard, C. R., Ambus, P., Skiba, U., Rees, R. M., Hensen, A., van Amstel, A., Dasselaar, A. v. d. P.-v., Soussana, J. F., Jones, M., Clifton-Brown, J., Raschi, A., Horvath, L., Neftel, A., Jocher, M., Ammann, C., Leifeld, J., Fuhrer, J., Calanca, P., Thalman, E., Pilegaard, K., Di Marco, C., Campbell, C., Nemitz, E., Hargreaves, K. J., Levy, P. E., Ball, B. C., Jones, S. K., van de Bulk, W. C. M., Groot, T., Blom, M., Domingues, R., Kasper, G., Allard, V., Ceschia, E., Cellier, P., Laville, P., Henault, C., Bizouard, F., Abdalla, M., Williams, M., Baronti, S., Berretti, F. et Grosz, B. (2007, 2007/06/01/). Effects of climate and management intensity on nitrous oxide emissions in grassland systems across Europe. *Agriculture, Ecosystems & Environment*, *121*(1), 135-152. https://doi.org/https://doi.org/10.1016/j.agee.2006.12.024

Flechard, C. R., Neftel, A., Jocher, M., Ammann, C. et Fuhrer, J. (2005, Dec). Bi-directional soil/atmosphere N2O exchange over two mown grassland systems with contrasting management practices. *Global Change Biology*, *11*(12), 2114-2127. https://doi.org/10.1111/j.1365-2486.2005.01056.x

Foley, J. A., Prentice, I. C., Ramankutty, N., Levis, S., Pollard, D., Sitch, S. et Haxeltine, A. (1996, Dec). An integrated biosphere model of land surface processes, terrestrial carbon balance, and vegetation dynamics. *Global Biogeochemical Cycles*, *10*(4), 603-628. https://doi.org/10.1029/96gb02692

Fuchs, K., Merbold, L., Buchmann, N., Bellocchi, G., Bindi, M., Brilli, L., Conant, R. T., Dorich, C. D., Ehrhardt, F., Fitton, N., Grace, P., Klumpp, K., Liebig, M., Lieffering, M., Martin, R., McAuliffe, R., Newton, P. C. D., Rees, R. M., Recous, S., Smith, P., Soussana, J.-F., Topp, C. F. E. et Snow, V. (2020). Evaluating the Potential of Legumes to Mitigate N2O Emissions From Permanent Grassland Using Process-Based Models. *Global Biogeochemical*

Cycles, *34*(12), e2020GB006561. https://doi.org/https://doi.org/10.1029/2020GB006561

Gao, X., Thomas, B. W., Beck, R., Thompson, D. J., Zhao, M., Willms, W. D. et Hao, X. (2018, Feb). LONG-TERM GRAZING ALTERS SOIL TRACE GAS FLUXES FROM GRASSLANDS IN THE FOOTHILLS OF THE ROCKY MOUNTAINS, CANADA. *Land Degradation & Development*, *29*(2), 292-302. https://doi.org/10.1002/ldr.2664

Geng, F., Li, K., Liu, X., Gong, Y., Yue, P., Li, Y. et Han, W. (2019, 2019/11/01/). Long-term effects of N deposition on N2O emission in an alpine grassland of Central Asia. *CATENA*, *182*, 104100. https://doi.org/https://doi.org/10.1016/j.catena.2019.104100

Gerber, P. J., Steinfeld, H., Henderson, B., Mottet, A., Opio, C., Dijkman, J., Falcucci, A. et Tempio, G. (2013). Tackling climate change through livestock – A global assessment of emissions and mitigation
opportunities. *Food and Agriculture Organization of the United Nations (FAO), Rome*.

Giese, M., Brueck, H., Gao, Y. Z., Lin, S., Steffens, M., Kögel-Knabner, I., Glindemann, T., Susenbeth, A., Taube, F., Butterbach-Bahl, K., Zheng, X. H., Hoffmann, C., Bai, Y. F. et Han, X. G. (2013). N balance and cycling of Inner Mongolia typical steppe: a comprehensive case study of grazing effects. *Ecological Monographs*, *83*(2), 195-219. https://doi.org/https://doi.org/10.1890/12-0114.1

Giltrap, D., Yeluripati, J., Smith, P., Fitton, N., Smith, W., Grant, B., Dorich, C. D., Deng, J., Topp, C. F., Abdalla, M., Liáng, L. L. et Snow, V. (2020). Global Research Alliance N2O chamber methodology guidelines: Summary of modeling approaches. *J Environ Qual*, *49*(5), 1168-1185. https://doi.org/https://doi.org/10.1002/jeq2.20119

Glatzel, S. et Stahr, K. (2001, Apr). Methane and nitrous oxide exchange in differently fertilised grassland in southern Germany. *Plant and Soil*, *231*(1), 21-35. https://doi.org/10.1023/a:1010315416866

Goldewijk, K. K., Beusen, A., Doelman, J. et Stehfest, E. (2017, Dec 1). Anthropogenic land use estimates for the Holocene - HYDE 3.2. *Earth System Science Data*, *9*(2), 927-953. https://doi.org/10.5194/essd-9-927-2017

Gong, Y., Yue, P., Li, K., Mohammat, A. et Liu, Y. (2021). Different responses of ecosystem CO2 and N2O emissions and CH4 uptake to seasonally asymmetric warming in an alpine grassland of the Tianshan. *Biogeosciences*, *18*(11), 3529-3537. https://doi.org/10.5194/bg-18-3529-2021

Harty, M. A., Forrestal, P. J., Watson, C. J., McGeough, K. L., Carolan, R., Elliot, C., Krol, D., Laughlin, R. J., Richards, K. G. et Lanigan, G. J. (2016, 2016/09/01/). Reducing nitrous oxide emissions by changing N fertiliser use from calcium ammonium nitrate (CAN) to urea based formulations. *Science of the Total Environment*, *563-564*, 576-586. https://doi.org/https://doi.org/10.1016/j.scitotenv.2016.04.120

Helfrich, M., Nicolay, G., Well, R., Buchen-Tschiskale, C., Dechow, R., Fuss, R., Gensior, A., Paulsen, H. M., Berendonk, C. et Flessa, H. (2020, Aug 15). Effect of chemical and mechanical grassland conversion to cropland on soil mineral N dynamics and N2O emission. *Agriculture Ecosystems & Environment*, *298*, Article 106975. https://doi.org/10.1016/j.agee.2020.106975

Horvath, L., Grosz, B., Machon, A., Balogh, J., Pinter, K. et Czobel, S. (2008, 2008). Influence of soil type on N2O and CH4 soil fluxes in Hungarian grasslands. *Community Ecology*, *9*, 75-80. https://doi.org/10.1556/ComEc.9.2008.S.11

Hyde, B. P., Hawkins, M. J., Fanning, A. F., Noonan, D., Ryan, M., O' Toole, P. et Carton, O. T. (2006, 2006/07/01). Nitrous Oxide Emissions from a Fertilized and Grazed Grassland in the South East of Ireland. *Nutrient Cycling in Agroecosystems*, *75*(1), 187-200. https://doi.org/10.1007/s10705-006-9026-x

Jones, S. K., Rees, R. M., Skiba, U. M. et Ball, B. C. (2005, 2005/07/01/). Greenhouse gas emissions from a managed grassland. *Global and Planetary Change*, *47*(2), 201-211. https://doi.org/https://doi.org/10.1016/j.gloplacha.2004.10.011

Kaltenegger, K., Erb, K.-H., Matej, S. et Winiwarter, W. (2021, 2021/05/01). Gridded soil surface nitrogen surplus on grazing and agricultural land: Impact of land use maps. *Environmental Research Communications*, *3*(5), 055003.

https://doi.org/10.1088/2515-7620/abedd8

Kariyapperuma, K. A., Wagner-Riddle, C., Furon, A. C. et Li, C. (2011, Mar-Apr). Assessing Spring Thaw Nitrous Oxide Fluxes Simulated by the DNDC Model for Agricultural Soils. *Soil Science Society of America Journal*, *75*(2), 678-690. https://doi.org/10.2136/sssaj2010.0264

Katayanagi, N., Sawamoto, T., Hayakawa, A. et Hatano, R. (2008, Aug). Nitrous oxide and nitric oxide fluxes from cornfield, grassland, pasture and forest in a watershed in Southern Hokkaido, Japan. *Soil Science and Plant Nutrition*, *54*(4), 662-680. https://doi.org/10.1111/j.1747-0765.2008.00284.x

Kendall, M. G. (1948). *Rank correlation methods*. Griffin.

Klein Goldewijk, K., Beusen, A., Doelman, J. et Stehfest, E. (2017). Anthropogenic land use estimates for the Holocene – HYDE 3.2. *Earth Syst. Sci. Data*, *9*(2), 927-953. https://doi.org/10.5194/essd-9-927-2017

Lessa, A. C. R., Madari, B. E., Paredes, D. S., Boddey, R. M., Urquiaga, S., Jantalia, C. P. et Alves, B. J. R. (2014, 2014/06/01/). Bovine urine and dung deposited on Brazilian savannah pastures contribute differently to direct and indirect soil nitrous oxide emissions. *Agriculture, Ecosystems & Environment*, *190*, 104-111. https://doi.org/https://doi.org/10.1016/j.agee.2014.01.010

Li, C., Salas, W., Zhang, R., Krauter, C., Rotz, A. et Mitloehner, F. (2012, 2012/06/01). Manure-DNDC: a biogeochemical process model for quantifying greenhouse gas and ammonia emissions from livestock manure systems. *Nutrient Cycling in Agroecosystems*, *93*(2), 163-200. https://doi.org/10.1007/s10705-012-9507-z

Li, C. S., Aber, J., Stange, F., Butterbach-Bahl, K. et Papen, H. (2000, Feb 27). A process-oriented model of N2O and NO emissions from forest soils: 1. Model development. *Journal of Geophysical Research-Atmospheres*, *105*(D4), 4369-4384. https://doi.org/10.1029/1999jd900949

Li, D., Lanigan, G. et Humphreys, J. (2011, Oct 10). Measured and Simulated Nitrous Oxide Emissions from Ryegrass- and Ryegrass/White Clover-Based Grasslands in a Moist Temperate Climate. *PLOS ONE*, *6*(10), Article e26176. https://doi.org/10.1371/journal.pone.0026176

Li, J., Luo, J., Shi, Y., Li, Y., Ma, Y., Ledgard, S., Wang, L., Houlbrooke, D., Bo, L. et Lindsey, S. (2016). Dung and farm dairy effluent affect urine patch nitrous oxide emissions from a pasture. *Animal Production Science*, *56*(3), 337-342. https://doi.org/https://doi.org/10.1071/AN15511

Li, K., Gong, Y., Song, W., Lv, J., Chang, Y., Hu, Y., Tian, C., Christie, P. et Liu, X. (2012, Aug). No significant nitrous oxide emissions during spring thaw under grazing and nitrogen addition in an alpine grassland. *Global Change Biology*, *18*(8), 2546-2554. https://doi.org/10.1111/j.1365-2486.2012.02704.x

Liang, D. et Robertson, G. P. (2021). Nitrification is a minor source of nitrous oxide (N2O) in an agricultural landscape and declines with increasing management intensity. *Global Change Biology*, *27*(21), 5599-5613. https://doi.org/https://doi.org/10.1111/gcb.15833

Liang, L. L., Campbell, D. I., Wall, A. M. et Schipper, L. A. (2018, 2018/12/01/). Nitrous oxide fluxes determined by continuous eddy covariance measurements from intensively grazed pastures: Temporal patterns and environmental controls. *Agriculture, Ecosystems & Environment*, *268*, 171-180. https://doi.org/https://doi.org/10.1016/j.agee.2018.09.010

Liebig, M. A., Faust, D. R., Archer, D. W., Kronberg, S. L., Hendrickson, J. R. et Aukema, K. D. (2020, Dec 1). Grazing Effects on Nitrous Oxide Flux in an Integrated Crop-Livestock System. *Agriculture Ecosystems & Environment*, *304*, Article 107146. https://doi.org/10.1016/j.agee.2020.107146

Liu, S., Lin, F., Wu, S., Ji, C., Sun, Y., Jin, Y., Li, S., Li, Z. et Zou, J. (2017). A meta-analysis of fertilizer-induced soil NO and combined NO+N2O emissions. *Global Change Biology*, *23*(6), 2520-2532. https://doi.org/https://doi.org/10.1111/gcb.13485

Liu, S., Zheng, Y., Ma, R., Yu, K., Han, Z., Xiao, S., Li, Z., Wu, S., Li, S., Wang, J., Luo, Y. et Zou, J. (2020). Increased soil release of greenhouse gases shrinks terrestrial carbon uptake enhancement under warming. *Global Change*

Biology, *26*(8), 4601-4613. https://doi.org/https://doi.org/10.1111/gcb.15156

López-Aizpún, M. et Horrocks, C. A. (2020, Jan 23). Meta-analysis of global livestock urine-derived nitrous oxide emissions from agricultural soils. *26*(4), 2002-2013. https://doi.org/10.1111/gcb.15012

Lopez-Aizpun, M., Horrocks, C. A., Charteris, A. F., Marsden, K. A., Ciganda, V. S., Evans, J. R., Chadwick, D. R. et Cardenas, L. M. (2020). Meta-analysis of global livestock urine-derived nitrous oxide emissions from agricultural soils. *Global Change Biology*. https://doi.org/10.1111/gcb.15012

Luo, J., Saggar, S., van der Weerden, T. et de Klein, C. (2019, 2019/02/01/). Quantification of nitrous oxide emissions and emission factors from beef and dairy cattle excreta deposited on grazed pastoral hill lands. *Agriculture, Ecosystems & Environment*, *270-271*, 103-113. https://doi.org/https://doi.org/10.1016/j.agee.2018.10.020

Luo, J., Wyatt, J., van der Weerden, T. J., Thomas, S. M., de Klein, C. A. M., Li, Y., Rollo, M., Lindsey, S., Ledgard, S. F., Li, J., Ding, W., Qin, S., Zhang, N., Bolan, N., Kirkham, M. B., Bai, Z., Ma, L., Zhang, X., Wang, H., Liu, H. et Rys, G. (2017). Chapter Five - Potential Hotspot Areas of Nitrous Oxide Emissions From Grazed Pastoral Dairy Farm Systems. Dans D. L. Sparks (dir.), *Advances in Agronomy* (vol. 145, p. 205-268). Academic Press. https://doi.org/https://doi.org/10.1016/bs.agron.2017.05.006.

Maire, J., Krol, D., Pasquier, D., Cowan, N., Skiba, U., Rees, R. M., Reay, D., Lanigan, G. J. et Richards, K. G. (2020, Mar 1). Nitrogen fertiliser interactions with urine deposit affect nitrous oxide emissions from grazed grasslands. *Agriculture Ecosystems & Environment*, *290*, Article 106784. https://doi.org/10.1016/j.agee.2019.106784

Mancia, A., Chadwick, D. R., Waters, S. M. et Krol, D. J. (2022, 2022/01/10/). Uncertainties in direct N2O emissions from grazing ruminant excreta (EF3PRP) in national greenhouse gas inventories. *Science of the Total Environment*, *803*, 149935. https://doi.org/https://doi.org/10.1016/j.scitotenv.2021.149935

Marsden, K. A., Holmberg, J. A., Jones, D. L., Charteris, A. F., Cardenas, L. M. et Chadwick, D. R. (2019, Dec 10). Nitrification represents the bottle-neck of sheep urine patch N2O emissions from extensively grazed organic soils. *Science of the Total Environment*, *695*, Article 133786. https://doi.org/10.1016/j.scitotenv.2019.133786

Marsden, K. A., Lush, L., Holmberg, J. A., Whelan, M. J., King, A. J., Wilson, R. P., Charteris, A. F., Cardenas, L. M., Jones, D. L. et Chadwick, D. R. (2020, 2020/10/15/). Sheep urination frequency, volume, N excretion and chemical composition: Implications for subsequent agricultural N losses. *Agriculture, Ecosystems & Environment*, *302*, 107073. https://doi.org/https://doi.org/10.1016/j.agee.2020.107073

Mori, A. et Hojito, M. (2015). Methane and nitrous oxide emissions due to excreta returns from grazing cattle in Nasu, Japan. *Grassland Science*, *61*(2), 109-120. https://doi.org/https://doi.org/10.1111/grs.12081

Morkved, P. T., Dorsch, P. et Bakken, L. R. (2007, Aug). The N2O product ratio of nitrification and its dependence on long-term changes in soil pH. *Soil Biology & Biochemistry*, *39*(8), 2048-2057. https://doi.org/10.1016/j.soilbio.2007.03.006

Mumford, M. T., Rowlings, D. W., Scheer, C., De Rosa, D. et Grace, P. R. (2019, Feb 15). Effect of irrigation scheduling on nitrous oxide emissions in intensively managed pastures. *Agriculture Ecosystems & Environment*, *272*, 126-134. https://doi.org/10.1016/j.agee.2018.11.011

Murphy, R. M., Saunders, M., Richards, K. G., Krol, D. J., Gebremichael, A. W., Rambaud, J., Cowan, N. et Lanigan, G. J. (2022, 2022/02/01/). Nitrous oxide emission factors from an intensively grazed temperate grassland: A comparison of cumulative emissions determined by eddy covariance and static chamber methods. *Agriculture, Ecosystems & Environment*, *324*, 107725. https://doi.org/https://doi.org/10.1016/j.agee.2021.107725

Nagatake, A., Mukumbuta, I., Yasuda, K., Shimizu, M., Kawai, M. et Hatano, R. (2018). Temporal Dynamics of Nitrous Oxide Emission and Nitrate Leaching in Renovated Grassland with Repeated Application of Manure and/or Chemical Fertilizer. *Atmosphere*, *9*(12), 485. https://www.mdpi.com/2073-4433/9/12/485

Nichols, K. L., Del Grosso, S. J., Derner, J. D., Follett, R. F., Archibeque, S. L., Stewart, C. E. et Paustian, K. H. (2016, 2016/06/01/). Nitrous oxide and methane fluxes from cattle excrement on C3 pasture and C4-dominated shortgrass steppe. *Agriculture, Ecosystems & Environment*, *225*, 104-115. https://doi.org/https://doi.org/10.1016/j.agee.2016.03.026

Nishina, K., Ito, A., Hanasaki, N. et Hayashi, S. (2017, Feb 20). Reconstruction of spatially detailed global map of NH4+ and NO3- application in synthetic nitrogen fertilizer. *Earth System Science Data*, *9*(1), 149-162. https://doi.org/10.1594/pangaea.861203

O'Neill, M., Saggar, S., Richards, K. G., Luo, J., Singh, B. P., Mehra, P. et Forrestal, P. J. (2021, 2021/12/01). Nitrous oxide emission factors in conventionally and naturally simulated cattle urine patches. *Nutrient Cycling in Agroecosystems*, *121*(2), 129-147. https://doi.org/10.1007/s10705-021-10162-5

Oenema, O., Velthof, G. L., Yamulki, S. et Jarvis, S. C. (1997). Nitrous oxide emissions from grazed grassland. *Soil Use and Management*, *13*(s4), 288-295. https://doi.org/https://doi.org/10.1111/j.1475-2743.1997.tb00600.x

Pärn, J., Verhoeven, J. T. A., Butterbach-Bahl, K., Dise, N. B., Ullah, S., Aasa, A., Egorov, S., Espenberg, M., Järveoja, J., Jauhiainen, J., Kasak, K., Klemedtsson, L., Kull, A., Laggoun-Défarge, F., Lapshina, E. D., Lohila, A., Lõhmus, K., Maddison, M., Mitsch, W. J., Müller, C., Niinemets, Ü., Osborne, B., Pae, T., Salm, J.-O., Sgouridis, F., Sohar, K., Soosaar, K., Storey, K., Teemusk, A., Tenywa, M. M., Tournebize, J., Truu, J., Veber, G., Villa, J. A., Zaw, S. S. et Mander, Ü. (2018, 2018/03/19). Nitrogen-rich organic soils under warm well-drained conditions are global nitrous oxide emission hotspots. *Nature communications*, *9*(1), 1135. https://doi.org/10.1038/s41467-018-03540-1

Pelster, D. E., Gisore, B., Koske, J. K., Goopy, J., Korir, D., Rufino, M. C. et Butterbach-Bahl, K. (2016, Sep-Oct). Methane and Nitrous Oxide Emissions from Cattle Excreta on an East African Grassland. *Journal of Environmental Quality*, *45*(5), 1531-1539. https://doi.org/10.2134/jeq2016.02.0050

Peng, C., Zhu, Q. et Chen, H. (2013). Integrating greenhouse gas emission processes into a dynamic global vegetation model of TRIPLEX-GHG. Egu General Assembly Conference,

Peng, C. H., Liu, J. X., Dang, Q. L., Apps, M. J. et Jiang, H. (2002, Jul 15). TRIPLEX: a generic hybrid model for predicting forest growth and carbon and nitrogen dynamics. *Ecological Modelling*, *153*(1-2), 109-130, Article Pii s0304-3800(01)00505-1. https://doi.org/10.1016/s0304-3800(01)00505-1

Peng, Q., Qi, Y., Dong, Y., Xiao, S. et He, Y. (2011, 2011/05/01). Soil nitrous oxide emissions from a typical semiarid temperate steppe in inner Mongolia: effects of mineral nitrogen fertilizer levels and forms. *Plant and Soil*, *342*(1), 345-357. https://doi.org/10.1007/s11104-010-0699-1

Powell, J. M. et Rotz, C. A. (2015). Measures of Nitrogen Use Efficiency and Nitrogen Loss from Dairy Production Systems. *Journal of Environmental Quality*, *44*(2), 336-344. https://doi.org/https://doi.org/10.2134/jeq2014.07.0299

Ramankutty, N., Evan, A. T., Monfreda, C. et Foley, J. A. (2008). Farming the planet: 1. Geographic distribution of global agricultural lands in the year 2000. *Global Biogeochemical Cycles*, *22*(1). https://doi.org/https://doi.org/10.1029/2007GB002952

Reay, D. S., Davidson, E. A., Smith, K. A., Smith, P., Melillo, J. M., Dentener, F. et Crutzen, P. J. (2012, 2012/06/01). Global agriculture and nitrous oxide emissions. *Nature Climate Change*, *2*(6), 410-416. https://doi.org/10.1038/nclimate1458

Reed, K. F., Moraes, L. E., Casper, D. P. et Kebreab, E. (2015). Predicting nitrogen excretion from cattle. *Journal of Dairy Science*, *98*(5), 3025-3035. https://doi.org/10.3168/jds.2014-8397

Risk, N., Snider, D. et Wagner-Riddle, C. (2013, Sep). Mechanisms leading to enhanced soil nitrous oxide fluxes induced by freeze-thaw cycles. *Canadian Journal of Soil Science*, *93*(4), 401-414. https://doi.org/10.4141/cjss2012-071

Rivera, J. E., Chará, J. et Barahona, R. (2019, 2019/06/01). CH4, CO2 and N2O emissions from grasslands and bovine excreta in two intensive tropical dairy production systems. *Agroforestry Systems*, *93*(3), 915-928. https://doi.org/10.1007/s10457-018-0187-9

Ruan, L. et Robertson, G. P. (2017, 2017/08/01). Reduced Snow Cover Increases Wintertime Nitrous Oxide (N2O) Emissions from an Agricultural Soil in the Upper U.S. Midwest. *Ecosystems*, *20*(5), 917-927. https://doi.org/10.1007/s10021-016-0077-9

Saggar, S., Hedley, C. B., Giltrap, D. L. et Lambie, S. M. (2007, Nov). Measured and modelled estimates of nitrous oxide emission and methane consumption from a sheep-grazed pasture. *Agriculture Ecosystems & Environment*, *122*(3), 357-365. https://doi.org/10.1016/j.agee.2007.02.006

Sauer, T. J., Compston, S. R., West, C. P., Hernandez-Ramirez, G., Gbur, E. E. et Parkin, T. B. (2009, Jul). Nitrous oxide emissions from a bermudagrass pasture: Interseeded winter rye and poultry litter. *Soil Biology & Biochemistry*, *41*(7), 1417-1424. https://doi.org/10.1016/j.soilbio.2009.03.019

Schils, R. L. M., van Groenigen, J. W., Velthof, G. L. et Kuikman, P. J. (2008, 2008/09/01). Nitrous oxide emissions from multiple combined applications of fertiliser and cattle slurry to grassland. *Plant and Soil*, *310*(1), 89-101. https://doi.org/10.1007/s11104-008-9632-2

Schirmann, J., de Bastos, D. F., Weiler, D. A., Veloso, M. G., Dieckow, J., Carvalho, P. C. d. F. et Bayer, C. (2020, 2020). Nitrous oxide emission factor from cattle urine and dung in native grassland of the Pampa biome, South Brazil. *Soil Research*, *58*(2), 198-206. https://doi.org/10.1071/sr19095

Shcherbak, I., Millar, N. et Robertson, G. P. (2014, Jun 24). Global metaanalysis of the nonlinear response of soil nitrous oxide (N2O) emissions to fertilizer nitrogen. *Proceedings of the National Academy of Sciences of the United States of America*, *111*(25), 9199-9204. https://doi.org/10.1073/pnas.1322434111

Sheldrick, W., Keith Syers, J. et Lingard, J. (2003, 2003/06/01). Contribution of livestock excreta to nutrient balances. *Nutrient Cycling in Agroecosystems*, *66*(2), 119-131. https://doi.org/10.1023/A:1023944131188

Simon, P. L., de Klein, C. A. M., Worth, W., Rutherford, A. J. et Dieckow, J. (2019, 2019/11/15/). The efficacy of Plantago lanceolata for mitigating nitrous oxide emissions from cattle urine patches. *Science of the Total Environment*, *691*, 430-441. https://doi.org/https://doi.org/10.1016/j.scitotenv.2019.07.141

Smith, K. A., Dobbie, K. E., Thorman, R., Watson, C. J., Chadwick, D. R., Yamulki, S. et Ball, B. C. (2012, 2012/06/01). The effect of N fertilizer forms on nitrous oxide emissions from UK arable land and grassland. *Nutrient Cycling in Agroecosystems*, *93*(2), 127-149. https://doi.org/10.1007/s10705-012-9505-1

Song, H., Peng, C., Zhang, K. et Zhu, Q. (2022, 2022/06/25/). Integrating major agricultural practices into the TRIPLEX-GHG model v2.0 for simulating global cropland nitrous oxide emissions: Development, sensitivity analysis and site evaluation. *Science of the Total Environment*, 156945. https://doi.org/https://doi.org/10.1016/j.scitotenv.2022.156945

Sordi, A., Dieckow, J., Bayer, C., Alburquerque, M. A., Piva, J. T., Zanatta, J. A., Tomazi, M., da Rosa, C. M. et de Moraes, A. (2014, 2014/06/01/). Nitrous oxide emission factors for urine and dung patches in a subtropical Brazilian pastureland. *Agriculture, Ecosystems & Environment*, *190*, 94-103. https://doi.org/https://doi.org/10.1016/j.agee.2013.09.004

Sordi, A., Dieckow, J., Bayer, C., Alburquerque, M. A., Piva, J. T., Zanatta, J. A., Tomazi, M., da Rosa, C. M. et de Moraes, A. (2014, Jun 1). Nitrous oxide emission factors for urine and dung patches in a subtropical Brazilian pastureland. *Agriculture Ecosystems & Environment*, *190*, 94-103. https://doi.org/10.1016/j.agee.2013.09.004

Stojanovic, B., Grubić, G., Božičković, A. et Davidović, V. (2019). *NITROGEN USE EFFICIENCY IN DAIRY CATTLE*.

Suter, H. C., Sultana, H., Davies, R., Walker, C. et Chen, D. (2016, 2016). Influence of enhanced efficiency fertilisation techniques on nitrous oxide emissions and productivity response from urea in a temperate Australian ryegrass pasture. *Soil Research*, *54*(5), 523-532. https://doi.org/10.1071/sr15317

Tang, S., Wang, K., Xiang, Y., Tian, D., Wang, J., Liu, Y., Cao, B., Guo, D. et Niu, S. (2019, 2019/03/01/). Heavy grazing reduces grassland soil greenhouse gas fluxes: A global meta-analysis. *Science of The Total Environment*, *654*, 1218-1224. https://doi.org/https://doi.org/10.1016/j.scitotenv.2018.11.082

Tenuta, M., Mkhabela, M., Tremorin, D., Coppi, L., Phipps, G., Flaten, D. et Ominski, K. (2010, 2010/06/15/). Nitrous oxide and methane emission from a coarse-textured grassland soil receiving hog slurry. *Agriculture, Ecosystems & Environment*, *138*(1), 35-43. https://doi.org/https://doi.org/10.1016/j.agee.2010.03.014

Thies, S., Joshi, D. R., Bruggeman, S. A., Clay, S. A., Mishra, U., Morile-Miller, J. et Clay, D. E. (2020, 2020/01/01). Fertilizer timing affects nitrous oxide, carbon dioxide, and ammonia emissions from soil [https://doi.org/10.1002/saj2.20010]. *Soil Science Society of America Journal*, *84*(1), 115-130. https://doi.org/https://doi.org/10.1002/saj2.20010

Thomas, B. W., Gao, X., Beck, R. et Hao, X. (2017, 2017/11/01). Are distinct nitrous oxide emission factors required for cattle urine and dung deposited on pasture in western Canada? *Environmental Science and Pollution Research*, *24*(33), 26142-26147. https://doi.org/10.1007/s11356-017-0392-5

Tian, H., Xu, R., Canadell, J. G., Thompson, R. L., Winiwarter, W., Suntharalingam, P., Davidson, E. A., Ciais, P., Jackson, R. B., Janssens-Maenhout, G., Prather, M. J., Regnier, P., Pan, N., Pan, S., Peters, G. P., Shi, H., Tubiello, F. N., Zaehle, S., Zhou, F., Arneth, A., Battaglia, G., Berthet, S., Bopp, L., Bouwman, A. F., Buitenhuis, E. T., Chang, J., Chipperfield, M. P., Dangal, S. R. S., Dlugokencky, E., Elkins, J. W., Eyre, B. D., Fu, B., Hall, B., Ito, A., Joos, F., Krummel, P. B., Landolfi, A., Laruelle, G. G., Lauerwald, R., Li, W., Lienert, S., Maavara, T., MacLeod, M., Millet, D. B., Olin, S., Patra, P. K., Prinn, R. G., Raymond, P. A., Ruiz, D. J., van der Werf, G. R., Vuichard, N., Wang, J., Weiss, R. F., Wells, K. C., Wilson, C., Yang, J. et Yao, Y. (2020, 2020/10/01). A comprehensive quantification of global nitrous oxide sources and sinks. *Nature*, *586*(7828), 248-256. https://doi.org/10.1038/s41586-020-2780-0

Tian, H., Yang, J., Xu, R., Lu, C., Canadell, J. G., Davidson, E. A., Jackson, R. B., Arneth, A., Chang, J., Ciais, P., Gerber, S., Ito, A., Joos, F., Lienert, S., Messina, P., Olin, S., Pan, S., Peng, C., Saikawa, E., Thompson, R. L., Vuichard, N., Winiwarter, W., Zaehle, S. et Zhang, B. (2019, Feb). Global soil nitrous oxide emissions since the preindustrial era estimated by an ensemble of terrestrial biosphere models: Magnitude, attribution, and uncertainty. *Global Change Biology*, *25*(2), 640-659. https://doi.org/10.1111/gcb.14514

Tully, K. L., Abwanda, S., Thiong'o, M., Mutuo, P. M. et Rosenstock, T. S. (2017, Jul-Aug). Nitrous Oxide and Methane Fluxes from Urine and Dung Deposited on Kenyan Pastures. *Journal of Environmental Quality*, *46*(4), 921-929. https://doi.org/10.2134/jeq2017.01.0040

van Delden, L., Rowlings, D. W., Scheer, C., De Rosa, D. et Grace, P. R. (2018, Dec). Effect of urbanization on soil methane and nitrous oxide fluxes in subtropical Australia. *Global Change Biology*, *24*(12), 5695-5707. https://doi.org/10.1111/gcb.14444

Van der Hoek, K. W. (1998, 1998/01/01/). Nitrogen efficiency in global animal production. *Environmental Pollution*, *102*(1, Supplement 1), 127-132. https://doi.org/https://doi.org/10.1016/S0269-7491(98)80025-0

van der Weerden, T. J., Noble, A. N., Luo, J., de Klein, C. A. M., Saggar, S., Giltrap, D., Gibbs, J. et Rys, G. (2020, 2020/08/25/). Meta-analysis of New Zealand's nitrous oxide emission factors for ruminant excreta supports disaggregation based on excreta form, livestock type and slope class. *Science of the Total Environment*, *732*, 139235. https://doi.org/https://doi.org/10.1016/j.scitotenv.2020.139235

Velthof, G. L., Brader, A. B. et Oenema, O. (1996, 1996/04/01). Seasonal variations in nitrous oxide losses from managed grasslands in The Netherlands. *Plant and Soil*, *181*(2), 263-274. https://doi.org/10.1007/BF00012061

Velthof, G. L., Hou, Y. et Oenema, O. (2015). Nitrogen excretion factors of livestock in the European Union: a review. *Journal of the Science of Food and Agriculture*, *95*(15), 3004-3014. https://doi.org/https://doi.org/10.1002/jsfa.7248

Voglmeier, K., Six, J., Jocher, M. et Ammann, C. (2019). Grazing-related nitrous oxide emissions: from patch scale to field scale. *Biogeosciences*, *16*(8), 1685-1703. https://doi.org/10.5194/bg-16-1685-2019

Wang, C., Zhang, R., Vilonen, L., Qu, Y., Fu, X., Shi, B., Cui, H., Gao, W., Cai, H. et Sun, W. (2021, 2021/12/01). Grazing and nitrogen addition restructure the spatial heterogeneity of soil microbial community structure and enzymatic activities [https://doi.org/10.1111/1365-2435.13926]. *Functional Ecology*, *35*(12), 2763-2777. https://doi.org/https://doi.org/10.1111/1365-2435.13926

Wang, J., Chadwick, D. R., Cheng, Y. et Yan, X. (2018, Mar). Global analysis of agricultural soil denitrification in response to fertilizer nitrogen. *Science of the Total Environment*, *616*, 908-917. https://doi.org/10.1016/j.scitotenv.2017.10.229

Wang, Q., Zhou, F., Shang, Z., Ciais, P., Winiwarter, W., Jackson, R. B., Tubiello, F. N., Janssens-Maenhout, G., Tian, H., Cui, X., Canadell, J. G., Piao, S. et Tao, S. (2019). Data-driven estimates of global nitrous oxide emissions from croplands. *National Science Review*. https://doi.org/10.1093/nsr/nwz087

Ward, G. N., Kelly, K. B. et Hollier, J. W. (2018). Greenhouse gas emissions from dung, urine and dairy pond sludge applied to pasture. 1. Nitrous oxide emissions. *Animal Production Science*, *58*(6), 1087-1093. https://doi.org/https://doi.org/10.1071/AN15595

Willmott, C. J. (1981). On the Validation of Model. *Physical Geography*, *2*(2), 219-232.

Wolf, B., Kiese, R., Chen, W., Grote, R., Zheng, X. et Butterbach-Bahl, K. (2012, 2012/01/01). Modeling N2O emissions from steppe in Inner Mongolia, China, with consideration of spring thaw and grazing intensity. *Plant and Soil*, *350*(1), 297-310. https://doi.org/10.1007/s11104-011-0908-6

Wolf, B., Zheng, X., Brueggemann, N., Chen, W., Dannenmann, M., Han, X., Sutton, M. A., Wu, H., Yao, Z. et Butterbach-Bahl, K. (2010, Apr 8). Grazing-induced reduction of natural nitrous oxide release from continental steppe. *Nature*, *464*(7290), 881-884. https://doi.org/10.1038/nature08931

Xu, L., Xu, X., Tang, X., Xin, X., Ye, L., Yang, G., Tang, H., Lv, S., Xu, D. et Zhang, Z. (2018, Apr). Managed grassland alters soil N dynamics and N2O emissions in temperate steppe. *Journal of Environmental Sciences*, *66*, 20-30. https://doi.org/10.1016/j.jes.2017.04.003

Xu, R., Prentice, I. C., Spahni, R. et Niu, H. S. (2012, Oct). Modelling terrestrial nitrous oxide emissions and implications for climate feedback. *New Phytologist*, *196*(2), 472-488. https://doi.org/10.1111/j.1469-8137.2012.04269.x

Yan, R., Tang, H., Xin, X., Chen, B., Murray, P. J., Yan, Y., Wang, X. et Yang, G. (2016, May). Grazing intensity and driving factors affect soil nitrous oxide fluxes during the growing seasons in the Hulunber meadow steppe of China. *Environmental Research Letters*, *11*(5), Article 054004. https://doi.org/10.1088/1748-9326/11/5/054004

Yang, X., Chen, H., Gong, Y., Zheng, X., Fan, M. et Kuzyakov, Y. (2015, 2015/12/25/). Nitrous oxide emissions from an agro-pastoral ecotone of northern China depending on land uses. *Agriculture, Ecosystems & Environment*, *213*, 241-251. https://doi.org/https://doi.org/10.1016/j.agee.2015.08.011

Yin, M., Gao, X., Tenuta, M., Li, L., Gui, D., Li, X. et Zeng, F. (2020, Oct 1). Enhancement of N2O emissions by grazing is related to soil physicochemical characteristics rather than nitrifier and denitrifier abundances in alpine grassland. *Geoderma*, *375*, Article 114511. https://doi.org/10.1016/j.geoderma.2020.114511

Yin, Y., Wang, Z., Tian, X., Wang, Y., Cong, J. et Cui, Z. (2021). Evaluation of variation in background nitrous oxide emissions: A new global synthesis integrating the impacts of climate, soil, and management conditions. *Global Change Biology*, *n/a*(n/a). https://doi.org/https://doi.org/10.1111/gcb.15860

Zhang, B., Tian, H., Lu, C., Dangal, S. R. S., Yang, J. et Pan, S. (2017, Sep 6). Global manure nitrogen production and application in cropland during 1860-2014: a 5 arcmin gridded global dataset for Earth system modeling. *Earth System Science Data*, *9*(2), 667-678. https://doi.org/10.5194/essd-9-667-2017

Zhang, F., Qi, J., Li, F. M., Li, C. S. et Li, C. B. (2010). Quantifying nitrous oxide emissions from Chinese grasslands with a process-based model. *Biogeosciences*, *7*(6), 2039-2050. https://doi.org/10.5194/bg-7-2039-2010

Zhang, H., Yao, Z., Wang, K., Zheng, X., Ma, L., Wang, R., Liu, C., Zhang, W., Zhu, B., Tang, X., Hu, Z. et Han, S. (2018, Jun 1). Annual N(2)O emissions from conventionally grazed typical alpine grass meadows in the eastern Qinghai-Tibetan Plateau. *Sci Total Environ*, *625*, 885-899. https://doi.org/10.1016/j.scitotenv.2017.12.216

Zhang, K., Peng, C., Wang, M., Zhou, X., Li, M., Wang, K., Ding, J. et Zhu, Q. (2017). Process-based TRIPLEX-GHG model for simulating N2O emissions from global forests and grasslands: Model development and evaluation. *Journal of Advances in Modeling Earth Systems*, *9*(5), 2079-2102. https://doi.org/https://doi.org/10.1002/2017MS000934

Zhang, K., Zhu, Q., Liu, J., Wang, M., Zhou, X., Li, M., Wang, K., Ding, J. et Peng, C. (2019, Mar 15). Spatial and temporal variations of N2O emissions from global forest and grassland ecosystems. *Agricultural and Forest Meteorology*, *266*, 129-139. https://doi.org/10.1016/j.agrformet.2018.12.011

Zhang, L., Hou, L., Guo, D., Li, L. et Xu, X. (2017, 2017/02/01/). Interactive impacts of nitrogen input and water amendment on growing season fluxes of CO2, CH4, and N2O in a semiarid grassland, Northern China. *Science of the Total Environment*, *578*, 523-534. https://doi.org/https://doi.org/10.1016/j.scitotenv.2016.10.219

Zhang, Y., Zhang, F., Abalos, D., Luo, Y., Hui, D., Hungate, B. A., García-Palacios, P., Kuzyakov, Y., Olesen, J. E., Jørgensen, U. et Chen, J. (2022, 2022/03/01). Stimulation of ammonia oxidizer and denitrifier abundances by nitrogen loading: Poor predictability for increased soil N2O emission [https://doi.org/10.1111/gcb.16042]. *Global Change Biology*, *28*(6), 2158-2168. https://doi.org/https://doi.org/10.1111/gcb.16042

Zhong, L., Hoogendoorn, C. J., Bowatte, S., Li, F. Y., Wang, Y. et Luo, D. (2016, Feb 1). Slope class and grazing intensity effects on microorganisms and nitrogen transformation processes responsible for nitrous oxide emissions from hill pastures. *Agriculture Ecosystems & Environment*, *217*, 70-78. https://doi.org/10.1016/j.agee.2015.11.009

Zhong, L., Zhou, X., Wang, Y., Li, F. Y., Zhou, S., Bai, Y. et Rui, Y. (2017, 2017/11/01/). Mixed grazing and clipping is beneficial to ecosystem recovery but may increase potential N2O emissions in a semi-arid grassland. *Soil Biology and Biochemistry*, *114*, 42-51. https://doi.org/https://doi.org/10.1016/j.soilbio.2017.07.002

Zhu, X., Luo, C., Wang, S., Zhang, Z., Cui, S., Bao, X., Jiang, L., Li, Y., Li, X., Wang, Q. et Zhou, Y. (2015, 2015/12/15/). Effects of warming, grazing/cutting and nitrogen fertilization on greenhouse gas fluxes during growing seasons in an alpine meadow on the Tibetan Plateau. *Agricultural and Forest Meteorology*, *214-215*, 506-514. https://doi.org/https://doi.org/10.1016/j.agrformet.2015.09.008

Zhu, Y., Butterbach-Bahl, K., Merbold, L., Leitner, S. et Pelster, D. E. (2021, 2021/12/01/). Nitrous oxide emission factors for cattle dung and urine deposited onto tropical pastures: A review of field-based studies. *Agriculture, Ecosystems & Environment*, *322*, 107637. https://doi.org/https://doi.org/10.1016/j.agee.2021.107637

Zhuang, Q., Lu, Y. et Chen, M. (2012, 2012/02/01/). An inventory of global N2O emissions from the soils of natural terrestrial ecosystems. *Atmospheric Environment*, *47*, 66-75. https://doi.org/https://doi.org/10.1016/j.atmosenv.2011.11.036

CHAPTER IV:

Central role of nitrogen fertilizer relative to water management in determining direct nitrous oxide emissions from global rice-based ecosystems

Hanxiong Song, Qiuan Zhu, Jean-Pierre Blanchet, Zhi Chen, Kerou Zhang, Tong Li, Feng Zhou, Changhui Peng

Article published in *Global Biogeochemical Cycles* 37.11 (2023): e2023GB007744.

4.1 Résumé

L'augmentation de la concentration atmosphérique de protoxyde d'azote (N_2O) résulte du développement de l'agriculture. Cependant, les émissions de N_2O provenant des écosystèmes rizicoles mondiaux n'ont pas encore été explicitement et systématiquement quantifiées. Cette étude vise donc à estimer l'ampleur spatio-temporelle des émissions de N_2O des écosystèmes rizicoles mondiaux et à déterminer les différents facteurs contributifs, en améliorant un modèle biogéochimique basé sur les processus, TRIPLEX-GHG v2.0. La validation du modèle a montré que les émissions de N_2O modélisées concordaient bien avec les observations de terrain sous différentes pratiques de gestion, aux échelles journalière, saisonnière et annuelle. Les émissions de N_2O simulées des écosystèmes rizicoles mondiaux ont montré des tendances à la hausse significatives, passant de 0.026 ± 0.0013 à 0.18 ± 0.003 TgN an^{-1} entre 1910 et 2020, avec environ 69.5 % des émissions attribuées aux saisons de culture du riz. Les écosystèmes rizicoles irrigués représentaient la majorité des émissions mondiales de N_2O liées au riz (~76.9 %) en raison de leurs taux d'émission de N_2O plus élevés par rapport aux systèmes pluviaux. En ce qui concerne l'analyse spatiale, le sud de la Chine, le nord-est de l'Inde et l'Asie du Sud-Est sont des points chauds pour les émissions de N_2O liées au riz. Les scénarios expérimentaux ont révélé que les engrais azotés sont la plus grande source de N_2O liée au riz au niveau mondial, en particulier depuis les années 1960 (0.047 ± 0.010 TgN an^{-1}, 35.24 %), tandis que l'impact de l'expansion de l'irrigation joue un rôle mineur. Globalement, cette étude fournit une meilleure compréhension des écosystèmes rizicoles dans le bilan mondial du N_2O agricole; de plus, elle a démontré quantitativement le rôle central des engrais azotés dans les émissions de N_2O liées au riz en incluant le calendrier de culture du riz, en couvrant les saisons hors riz, en différenciant les effets des différents régimes hydriques et des formes d'apports en azote. Nos résultats soulignent l'importance de la co-gestion des engrais azotés et des régimes hydriques pour réduire l'impact climatique net de la culture mondiale du riz.

4.2 Abstract

The increasing atmospheric nitrous oxide (N_2O) concentration stems from the development of agriculture. As an important agricultural land type, N_2O emissions from global rice-based ecosystems have not been explicitly and systematically quantified. Therefore, this study aims to estimate the spatiotemporal magnitudes of the N_2O emissions from global rice-based ecosystems and determine different contribution factors, by improving a process-based biogeochemical model, TRIPLEX-GHG v2.0. Model validation suggested the modeled N_2O agreed well with field observations under varying management practices at daily, seasonal, and annual steps. Simulated N_2O emissions from global rice-based ecosystems exhibited significant increasing trends from 0.026 ± 0.0013 to 0.18 ± 0.003 TgN yr^{-1} from 1910 – 2020, with ~69.5% emissions attributed to the rice-growing seasons. Irrigated rice ecosystems accounted for a majority of global rice N_2O emissions (~ 76.9%) because of their higher N_2O emission rates than rainfed systems. Regarding spatial analysis, Southern China, Northeast India, and Southeast Asia are hotspots for rice-based N_2O emissions. Experimental scenarios revealed that N fertilizer is the largest global rice-N_2O source, especially since the 1960s (0.047 ± 0.010 TgN yr^{-1}, 35.24%), while the impact of expanded irrigation plays a minor role. Overall, this study provides a better understanding of rice-based ecosystem in global agricultural N_2O budget; further it quantitively demonstrated the central role of N fertilizer in rice-based N_2O emissions by including rice crop calendar, covering non-rice growing seasons, differentiating the effects of various water regimes and input N forms. Our findings emphasize the significance of co-management of N fertilizer and water regimes in reducing the net climate impact of global rice cultivation.

4.3 Introduction

Nitrous oxide (N_2O), is an important green-house gas with 265 – 298 times larger global warming potential than CO_2 on a 100-year timescale and is a persistent trace gas that induces ozone depletion (Canadell, 2021). The increasing atmospheric concentration of N_2O is largely attributed to the development of agricultural lands under intensive agricultural practices, including N fertilizer application, irrigation, and tillage (Davidson & Kanter, 2014; Tian et al., 2020). Rice (*Oryza sativa* L.), a staple food crop that sustains a large population, accounts for ~ 8 – 11% of the global cultivation area (121.4 million ha) in the 21st century (Klein Goldewijk et al., 2017). N_2O production and emissions from rice-based ecosystems are driven by microbial nitrification and denitrification processes and are regulated by multiple environmental and management factors (Akiyama et al., 2005; Butterbach-Bahl et al., 2013; Zou et al., 2009).

Attempts to quantify the magnitude of rice-based N_2O emissions found strong spatiotemporal variations across the globe. For instance, Kritee et al. (2018) reported that the N_2O emission rate during one growing season in an intermittently flooded Indian fields was 21 kgN ha^{-1}. Meanwhile, the mean emission rates obtained under varying fertilization regimes in a long-term flooded rice-paddy in southern China was ~2.5 kgN ha^{-1} yr^{-1} (Zhou et al., 2018). However, emissions less than 1 kgN ha^{-1} yr^{-1} were also widely observed at continuous flooded rice fields in China (Liu et al., 2014), USA (Pittelkow et al., 2013), and Southeast Asia (Chidthaisong et al., 2018). Flooded rice-based ecosystem soils exhibit low N_2O emissions because nitrification processes are strongly inhibited, while the complete reduction of N_2O to N_2 via denitrification is favored under the long-term anaerobic conditions (Kritee et al., 2018; W. Zhou et al., 2017). In addition, the high solubility of N_2O combined with the strong run-off and leaching, account for this phenomenon during the flooding periods (Jian-She et al., 2011; Xiong et al., 2006). Direct N_2O emissions from rice-based ecosystems mainly occurs during midseason aeration in the rice-growing season and subsequent dry–wet alternations driven by local climates in the non-rice-growing (e.g., winter crops) or fallow seasons (Zhang et al., 2016; M. Zhou et al., 2017). Year-round observations found 4-fold higher N_2O emissions during the non-rice-growing seasons than during the rice-growing seasons (Pittelkow et al., 2013; Xie et al., 2022; M. Zhou et al., 2017); however, availability of annual continuous N_2O emission measurements is limited. Therefore, owing to the inconsistent observed emission data, there is an incomplete understanding of the contribution of rice-based ecosystems to the global N_2O budget (Shang et al., 2020; Zhou et al., 2014).

The modeling approach is an essential tool to assess measurements and incorporate the spatiotemporal variations in N_2O emissions from rice-based ecosystems. However, the development and application of such models remain insufficient due to an incomplete knowledge of the mechanisms and driving forces of rice ecosystem N_2O emissions. Thus, existing model conceptualizations and descriptions lead to uncertainties in the outcomes, especially on large geographical scales. The Intergovernmental Panel on Climate Change (IPCC) recommends an empirical model that assigns different emission factors (EFs, percentage of N loss as N_2O emission) for continuous flooded (0.22%) and intermittent flooded (0.37%) rice-paddies with background emissions (1.82 kgN ha^{-1} yr^{-1}) (Akiyama et al., 2005). However, large discrepancies were widely detected between the IPCC modeled and observed emissions because EF-based models ignored the effects of environmental variables (Kritee et al., 2018; Xie et al., 2022; Zhou et al., 2018). Another source of uncertainty is that most models quantify N_2O emissions during the rice-growing seasons exclusively, which only covers ~100–240 days in a year, thus leading to an underestimated annual N_2O budget (Bo et al., 2022; Shang et al., 2020). Moreover, several empirical models only simulate fertilization-induced N_2O emissions but excluded background emissions (Zou et al., 2009) which may account for more than 50% of annual emissions from paddy soils, thereby introducing large uncertainties in total emissions (Akiyama et al., 2005). In addition to the empirical approaches, biogeochemical process-based models estimate N_2O fluxes from rice-based ecosystems by providing detailed descriptions of microbial activities and nutrient cycles. In contrast, their application is area dependent and mainly limited to a particular case study at the site level. For instance, the DeNitrification and DeComposition Model (DNDC) showed different performances in estimating seasonal N_2O emissions when implemented in various fields in California, USA (Simmonds, Li, et al., 2015), China (Cai et al., 2003), the Philippines (Kraus et al., 2015), and India (Babu et al., 2006). To the best of our knowledge, the specific contribution of global rice-based ecosystems to the total N_2O budget has not been systematically quantified using the process-based models, and the global N_2O Model Inter-comparison Project (NMIP), which aimed to determine the global N_2O budget, along with all the uncertainties, also did not document the explicit estimation of rice-based N_2O emissions (Tian et al., 2019). This research gap can be attributed to the following: 1) existing models did not have extensive validation against the long-term field observations across large areas, and 2) lack of information on various management factors, especially the geographic distribution of the global rice area, numbers of growing seasons, and decision to alter management practices within a year.

Recently developed spatially global rice crop calendar datasets, agricultural management information, and a growing number of long-term continuous measurements would provide good opportunities to better quantify the spatiotemporal variations in N_2O emissions from rice-based ecosystems (Laborte et al., 2017; Tian et al., 2022). The TRIPLEX-GHG model v2.0 is a process-based biogeochemical model that can simulate N_2O emissions from upland soils on a global scale; however, its descriptions of the dynamics of rice-based N_2O fluxes are lacking (Song et al., 2022; Zhang et al., 2017). Therefore, the main objective of this study was to improve and implement the TRIPLEX-GHG model v2.0 to better understand the spatiotemporal magnitudes and sources of N_2O emissions from global rice-based ecosystems, and provide scientific basis for possible mitigation strategies. We hypothesized that: 1) irrigated rice-based ecosystems is a more significant N_2O source than rainfed rice-based ecosystems during 1910—2020; and that 2) N fertilizer application is the largest contributor to the total rice-based N_2O emissions.

4.4 Materials and methods

4.4.1 Model description and improvements

The TRIPLEX-GHG model v2.0 is a biogeochemical process-based ecosystem model (Song et al., 2022), which considers various factors, including the dynamic vegetation, water movement, and C and N cycling in terrestrial ecosystems (Zhang et al., 2019; Zhu et al., 2017). As shown in Figure 4.1, the key submodules of the model include: A land surface submodule which simulates the energy and water fluxes between the soil surface, vegetation, and the atmosphere; a vegetation dynamic submodule and a plant phenology submodule describe the phenological behaviors of different plant functional types (PFTs) and their responses to changing climate factors; the soil biogeochemical submodule simulates the dynamics of soil organic matter decomposition, nutrient mineralization, immobilization, and microbial activities (Foley et al., 1996; Kucharik et al., 2000). The results are further utilized by methane (CH_4) and nitrous oxide (N_2O) submodules to estimate the emission of greenhouse gases (Zhang et al., 2017; Zhu et al., 2014). The management submodule interacts with others to simulate the effects of agricultural management (Song et al., 2022).

Rice-based cropping systems are characterized by strong variations in soil water conditions, including both rice-growing seasons and fallow, or second crop seasons. Redox potential oscillations induced by changes in water regime control the compositions and functions of microbial communities and, thus, short-term biogeochemical processes, especially N losses, accompanied by the emission of trace gases (Cowan et al., 2021; Kögel-Knabner et al., 2010; Zou et al., 2007). The current TRIPLEX-GHG v2.0 does not include the above-mentioned biogeochemical features of rice-paddies which is significantly different from that of upland soil (Kögel-Knabner et al., 2010). Therefore, the current structure of the TRIPLEX-GHGv2.0 was modified to simulate the dynamics of N_2O emissions from rice-based ecosystems (Figure 4.1).

First, we changed the composition of soil profile in the model for flooding rice paddies. The original horizon sequence of soil profile of TRIPLEX-GHG modelv2.0 comprised six layers, with depths of 0.1, 0.15, 0.25, 0.5, 1.0, and 2.0 m, respectively. However, paddy management results in the development of pedogenetic horizons that are specific to paddy soils. Therefore, we refined the model structure of surface soil (down to 25cm) into three different zones: below the standing water layer (above soil profile), there are partly oxic zone (0–5cm), the upper part of the anthraquic horizon (5–15cm), and the lower part of the anthraquic horizon (15–25cm), respectively (Figure 4.1) (Kögel-Knabner et al., 2010).

Second, we incorporated the major microbial-driven N-cycle processes into the model structure, namely, anaerobic ammonium oxidation and nitrifier denitrification. The anaerobic ammonium oxidation (ANAMMOX) process is an important N loss pathway in rice-paddy soil, although its direct contribution to N_2O production and emissions is limited (Nie et al., 2019; Zhu et al., 2011). Mediated by anammox bacteria within the *Plantomycetes* phylum, ammonium (NH_4^+) is oxidized by nitrite (NO_2^-) to N_2 under low oxygen availability conditions. We used the Michaelis-Menten function to describe the relationship between NH_4^+ concentration and ANAMMOX rate ($Ranammox$) using the following equations:

$$Ranammox = V_{anmmax} \cdot \frac{anvf \cdot [NH_4{}^+]}{K_{NH4} + anvf \cdot [NH_4{}^+]} \cdot exp^{-anvf \cdot [NO_3{}^-]} \cdot f_{temp} \cdot f_{pH} \tag{3}$$

Where V_{anmmax} is the maximum ANAMMOX rate; $anvf$ is the size of anaerobic balloon of the soil profile; $[NH_4{}^+]$ and $[NO_3{}^-]$ indicate the concentration of NH_4^+ and NO_3^-, respectively; K_{NH4} is the half-saturation coefficient of NH_4^+ (Shan et al., 2018).

Nitrifier denitrification is a key N-loss pathway under anaerobic conditions that reduces nitrite by ammonia-oxidizing bacteria (AOB) in sequential reactions. This process is favored under low-oxygen, low-carbon, and low pH conditions and significantly contributes to N_2O production in rice-paddy soils. Based on the experiments by Kool et al. (2011) and Zhu et al. (2013), the following equation was applied to describe nitrifier denitrification rates:

$$R_{NOx} = V_{NOxmax} \cdot B_{AOB} \cdot \frac{[NO_x]}{K_{NOx}+[NO_x]} \cdot f_{temp} \cdot f_{pH} \cdot f_{wfps} \quad (4)$$

where R_{NOx} denotes the reduction rate of NOx by AOB and the V_{NOxmax} represent the maximum NOx reduction rates (i.e., 0.01, 0.01, and 0.0053 for NO_2^-, NO, and N_2O, respectively); B_{AOB} indicates the biomass of AOB (gC m^{-2}); K_{NOx} and $[NO_x]$ are the half-saturation coefficient of NO_x and soil concentration of NO_x (kg ha^{-1}), respectively.

Finally, the model descriptions associated with the gases exchange processes between the paddy soil and the atmosphere, was improved. Rice and other hydrophytes develop aerenchyma under an inundation environment to facilitate the gas transport between the atmosphere and rhizosphere. In the presence of flooding water, a large proportion of N_2O is emitted by rice plants. The solubility of N_2O for standing water is consistent with that of soil solutions (i.e., 0.5 g L^{-1}) in original model. The model structure of Zhu et al. (2014) and Song et al. (2020) were adapted to estimate the rice plant-mediated N_2O emissions ($PMTN_2O$, mgN m^{-2} day^{-1}):

$$PMTN_2O = D \cdot \varepsilon(z) \cdot \frac{Dif\_N_2O}{z} \quad (5)$$

where $\varepsilon(z)$ denote the plant aerenchyma factor at soil depth z, which is based on the cross-sectional area of root endings per root biomass (0.085 m^2 kg^{-1}), specific leaf area (20 m^2 kg^{-1}) as well as model estimated root biomass (gC m^{-2}) and leaf area index (m^2 m^{-2}). $Dif\_N_2O(z)$ is the N_2O deficit between the soil profile and the atmosphere (mgN m^{-2}) and z represents the depth of the soil layer.

The existence of oxic and partly oxic zones in paddy soil results from the oxygen released from the grown rice-root systems (Frenzel et al., 1992; Kögel-Knabner et al., 2010). This aerobic niche of the soil is one of the major hotspots for biogeochemical processes, including nitrification (Li et al., 2007). A simple linear relationship was applied to root biomass to estimate the partial pressure of soil oxygen in the first paddy layer.

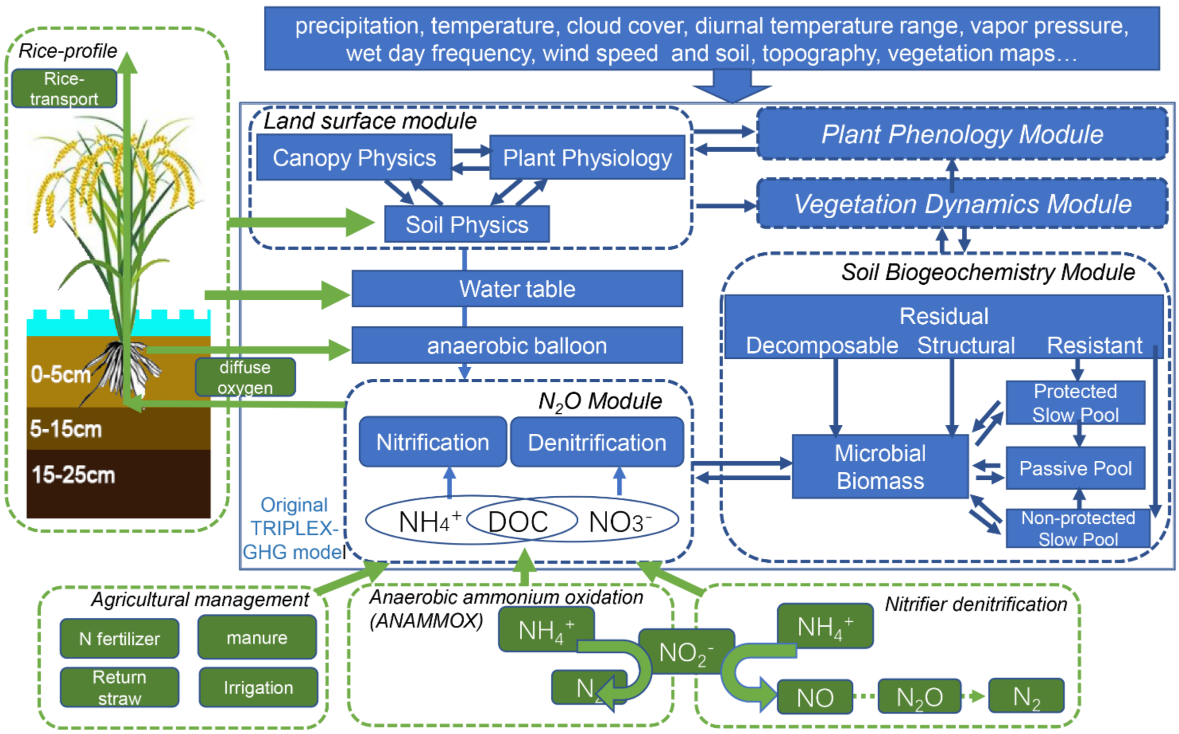

Figure 4.1 Schematic representation of the key processes of rice-based ecosystems integrated into the original TRIPLEX-GHGv2.0 model. The green boxes indicate the newly integrated management or biogeochemical processes, while the blue boxes indicate the structure of the original model.

4.4.2 Model calibration and validation

The improved model was applied to simulate rice-based N_2O fluxes at the site level to evaluate model performance. Overall, 152 independent field experiments from 32 published papers (see supporting material 2 Table 4.S1) were collected based on the following criteria: (1) measurement of N_2O flux must cover at least one rice-growing season; (b) the N_2O fluxes were observed using the static chamber method to minimize the influence of measurement across the sites; and (3) the water regime was reported in detail for model input. The collected sites covered major rice cultivation regions across the globe, and ~70% of the sites are located in eastern Asia (e.g., China).

For model simulations at the site level, site-specific environmental factors were used to drive model. Soil properties (e.g., pH, clay, sand content), and management practices (e.g., fertilizer application time, amount, and type; irrigation frequency and water regime; plantation and harvesting), were extracted from the corresponding literatures. As for daily climate information, we obtained the data from the Climatic Research Unit grided Time Series v4.3 (CRUTS) datasets to drive the model (1910—2020). However, if accessible, we applied daily recorded climate data from corresponding meteorological stations (mostly located in China, e.g., Figure 4.3, http://www.cnern.org.cn/data/initDRsearch) to fill the CRUTSv4.3 data in the experimental years as an alternative.

We randomly selected 10 sites to conduct an initial sensitivity analysis of the parameters to obtain the most sensitive parameters for the production of N_2O before testing the model. According to previous N_2O modeling studies, the coefficient of nitrification (COE_{NR}) and coefficient of nitrate consumption (COE_{dNOX}) are key parameters that drive the production and emissions of N_2O in natural and cropland ecosystems (Eq. 1,2) (Song et al., 2022; Zhang et al., 2017). Therefore, 10 major parameters were included that directly control nitrification, denitrification, nitrifier denitrification, and ANAMMOX to compare their sensitivities (Table 4.1). The model was run in a site-specific manner, and input with different environmental information. The parameters related to management (e.g., fertilizer NH_4^+ fraction) were excluded at this stage. We changed one parameter at a time by 20% while maintaining the others at a fixed default value to evaluate the responses of the N_2O emissions to the changed parameter (Pappas et al., 2013) based on the sensitivity index (SI, Supporting material 1). We set up the default values of the two highly sensitive parameters for N_2O emissions to fit the best model performance through trial and error (Liang et al., 2022; Zhang et al., 2017). For model evaluation, four long-term continuous measurements (≥ 2 years) covering both rice-growing, non-rice-growing, and fallow seasons and another four short-term (≤1year) observations were collected to test the model performance by comparing the modelled daily N_2O fluxes with the measured results obtained using the GetData Graph Digitizer software (v2.26; getdata-graph-digitizer.com). We used the index of agreement (D), root mean square error (RMSE), and coefficient of determination (R^2) to quantify model performances (Supporting information 1). Subsequently, we compared the modeled results with 152 observation records of cumulative N_2O emissions by calculating the daily mean N_2O emission rates (reported in the literature) during the experiment periods (Table 4.S1).

Table 4.1 Major parameters associated with N_2O production used in model validation.

Parameter	Explanation	Values	Types*	Unit	References
COE_{NR}	Nitrification rate coefficient	0.03	Upland cropland		(Zhang et al., 2017)
		0.5	Continuous flooding#		(Liang et al., 2022; Zhou et al., 2012)
		1.0	Intermittent flooding#		

COE_{dNO3}	Coefficient for consumption rate of NO_3^-	0.05	Upland cropland		(Song et al., 2022)
		0.5	Continuous flooding#		(Zhou et al., 2012)
		0.1	Intermittent flooding#		
V_{no2ox}	Maximum rate of nitrite oxidizing during nitrification	13.2	Upland cropland	kgN ha^{-1} $layer^{-1}$ d^{-1}	(Ma et al., 2022)
		9.8	Flooding		
K_{ox_NO2}	Half-saturation coefficient of NO_2^-	40	Upland cropland	mgN L^{-1}	(Ma et al., 2022)
		40	Flooding		
COE_{dNO2}	Coefficient for consumption rate of NO_2^-	1.0	Upland cropland		(Li et al., 2000; Song et al., 2022)
		2.0	Flooding		
COE_{dN2O}	Coefficient for consumption rate of N_2O	1.0	Upland cropland		(Li et al., 2000; Song et al., 2022)
		2.0	Flooding		
V_{anmmax}	Maximum ANAMMOX rate	0.187	Upland cropland	kgN ha^{-1} $layer^{-1}$ d^{-1}	(Shan et al., 2018; Yao et al., 2023)
		0.3992	Flooding		
K_{NH4}	Half-saturation coefficient of NH_4^+ for ANAMMOX	6.3	Upland cropland	mgN L^{-1}	(Nie et al., 2019; Shan et al., 2018)
		6.3	Flooding		
V_{NO2max}	Maximum consumption rate of NO_2^- during nitrifier denitrification	2.4	Upland cropland	kgN ha^{-1} $layer^{-1}$ d^{-1}	(Ma et al., 2022)
		2.0	Flooding		
K_{nid_NO2}	Half-saturation coefficient of NO_2^- for nitrifier denitrification	1.4	Upland cropland	mgN L^{-1}	(Ma et al., 2022)
		1.4	Flooding		

*Except for the two important parameters COE_{NR} and COE_{dNO3}, other parameter values were constant for intermittent and continuous flooding conditions but different with aeration.

#The differentiated parameter values for COE_{NR} and COE_{dNO3} are based on the divergent ammonium consumption (nitrification) and nitrate reduction (first step of denitrification in chain-reaction) rates under different water management regimes (Zhou et al., 2012).

4.4.3 Simulation scenarios designs

Generally, rice-based ecosystems can be classified into three major categories based on the different water regimes applied during the rice-growing season: continuous flooding rice-paddies, intermittent flooding rice-paddies, and dryland rice (rarely found). With respect to the geographic distribution of rice-paddies, it was simply assumed that all irrigated rice fields were assumed to be under the intermittently flooded management regime, because the associated irrigation equipment offers opportunities to freely drain and reflood paddies. In contrast, the flooding conditions of rainfed rice after the initial flooding were dependent on the natural water balance. The model designs for rice management practices were based on the global rice crop calendar and conventional farmers practices. For all rice paddies, the field is flooded for seedling transplanting at the one day before the start of the growing season (dependent on climate conditions), and is drained at 10 days before harvesting (Linquist et al., 2015; Wang et al., 2021). Meanwhile, midseason aeration only occurs once per rice-growing season for the intermittent flooded rice-paddies and lasts 7–10 days after being flooded for 30 days since the start of growing season (Li et al., 2011; Ma et al., 2013). No midseason drainage is conducted for rainfed rice-based ecosystems. Basal, tiller, and panicle fertilizer were applied 1 day before transplanting, 1 week after transplanting, and 1 week after the jointing stage (ratio of each application, 5:3:2), respectively (Z. Wang et al., 2020; Zeng et al., 2012).

Global simulations were conducted at a spatial resolution of 0.5 × 0.5° latitude/longitude from 1860–2020 using a high-performance computer system. The model simulation underwent an initial 300-year spin-up procedure driven by the multi-year averaged historical meteorological data to reach a state of relative equilibrium in the soil carbon and nitrogen pools before the analysis. For the period 1860–1910, the multi-year average climate data (1910—1920) were used. Subsequently, since 1910, the following nine scenarios were designed to simulate the spatiotemporal variation pattern of N_2O emissions from rice-based ecosystems globally and were used to allocate the total emissions to different driving factors (Table 4.2): SH0 represented the baseline estimate; SH1 represented the multifactor simulation with all driving data to obtain the best estimation of historical rice-based N_2O emissions; SH2 and SH3 quantified the contribution of the application of chemical fertilizer and manure to total emissions by subtracting with the SH1; While SH4 and SH5 estimated the interactive effects of different N inputs; SH6 and SH7 assessed the effects of the increasing irrigated rice area with or without fertilization; SH8 and SH9 quantified the effects of climate change and increased atmospheric CO_2 concentration on rice-based N_2O emissions. This study does not account for the effects of land use changes on direct N_2O emissions from rice-based ecosystems due to the model's lack of a comprehensive land-use module

Analysis of the modeled results was all processed by R software (version 4.3.1) using the packages "ncdf4", "raster", "terra", and "ggplot2".

Table 4.2 Scenario designs of the simulation experiments to attribute changes in N_2O emissions to different driving factors.

Scenario ID	Changing variables					
	Climate	CO_2	Irrigation	N deposition	Manure	Fertilizer N
SH0, Reference run	M1910–1920#	1910	1910*	1910*	1910*	1910*
SH1, Multifactor	1910–2020	1910–2020	1910–2020	1910–2020	1910–2020	1910–2020
SH2, No fertilizer	1910–2020	1910–2020	1910–2020	1910–2020	1910–2020	1910*
SH3, No manure	1910–2020	1910–2020	1910–2020	1910–2020	1910*	1910–2020
SH4, No N application	1910–2020	1910–2020	1910–2020	1910–2020	1910*	1910*
SH5, No N deposition	1910–2020	1910–2020	1910–2020	1910*	1910–2020	1910–2020
SH6, No irrigation	1910–2020	1910–2020	1910*	1910–2020	1910–2020	1910–2020
SH7, No irrigation&fertilizer	1910–2020	1910–2020	1910*	1910–2020	1910–2020	1910*
SH8, No climate	M1910–1920#	1910–2020	1910–2020	1910–2020	1910–2020	1910–2020
SH9, No CO_2	1910–2020	1910	1910–2020	1910–2020	1910–2020	1910–2020

1910–2020 indicates the forcing from 1910–2020 because the entire simulation period was included; #: mean climate value from 1910–1920; *: driving variable is fixed at the level of 1910 over the entire simulation period.

4.4.4 Input datasets

For global simulations, a series of spatial data sets was applied to represent environmental and management changes on a global scale. The climate data we used to drive the model were derived from the daily version of the Climatic Research Unit grided Time Series v4.3 (CRUTS) datasets and included daily mean air temperature, precipitation, relative humidity, wind speed, and air pressure covering from 1910 to 2020 (Harris et al., 2020). In context of soil information, the soil physical (e.g., sand, slit, and clay content) properties and pH data were based on the Digital Soil Map of the World (FAO, Reynolds et al., 2000). The soil organic C (SOC) data and soil C:N ratio data were adopted from the global soil dataset (IGBP-DIS;2000) as reference to constrain the model, thereby preventing imbalanced soil C and N status under disturbances. Topographic information was based on digital elevation model (DEM, 1km; https://lta.cr.usgs.gov/GTOPO30). Regarding historical atmospheric N deposition (NH_x and NO_x), outcomes from the International Global Atmospheric Chemistry (IGAC)/SPARC Chemistry-Climate Model Initiative (CCMI) were used.

All agricultural management information was based on published datasets (from 1910 to 2020), which were successfully applied in global modeling studies (Ito et al., 2018; Tian et al., 2019). The amount (kgN ha^{-1}) and properties (NH_4^+:NO_3^-) of the chemical N fertilizer application data were obtained from the History of anthropogenic Nitrogen inputs (HaNi) dataset (Tian et al., 2022), which incorporates the information provided by the International Fertilizer Association country-level inventory, crop-specific N fertilizer use rates, major crop calendar, and FAOSTAT fertilizer types. The manure application data were also derived from HaNi dataset, while the manure chemical properties (e.g., C:N ratios, inorganic N proportion etc.) were based on our previous studies and model descriptions (Song et al., 2023; Song et al., 2022). The historical geographic distribution of rice-based ecosystems was obtained from the Land-Use Harmonization dataset (LUH2, flooded C3 crops) (Hurtt et al., 2020). The History Database of the Global Environment (HYDE 3.2) was used to attribute rice-ecosystems into rainfed rice-paddy and irrigated rice-paddy by integrating the FAO's category "area equipped for irrigation" (Klein Goldewijk et al., 2017). The decisions of rice cropping seasons are largely inconsistent across the globe, which constrained the applications of process-based models' estimations at large scales (Tian et al., 2018). To overcome this, a global spatial rice crop calendar, RiceAtlas, was employed to define the total number, start and end dates of rice-growing seasons, thus, considering the water regimes and timing of fertilizer applications of rice paddies each year (see section 2.5) (Laborte et al., 2017). Considering the management experience and previous modeling studies (Wang et al., 2021; Zhang et al., 2016), maximum two rice-cropping seasons per year was chosen for current study to prevent unrealistic situations. All datasets were transformed into the same spatial resolution at 0.5×0.5° using the ArcMap software.

4.5 Results

4.5.1 Parameter sensitivity and model validation

A sensitivity analysis revealed large variations in the sensitivities of modeled N_2O to model parameters (Figure. 2). Most parameters showed a non-unique effect on the N_2O emissions from the different rice-paddy sites. COE_{NR} and COE_{dNO2} exhibited consistent positive effects; COE_{dNO3}, COE_{dN2O}, and V_{anmmax} mostly presented negative effects; and other parameters had non-significant effects. Overall, the coefficient of nitrification (COE_{NR}) was the most sensitive parameter that is directly associated with microbial N cycles (SI = 1.56) and controls the consumption of NH_4^+ by nitrifiers.

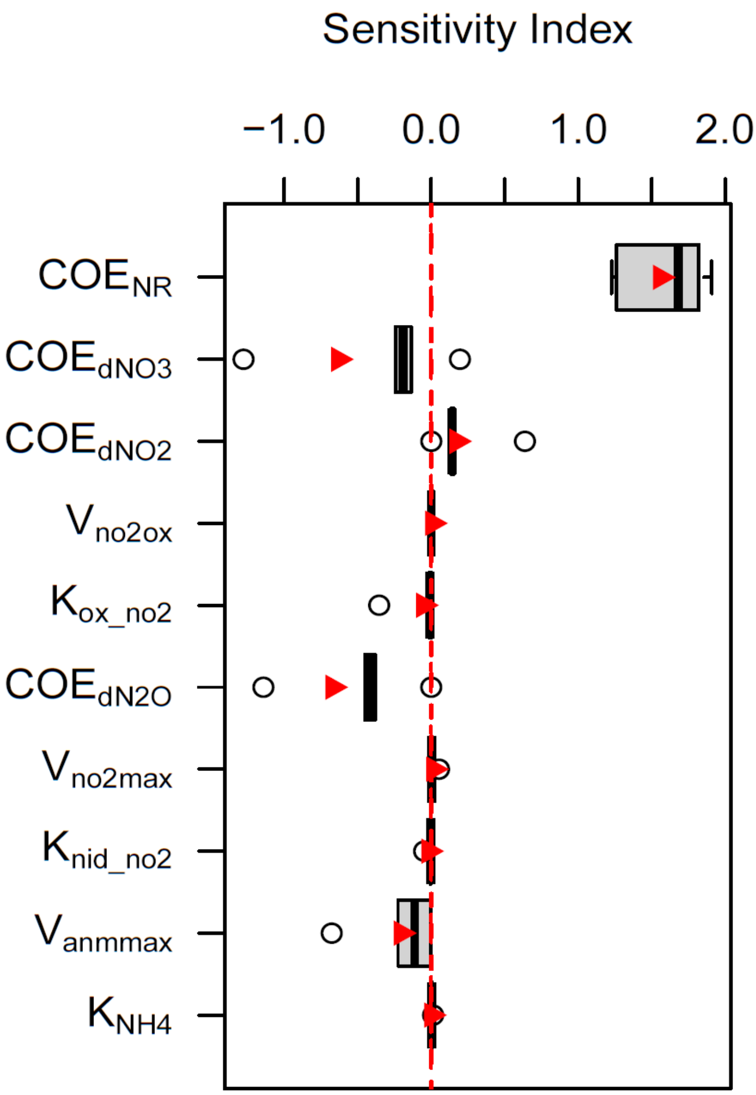

Figure 4.2 Sensitivity analysis of different parameters (descriptions and default values of parameters are listed in Table 4.1). The closed red triangles indicate the mean sensitivity index value of the parameters, the dashed red line suggests the SI=0, and open dots indicate outliers.

Subsequently, the continuous long-term observed data from rice-based cultivation sites were compared with the modeled daily N_2O fluxes. Generally, the modeled results were consistent with the observations from selected sites under different management practices and environmental conditions. For the continuously flooded double-rice field located in California, USA, the improved model reasonably captured the seasonal variability in N_2O emissions (D = 0.74, RMSE = 0.52, R=0.58; Figure 4.3a). The emissions during the fallow seasons accounted for most of annual emissions. A good consistency was also found between the simulated and measured N_2O fluxes from rice-based cropping systems (e.g., single and double rice) in southern China, with different water regimes located in southern China. The responses of N_2O emissions to fertilizer application were well simulated for the continuous flooded rice and rapeseed seasons (D = 0.77, RMSE = 1.89, R=0.61, Figure 4.3b). The N_2O pulses induced by intermittent flooding practices were well estimated for the rice-wheat rotation system in Jiangdu County in China, contributing to the good model performance (D = 0.85, RMSE = 2.00, R=0.74, Figure 4.3c). Although the model well reporduced a general trend of the variation in N_2O fluxes from intensively managed rice-based croplands in Suzhou, discrepancies were observed because the N addition effects were occasionally underestimating during rice-growing seasons (D = 0.62, RMSE = 0.66, R=0.45 Figure 4.3d). More site evaluations (one-year measurements) are presented in the supporting material2 (Figure 4.S1).

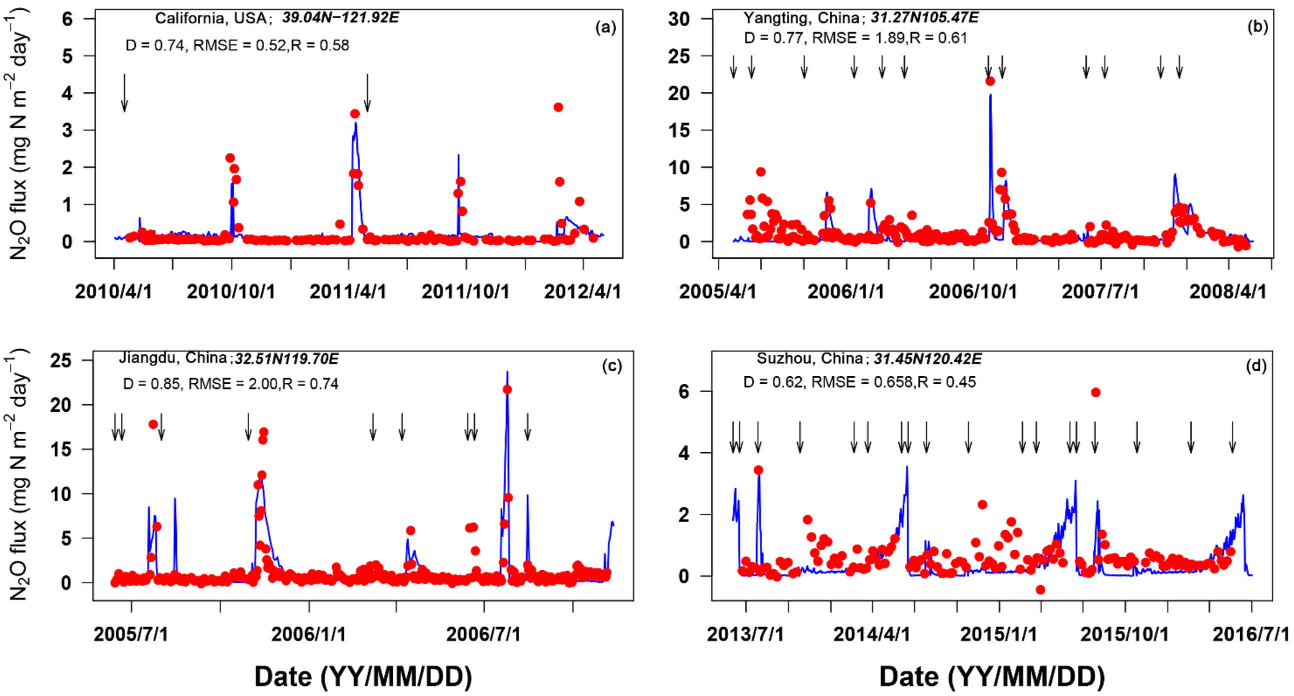

Figure 4.3 Comparison of modeled (blue lines) and observed (red dots) daily N_2O emissions from long-term continuous measurements. The model was driven by site-specific environmental variables and management information. Solid arrows indicate the timing of fertilizer (chemical or manure) applications. (a) and (b): continuous flooded rice (c) and (d): intermittent flooded rice.

We further evaluated the model performance by comparing the modeled daily mean N_2O emissions during the experiment periods with the data from 152 site measurements globally. Varying field measurement durations (i.e., covering the rice-growing season only, both rice and non-rice seasons) and water regime managements (i.e., continuous and intermittent flooding) were included (Table 4.1). Generally, the improved TRIPLEX-GHG model v2.0 explained 78% of the variances in the N_2O

emissions from rice-based ecosystems, and the regression result was close to 1:1 line over a wide range of daily mean N_2O emissions (slope = 1.001, Figure. 4). Results suggest that the model can simulate the dynamics of rice N_2O emissions on a global scale.

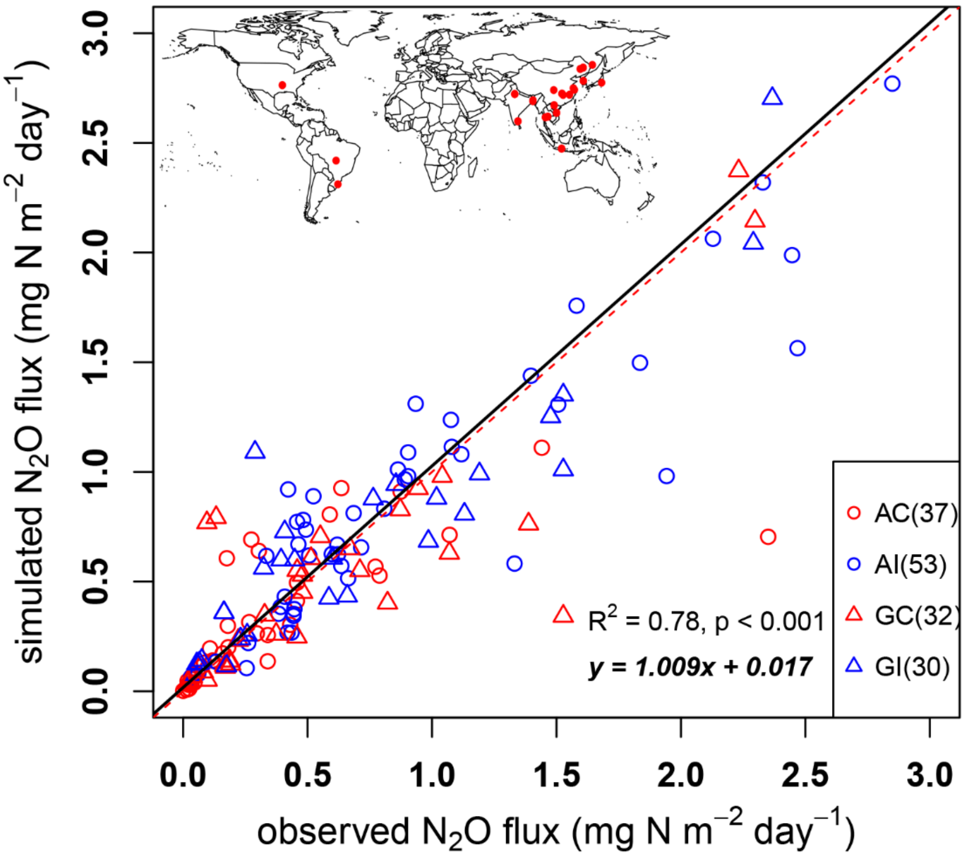

Figure 4.4 Comparison of modeled and observed N_2O emissions from 152 rice-based cropping systems during the experiment period. The red dashed line is the 1:1 line and the closed red dots on the map represent the locations of the included sites. AC: annual measurement (covers both the rice-growing seasons and non-rice seasons) for continuous flooding rice; AI: annual measurement for intermittent flooding rice; GC: measurement covers the growing season only for continuous flooding rice; GI: measurement covers the growing season only for intermittent flooding rice.

4.5.2 Temporal variations of N_2O emissions from global rice-based ecosystems

Based on the simulated results for scenario SH1, a strong temporal and spatial variations were observed in the N_2O emissions from global rice-based ecosystems during the historical period.

From 1910–2020, rice-based ecosystems N_2O emissions exhibited a general increasing trend (5.8 times) from 0.026 (±0.002, mean ± 0.5×sd) in the 1910s to 0.177±0.003 Tg N yr^{-1} in the 2010s, and it represents a linear rate of 0.00157 Tg N yr^{-2} ($p < 0.05$, $R^2 = 0.97$, Figure 4.5a). Specifically, the general increase was suppressed and shifted to a declining trend after 2010, which was probably driven by the decrease in fertilizer applications (Figure 4.S2). Irrigated rice-paddies showed increases in emissions from 0.021±0.002 to 0.148±0.003 TgN yr^{-1}, which accounted for 76.93% of the total emission during the study period, while the emission growth of rainfed rice-base fields showed a slower rising trend (0.00022 TgN yr^{-2}). Regarding simulated seasonal variations results, the monthly N_2O emissions from global rice-based ecosystems, which are mostly located in the North Hemisphere, showed a bell-shape pattern (Figure 4.5c-d). In the Northern Hemisphere, irrigated rice-based ecosystems soils showed significantly larger N_2O fluxes than rainfed rice soils, especially in May and June (0.29 and 0.30 kgN ha^{-1} $month^{-1}$, respectively). Similarly, in the Southern Hemisphere, the major rice-growing seasons had larger fluxes but had less variations for both rice-based ecosystem types. Generally, the rice-growing seasons, including both single and double cropping systems, accounted for 69.52±8.64 % of the total N_2O emissions in 1910–2020. The contributions of N_2O emission in non-rice-growing season showed strong spatial heterogeneities for different regions (Figure 4.S7).

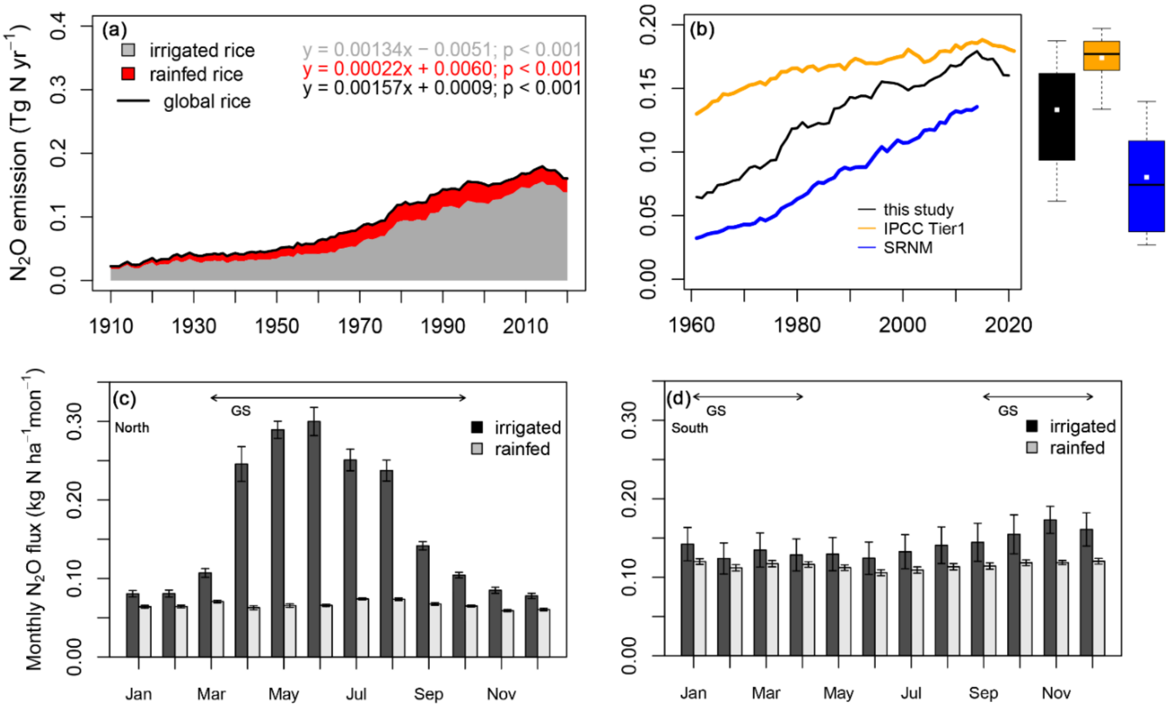

Figure 4.5 Annual total N_2O emissions from global rice-based ecosystems from 1910–2020 (a). Comparison with previous modeled results (b). Notably, the IPCC Tier1 method applied the same N input dataset as that used in this study, while the SRNM applied their aggregated high-resolution, crop-specific data on the N application rates from 1961–2014 as described in Wang et al. (2020). The white dots in the boxplot indicate the mean values. The seasonal variation

patterns (monthly) of rice-based N_2O emissions are also presented for the Northern (c) and Southern (d) Hemispheres. GS represents growing season, and horizontal arrows indicate the potential length of the rice-growing seasons (covering both single and double rice systems).

4.5.3 Spatial variations of N_2O emissions from global rice-based ecosystems

Simulated results suggested that the N_2O emissions from global rice-based ecosystems exhibit a strong spatial variation pattern depending on multiple factors, including variations in climate, number of rice-cropping seasons, and fertilizer applications. Irrigated rice ecosystems presented higher N_2O fluxes, which increased from 1.07±0.05 kgN ha^{-1} yr^{-1} in the 1910s to 1.82±0.09 kgN ha^{-1} yr^{-1} in the 2010s (Figure 4.6a). In contrast, N_2O fluxes from rainfed rice fields experienced lower increases (0.97±0.03 to 1.35±0.02) during the study period (Figure 4.6b). Consequently, southeastern China, northern India, and Southeast Asia were identified as the hotspots of rice N_2O emissions across the globe as a result of the large fertilizer application rates and broad irrigated area (Figure 4.S3). More than 3.0 kgN ha^{-1} yr^{-1} emissions were obtained from the rice-based ecosystems in the eastern coastal provinces of China (e.g., Jiangsu province), as well as in northern India, and they were mostly emitted from irrigated rice systems (Figure 4.S3, S4). As the most important and consistent hotspot of rice N_2O emissions, Asia had a rapid increase in emissions of 469.6% and contributed 81.9±0.014% of the total emissions during the study period, thus demonstrating the major role of Asia in rice-cultivation and N_2O emissions globally (Figure 4.S4).

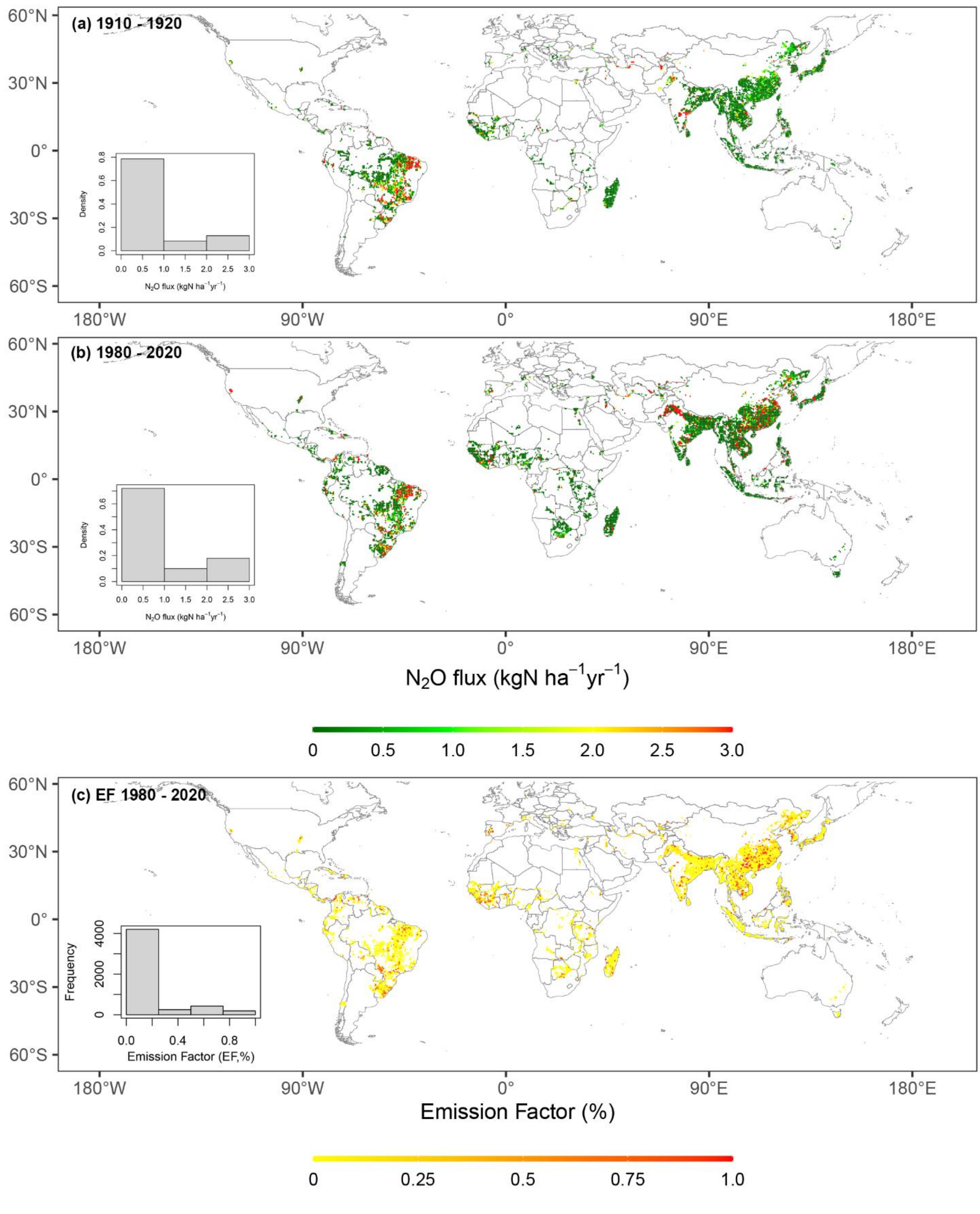

Figure 4.6 Spatial variations in the weighted mean N_2O emissions from rice-based ecosystems during (a) 1910–1920 and (b) 1980–2020, and (c) Emission Factor of N fertilizer (EF) during 1980–2020. Both the mean emissions and EFs are for the weighted rice-based ecosystem fraction, not grid cells.

More specifically, China contributed 33.35±2.26% of the net N_2O emissions from rice-based ecosystems between 1910 and 2020, followed by the Indian subcontinent (19.76±2.52%), Southeast Asia (17.46±2.15%), and East Asia (6.35±1.08%). Consistent with the global level, a general increasing trend in simulated rice-based N_2O emissions was obtained for major rice-cultivation countries and regions. During the study period, China experienced both the largest increases in total rice-N_2O emissions (from 11.01±1.07 to 62.61±1.35 GgN yr^{-1}), and weighted mean fluxes (from 0.72±0.06 to 3.26±0.07 kgN ha^{-1} yr^{-1}), representing a 4.5-fold increase from 1910 to 2010 (Figure 4.7a). Similarly, a rapid increase in rice-based N_2O emissions was observed in the Indian subcontinent, although the growth of N_2O fluxes was only observed after the 1970s (Figure 4.7b). Korea, Japan, and countries in Southeast Asia (e.g., Thailand and Indonesia) presented relatively low but consistently increasing N_2O fluxes during the study period (Figure 4.7c-d). In contrast, although large emission rates (>1.5 kgN ha^{-1} yr^{-1}) from South America (e.g., Brazil) and Africa (e.g., Liberia) were obtained through simulations (Figure 4.7e-f), the small rice cultivated area resulted in small contributions to historical N_2O emissions (4.50±1.14% and 6.19±1.08%, respectively).

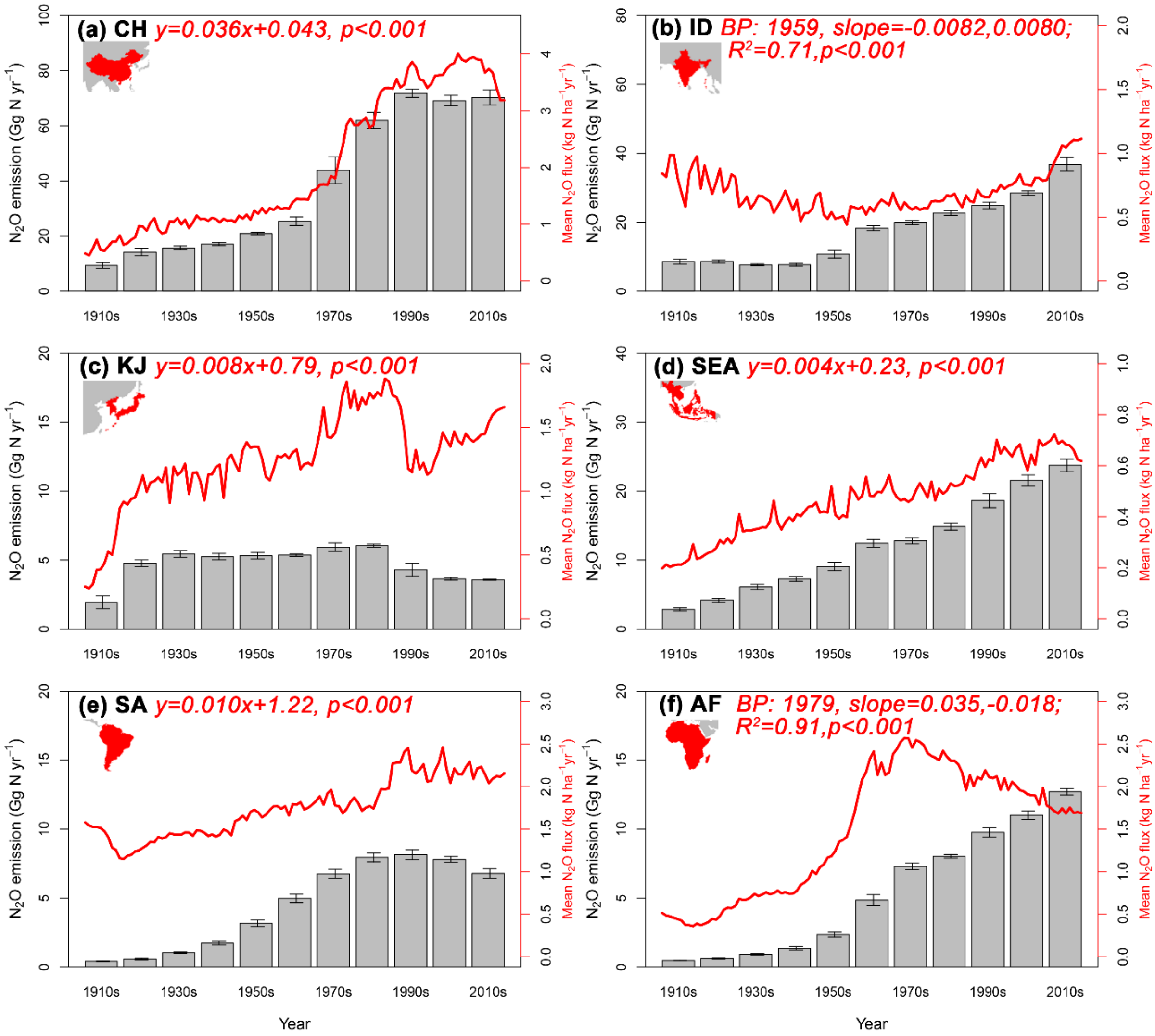

Figure 4.7 Regional variations in N_2O emissions and fluxes from 1910–2020. North America and Europe were not included because of the limited rice cultivation area. (a) CH: China; (b) ID: India, Nepal, and Bangladesh; (c) KJ: North, South Korea and Japan; (d) SEA: Southeast Asia; (e) SA: South America; and (f) AF: Africa. BP: break point produced by piece-wise regression.

4.5.4 Contribution of driving forces to total rice-based N_2O emission

The influence of multiple management practices such as chemical fertilizer applications, manure additions, and increased irrigation, are responsible for the overall global variation patterns (Figure 4.8).

We found that increased fertilizer application (FER) was the predominant contributor to the total increase in rice-based N_2O emissions based on the difference between SH1 and SH2, especially since the 1980s. The FER accounted for 26.48% (0.030±0.013 TgN yr^{-1}) of the historical rice-based N_2O emissions and 43.32% of emissions since the 2000s. As the most important driver, we found the sensitivity of rice-N_2O emission to N fertilizer, the weighted mean Emission Factors (EF), in 1980—

2020 also exhibit a strong spatial heterogeneity on a global scale (Figure 4.6c). A majority of rice-based ecosystem grid cells have EFs < 0.2% while ~10% of rice-distributed grids show EFs larger than 1.0%. In consistent with rice-N_2O emission hotspots, large EF values were mostly observed in southern China and southeast Asia. Such pattern is determined by multiple management and environmental factors. Particularly, both N fertilizer input rates and fertilizer chemical quality significantly affect variations in EFs of rice-based ecosystems globally (Table 4.S2). In contrast, manure, as an organic N source (MAN), was responsible for 0.018±0.004 TgN yr^{-1} emissions during the study period. The increasing atmospheric N deposition (NDP) also increased the rice-based N_2O emissions at an average rate of 0.017±0.006 TgN yr^{-1} (16.97%). By comparing the differences between scenarios SH1 and SH6, 9.78% of the N_2O emission growth could be attributed to increased implementation of irrigation in rice cultivation on a global scale. Moreover, this impact size constantly increased along with fertilizer application, corresponding to 0.027±0.002 TgN yr^{-1} in the 21st century. Notably, a strong correlation was detected for the effect of irrigation and fertilizer application without fertilizer input, and the increased irrigation had a limiting impact on rice-N_2O emissions globally (Figure 4.8b). Regarding the change in climates (CLM) and atmospheric CO_2 concentrations, climate changes showed a positive impact on rice-based N_2O emissions before the 1960s, but an overall negative response was observed in recent decades as a result of combined management effects. Increased CO_2 concentration showed a consistent negative effect on rice-based N_2O emissions during study period (at a rate of 0.0039±0.0016TgN yr^{-1}) by enhancing vegetation N uptake. Importantly, the contributions of the driving factors varied for different regions. Since the start of the 21st century, N_2O emissions generated by synthetic N fertilizer accounted for 52% and 9.7% of the emissions from China and India, respectively. However, for the Indian subcontinent, increased irrigated rice ecosystem was identified as the more substantial contributor to increases in N_2O emissions than the increased usage of N fertilizer (Figure 4.8c).

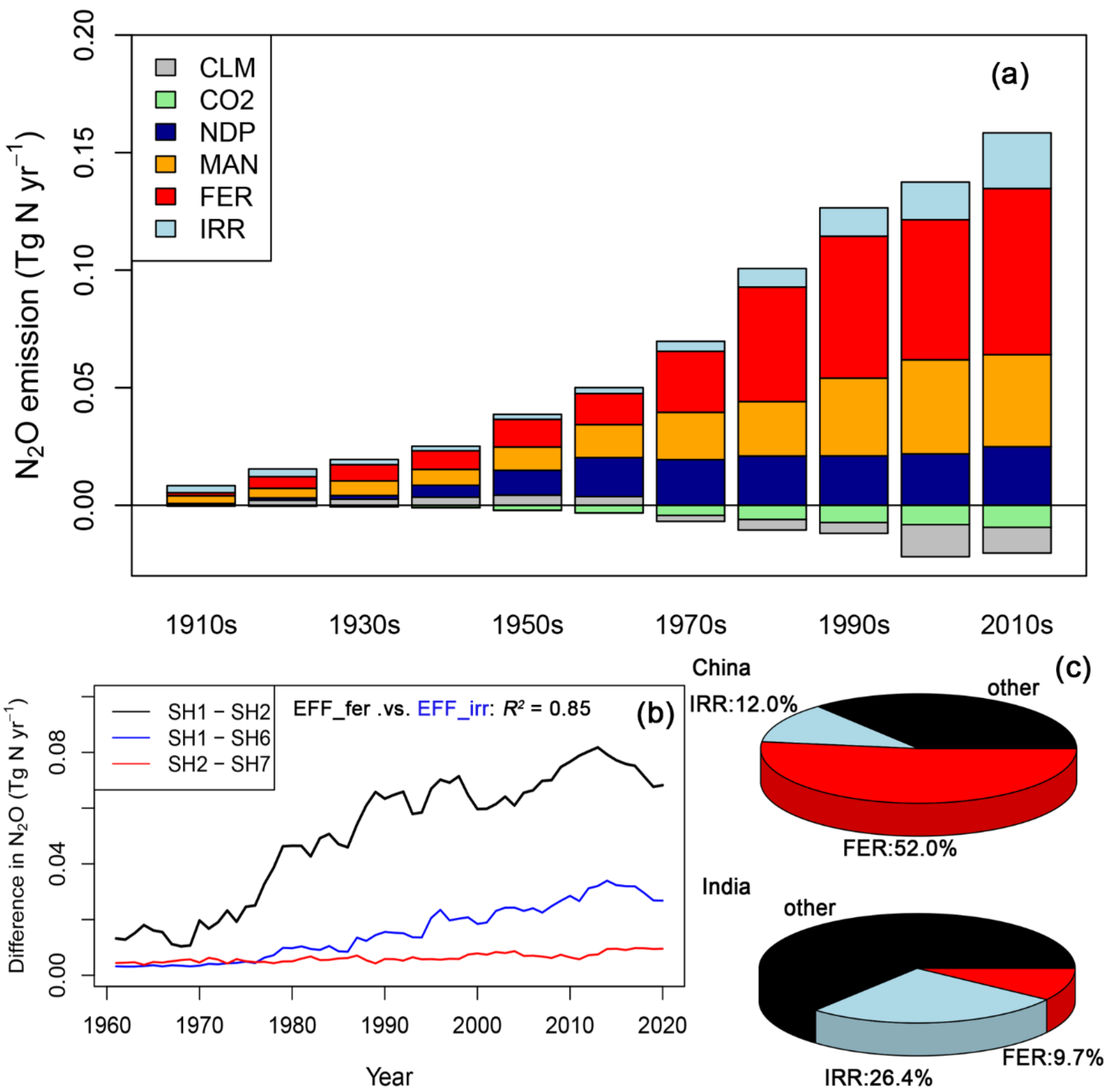

Figure 4.8 (a) Contributions of driving factors to decadal N_2O emissions from global rice-based ecosystems. CLM: climate (SH1-SH8), CO2: atmospheric CO_2 concentration (SH1-SH9); NDP: atmospheric N deposition, MAN: manure application (SH1-SH3); FER: N fertilizer application (SH1-SH2); IRR: expansion of irrigated area (SH1-SH6). (b) Coupled effects between fertilization and expanding irrigated area. (c) Comparison of the relative contributions of irrigation (IRR) and fertilization (FER) for the two most important emission sources, China and India.

4.6 Discussion

4.6.1 Global rice-based N_2O emissions compared with previous studies

Simulation results suggested that global rice-based ecosystems are responsible for a net N_2O flux of 0.104±0.024 TgN yr^{-1} during the study period (1910–2020). In particular, rice-based ecosystems have emitted 0.17±0.005 TgN yr^{-1} in the 21^{st} century which account for ~2% of the global terrestrial soil emissions in the most updated global N_2O budget for the most recent decade (Tian et al., 2020). This finding indicates that rice-based ecosystems, including those rainfed and irrigated, are a minor contributor to the global total N_2O emissions compared to upland agriculture (Akiyama et al., 2005; Tian et al., 2020).

We further compared our explicit estimation of rice-based N_2O emissions with those observed by previous modeling studies. Based on the most widely applied default Emission Factor (EF) values and the same N fertilization datasets used in this study, the IPCC Tier1 model obtained a mean of global rice N_2O emission level at 0.17±0.007 Tg N yr^{-1} from 1961–2020 (EF for all flooding regimes). The IPCC results generally overestimated the rice-N_2O emissions in recent decades (slight overestimation from the 1980s to 2010s) and during the historical period compared with the results obtained in this study (Figure 4.5b). This discrepancy is likely attributed to the overestimation of the background emissions (1.82 kgN ha^{-1} yr^{-1}, IPCC), which greatly vary with climate changes and land management intensifications (Kim et al., 2013; Xu et al., 2020). The recommended background emissions were based on observations conducted in the early 21st century, although these values are likely to be higher than those of the historical period owing to increasing N deposition and warming temperature (Aliyu et al., 2018; Q. Wang et al., 2020). Our estimated rice-based N_2O emissions were larger than those of recent modeling studies. Wang et al. (2020) utilized a data-driven upscaling model (SRNM), estimating 0.133 (±0.0008) TgN yr^{-1} emission for 2010 to 2014, which was lower than our obtained result (i.e., 0.168±0.02) TgN yr^{-1}. Despite the different spatial resolutions and N input rates, the SRNM model did not account for the influence of the accumulated input N from previous years (Q. Wang et al., 2020). Additionally, historical water management (i.e., legacy effect) may explain the resulting discrepancy (A. Lagomarsino et al., 2016). Another biogeochemical process-based model, DLEM reported rice-N_2O emissions were less than 0.1 TgN yr^{-1} in the 21st century; the discrepancy may be attributed to the structure of the DLEM, which assigns permanent flooding conditions during rice growth, resulting in underestimated rice-based N_2O emissions (i.e., < 2kgN ha^{-1}, Figure 4.1; Xu et al. 2020).

At the country level, Zou et al. (2009) reported emissions of 32.3 GgN yr^{-1} (Gg=10^9g) from rice-based soils in China in the 1990s by assigning different EFs based on the flooding regimes (i.e., F-D-F and F-D-F-M). Our estimated result for the growing seasons (50.12±1.08 GgN yr^{-1}) was approximately 55% higher for the same period in China, which was partly because our study differentiated fertilizer types into NH_4^+, NO_3^-, and organic manure; meanwhile, Zou et al. (2009) only incorporated the amount of N input. The estimated contribution of Indian rice-based ecosystems after the 2000s that we obtained is close to that by Pathak et al. (2005) (0.03–0.06 TgN yr^{-1}); however, it is 57% higher than that by a non-linear statistical model (18.0 GgN yr^{-1}) (Gerber et al., 2016) and only ~ 20% of the value estimated by Kritee (2018) (146.0 GgN yr^{-1}). The large discrepancy here may have been caused by the diverse assumptions of the flooding regimes (e.g., up to 90% and less than 30% continuous flooded areas in the study by Gerber and Kritee, respectively) and static soil moisture conditions applied in their simulations (Gupta et al., 2021).

Therefore, our historical estimation of global rice-based ecosystems is generally consistent with the range of existing estimations in the literature. We improved the quality of this estimation by conducting more extensive model validation and carefully considering the effect of different water management, N forms, and their contribution during non-rice-growing seasons.

4.6.2 Spatial and temporal variations and driving forces

The simulated results indicated that the strong spatiotemporal variations in rice-based N_2O emissions are strongly dependent on the difference in environmental factors and varying management types.

Consistent with the first hypothesis, the irrigated rice-based ecosystem contributed to most of the total rice N_2O emissions (Figure. 5a) and attributed the higher N_2O emission per unit of area in irrigated rice paddies to the growing N fertilizer application rate, frequent flood-aeration cycles induced by midseason drainage practices, and less annual precipitations. The weighted mean fertilizer application rate for irrigated rice ecosystems (0.28±0.044 kgN ha^{-1} yr^{-1}) was approximately two times larger than that for rainfed rice ecosystems (0.13±0.042 kgN ha^{-1} yr^{-1}) ($p < 0.001$, Figure 4.S6a). As the most important soil N source for agricultural soils, the significantly higher N fertilizer inputs stimulate substrate availability for nitrification and denitrification in irrigated rice soils (Davidson, 2009; Xu et al., 2020). Globally, major N_2O emission pulses were often observed during the midseason aeration period, which was well presented by our model (Figure 4.3) (Cowan et al., 2021; Li et al., 2011). In this study, irrigated rice soils were all under intermittent flooding management, which generates more N_2O than rainfed fields because of the longer aeration period, thus favoring nitrification during growing seasons (Zou et al., 2007). In comparison, the low N_2O flux from rainfed rice-based ecosystems is associated with climate factors in addition to lower N application rates. As these ecosystems are mostly distributed in subtropical and tropical climate regions (Northeast India, South east Asia, and Brazilian Amazon), significantly larger mean annual rainfall is provided as water supply (Figure 4.S6b). Therefore, owing to good water and temperature conditions (Figure 4.S6c), rainfed rice fields have standing water for most of the time during the rice-growing seasons (but not necessarily continuously flooded), as indicated by the water table balance module in this study. Local field studies confirmed the high water table level of rainfed rice (Bhattacharyya, Sinhababu, et al., 2013; Datta et al., 2009) and low rice-N_2O emissions in these regions (e.g., 0.093 kgN ha^{-1} for 155 days in Brazil and 0.45–0.64 kgN ha^{-1} $season^{-1}$ in India) (Datta et al., 2009; Metay et al., 2011), which is in line with our simulated data.

Our modeled results suggest that during the study period, China, the Indian subcontinent (mostly India), and Southeast Asia were the largest hotspots of global rice-based N_2O emissions. The different regional temporal variation patterns in rice-N_2O emission are highly dependent on N fertilizer application and flooding water management. As the largest rice-produce and consuming market, China accounts for 40.17±2.8% of the global rice-based N_2O emissions. This substantial contribution arises from the largest N inputs in the forms of fertilizer and manure across its vast rice cultivation area (26.79% of global total) (Figure 4.S2). The robust correlation between mean fertilizer input rates and averaged N_2O flux implies the dominant role of N fertilizer in controlling the significant increasing trend of rice-N_2O emissions in China at a rate of 0.68 GgN yr^{-2} 1910—2020 (Shang et al., 2019; Xu et al., 2020). In comparison, India and Southeast Asia, the second and third largest contributors to rice N_2O emissions, are collectively responsible for approximately half of China's emissions. The smaller N_2O fluxes in these regions, especially for irrigated rice during growing seasons (Figure 4.S7), is not only attributed to the less intensive N input but also water regimes since double seasons rainfed rice takes the majority until recent decades (Figure 4.S2) (Gaihre et al., 2015; Laborte et al., 2017). As a non-neglectable feature, non-growing seasons contribute substantially to the annual N_2O emission from rainfed rice, but large N_2O fluxes emitted from irrigated rice-based ecosystems during mid-season drainage constitutes a more important N_2O source than non-rice-growing seasons, despite the similar aeration conditions (Cowan et al., 2021; LaHue et al., 2016). The overall insignificant correlation between EF and length of non-growing period suggests that applied fertilizer might exert limited residual impact on non-growing seasons' emission from rice-based ecosystems. This is likely due to the rapid loss of added N in flooded rice-paddies via severe leaching, run-off, NH_3 volatilization, and denitrification processes (Weller et al., 2016; Zhou et al., 2014; M. Zhou et al., 2017). Thus, the transition to irrigated rice cultivation further resulted in a marked increase in mean rice-N_2O fluxes in these regions, especially since the 2000s (Figure 4.7) (Kritee et al., 2018; Weller et al., 2015). Meanwhile, reductions in the rice cultivation area in Korea, Japan and South America (primarily Brazil) drove the lower rice-N_2O emissions from rice-based ecosystems in these regions (Figure 4.7 and Figure 4.S2). However, such effects were neglectable on a global level. Interestingly, the combination of the overall low N application rates (< 4 kgN ha^{-1} yr^{-1}, Figure 4.S2f) and a pronounced decrease in NO_3^- fraction of fertilizer (Figure 4.S8) may be responsible for the declining mean rice-N_2O flux in Africa after the 1980s (significant correlation between EF and fertilizer NO_3^- fraction, $r = 0.11$, $p < 0.001$, $n=4016$) even though with rapidly increasing total fertilizer use and rice cultivation.

4.6.3 Role of N fertilizer applications and water regime management

Previous studies reported that flooding regime strategies and N fertilizer management might be predominantly responsible for rice-based ecosystem N_2O emissions, which implies different potential trajectories in GHG mitigation. For instance, Kritee et al. (2018) emphasized the central role of water management in regulating N_2O, especially considering the frequency of midseason aeration during the growing seasons. However, studies have also suggested that N management still plays a key role in contributing to N_2O emissions from rice fields (Yan & Akiyama, 2018). Our results showed the N fertilizer application represented the largest source underlying increases in N_2O emissions (~25%) during the study period, which supported the second hypothesis (Figure. 8).

As the most important driver, synthetic N fertilizer inputs were strongly correlated with the spatiotemporal variations in N_2O emissions and EFs from global rice-based ecosystems. In particular, decreased synthetic N fertilizer application was the predominant driver of the weakened growth trend and subsequent decline in total N_2O emissions from rice-based ecosystems after 2010 (Figure 4.5a, Figure 4.S2) (Shang et al., 2019). Fertilizer is the key N supply for soil microbial nitrification and denitrification in both the short and long term (Lan et al., 2015; Li et al., 2018). Previous studies might have underestimated fertilizer-induced N_2O emissions in rice-based systems. Thus, a weighted mean EF of paddy soils was obtained at 0.63%, which is generally in line with majority of field studies but was greater than 0.31% reported by IPCC Tier1 (Davidson, 2009; Kritee et al., 2018; Shcherbak et al., 2014; Yao et al., 2012; Zhang et al., 2010). There are two reasons for this phenomenon. Firstly, excluding the non-rice-growing seasons led to a significant underestimation (up to 40%) of the rice-based ecosystem contribution to the N_2O budget, as suggested by the simulated seasonal variations (Figure 4.5c-d). Numerous measurements have revealed the significance of the non-growing season to annual N_2O emissions from rice-based ecosystems (Bhattacharyya, Nayak, et al., 2013; LaHue et al., 2016; Zhou et al., 2014). The rice-paddy EF calculated from whole-year measurements can be 30% larger than that of growing seasons-only measurements, indicating that external N additions not only promotes N_2O emissions during rice-growing seasons but also enhances N_2O fluxes during non-rice and fallow seasons (Shang et al., 2020). Field and incubation studies revealed that the enrichment in mineral N and increased abundance of nitrifiers (e.g., ammonium-oxidizing archaea) (L. Wang et al., 2019) and denitrifier communities (Liu et al., 2012), especially in the surface soil layer, and are responsible for large paddy soil N_2O concentration and emissions after the fallow drainage (Yang et al., 2016). Second, considering the effects of changing input N amounts and forms in this study, significant positive correlation was obtained between EF and N fertilizer application rates (Table 4.S2), supporting the non-linear response of N_2O emission to N inputs (Shcherbak et al., 2014; Yao et al., 2012). Moreover, fertilizer NO_3^- fraction show a significantly negative effect on EFs for global rice-based ecosystems. On the one hand, both field experiments and our model sensitivity analysis confirmed that nitrification (requires NH_4^+) is the most important N_2O contributor in rice-based ecosystems (Malla et al., 2005; Yang et al., 2017), which is different in upland soils where NO_3^- has a greater potential to emit N_2O as the direct substrate for denitrification (Das & Adhya, 2014; Lan et al., 2015). On the other hand, added NO_3^- is highly mobile and likely to be rapidly removed from rice-based ecosystems due to enhanced denitrification and leaching processes under oxygen-depleted, water saturation conditions (Kögel-Knabner et al., 2010; Silver et al., 2001).

However, the magnitude of N fertilizer effect displays notable regional variations. Specifically, in Indian subcontinent, N fertilizer application only account for ~9.7% rice-based N_2O emissions. Moreover, the increasing N fertilizer rate during study period does not predominantly dictate the trends in both weighted mean N_2O flux and mean EF (Figure 4.7b, Table 4.S3). Instead, there are significantly negative correlations between these metrics and the fraction of rainfed rice-based ecosystem ($r = -0.55$ and -0.68, respectively; $p < 0.001$). The large rainfed rice-field area (~60%) takes primary responsibility for the different patterns of overall contribution and mean N_2O flux variations in India due to the less sensitivity of N_2O emission to N additions under prolonged flooding conditions of rainfed rice-based ecosystems (Table 4.S3) (Kritee et al., 2018). In agreement, our simulations also reflected that the increased rice irrigation had a significant positive effect on increasing global rice-N_2O emissions (Figure 4.8). The increased irrigation led to shifts between aeration and flooding conditions in rice-based systems, which favor the mineralization, nitrification, and incomplete denitrification processes to produce and emit N_2O (Figure 4.2) (Johnson-Beebout et al., 2009; Li et al., 2011; Verhoeven et al., 2019). In contrast, a previous study pointed out that without significantly increasing soil NO_3^- availability prior to flooding, the frequent changes in flooding conditions have limited effects on total N_2O emissions (Jørgensen & Elberling, 2012). Similarly, significant N_2O pulses were not detected in a number of the fertilizer-free treatments, despite fluctuations in water levels (Cowan et al., 2021; Islam et al., 2018; Kritee et al., 2018). Microbial N_2O production in paddy soils is mostly limited by substrates availability (i.e., inorganic N) owing to intensive run off and leaching (Hou et al., 2016; Verhoeven et al., 2019; Zhao et al., 2012). Thus, we conclude that the changing water regimes can act as a trigger to stimulate nitrification and denitrification only when soil nutrients are not N limited (Jørgensen & Elberling, 2012). This result has been confirmed by this study based on the comparable weighted mean N_2O fluxes of irrigated and rainfed rice ecosystems before the 1950s (Figure 4.S5) and without fertilizer application (Figure 4.8b).

Consequently, our study showed the dominant role of N fertilizer in regulating rice-based N_2O emissions compared with irrigation and environmental changes (discussion in supporting material 1). The quantity and quality of N fertilizer are also identified as the key factors for controlling the sensitivity of rice-N_2O emission responses to N addition. However, decoupling the impact of different flooding regimes with N fertilization is difficult. Co-management of water regimes and N fertilizer is recommended to mitigate N_2O emissions from rice-based ecosystems (Kritee et al., 2018).

4.6.4 Current limitations and future work

Although this model-based study improved the understanding of the dynamics of N_2O emissions from rice-based ecosystems on a global scale, uncertainties still exist because the results are influenced by the quality of input information, model structure, and parameter settings.

First and foremost, better global gridded datasets on crop-specific N input are crucial to accurately estimate the spatiotemporal heterogeneity of rice-based N_2O emissions, particularly regarding the key driver, anthropogenic N inputs (Xu et al., 2020). Current study used global N fertilizer and manure application data represent the crop-area-weighted average N fertilizer and manure rates in each grid cell (0.5°) (Tian et al., 2022) rather than crop-specific N input rates (e.g., Wang et al., 2020). This discrepancy could cause significant uncertainties in the estimation of N_2O emissions because different crop species have diverse N demands, influencing soil N availability for producing N_2O (Shcherbak et al., 2014). For example, commonly utilized N fertilizer application rates of single rice-based ecosystems in Northeast China (e.g., 150kgN ha^{-1} yr^{-1}, Table 4.S1, Chen et al., 2013) exceed those provided by the HaNi dataset that we employed in this study (e.g., ~100kgN ha^{-1} yr^{-1}). The prevalence of soybean cultivation in this region, which has a low N fertilizer requirement, leads to smaller averaged N application rate for the grid cells, consequently underestimates N_2O emissions. However, utilization of rice-specific N fertilizer application might introduce more uncertainty because of lack in crop rotation information, which is another limitation of the current study. For some regions with two cropping seasons, such as southern China and mid-India, rice-based rotation systems are widely accepted, meaning that after rice cultivation (as primary crop species), another crop (mostly upland crops such as wheat) can be grown. This practice results in significantly larger N_2O emissions compared with double rice-systems or rice-fallow systems because a longer soil aeration period favors incomplete denitrification and the growth of the second crop requires additional fertilization to produce and emit N_2O (Weller et al., 2016; Zhou et al., 2014; M. Zhou et al., 2017). In addition, different options of second crop have been proved to show varying effects on N_2O flux in rice-growing seasons (Xu et al., 2023). In the future, improved anthropogenic N input datasets with crop-specific and general rotation information at a fine resolution are required to better estimate rice-based N_2O emissions.

Regarding model structure, one major uncertainty source is the limited consideration and description of rice flooding regimes. Intermittent flooding practices can be further divided into flooding-drainage-flooding (F-D-F), flooding-drainage-flooding-moist without water logging (F-D-F-M), and alternative wetting and drying (AWD) practices (Zou et al., 2009). However, this study did not include AWD practices, which significantly increases the N_2O fluxes (Alessandra Lagomarsino et al., 2016; Oo et al., 2018), because they are difficult to simulate the randomly frequent flooding-drying transitions and inconsistent timing and duration of midseason drainage (Ma et al., 2013). In addition, the geographic distributions of these practices cannot be obtained on a large-scale basis because the water regime is determined by individual farmers, and has no clear global distribution patterns, unlike those for soil and climate (Wang et al., 2018). Moreover, negative N_2O fluxes have been reported in a few paddy soils (Berger et al., 2013; Shang et al., 2011) and some natural wetlands (Audet et al., 2014; Jørgensen & Elberling, 2012; Majumdar, 2013). Plus, indirect N_2O emissions are vital for rice-based ecosystems, possibly accounting for up to ~50% of annual budget (Xie et al., 2022). However, the mechanisms underlying these N_2O dynamics are not yet well understood yet but may be related to the depletion of soil N availability for denitrification (Wu et al., 2013), high content of SOC, such as in peatlands (Majumdar, 2013), and level of the wetland water table that restricts the diffusion of O_2 (Ye & Horwath, 2016).

Finally, the effect of land-use changes (LUC) associated with expansion of rice-based ecosystem on direct rice-N_2O emission remains unquantified for this study. Because current TRIPLEX-GHG model v2.0 is not equipped with a module that describes changes in soil properties and biogeochemical processes resulting from land-use transitions. LUC have major impacts on terrestrial N_2O emissions, especially for converting natural to agricultural lands (Meurer et al., 2016; van Lent et al., 2015). However, the magnitude of such effect is largely uncertain because when excluding anthropogenic N inputs, land-use changes exhibit divergent influences on soil N_2O fluxes globally (Tian et al., 2019; van Lent et al., 2015). Regarding rice-based ecosystems, studies have reported insignificant effects on soil N_2O emission after conversion of upland wet soils to rice-paddy through flooding, the commonest practice (Liu et al., 2020; Ye & Horwath, 2016). One explanation is that the seasonal flooding condition in most rice-based ecosystems promote mineral N loss by complete denitrification to N_2 under strict anaerobiosis (Peng et al., 2006; Zou et al., 2007). In contrast, loss of rice-based ecosystems (i.e., transformation of rice-paddy into upland ecosystems) has been observed to significantly enhance N_2O emission (L. Wu et al., 2017; Xu et al., 2022). Drainage exposes accumulated soil NH_4^+ to nitrification, thereby favoring nitrifier abundance and activity, stimulating production and emission of N_2O (Butterbach-Bahl et al., 2013; X. Wu et al., 2017). Given the doubling of global rice-field during study period, it seems that the expansion of rice-area might have limited contribution to N_2O emission. But the more frequent transitions between rice and upland crops, coupled with recent decreasing rice-cultivation area in eastern Asia, could potentially act as a crucial factor in inducing N_2O emission (Farquharson & Baldock, 2008; Zhang et al., 2020). These changes warrant further modeling to address the role of LUC (Farquharson & Baldock, 2008; Zhang et al., 2020).

Overall, constructing reliable N fertilizer application data, improving model representations on water management and land-use changes, and validating models using more available site-level observations are essential for reducing the uncertainty and improving the accurate estimation of rice-based ecosystem N_2O emissions in the future for sustainable agriculture (Xu et al., 2020).

4.7 Conclusion

To our knowledge, this study is the first attempt to explicitly quantify the spatiotemporal magnitude and sources of global rice-based N_2O emissions from 1910–2020 by carefully considering the heterogeneity in environmental factors and changes in detailed managements based on the rice-crop calendar, with an application of the biogeochemical process-based model TRIPLEX-GHG v2.0. The model was well improved and extensively validated globally by incorporating different management practices and key biogeochemical processes for rice-based ecosystems. Simulated results showed that total N_2O emissions from global rice-based ecosystems increased by more than five times from 1910 to present period (0.18 ± 0.003 TgN yr^{-1}). Notably, the importance of non-growing seasons' emissions to the annual global rice-based N_2O emissions (~30.5%) is emphasized in this study. Spatial variations suggest that the irrigated rice ecosystems play a vital role in N_2O emissions as compared to rainfed rice during the study period. China was identified as the largest source of rice-N_2O emissions, followed by the Indian subcontinent and Southeast Asia. Additionally, we found that synthetic N fertilizer application is the largest source of rice-based N_2O emissions, with an increasingly important role over time. However, increased irrigation of rice-based ecosystem areas was only responsible for 9.7% of the total emissions, and its extent highly correlated with the N fertilizer effect. These results highlight the importance of integrating emissions during non-growing seasons, the different effects of water regimes, and diverse N forms in the estimation. We concluded that the co-management of N fertilizer and flooding regimes is an effective approach for mitigating N_2O emissions from global rice-based ecosystems under global climate change.

4.8 Supplementary materials

4.8.1 Evaluation of model parameters and performances

The SI is calculated based on the following equation:

$$\mathrm{SI} = \frac{1}{n} \cdot \sum_{j=1}^{n} \left(\frac{(y_{2j} - y_{1j})/y_{0j}}{2 \cdot \Delta x / x_0} \right)$$

where n is the total number of months from 1961 to 2015 (because in our model, chemical fertilizer application started in 1961); j accounts for the number of months from 1961 to 2015; y_{0j} represents the jth monthly N_2O emissions with an initial parameter x_0; and $y_{2j}\ and\ y_{1j}$ are the N_2O emission values produced for $+\Delta x$ and $-\Delta x$, respectively. Δx was set as 20% of x_0.

The index of agreement (*D*), the root mean square error (*RMSE*), and the coefficient of determination (R^2) were used to evaluate our model's performance in daily time step, and the D-value and *RMSE* were calculated as follows:

$$D = 1 - \frac{\sum_{i=1}^{n}(S_i - O_i)^2}{\sum_{i=1}^{n}(|S_i - \bar{O}| + |O_i - \bar{O}|)^2},$$

$$RMSE = \sqrt{\frac{\sum_{i=1}^{n}(S_i - O_i)^2}{n}}.$$

Here, S_i is the ith simulated result corresponding to the number of observations; O_i is the ith observed value; and $\overline{O}$ is the mean of the observed values during the experimental period. D varies between 0 and 1, and is excessively sensitive to extreme values (Willmott, 1981). The model performance was considered to be perfect and unmeaningful when the D value was set to 1 and 0, respectively. The *RMSE* is the key value representing the difference between the simulated and observed values, and is significantly affected by the data units (e.g., mg N m^{-2} day^{-1} compared with kg N ha^{-1} day^{-1}).

4.8.2 Supplementary Figures

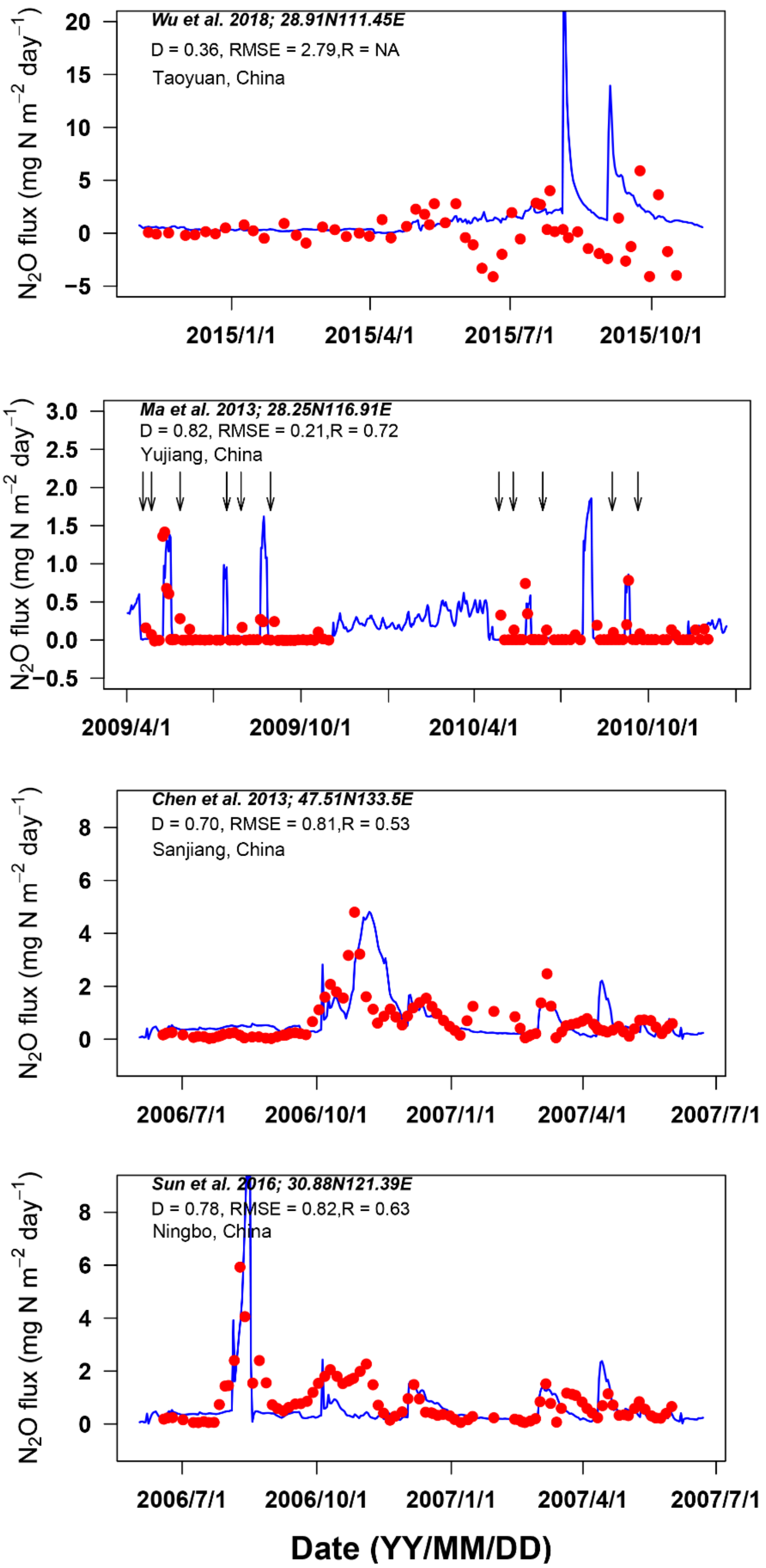

Figure 4. S1 Comparison of modeled (blue lines) and observed (red dots) daily N_2O emissions for short term (~1 year). The model was driven by site-specific environment and management information.

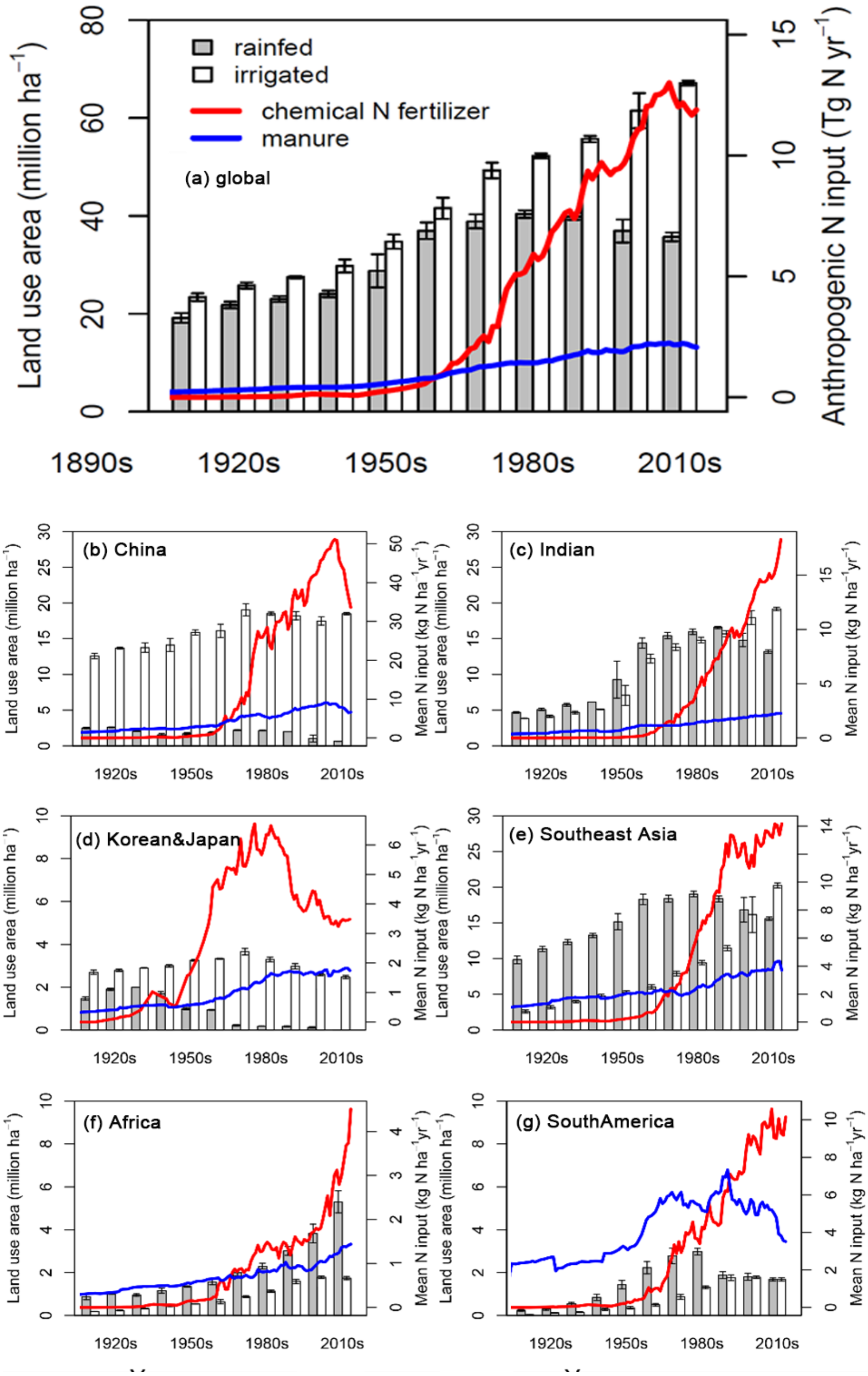

Figure 4. S2 Changes in irrigated and rainfed rice-based ecosystem area and the application rate of chemical fertilizer and manure. The land use change data were derived from LUH2.0 (Hurtt et al., 2020) and HYDE3.2 (Klein Goldewijk et al., 2017). While the N fertilizer datasets were obtained from HANI (Tian et al., 2022).

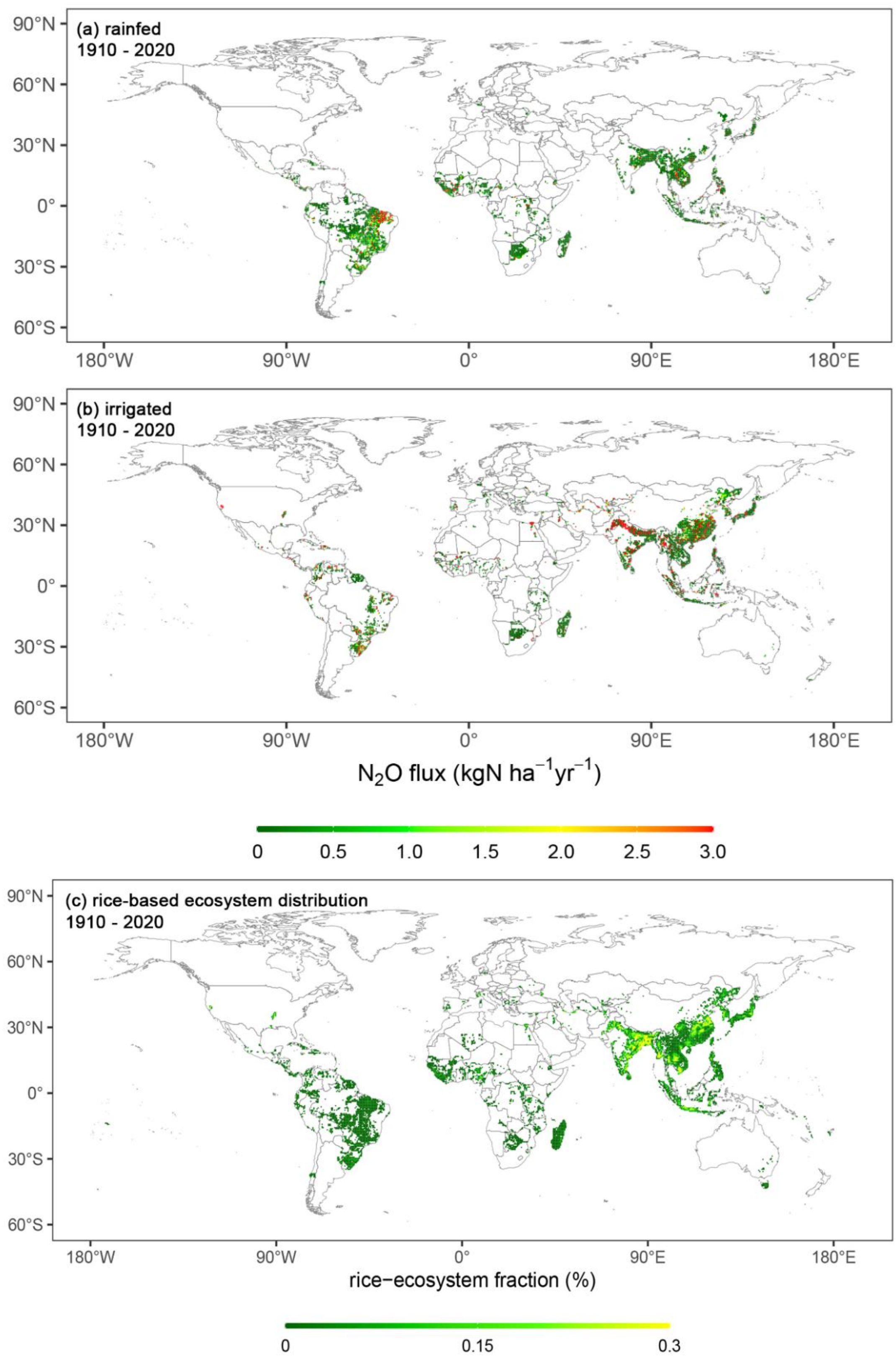

Figure 4. S3 Spatial pattern of mean N_2O emissions (not area weighted) from rainfed (a) and irrigated (b) rice-based ecosystems during 1910 – 2020 as a result of multiple environmental changes. The results are based on Multifactor simulation (SH1). (c) presents geographic distribution of all rice-based ecosystems during the study period.

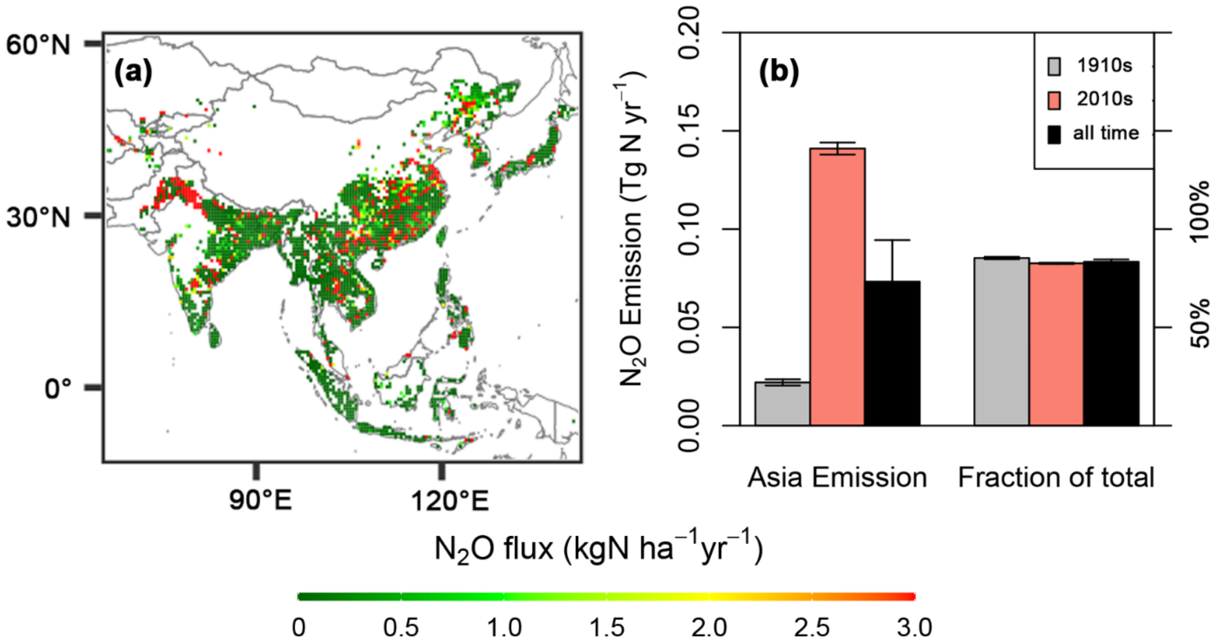

Figure 4. S4 (a) Spatial variations in the weighted mean N_2O emissions from rice-based ecosystems in Asia during 1980—2020; and (b) Quantification of the contribution (emission rate and proportion) of Asia to global rice-based N_2O emissions during the whole study period.

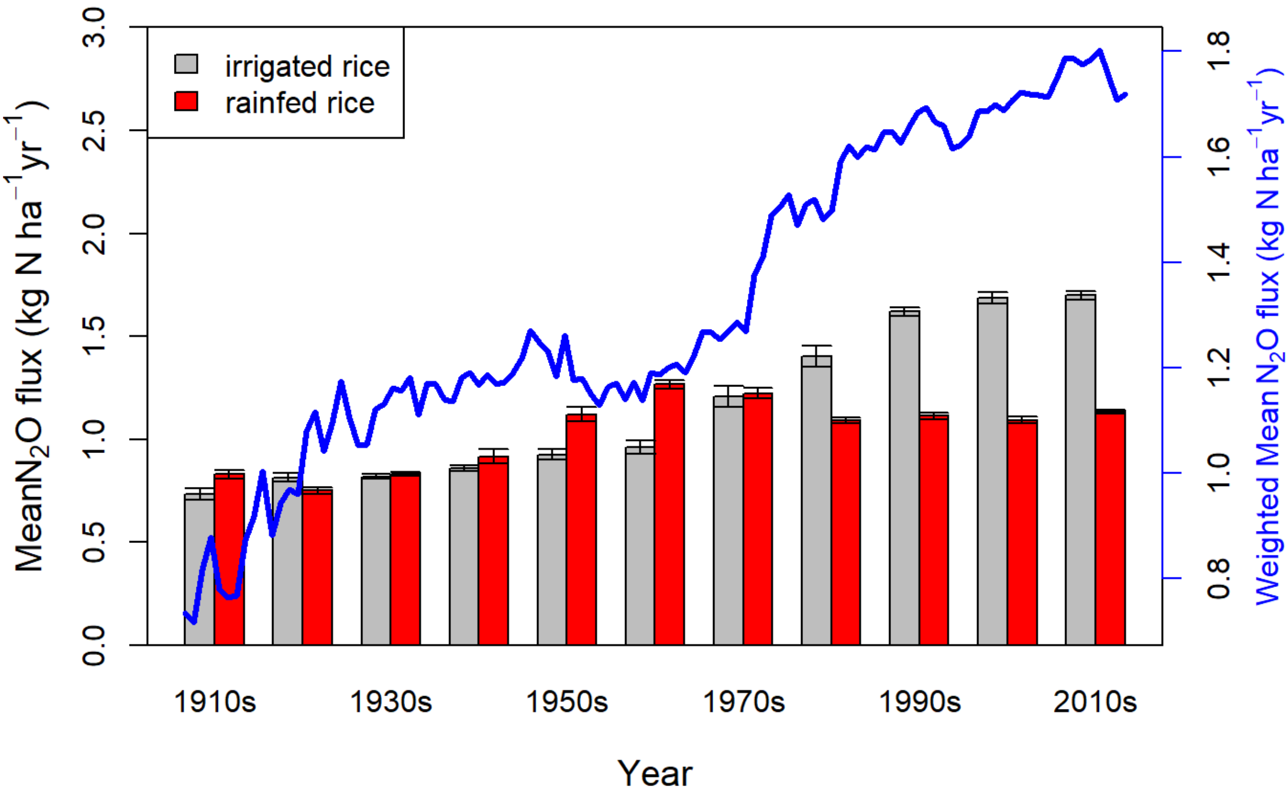

Figure 4. S5 Global weighted mean N_2O flux from rice-based ecosystems (blue line) and mean annual N_2O fluxes (mean±0.5standard division) from irrigated and rainfed rice ecosystems.

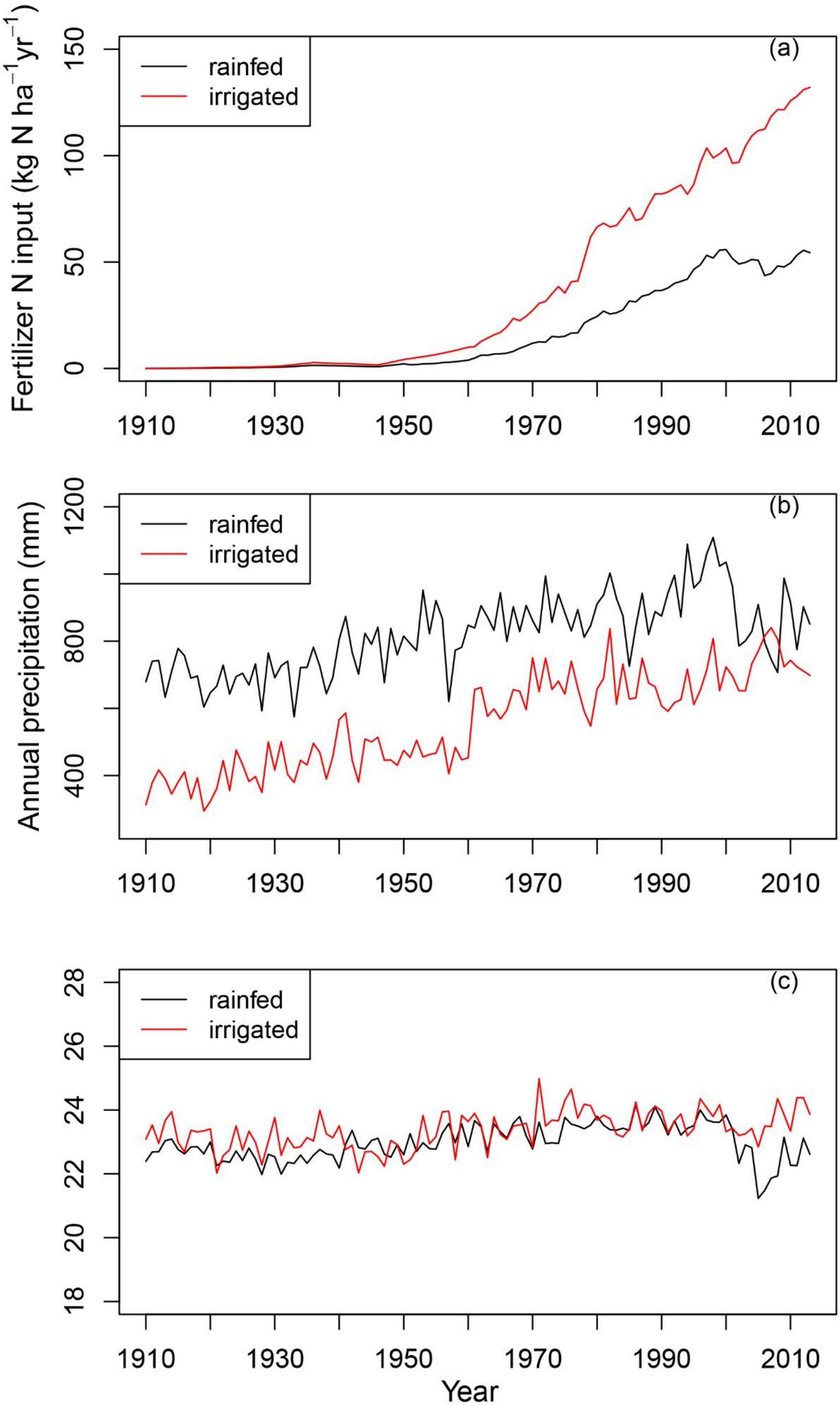

Figure 4. S6 Temporal variations of the weighted mean fertilizer N application (a), annual precipitation (b), and annual mean temperature (c) of rice-based ecosystems on a global scale.

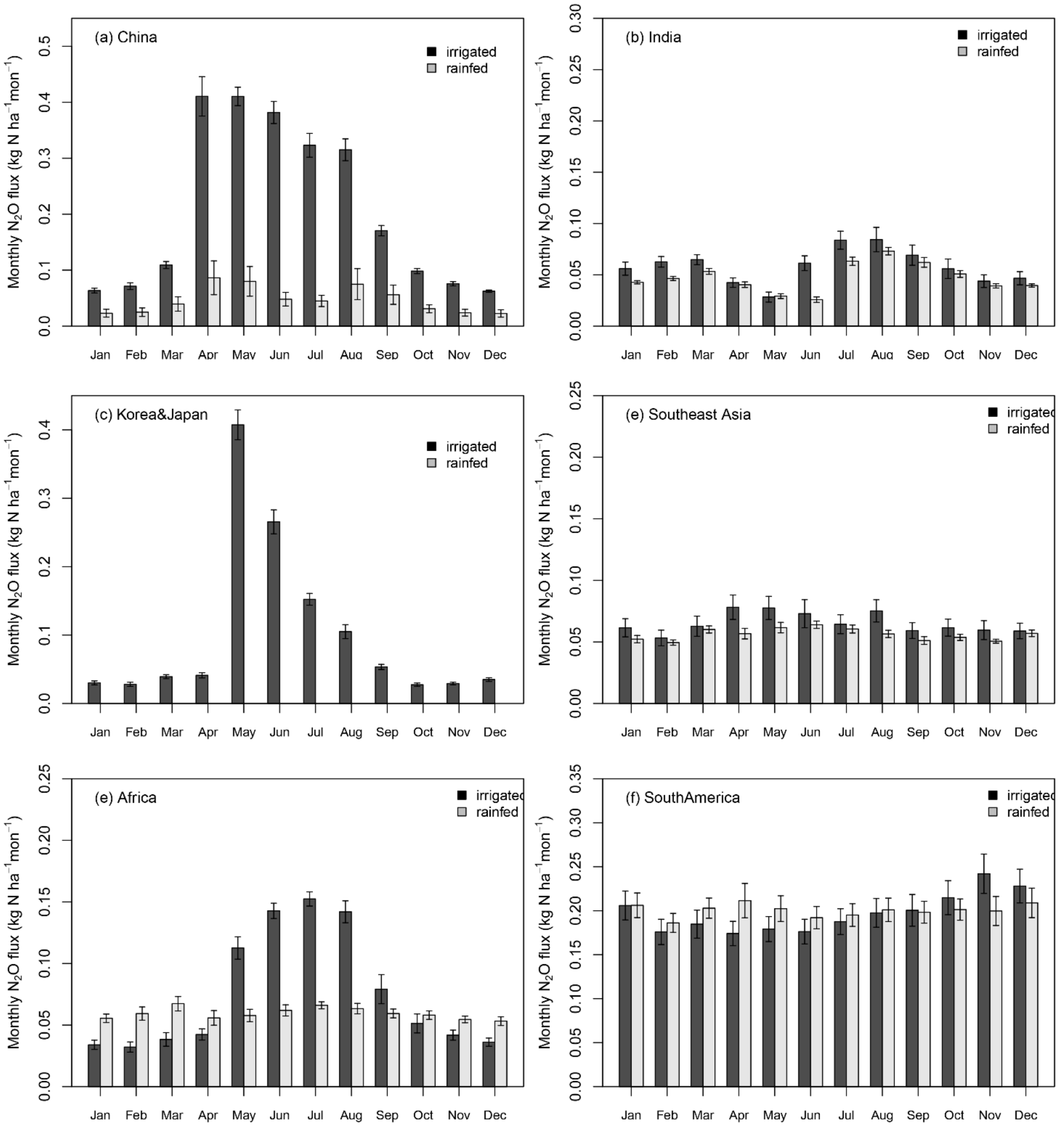

Figure 4. S7 Seasonal variation patterns (monthly) of rice-based N_2O emissions for different regions

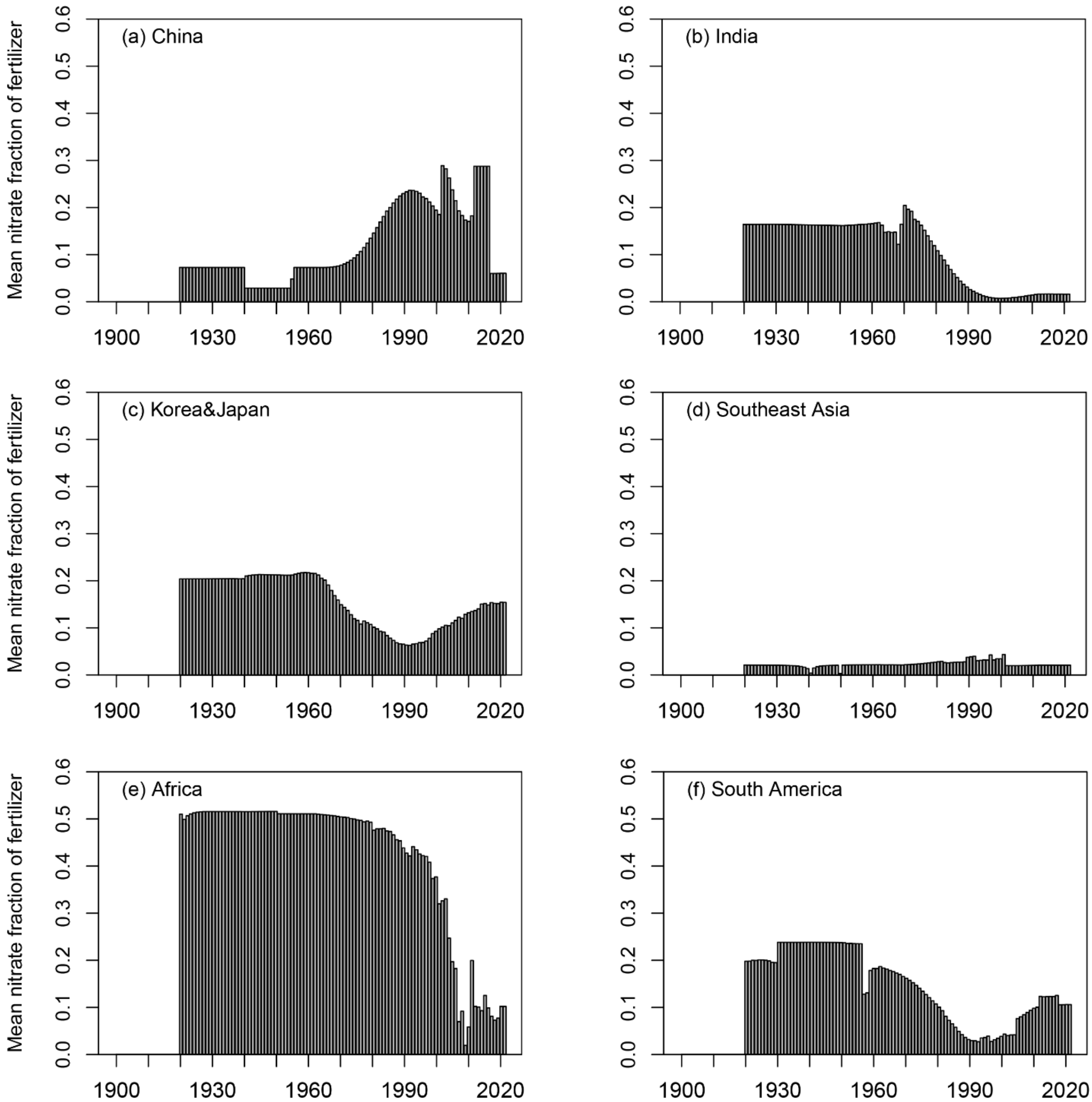

Figure 4. S8 Fraction of nitrate for applied N fertilizer in rice-based ecosystems for different regions.

4.8.3 Supplementary Tables

Table 4. S1 Site climate, environment, and management information for model validation. For the volume Duration, A and B indicate the experiment was conducted annually or just growing season only. For the flood category, C and D denote continuous and intermittent flooding, respectively.

Ref.	Lon.	Lat.	Country	Duration	Period	Prec, mm	Temp, °C	Clay, %	SOC, %	pH	N fer rate kgNha^{-1}yr^{-1}	flood	rotation	Observed (mgN m^{-2} d^{-1})	Estimated (mgN m^{-2} d^{-1})
(Shang et al., 2011)	111.5	28.91	China, Taoyuan	2006.11-2007.10	A	1448	16.5	37.5	1.8	5.2	0	C	rice-rice	0.18	0.61
	111.5	28.91	China, Taoyuan	2006.11-2007.10	A	1448	16.5	37.9	1.9	5.3	183	C	rice-rice	0.87	0.91
	111.5	28.91	China, Taoyuan	2006.11-2007.10	A	1448	16.5	39.6	2.6	5.1	183	C	rice-rice	2.35	0.70
	111.5	28.91	China, Taoyuan	2006.11-2007.10	A	1448	16.5	40.7	2.38	5	122	C	rice-rice	1.44	1.11
	111.5	28.91	China, Taoyuan	2007.11-2008.10	A	1448	16.5	37.5	1.8	5.2	0	C	rice-rice	0.30	0.26
	111.5	28.91	China, Taoyuan	2007.11-2008.10	A	1448	16.5	37.9	1.9	5.3	183	C	rice-rice	0.59	0.81
	111.5	28.91	China, Taoyuan	2007.11-2008.10	A	1448	16.5	39.6	2.6	5.1	183	C	rice-rice	0.77	0.57
	111.5	28.91	China, Taoyuan	2007.11-2008.10	A	1448	16.5	40.7	2.38	5	122	C	rice-rice	0.79	0.53
	111.5	28.91	China, Taoyuan	2008.11-2009.10	A	1448	16.5	37.5	1.8	5.2	0	C	rice-rice	0.43	0.30
	111.5	28.91	China, Taoyuan	2008.11-2009.10	A	1448	16.5	37.9	1.9	5.3	183	C	rice-rice	0.64	0.93
	111.5	28.91	China, Taoyuan	2008.11-2009.10	A	1448	16.5	39.6	2.6	5.1	183	C	rice-rice	0.30	0.64
	111.5	28.91	China, Taoyuan	2008.11-2009.10	A	1448	16.5	40.7	2.38	5	122	C	rice-rice	0.46	0.50
(Yao et al., 2010)	120.48	31.51	Wuxi, China	2002.6-2003.6	A	1079	15.6	31	1.5	6.8	430	D	rice-wheat	0.90	0.98
	120.48	31.51	Wuxi, China	2002.6-2003.6	A	1079	15.6	31	1.5	6.8	430	D	rice-wheat	2.33	2.32
	120.48	31.51	Wuxi, China	2002.6-2003.6	A	1079	15.6	31	1.5	6.8	430	D	rice-wheat	1.40	1.44
	119.7	32.51	Jiangdu, China	2005.6-2006.6	A	1136	14.9	14	1.84	8	475	D	rice-wheat	0.38	0.35
	119.7	32.51	Jiangdu, China	2005.6-2006.6	A	1136	14.9	14	1.84	8	475	D	rice-wheat	1.51	1.31
	119.7	32.51	Jiangdu, China	2005.6-2006.6	A	1136	14.9	14	1.84	8	475	D	rice-wheat	0.90	1.09
	119.7	32.51	Jiangdu, China	2006.6-2007.6	A	625	23.8	14	1.84	8	475	D	rice-wheat	0.51	0.62
	119.7	32.51	Jiangdu, China	2006.6-2007.6	A	625	23.8	14	1.84	8	475	D	rice-wheat	1.84	1.50
	119.7	32.51	Jiangdu, China	2006.6-2007.6	A	625	23.8	14	1.84	8	475	D	rice-wheat	1.08	1.24
(Zhang et al., 2013)	112.3	28.11	Ningxiang, China	2007.4-2007.10	B	1358.3	16.8	26	3.49	6.26	266	D	rice-rice	0.45	0.60

	112.3	28.11	Ningxiang, China	2007.4-2007.10	B	1358.3	16.8	26	3.49	6.26	266	D	rice-rice	0.39	0.60
	112.3	28.11	Ningxiang, China	2008.4-2008.10	B	1358.3	16.8	26	3.49	6.26	266	D	rice-rice	0.16	0.36
	112.3	28.11	Ningxiang, China	2008.4-2008.10	B	1358.3	16.8	26	3.49	6.26	266	D	rice-rice	0.16	0.36
(Zhou et al., 2015)	105.48	31.27	Yanting, China	2005-2006	A	826	17.3	13.4	0.86	8.5	0	C	rice-rapeseed	0.34	0.14
	105.48	31.27	Yanting, China	2005-2006	A	826	17.3	13.4	0.86	8.5	0	D	rice-rapeseed	1.33	0.58
	105.48	31.27	Yanting, China	2005-2006	A	826	17.3	13.4	0.86	8.5	0	D	rice-rapeseed	1.94	0.98
	105.48	31.27	Yanting, China	2006-2007	A	826	17.3	13.4	0.86	8.5	150	C	rice-rapeseed	0.12	0.14
	105.48	31.27	Yanting, China	2006-2007	A	826	17.3	13.4	0.86	8.5	150	D	rice-rapeseed	0.72	0.66
	105.48	31.27	Yanting, China	2006-2007	A	826	17.3	13.4	0.86	8.5	150	D	rice-rapeseed	1.12	1.08
	105.48	31.27	Yanting, China	2007-2008	A	826	17.3	13.4	0.86	8.5	250	C	rice-rapeseed	0.08	0.13
	105.48	31.27	Yanting, China	2007-2008	A	826	17.3	13.4	0.86	8.5	250	D	rice-rapeseed	0.49	0.74
	105.48	31.27	Yanting, China	2007-2008	A	826	17.3	13.4	0.86	8.5	250	D	rice-rapeseed	1.08	1.11
(H. Wang et al., 2019)	120.41	31.45	China	2013.6-2014.6	A	1094	15.7	30.8	1.4	6.1	425	D	rice-wheat	0.44	0.35
	120.41	31.45	China	2013.6-2014.6	A	1094	15.7	30.8	1.4	6.1	425	D	rice-wheat	0.64	0.57
	120.41	31.45	China	2013.6-2014.6	A	1094	15.7	30.8	1.4	6.1	425	D	rice-wheat	0.60	0.63
	120.41	31.45	China	2013.6-2014.6	A	1094	15.7	30.8	1.4	6.1	425	D	rice-wheat	0.81	0.83
	120.41	31.45	China	2014.6-2015.6	A	1109	15.8	30.8	1.4	6.1	425	D	rice-wheat	0.44	0.34
	120.41	31.45	China	2014.6-2015.6	A	1109	15.8	30.8	1.4	6.1	425	D	rice-wheat	0.62	0.62
	120.41	31.45	China	2014.6-2015.6	A	1109	15.8	30.8	1.4	6.1	425	D	rice-wheat	0.62	0.67
	120.41	31.45	China	2014.6-2015.6	A	1109	15.8	30.8	1.4	6.1	425	D	rice-wheat	0.89	0.97
	120.41	31.45	China	2015.6-2016.6	A	1059	15.7	30.8	1.4	6.1	425	D	rice-wheat	0.45	0.37
	120.41	31.45	China	2015.6-2016.6	A	1059	15.7	30.8	1.4	6.1	425	D	rice-wheat	0.66	0.52
	120.41	31.45	China	2015.6-2016.6	A	1059	15.7	30.8	1.4	6.1	425	D	rice-wheat	0.68	0.81
	120.41	31.45	China	2015.6-2016.6	A	1059	15.7	30.8	1.4	6.1	425	D	rice-wheat	0.86	1.01

(Huang et al., 2019)	116.92	28.25	China	2010.11-2011.11	A	1789	17.6	35.2	1.7	4.74	180	D	rice-rice	0.04	0.07
	116.92	28.25	China	2010.11-2011.11	A	1789	17.6	35.2	1.7	4.74	180	C	rice-rice	0.03	0.03
	116.92	28.25	China	2011.11-2012.11	A	1789	17.6	35.2	1.7	4.74	180	D	rice-rice	0.03	0.07
	116.92	28.25	China	2011.11-2012.11	A	1789	17.6	35.2	1.7	4.74	180	C	rice-rice	0.02	0.03
	116.92	28.25	China	2012.11-2013.11	A	1789	17.6	35.2	1.7	4.74	180	D	rice-rice	0.03	0.07
	116.92	28.25	China	2012.11-2013.11	A	1789	17.6	35.2	1.7	4.74	180	C	rice-rice	0.03	0.03
	116.92	28.25	China	2013.11-2014.11	A	1789	17.6	35.2	1.7	4.74	180	D	rice-rice	0.03	0.07
	116.92	28.25	China	2013.11-2014.11	A	1789	17.6	35.2	1.7	4.74	180	C	rice-rice	0.03	0.03
(Ma et al., 2013)	119.61	26.29	China	2009	B	1500	18.3	30	2.56	5.3	180	C	rice-rice	0.02	0.04
	119.61	26.29	China	2009	B	1500	18.3	30	2.56	5.3	180	D	rice-rice	0.07	0.14
	119.61	26.29	China	2009	B	1500	18.3	30	2.56	5.3	180	D	rice-rice	0.17	0.12
	119.61	26.29	China	2010	B	1500	18.3	30	2.56	5.3	180	C	rice-rice	0.02	0.04
	119.61	26.29	China	2010	B	1500	18.3	30	2.56	5.3	180	D	rice-rice	0.05	0.12
	119.61	26.29	China	2010	B	1500	18.3	30	2.56	5.3	180	D	rice-rice	0.06	0.13
(Simmonds, Anders, et al., 2015)	-91.42	34.46	Arkansas, USA	2011.5-2011.10	B	288	26.5	18	0.65	6.25	168	C	rice-fallow	0.08	0.09
	-91.42	34.46	Arkansas, USA	2012.4-2012.8	B	400	25.2	18	0.65	6.25	134	C	rice-fallow	0.04	0.07
(Linquist et al., 2015)	-91.4	34.47	Stuttgart,USA	2012.4-2012.10	A				0.67	5.6	144	C	rice-soybean	0.02	0.05
	-91.4	34.47	Stuttgart,USA	2012.4-2012.10	A				0.67	5.6	144	D	rice-soybean	0.06	0.08
	-91.4	34.47	Stuttgart,USA	2012.4-2012.10	A				0.67	5.6	144	D	rice-soybean	0.13	0.14
	-91.4	34.47	Stuttgart,USA	2013.4-2013.9	A				0.67	5.6	144	C	rice-soybean	0.05	0.04
	-91.4	34.47	Stuttgart,USA	2013.4-2013.9	A				0.67	5.6	144	D	rice-soybean	0.25	0.11
	-91.4	34.47	Stuttgart,USA	2013.4-2013.9	A				0.67	5.6	144	D	rice-soybean	0.26	0.22
(Kim et al., 2014)	126.99	37.26	Korea	2008.5-2008.10	B	571.6602	21.00185	32	0.986	5.8	0	C	rice-fallow	0.22	0.23
	126.99	37.26	Korea	2008.5-2008.10	B	571.6602	21.00185	32	0.986	5.8	160	C	rice-fallow	0.46	0.25
	126.99	37.26	Korea	2008.5-2008.10	B	571.6602	21.00185	32	0.986	5.8	0	D	rice-fallow	0.26	0.26
	126.99	37.26	Korea	2008.5-2008.10	B	571.6602	21.00185	32	0.986	5.8	160	D	rice-fallow	0.59	0.43

(Wu et al., 2018)	111.45	28.91	Taoyuan, China	2014.11-2015.11	A	1448	16.5	32	1.76	7.8	182	C	rice-rice	0.00	0.00
	111.45	28.91	Taoyuan, China	2014.11-2015.11	A	1448	16.5	32	1.76	7.8	182	C	rice-rice	0.11	0.20
	111.45	28.91	Taoyuan, China	2014.11-2015.11	A	1448	16.5	32	1.76	7.8	182	C	rice-rice	0.01	0.01
	111.45	28.91	Taoyuan, China	2014.11-2015.11	A	1448	16.5	32	1.76	7.8	182	C	rice-rice	0.27	0.32
(Setyanto et al., 2018)	111.2	-6.78	Indonesia	2013.10-2014.3	B	1142.34	26.95	22.5	0.53	6.48	120	C	rice-rice	0.51	0.61
	111.2	-6.78	Indonesia	2014.10-2015.3	B	1117.24	27.02	22.5	0.53	6.48	120	C	rice-rice	0.48	0.53
	111.2	-6.78	Indonesia	2013.10-2014.4	B	1142.34	26.95	22.5	0.53	6.48	120	D	rice-rice	0.32	0.56
	111.2	-6.78	Indonesia	2014.10-2015.4	B	1117.24	27.02	22.5	0.53	6.48	120	D	rice-rice	0.60	0.61
(Chidthaisong et al., 2018)	101.22	14.01	Thailand	2013.12-2014.4	B	96.02	26.62	62	1.74	4.6	70	C	rice-rice	0.17	0.12
	101.22	14.01	Thailand	2015.2-2016.5	B	1309.64	28.74	62	1.74	4.6	70	C	rice-rice	0.37	0.26
	101.22	14.01	Thailand	2013.12-2014.4	B	96.02	26.62	62	1.74	4.6	70	D	rice-rice	0.23	0.24
	101.22	14.01	Thailand	2015.2-2016.5	B	1309.64	28.74	62	1.74	4.6	70	D	rice-rice	0.66	0.43
	107.52	16.47	Vietnam	2014.6-2014.9	B	393	28.95	37.5	1.14	4.1	100	C	rice-rice	0.17	0.11
	107.52	16.47	Vietnam	2014.6-2014.9	B	393	28.95	37.5	1.14	4.1	100	C	rice-rice	0.19	0.12
	107.52	16.47	Vietnam	2015.1-2015.5	B	473.2	24.36	37.5	1.14	4.1	100	C	rice-rice	0.10	0.77
	107.52	16.47	Vietnam	2015.1-2015.5	B	473.2	24.36	37.5	1.14	4.1	100	C	rice-rice	0.13	0.79
	107.52	16.47	Vietnam	2014.6-2014.9	B	393	28.95	37.5	1.14	4.1	100	D	rice-rice	0.41	0.73
	107.52	16.47	Vietnam	2015.1-2015.5	B	473.2	24.36	37.5	1.14	4.1	100	D	rice-rice	0.29	1.09
(Cha-un et al., 2017)	99.5	13.59	Vietnam	2010.1-2011.1	A	1063	27.9	2	0.4	5.8	150	D	rice-fallow	1.58	1.76
	99.5	13.59	Vietnam	2010.1-2011.1	A	1063	27.9	2	0.4	5.8	150	D	rice-rice	0.42	0.92
	99.5	13.59	Vietnam	2010.1-2011.1	A	1063	27.9	2	0.4	5.8	150	D	rice-Corn	2.13	2.06
	99.5	13.59	Vietnam	2010.1-2011.1	A	1063	27.9	2	0.4	5.8	150	D	rice-Spream	2.45	1.99
	99.5	13.59	Vietnam	2010.1-2011.1	A	1063	27.9	2	0.4	5.8	150	D	rice-fallow	0.93	1.31
	99.5	13.59	Vietnam	2010.1-2011.1	A	1063	27.9	2	0.4	5.8	150	D	rice-rice	0.33	0.62
	99.5	13.59	Vietnam	2010.1-2011.1	A	1063	27.9	2	0.4	5.8	150	D	rice-Corn	2.47	1.56
	99.5	13.59	Vietnam	2010.1-2011.1	A	1063	27.9	2	0.4	5.8	150	D	rice-Spream	2.85	2.77

(Quang et al., 2019)	105.77	21.42	Vietnam	2015.2-2015.6	B	157.2	23.68	23	1.9	5.03	100	C	rice-rice	0.67	0.65
	105.77	21.42	Vietnam	2015.7-2016.6	B	157.2	23.68	23	1.9	5.03	100	C	rice-rice	0.48	0.45
	105.77	21.42	Vietnam	2016.7-2016.10	B	156.8	28.81	23	1.9	5.03	100	C	rice-rice	0.33	0.35
(Dong et al., 2018)	126.8	45.82	Harbin, China	2012.6-2012.10	B	540	6.9	20.25	1.83	6.5	0	C	rice-fallow	0.87	0.83
	126.8	45.82	Harbin, China	2012.6-2012.11	B	540	6.9	20.25	1.83	6.5	75	C	rice-fallow	1.39	0.76
	126.8	45.82	Harbin, China	2012.6-2012.12	B	540	6.9	20.25	1.83	6.5	150	C	rice-fallow	2.23	2.37
	126.8	45.82	Harbin, China	2013.5-2013.10	B	540	6.9	20.25	1.83	6.5	0	C	rice-fallow	1.04	0.98
	126.8	45.82	Harbin, China	2013.5-2013.11	B	540	6.9	20.25	1.83	6.5	75	C	rice-fallow	1.53	0.34
	126.8	45.82	Harbin, China	2013.5-2013.12	B	540	6.9	20.25	1.83	6.5	150	C	rice-fallow	2.30	2.14
	126.8	45.82	Harbin, China	2012.6-2012.10	B	540	6.9	20.25	1.83	6.5	0	D	rice-fallow	1.02	0.88
	126.8	45.82	Harbin, China	2012.6-2012.11	B	540	6.9	20.25	1.83	6.5	75	D	rice-fallow	1.53	1.35
	126.8	45.82	Harbin, China	2012.6-2012.12	B	540	6.9	20.25	1.83	6.5	150	D	rice-fallow	2.29	2.04
	126.8	45.82	Harbin, China	2013.5-2013.10	B	540	6.9	20.25	1.83	6.5	0	D	rice-fallow	1.53	1.01
	126.8	45.82	Harbin, China	2013.5-2013.11	B	540	6.9	20.25	1.83	6.5	75	D	rice-fallow	1.48	1.25
	126.8	45.82	Harbin, China	2013.5-2013.12	B	540	6.9	20.25	1.83	6.5	150	D	rice-fallow	2.37	2.70
(Tang et al., 2018)	124.72	45.01	Qiangguo, China	2012.5-2012.10	B	423.88	17.83	28.75	0.43	9.72	150	C	rice-fallow	0.94	0.92
	124.71	45	Qiangguo, China	2012.5-2012.11	B	423.88	17.83	28.75	2.31	8.31	150	C	rice-fallow	0.82	0.40
	124.72	45.01	Qiangguo, China	2012.5-2012.12	B	423.88	17.83	28.75	4.19	6.9	150	D	rice-fallow	1.19	0.99
	124.72	45	Qiangguo, China	2012.5-2012.13	B	423.88	17.83	28.75	6.07	5.49	150	D	rice-fallow	0.99	0.68
(Oo et al., 2018)	79.5	11	India	2016.6-2016.9	B	1292	30.15	25.3	1.96	7.5	150	C	rice-rice	0.71	0.55
	79.5	11	India	2016.10-2017.1	B	1292	30.15	25.3	1.96	7.5	150	C	rice-rice	0.46	0.55
	79.5	11	India	2016.6-2016.9	B	1292	30.15	25.3	1.96	7.5	150	D	rice-rice	1.13	0.81
	79.5	11	India	2016.10-2017.1	B	1292	26.15	25.3	1.96	7.5	150	D	rice-rice	0.86	0.94

	79.5	11	India	2016.6-2016.9	B	1292	26.15	25.3	1.96	7.5	150	C	rice-rice	1.07	0.63
	79.5	11	India	2016.10-2017.1	B	1292	30.15	25.3	1.96	7.5	150	D	rice-rice	0.76	0.88
(Gupta et al., 2016)	77.2	28.67	New Delhi	2011.11-2012.11	A	750	24.5	21	0.46	8.1	240	D	rice-wheat	0.39	0.38
	77.2	28.67	New Delhi	2011.11-2012.11	A	750	24.5	21	0.46	8.1	240	D	rice-wheat	0.41	0.43
	77.2	28.67	New Delhi	2011.11-2012.11	A	750	24.5	21	0.46	8.1	240	D	rice-wheat	0.46	0.67
	77.2	28.67	New Delhi	2011.11-2012.11	A	750	24.5	21	0.46	8.1	240	D	rice-wheat	0.46	0.77
	77.2	28.67	New Delhi	2012.11-2013.11	A	750	24.5	21	0.46	8.1	240	D	rice-wheat	0.42	0.27
	77.2	28.67	New Delhi	2012.11-2013.11	A	750	24.5	21	0.46	8.1	240	D	rice-wheat	0.44	0.27
	77.2	28.67	New Delhi	2012.11-2013.11	A	750	24.5	21	0.46	8.1	240	D	rice-wheat	0.48	0.78
	77.2	28.67	New Delhi	2012.11-2013.11	A	750	24.5	21	0.46	8.1	240	D	rice-wheat	0.52	0.89
(Gaihre et al., 2015)	90.43	24.7	BAU	2013.5-2014.5	A	1500	25.3	29.96	1.18	6.2	0	C	rice-rice	0.04	0.08
	90.43	24.7	BAU	2013.5-2014.5	A	1500	25.3	29.96	1.18	6.2	130	C	rice-rice	0.16	0.17
	90.43	24.7	BAU	2013.5-2014.5	A	1500	25.3	29.96	1.18	6.2	182	C	rice-rice	0.07	0.11
	90.4	23.99	BRRI	2013.5-2014.5	A	1500	25.3	11.44	1.76	5.5	0	C	rice-rice	0.02	0.03
	90.4	23.99	BRRI	2013.5-2014.5	A	1500	25.3	11.44	1.76	5.5	130	C	rice-rice	0.03	0.06
	90.4	23.99	BRRI	2013.5-2014.5	A	1500	25.3	11.44	1.76	5.5	182	C	rice-rice	0.02	0.01
(Petter et al., 2016)	-52.4	-14.56	Brazil	2013.1-2013.4	B	1534	23.6	17	1.13	5.3	0	C	rice-fallow	0.10	0.05
	-52.4	-14.56	Brazil	2013.1-2013.4	B	1534	23.6	17	1.13	5.3	100	C	rice-fallow	0.19	0.14
	-52.4	-14.56	Brazil	2013.1-2013.4	B	1534	23.6	17	1.13	5.3	32Mgha	C	rice-fallow	0.55	0.71
(Zschornack et al. 2017)	-51.12	-29.94	Brazil	2009.10-2010.10	A	1394	20	17	0.13	5.3	210	C	rice-regrass	0.46	0.41
	-51.12	-29.94	Brazil	2010.10-2011.10	A	1394	20	17	0.13	5.3	210	C	rice-regrass	0.34	0.26
	-51.12	-29.94	Brazil	2011.10-2012.5	A	1394	20	17	0.13	5.3	210	C	rice-regrass	0.18	0.30
	-51.12	-29.94	Brazil	2009.10-2010.10	A	1394	20	17	0.13	5.3	300	C	rice-regrass	1.07	0.71
	-51.12	-29.94	Brazil	2010.10-2011.10	A	1394	20	17	0.13	5.3	300	C	rice-regrass	0.27	0.69
	-51.12	-29.94	Brazil	2011.10-2012.5	A	1394	20	17	0.13	5.3	300	C	rice-regrass	0.18	0.20

Table 4. S2 The global correlation results between weighted mean Emission Factors (EF) and related management, environmental factors.

	Variables	t	df	cor	*p*-value
$EF_{1980-2020}$ .vs. $Variable_{1980-2020}$	Fraction of fertilizer NO_3^-	-22.98	155434	-0.058**	<0.0001
	Total fertilizer application rate	41.337	155698	0.104**	<0.0001
	Atmospheric N deposition rate	-10.698	155698	-0.029**	<0.0001
	Mean daily temperature	12.56	155698	0.0334**	<0.0001
	Mean daily precipitation	2.215	155698	0.0059	0.0268
EF_{mean} .vs. $Variable_{mean}$	Annual rice non-growing season days	2.11	5071	0.030	0.034
	Soil pH	-1.72	5071	-0.024	0.084
	Soil clay content	4.28	5071	0.060**	<0.0001
	Soil sand content	-4.81	5071	-0.067**	<0.0001

All the data was log transformed before processing.

Table 4. S3 The regional correlation results between weighted mean N_2O emissions and rainfed rice-based ecosystem fraction, annual precipitation level, and weighted mean N fertilizer application rate during different time period in three key rice-cultivation regions.

Region	Variables	Periods	t	cor	*p*-value
China	Rainfed fraction	1910-2020	-10.50	-0.71	<0.001
		1960-2020	-4.99	-0.54	<0.001
	Precipitation	1910-1960	0.14	0.95	0.34
	Trend#		Slope=0.11	R^2=0.11	0.02
	Mean N application rate	1910-2020	22.68	0.91	<0.001
		1960-2020	27.96	0.96	<0.001
India	Rainfed fraction	1910-2020	-6.87	-0.55	<0.001
		1960-2020	-17.93	-0.92	<0.001
	Precipitation	1910-1960	-6.71	-0.70	<0.001
	Trend#		Slope=0.23	R^2=0.47	<0.001
	Mean N application rate	1910-2020	0.71	0.07	0.48
		1960-2020	8.22	0.73	<0.001
Southeast Aisa	Rainfed fraction	1910-2020	-11.45	-0.74	<0.001
		1960-2020	-11.42	-0.83	<0.001
	Precipitation	1910-1960	1.41	0.20	0.16
	Trend#		Slope=0.07	R^2=0.014	0.41
	Mean N application rate	1910-2020	25.04	0.92	<0.001
		1960-2020	9.72	0.78	<0.001

#: time series trend of annual precipitation during 1910-1960. The break point is set as 1960 because after the 1960s, chemical N fertilizer become widely used (green revolution), which dominate the trend of N_2O emission.

4.9 References

Akiyama, H., Yagi, K., & Yan, X. (2005). Direct N2O emissions from rice paddy fields: Summary of available data. *Global Biogeochemical Cycles*, *19*(1). https://doi.org/https://doi.org/10.1029/2004GB002378

Aliyu, G., Sanz-Cobena, A., Mueller, C., Zaman, M., Luo, J., Liu, D., Yuan, J., Chen, Z., Niu, Y., Arowolo, A., & Ding, W. (2018). A meta-analysis of soil background N2O emissions from croplands in China shows variation among climatic zones. *Agriculture Ecosystems & Environment*, *267*, 63-73. https://doi.org/10.1016/j.agee.2018.08.003

Audet, J., Hoffmann, C. C., Andersen, P. M., Baattrup-Pedersen, A., Johansen, J. R., Larsen, S. E., Kjaergaard, C., & Elsgaard, L. (2014). Nitrous oxide fluxes in undisturbed riparian wetlands located in agricultural catchments: Emission, uptake and controlling factors. *Soil Biology and Biochemistry*, *68*, 291-299. https://doi.org/https://doi.org/10.1016/j.soilbio.2013.10.011

Babu, Y. J., Li, C., Frolking, S., Nayak, D. R., & Adhya, T. K. (2006). Field Validation of DNDC Model for Methane and Nitrous Oxide Emissions from Rice-based Production Systems of India. *Nutrient Cycling in Agroecosystems*, *74*(2), 157-174. https://doi.org/10.1007/s10705-005-6111-5

Berger, S., Jang, I., Seo, J., Kang, H., & Gebauer, G. (2013). A record of N2O and CH4 emissions and underlying soil processes of Korean rice paddies as affected by different water management practices. *Biogeochemistry*, *115*(1), 317-332. https://doi.org/10.1007/s10533-013-9837-1

Bhattacharyya, P., Nayak, A. K., Mohanty, S., Tripathi, R., Shahid, M., Kumar, A., Raja, R., Panda, B. B., Roy, K. S., Neogi, S., Dash, P. K., Shukla, A. K., & Rao, K. S. (2013). Greenhouse gas emission in relation to labile soil C, N pools and functional microbial diversity as influenced by 39 years long-term fertilizer management in tropical rice. *Soil and Tillage Research*, *129*, 93-105. https://doi.org/https://doi.org/10.1016/j.still.2013.01.014

Bhattacharyya, P., Sinhababu, D. P., Roy, K. S., Dash, P. K., Sahu, P. K., Dandapat, R., Neogi, S., & Mohanty, S. (2013). Effect of fish species on methane and nitrous oxide emission in relation to soil C, N pools and enzymatic activities in rainfed shallow lowland rice-fish farming system. *Agriculture, Ecosystems & Environment*, *176*, 53-62. https://doi.org/https://doi.org/10.1016/j.agee.2013.05.015

Bo, Y., Jägermeyr, J., Yin, Z., Jiang, Y., Xu, J., Liang, H., & Zhou, F. (2022). Global benefits of non-continuous flooding to reduce greenhouse gases and irrigation water use without rice yield penalty [https://doi.org/10.1111/gcb.16132]. *Global change biology*, *28*(11), 3636-3650. https://doi.org/https://doi.org/10.1111/gcb.16132

Butterbach-Bahl, K., Baggs, E. M., Dannenmann, M., Kiese, R., & Zechmeister-Boltenstern, S. (2013). Nitrous oxide emissions from soils: how well do we understand the processes and their controls? *Philosophical Transactions of the Royal Society B: Biological Sciences*, *368*(1621), 20130122. https://doi.org/10.1098/rstb.2013.0122

Cai, Z., Sawamoto, T., Li, C., Kang, G., Boonjawat, J., Mosier, A., Wassmann, R., & Tsuruta, H. (2003). Field validation of the DNDC model for greenhouse gas emissions in East Asian cropping systems. *Global Biogeochemical Cycles*, *17*(4). https://doi.org/https://doi.org/10.1029/2003GB002046

Canadell, J. G., Monteiro, P. M. S., Costa, M. H., Cotrim da Cunha, L., Cox, P. M., Eliseev, A. V., Henson, S., Ishii, M., Jaccard, S., Koven, C., Lohila, A., Patra, P. K., Piao, S., Rogelj, J., Syampungani, S., Zaehle, S., & Zickfeld, K. (2021). . (2021). Global carbon and other biogeochemical cycles and feedbacks. *Climate change 2021: The physical science basis. Contribution of Working Group I to the Sixth Assessment Report of the Intergovernmental Panel on Climate Change. Cambridge University Press, in press.*

.

Cha-un, N., Chidthaisong, A., Yagi, K., Sudo, S., & Towprayoon, S. (2017). Greenhouse gas emissions, soil carbon sequestration and crop yields in a rain-fed rice field with crop rotation management. *Agriculture, Ecosystems & Environment*, *237*, 109-120. https://doi.org/https://doi.org/10.1016/j.agee.2016.12.025

Chidthaisong, A., Cha-un, N., Rossopa, B., Buddaboon, C., Kunuthai, C., Sriphirom, P., Towprayoon, S., Tokida, T., Padre,

A. T., & Minamikawa, K. (2018). Evaluating the effects of alternate wetting and drying (AWD) on methane and nitrous oxide emissions from a paddy field in Thailand. *Soil Science and Plant Nutrition*, *64*(1), 31-38. https://doi.org/10.1080/00380768.2017.1399044

Cowan, N., Bhatia, A., Drewer, J., Jain, N., Singh, R., Tomer, R., Kumar, V., Kumar, O., Prasanna, R., Ramakrishnan, B., Kumar, D., Bandyopadhyay, S. K., Sutton, M., & Pathak, H. (2021). Experimental comparison of continuous and intermittent flooding of rice in relation to methane, nitrous oxide and ammonia emissions and the implications for nitrogen use efficiency and yield. *Agriculture, Ecosystems & Environment*, *319*, 107571. https://doi.org/https://doi.org/10.1016/j.agee.2021.107571

Das, S., & Adhya, T. K. (2014). Effect of combine application of organic manure and inorganic fertilizer on methane and nitrous oxide emissions from a tropical flooded soil planted to rice. *Geoderma*, *213*, 185-192. https://doi.org/https://doi.org/10.1016/j.geoderma.2013.08.011

Datta, A., Nayak, D. R., Sinhababu, D. P., & Adhya, T. K. (2009). Methane and nitrous oxide emissions from an integrated rainfed rice–fish farming system of Eastern India. *Agriculture, Ecosystems & Environment*, *129*(1), 228-237. https://doi.org/https://doi.org/10.1016/j.agee.2008.09.003

Davidson, E. A. (2009). The contribution of manure and fertilizer nitrogen to atmospheric nitrous oxide since 1860. *Nature Geoscience*, *2*(9), 659-662. https://doi.org/10.1038/ngeo608

Davidson, E. A., & Kanter, D. (2014). Inventories and scenarios of nitrous oxide emissions. *Environmental Research Letters*, *9*(10), Article 105012. https://doi.org/10.1088/1748-9326/9/10/105012

Dong, W., Guo, J., Xu, L., Song, Z., Zhang, J., Tang, A., Zhang, X., Leng, C., Liu, Y., Wang, L., Wang, L., Yu, Y., Yang, Z., Yu, Y., Meng, Y., & Lai, Y. (2018). Water regime-nitrogen fertilizer incorporation interaction: Field study on methane and nitrous oxide emissions from a rice agroecosystem in Harbin, China. *Journal of Environmental Sciences*, *64*, 289-297. https://doi.org/https://doi.org/10.1016/j.jes.2017.06.007

Farquharson, R., & Baldock, J. (2008). Concepts in modelling N2O emissions from land use. *Plant and Soil*, *309*(1), 147-167. https://doi.org/10.1007/s11104-007-9485-0

Foley, J. A., Prentice, I. C., Ramankutty, N., Levis, S., Pollard, D., Sitch, S., & Haxeltine, A. (1996). An integrated biosphere model of land surface processes, terrestrial carbon balance, and vegetation dynamics. *Global Biogeochemical Cycles*, *10*(4), 603-628. https://doi.org/10.1029/96gb02692

Frenzel, P., Rothfuss, F., & Conrad, R. (1992). Oxygen profiles and methane turnover in a flooded rice microcosm. *Biology and Fertility of Soils*, *14*(2), 84-89. https://doi.org/10.1007/BF00336255

Gaihre, Y. K., Singh, U., Islam, S. M. M., Huda, A., Islam, M. R., Satter, M. A., Sanabria, J., Islam, M. R., & Shah, A. L. (2015). Impacts of urea deep placement on nitrous oxide and nitric oxide emissions from rice fields in Bangladesh. *Geoderma*, *259-260*, 370-379. https://doi.org/https://doi.org/10.1016/j.geoderma.2015.06.001

Gerber, J. S., Carlson, K. M., Makowski, D., Mueller, N. D., Garcia de Cortazar-Atauri, I., Havlík, P., Herrero, M., Launay, M., O'Connell, C. S., Smith, P., & West, P. C. (2016). Spatially explicit estimates of N2O emissions from croplands suggest climate mitigation opportunities from improved fertilizer management [https://doi.org/10.1111/gcb.13341]. *Global change biology*, *22*(10), 3383-3394. https://doi.org/https://doi.org/10.1111/gcb.13341

Gupta, D. K., Bhatia, A., Kumar, A., Das, T. K., Jain, N., Tomer, R., Malyan, S. K., Fagodiya, R. K., Dubey, R., & Pathak, H. (2016). Mitigation of greenhouse gas emission from rice–wheat system of the Indo-Gangetic plains: Through tillage, irrigation and fertilizer management. *Agriculture, Ecosystems & Environment*, *230*, 1-9. https://doi.org/https://doi.org/10.1016/j.agee.2016.05.023

Gupta, K., Kumar, R., Baruah, K. K., Hazarika, S., Karmakar, S., & Bordoloi, N. (2021). Greenhouse gas emission from rice fields: a review from Indian context. *Environmental Science and Pollution Research*, *28*(24), 30551-30572. https://doi.org/10.1007/s11356-021-13935-1

Harris, I., Osborn, T. J., Jones, P., & Lister, D. (2020). Version 4 of the CRU TS monthly high-resolution gridded multivariate climate dataset. *Scientific Data*, *7*(1), 109. https://doi.org/10.1038/s41597-020-0453-3

Hou, X., Zhou, F., Leip, A., Fu, B., Yang, H., Chen, Y., Gao, S., Shang, Z., & Ma, L. (2016). Spatial patterns of nitrogen runoff from Chinese paddy fields. *Agriculture, Ecosystems & Environment*, *231*, 246-254. https://doi.org/https://doi.org/10.1016/j.agee.2016.07.001

Huang, Y., Wang, C., Lin, C., Zhang, Y., Chen, X., Tang, L., Liu, C., Chen, Q., Onwuka, M. I., & Song, T. (2019). Methane and Nitrous Oxide Flux after Biochar Application in Subtropical Acidic Paddy Soils under Tobacco-Rice Rotation. *Scientific Reports*, *9*(1), 17277. https://doi.org/10.1038/s41598-019-53044-1

Hurtt, G. C., Chini, L., Sahajpal, R., Frolking, S., Bodirsky, B. L., Calvin, K., Doelman, J. C., Fisk, J., Fujimori, S., Klein Goldewijk, K., Hasegawa, T., Havlik, P., Heinimann, A., Humpenöder, F., Jungclaus, J., Kaplan, J. O., Kennedy, J., Krisztin, T., Lawrence, D., . . . Zhang, X. (2020). Harmonization of global land use change and management for the period 850–2100 (LUH2) for CMIP6. *Geosci. Model Dev.*, *13*(11), 5425-5464. https://doi.org/10.5194/gmd-13-5425-2020

Islam, S. M. M., Gaihre, Y. K., Biswas, J. C., Singh, U., Ahmed, M. N., Sanabria, J., & Saleque, M. A. (2018). Nitrous oxide and nitric oxide emissions from lowland rice cultivation with urea deep placement and alternate wetting and drying irrigation. *Scientific Reports*, *8*(1), 17623. https://doi.org/10.1038/s41598-018-35939-7

Ito, A., Nishina, K., Ishijima, K., Hashimoto, S., & Inatomi, M. (2018). Emissions of nitrous oxide (N2O) from soil surfaces and their historical changes in East Asia: a model-based assessment. *Progress in Earth and Planetary Science*, *5*. https://doi.org/10.1186/s40645-018-0215-4

Jian-She, Z., Fu-Ping, Z., Jin-Hua, Y., Jin-Ping, W., Ming-Li, C., Li, C.-F., & Cao, C.-G. (2011). Emissions of N2O and NH3, and nitrogen leaching from direct seeded rice under different tillage practices in central China. *Agriculture, Ecosystems & Environment*, *140*(1), 164-173. https://doi.org/https://doi.org/10.1016/j.agee.2010.11.023

Johnson-Beebout, S. E., Angeles, O. R., Alberto, M. C. R., & Buresh, R. J. (2009). Simultaneous minimization of nitrous oxide and methane emission from rice paddy soils is improbable due to redox potential changes with depth in a greenhouse experiment without plants. *Geoderma*, *149*(1), 45-53. https://doi.org/https://doi.org/10.1016/j.geoderma.2008.11.012

Jørgensen, C. J., & Elberling, B. (2012). Effects of flooding-induced N2O production, consumption and emission dynamics on the annual N2O emission budget in wetland soil. *Soil Biology and Biochemistry*, *53*, 9-17. https://doi.org/https://doi.org/10.1016/j.soilbio.2012.05.005

Kim, D.-G., Giltrap, D., & Hernandez-Ramirez, G. (2013). Background nitrous oxide emissions in agricultural and natural lands: a meta-analysis. *Plant and Soil*, *373*(1), 17-30. https://doi.org/10.1007/s11104-013-1762-5

Kim, G.-Y., Gutierrez, J., Jeong, H.-C., Lee, J.-S., Haque, M. D. M., & Kim, P. J. (2014). Effect of intermittent drainage on methane and nitrous oxide emissions under different fertilization in a temperate paddy soil during rice cultivation. *Journal of the Korean Society for Applied Biological Chemistry*, *57*(2), 229-236. https://doi.org/10.1007/s13765-013-4298-8

Klein Goldewijk, K., Beusen, A., Doelman, J., & Stehfest, E. (2017). Anthropogenic land use estimates for the Holocene – HYDE 3.2. *Earth Syst. Sci. Data*, *9*(2), 927-953. https://doi.org/10.5194/essd-9-927-2017

Kögel-Knabner, I., Amelung, W., Cao, Z., Fiedler, S., Frenzel, P., Jahn, R., Kalbitz, K., Kölbl, A., & Schloter, M. (2010). Biogeochemistry of paddy soils. *Geoderma*, *157*(1), 1-14. https://doi.org/https://doi.org/10.1016/j.geoderma.2010.03.009

Kraus, D., Weller, S., Klatt, S., Haas, E., Wassmann, R., Kiese, R., & Butterbach-Bahl, K. (2015). A new LandscapeDNDC biogeochemical module to predict CH4 and N2O emissions from lowland rice and upland cropping systems. *Plant and Soil*, *386*(1), 125-149. https://doi.org/10.1007/s11104-014-2255-x

Kritee, K., Nair, D., Zavala-Araiza, D., Proville, J., Rudek, J., Adhya, T. K., Loecke, T., Esteves, T., Balireddygari, S., Dava, O., Ram, K., S. R., A., Madasamy, M., Dokka, R. V., Anandaraj, D., Athiyaman, D., Reddy, M., Ahuja, R., & Hamburg, S. P. (2018). High nitrous oxide fluxes from rice indicate the need to manage water for both long- and short-term climate impacts. *Proceedings of the National Academy of Sciences*, *115*(39), 9720-9725. https://doi.org/doi:10.1073/pnas.1809276115

Kucharik, C. J., Foley, J. A., Delire, C., Fisher, V. A., Coe, M. T., Lenters, J. D., Young-Molling, C., Ramankutty, N., Norman, J. M., & Gower, S. T. (2000). Testing the performance of a Dynamic Global Ecosystem Model: Water balance, carbon balance, and vegetation structure. *Global Biogeochemical Cycles*, *14*(3), 795-825. https://doi.org/10.1029/1999gb001138

Laborte, A. G., Gutierrez, M. A., Balanza, J. G., Saito, K., Zwart, S. J., Boschetti, M., Murty, M. V. R., Villano, L., Aunario, J. K., Reinke, R., Koo, J., Hijmans, R. J., & Nelson, A. (2017). RiceAtlas, a spatial database of global rice calendars and production. *Scientific Data*, *4*(1), 170074. https://doi.org/10.1038/sdata.2017.74

Lagomarsino, A., Agnelli, A. E., Linquist, B., Adviento-Borbe, M. A., Agnelli, A., Gavina, G., Ravaglia, S., & Ferrara, R. M. (2016). Alternate Wetting and Drying of Rice Reduced CH4 Emissions but Triggered N2O Peaks in a Clayey Soil of Central Italy. *Pedosphere*, *26*(4), 533-548. https://doi.org/https://doi.org/10.1016/S1002-0160(15)60063-7

Lagomarsino, A., Agnelli, A. E., Pastorelli, R., Pallara, G., Rasse, D. P., & Silvennoinen, H. (2016). Past water management affected GHG production and microbial community pattern in Italian rice paddy soils. *Soil Biology and Biochemistry*, *93*, 17-27. https://doi.org/https://doi.org/10.1016/j.soilbio.2015.10.016

LaHue, G. T., Chaney, R. L., Adviento-Borbe, M. A., & Linquist, B. A. (2016). Alternate wetting and drying in high yielding direct-seeded rice systems accomplishes multiple environmental and agronomic objectives. *Agriculture, Ecosystems & Environment*, *229*, 30-39. https://doi.org/https://doi.org/10.1016/j.agee.2016.05.020

Lan, T., Han, Y., & Cai, Z. (2015). Denitrification and its product composition in typical Chinese paddy soils. *Biology and Fertility of Soils*, *51*(1), 89-98. https://doi.org/10.1007/s00374-014-0953-4

Li, C. S., Aber, J., Stange, F., Butterbach-Bahl, K., & Papen, H. (2000). A process-oriented model of N2O and NO emissions from forest soils: 1. Model development. *Journal of Geophysical Research-Atmospheres*, *105*(D4), 4369-4384. https://doi.org/10.1029/1999jd900949

Li, G., Lin, J., Xue, L., Ding, Y., Wang, S., & Yang, L. (2018). Fate of Basal N Under Split Fertilization in Rice with 15N Isotope Tracer. *Pedosphere*, *28*(1), 135-143. https://doi.org/https://doi.org/10.1016/S1002-0160(17)60407-7

Li, X., Yuan, W., Xu, H., Cai, Z., & Yagi, K. (2011). Effect of timing and duration of midseason aeration on CH4 and N2O emissions from irrigated lowland rice paddies in China. *Nutrient Cycling in Agroecosystems*, *91*(3), 293-305. https://doi.org/10.1007/s10705-011-9462-0

Li, Y. L., Zhang, Y. L., Hu, J., & Shen, Q. R. (2007). Contribution of nitrification happened in rhizospheric soil growing with different rice cultivars to N nutrition. *Biology and Fertility of Soils*, *43*(4), 417-425. https://doi.org/10.1007/s00374-006-0119-0

Liang, H., Xu, J., Hou, H., Qi, Z., Yang, S., Li, Y., & Hu, K. (2022). Modeling CH4 and N2O emissions for continuous and noncontinuous flooding rice systems. *Agricultural Systems*, *203*, 103528. https://doi.org/https://doi.org/10.1016/j.agsy.2022.103528

Linquist, B. A., Anders, M. M., Adviento-Borbe, M. A. A., Chaney, R. L., Nalley, L. L., Da Rosa, E. F., & Van Kessel, C. (2015). Reducing greenhouse gas emissions, water use, and grain arsenic levels in rice systems. *Global change biology*, *21*(1), 407-417.

Liu, H., Wrage-Mönnig, N., & Lennartz, B. (2020). Rewetting strategies to reduce nitrous oxide emissions from European peatlands. *Communications Earth & Environment*, *1*(1), 17. https://doi.org/10.1038/s43247-020-00017-2

Liu, J., Hou, H., Sheng, R., Chen, Z., Zhu, Y., Qin, H., & Wei, W. (2012). Denitrifying communities differentially respond to flooding drying cycles in paddy soils. *Applied Soil Ecology*, *62*, 155-162.

https://doi.org/https://doi.org/10.1016/j.apsoil.2012.06.010

Liu, S., Zhang, Y., Lin, F., Zhang, L., & Zou, J. (2014). Methane and nitrous oxide emissions from direct-seeded and seedling-transplanted rice paddies in southeast China. *Plant and Soil*, *374*(1), 285-297. https://doi.org/10.1007/s11104-013-1878-7

Ma, J., Ji, Y., Zhang, G., Xu, H., & Yagi, K. (2013). Timing of midseason aeration to reduce CH4 and N2O emissions from double rice cultivation in China. *Soil Science and Plant Nutrition*, *59*(1), 35-45. https://doi.org/10.1080/00380768.2012.730477

Ma, M., Song, C., Fang, H., Zhang, J., Wei, J., Liu, S., Chen, X., Zhang, K., Yuan, W., & Lu, H. (2022). Development of a Process-Based N2O Emission Model for Natural Forest and Grassland Ecosystems. *Journal of Advances in Modeling Earth Systems*, *14*(3), e2021MS002460. https://doi.org/https://doi.org/10.1029/2021MS002460

Majumdar, D. (2013). Biogeochemistry of N2O Uptake and Consumption in Submerged Soils and Rice Fields and Implications in Climate Change. *Critical Reviews in Environmental Science and Technology*, *43*(24), 2653-2684. https://doi.org/10.1080/10643389.2012.694332

Malla, G., Bhatia, A., Pathak, H., Prasad, S., Jain, N., & Singh, J. (2005). Mitigating nitrous oxide and methane emissions from soil in rice–wheat system of the Indo-Gangetic plain with nitrification and urease inhibitors. *Chemosphere*, *58*(2), 141-147. https://doi.org/https://doi.org/10.1016/j.chemosphere.2004.09.003

Metay, A., Chapuis-Lardy, L., Findeling, A., Oliver, R., Alves Moreira, J. A., & Feller, C. (2011). Simulating N2O fluxes from a Brazilian cropped soil with contrasted tillage practices. *Agriculture, Ecosystems & Environment*, *140*(1), 255-263. https://doi.org/https://doi.org/10.1016/j.agee.2010.12.012

Meurer, K. H. E., Franko, U., Stange, C. F., Rosa, J. D., Madari, B. E., & Jungkunst, H. F. (2016). Direct nitrous oxide (N2O) fluxes from soils under different land use in Brazil—a critical review. *Environmental Research Letters*, *11*(2), 023001. https://doi.org/10.1088/1748-9326/11/2/023001

Nie, S. a., Zhu, G.-B., Singh, B., & Zhu, Y.-G. (2019). Anaerobic ammonium oxidation in agricultural soils-synthesis and prospective. *Environmental Pollution*, *244*, 127-134. https://doi.org/https://doi.org/10.1016/j.envpol.2018.10.050

Oo, A. Z., Sudo, S., Inubushi, K., Mano, M., Yamamoto, A., Ono, K., Osawa, T., Hayashida, S., Patra, P. K., Terao, Y., Elayakumar, P., Vanitha, K., Umamageswari, C., Jothimani, P., & Ravi, V. (2018). Methane and nitrous oxide emissions from conventional and modified rice cultivation systems in South India. *Agriculture, Ecosystems & Environment*, *252*, 148-158. https://doi.org/https://doi.org/10.1016/j.agee.2017.10.014

Pappas, C., Fatichi, S., Leuzinger, S., Wolf, A., & Burlando, P. (2013). Sensitivity analysis of a process-based ecosystem model: Pinpointing parameterization and structural issues [https://doi.org/10.1002/jgrg.20035]. *Journal of Geophysical Research: Biogeosciences*, *118*(2), 505-528. https://doi.org/https://doi.org/10.1002/jgrg.20035

Peng, S., Buresh, R. J., Huang, J., Yang, J., Zou, Y., Zhong, X., Wang, G., & Zhang, F. (2006). Strategies for overcoming low agronomic nitrogen use efficiency in irrigated rice systems in China. *Field Crops Research*, *96*(1), 37-47. https://doi.org/https://doi.org/10.1016/j.fcr.2005.05.004

Petter, F. A., Borges de Lima, L., Marimon Júnior, B. H., Alves de Morais, L., & Marimon, B. S. (2016). Impact of biochar on nitrous oxide emissions from upland rice. *Journal of Environmental Management*, *169*, 27-33. https://doi.org/https://doi.org/10.1016/j.jenvman.2015.12.020

Pittelkow, C. M., Adviento-Borbe, M. A., Hill, J. E., Six, J., van Kessel, C., & Linquist, B. A. (2013). Yield-scaled global warming potential of annual nitrous oxide and methane emissions from continuously flooded rice in response to nitrogen input. *Agriculture, Ecosystems & Environment*, *177*, 10-20. https://doi.org/https://doi.org/10.1016/j.agee.2013.05.011

Quang, L. X., Nakamura, K., Hung, T., Tinh, N. V., Matsuda, S., Kadota, K., Horino, H., Hai, P. T., Komatsu, H., Hasegawa, K., Fukuda, S., Hirata, J., Oura, N., Kishimoto-Mo, A. W., Yonemura, S., & Onishi, T. (2019). Effect of organizational paddy water management by a water user group on methane and nitrous oxide emissions and rice yield in the Red River Delta, Vietnam. *Agricultural Water Management*, *217*, 179-192. https://doi.org/https://doi.org/10.1016/j.agwat.2019.02.015

Setyanto, P., Pramono, A., Adriany, T. A., Susilawati, H. L., Tokida, T., Padre, A. T., & Minamikawa, K. (2018). Alternate wetting and drying reduces methane emission from a rice paddy in Central Java, Indonesia without yield loss. *Soil Science and Plant Nutrition*, *64*(1), 23-30. https://doi.org/10.1080/00380768.2017.1409600

Shan, J., Yang, P., Shang, X., Rahman, M. M., & Yan, X. (2018). Anaerobic ammonium oxidation and denitrification in a paddy soil as affected by temperature, pH, organic carbon, and substrates. *Biology and Fertility of Soils*, *54*(3), 341-348. https://doi.org/10.1007/s00374-018-1263-z

Shang, Q., Yang, X., Gao, C., Wu, P., Liu, J., Xu, Y., Shen, Q., Zou, J., & Guo, S. (2011). Net annual global warming potential and greenhouse gas intensity in Chinese double rice-cropping systems: a 3-year field measurement in long-term fertilizer experiments [https://doi.org/10.1111/j.1365-2486.2010.02374.x]. *Global change biology*, *17*(6), 2196-2210. https://doi.org/https://doi.org/10.1111/j.1365-2486.2010.02374.x

Shang, Z., Abdalla, M., Kuhnert, M., Albanito, F., Zhou, F., Xia, L., & Smith, P. (2020). Measurement of N2O emissions over the whole year is necessary for estimating reliable emission factors. *Environmental Pollution*, *259*, 113864. https://doi.org/https://doi.org/10.1016/j.envpol.2019.113864

Shang, Z., Zhou, F., Smith, P., Saikawa, E., Ciais, P., Chang, J., Tian, H., Del Grosso, S. J., Ito, A., Chen, M., Wang, Q., Bo, Y., Cui, X., Castaldi, S., Juszczak, R., Kasimir, A., Magliulo, V., Medinets, S., Medinets, V., . . . Sabbatini, S. (2019). Weakened growth of cropland-N2O emissions in China associated with nationwide policy interventions. *Global Change Biology*, *25*(11), 3706-3719. https://doi.org/10.1111/gcb.14741

Shcherbak, I., Millar, N., & Robertson, G. P. (2014). Global metaanalysis of the nonlinear response of soil nitrous oxide (N2O) emissions to fertilizer nitrogen. *Proceedings of the National Academy of Sciences*, *111*(25), 9199-9204. https://doi.org/10.1073/pnas.1322434111

Silver, W. L., Herman, D. J., & Firestone, M. K. (2001). DISSIMILATORY NITRATE REDUCTION TO AMMONIUM IN UPLAND TROPICAL FOREST SOILS [https://doi.org/10.1890/0012-9658(2001)082 2410:DNRTAI 2.0.CO;2]. *Ecology*, *82*(9), 2410-2416. https://doi.org/https://doi.org/10.1890/0012-9658(2001)082[2410:DNRTAI]2.0.CO;2

Simmonds, M. B., Anders, M., Adviento-Borbe, M. A., van Kessel, C., McClung, A., & Linquist, B. A. (2015). Seasonal Methane and Nitrous Oxide Emissions of Several Rice Cultivars in Direct-Seeded Systems [https://doi.org/10.2134/jeq2014.07.0286]. *Journal of Environmental Quality*, *44*(1), 103-114. https://doi.org/https://doi.org/10.2134/jeq2014.07.0286

Simmonds, M. B., Li, C., Lee, J., Six, J., van Kessel, C., & Linquist, B. A. (2015). Modeling methane and nitrous oxide emissions from direct-seeded rice systems. *Journal of Geophysical Research: Biogeosciences*, *120*(10), 2011-2035. https://doi.org/https://doi.org/10.1002/2015JG002915

Song, H., Peng, C., Zhang, K., Li, T., Yang, M., Liu, Q., & Zhu, Q. (2023). Quantifying patterns, sources and uncertainty of nitrous oxide emissions from global grazing lands: Nitrogen forms are the determinant factors for estimation and mitigation. *Global and Planetary Change*, *223*, 104080. https://doi.org/https://doi.org/10.1016/j.gloplacha.2023.104080

Song, H., Peng, C., Zhang, K., & Zhu, Q. (2022). Integrating major agricultural practices into the TRIPLEX-GHG model v2.0 for simulating global cropland nitrous oxide emissions: Development, sensitivity analysis and site evaluation. *Science of The Total Environment*, *843*, 156945. https://doi.org/https://doi.org/10.1016/j.scitotenv.2022.156945

Tang, J., Wang, J., Li, Z., Wang, S., & Qu, Y. (2018). Effects of Irrigation Regime and Nitrogen Fertilizer Management on CH4, N2O and CO2 Emissions from Saline–Alkaline Paddy Fields in Northeast China. *Sustainability*, *10*(2).

Tian, H., Bian, Z., Shi, H., Qin, X., Pan, N., Lu, C., Pan, S., Tubiello, F. N., Chang, J., Conchedda, G., Liu, J., Mueller, N., Nishina, K., Xu, R., Yang, J., You, L., & Zhang, B. (2022). History of anthropogenic Nitrogen inputs (HaNi) to the terrestrial biosphere: a 5 arcmin resolution annual dataset from 1860 to 2019. *Earth Syst. Sci. Data*, *14*(10), 4551-4568. https://doi.org/10.5194/essd-14-4551-2022

Tian, H., Xu, R., Canadell, J. G., Thompson, R. L., Winiwarter, W., Suntharalingam, P., Davidson, E. A., Ciais, P., Jackson, R. B., Janssens-Maenhout, G., Prather, M. J., Regnier, P., Pan, N., Pan, S., Peters, G. P., Shi, H., Tubiello, F. N., Zaehle, S., Zhou, F., . . . Yao, Y. (2020). A comprehensive quantification of global nitrous oxide sources and sinks. *Nature*, *586*(7828), 248-256. https://doi.org/10.1038/s41586-020-2780-0

Tian, H., Yang, J., Lu, C., Xu, R., Canadell, J. G., Jackson, R. B., Arneth, A., Chang, J., Chen, G., Ciais, P., Gerber, S., Ito, A., Huang, Y., Joos, F., Lienert, S., Messina, P., Olin, S., Pan, S., Peng, C., . . . Zhu, Q. (2018). The Global N2O Model Intercomparison Project. *Bulletin of the American Meteorological Society*, *99*(6), 1231-1251. https://doi.org/10.1175/bams-d-17-0212.1

Tian, H., Yang, J., Xu, R., Lu, C., Canadell, J. G., Davidson, E. A., Jackson, R. B., Arneth, A., Chang, J., & Ciais, P. (2019). Global soil nitrous oxide emissions since the preindustrial era estimated by an ensemble of terrestrial biosphere models: Magnitude, attribution, and uncertainty. *Global change biology*, *25*(2), 640-659.

van Lent, J., Hergoualc'h, K., & Verchot, L. V. (2015). Reviews and syntheses: Soil N₂O and NO emissions from land use and land-use change in the tropics and subtropics: a meta-analysis. *Biogeosciences*, *12*(23), 7299-7313. https://doi.org/10.5194/bg-12-7299-2015

Verhoeven, E., Barthel, M., Yu, L., Celi, L., Said-Pullicino, D., Sleutel, S., Lewicka-Szczebak, D., Six, J., & Decock, C. (2019). Early season N2O emissions under variable water management in rice systems: source-partitioning emissions using isotope ratios along a depth profile. *Biogeosciences*, *16*(2), 383-408. https://doi.org/10.5194/bg-16-383-2019

Wang, H., Shen, M., Hui, D., Chen, J., Sun, G., Wang, X., Lu, C., Sheng, J., Chen, L., Luo, Y., Zheng, J., & Zhang, Y. (2019). Straw incorporation influences soil organic carbon sequestration, greenhouse gas emission, and crop yields in a Chinese rice (Oryza sativa L.) –wheat (Triticum aestivum L.) cropping system. *Soil and Tillage Research*, *195*, 104377. https://doi.org/https://doi.org/10.1016/j.still.2019.104377

Wang, L., Li, K., Sheng, R., Li, Z., & Wei, W. (2019). Remarkable N2O emissions by draining fallow paddy soil and close link to the ammonium-oxidizing archaea communities. *Scientific Reports*, *9*(1), 2550. https://doi.org/10.1038/s41598-019-39465-y

Wang, Q., Zhou, F., Shang, Z., Ciais, P., Winiwarter, W., Jackson, R. B., Tubiello, F. N., Janssens-Maenhout, G., Tian, H., Cui, X., Canadell, J. G., Piao, S., & Tao, S. (2020). Data-driven estimates of global nitrous oxide emissions from croplands. *National Science Review*, *7*(2), 441-452. https://doi.org/10.1093/nsr/nwz087

Wang, Y., Guo, J., Vogt, R. D., Mulder, J., Wang, J., & Zhang, X. (2018). Soil pH as the chief modifier for regional nitrous oxide emissions: New evidence and implications for global estimates and mitigation. *Global Change Biology*, *24*(2), E617-E626. https://doi.org/10.1111/gcb.13966

Wang, Z., Zhang, X., Liu, L., Wang, S., Zhao, L., Wu, X., Zhang, W., & Huang, X. (2020). Inhibition of methane emissions from Chinese rice fields by nitrogen deposition based on the DNDC model. *Agricultural Systems*, *184*, 102919. https://doi.org/https://doi.org/10.1016/j.agsy.2020.102919

Wang, Z., Zhang, X., Liu, L., Wang, S., Zhao, L., Wu, X., Zhang, W., & Huang, X. (2021). Estimates of methane emissions from Chinese rice fields using the DNDC model. *Agricultural and Forest Meteorology*, *303*, 108368. https://doi.org/https://doi.org/10.1016/j.agrformet.2021.108368

Weller, S., Janz, B., Jörg, L., Kraus, D., Racela, H. S. U., Wassmann, R., Butterbach-Bahl, K., & Kiese, R. (2016). Greenhouse gas emissions and global warming potential of traditional and diversified tropical rice rotation systems [https://doi.org/10.1111/gcb.13099]. *Global change biology*, *22*(1), 432-448. https://doi.org/https://doi.org/10.1111/gcb.13099

Weller, S., Kraus, D., Ayag, K. R. P., Wassmann, R., Alberto, M. C. R., Butterbach-Bahl, K., & Kiese, R. (2015). Methane and nitrous oxide emissions from rice and maize production in diversified rice cropping systems. *Nutrient Cycling in Agroecosystems*, *101*(1), 37-53. https://doi.org/10.1007/s10705-014-9658-1

Willmott, C. J. (1981). On the Validation of Model. *Physical Geography*, *2*(2), 219-232.

Wu, D., Dong, W., Oenema, O., Wang, Y., Trebs, I., & Hu, C. (2013). N2O consumption by low-nitrogen soil and its regulation by water and oxygen. *Soil Biology and Biochemistry*, *60*, 165-172. https://doi.org/https://doi.org/10.1016/j.soilbio.2013.01.028

Wu, L., Tang, S., He, D., Wu, X., Shaaban, M., Wang, M., Zhao, J., Khan, I., Zheng, X., Hu, R., & Horwath, W. R. (2017). Conversion from rice to vegetable production increases N2O emission via increased soil organic matter mineralization. *Science of The Total Environment*, *583*, 190-201. https://doi.org/https://doi.org/10.1016/j.scitotenv.2017.01.050

Wu, X., Liu, H., Fu, B., Wang, Q., Xu, M., Wang, H., Yang, F., & Liu, G. (2017). Effects of land-use change and fertilization on N2O and NO fluxes, the abundance of nitrifying and denitrifying microbial communities in a hilly red soil region of southern China. *Applied Soil Ecology*, *120*, 111-120. https://doi.org/https://doi.org/10.1016/j.apsoil.2017.08.004

Wu, X., Wang, W., Xie, X., Hou, H., & Yin, C. (2018). Response of N2O emission to straw retention under two contrasting paddy water conditions: a field experiment over rice–rice-fallow rotation. *Paddy and Water Environment*, *16*(1), 199-205. https://doi.org/10.1007/s10333-017-0621-z

Xie, Y., Zhang, M., Xiao, W., Zhao, J., Huang, W., Zhang, Z., Hu, Y., Qin, Z., Jia, L., Pu, Y., Chu, H., Wang, J., Shi, J., Liu, S., & Lee, X. (2022). Nitrous oxide flux observed with tall-tower eddy covariance over a heterogeneous rice cultivation landscape. *Science of the Total Environment*, *810*, 152210. https://doi.org/https://doi.org/10.1016/j.scitotenv.2021.152210

Xiong, Z. Q., Xing, G. X., & Zhu, Z. L. (2006). Water dissolved nitrous oxide from paddy agroecosystem in China. *Geoderma*, *136*(3), 524-532. https://doi.org/https://doi.org/10.1016/j.geoderma.2006.04.010

Xu, P., Han, Z., Wu, J., Li, Z., Wang, J., & Zou, J. (2022). Emissions of Greenhouse Gases and NO from Rice Fields and a Peach Orchard as Affected by N Input and Land-Use Conversion. *Agronomy*, *12*(8), 1850. https://www.mdpi.com/2073-4395/12/8/1850

Xu, P., Jiang, M., Khan, I., Shaaban, M., Zhao, J., Yang, T., & Hu, R. (2023). The effect of upland crop planting on field N2O emission from rice-growing seasons: A case study comparing rice-wheat and rice-rapeseed rotations. *Agriculture, Ecosystems & Environment*, *347*, 108365. https://doi.org/https://doi.org/10.1016/j.agee.2023.108365

Xu, R., Tian, H., Pan, S., Prior, S. A., Feng, Y., & Dangal, S. R. S. (2020). Global N2O Emissions From Cropland Driven by Nitrogen Addition and Environmental Factors: Comparison and Uncertainty Analysis [https://doi.org/10.1029/2020GB006698]. *Global Biogeochemical Cycles*, *34*(12), e2020GB006698. https://doi.org/https://doi.org/10.1029/2020GB006698

Yan, X., & Akiyama, H. (2018). Overestimation of N2O mitigation potential by water management in rice paddy fields. *Proceedings of the National Academy of Sciences*, *115*(48), E11204-E11205. https://doi.org/10.1073/pnas.1816208115

Yang, H., Sheng, R., Zhang, Z., Wang, L., Wang, Q., & Wei, W. (2016). Responses of nitrifying and denitrifying bacteria to flooding-drying cycles in flooded rice soil. *Applied Soil Ecology*, *103*, 101-109. https://doi.org/https://doi.org/10.1016/j.apsoil.2016.03.008

Yang, Y., Meng, T., Qian, X., Zhang, J., & Cai, Z. (2017). Evidence for nitrification ability controlling nitrogen use efficiency and N losses via denitrification in paddy soils. *Biology and Fertility of Soils*, *53*(3), 349-356. https://doi.org/10.1007/s00374-017-1185-1

Yao, Y., Han, B., Liu, B., Wang, Y., Su, X., Ma, L., Zhang, T., Niu, S., Chen, X., & Li, Z. (2023). Global variations and controlling factors of anammox rates [https://doi.org/10.1111/gcb.16715]. *Global change biology*, *n/a*(n/a).

https://doi.org/https://doi.org/10.1111/gcb.16715

Yao, Z., Zheng, X., Dong, H., Wang, R., Mei, B., & Zhu, J. (2012). A 3-year record of N2O and CH4 emissions from a sandy loam paddy during rice seasons as affected by different nitrogen application rates. *Agriculture, Ecosystems & Environment*, *152*, 1-9. https://doi.org/https://doi.org/10.1016/j.agee.2012.02.004

Yao, Z., Zhou, Z., Zheng, X., Xie, B., Mei, B., Wang, R., Butterbach-Bahl, K., & Zhu, J. (2010). Effects of organic matter incorporation on nitrous oxide emissions from rice-wheat rotation ecosystems in China. *Plant and Soil*, *327*(1), 315-330. https://doi.org/10.1007/s11104-009-0056-4

Ye, R., & Horwath, W. R. (2016). Nitrous oxide uptake in rewetted wetlands with contrasting soil organic carbon contents. *Soil Biology and Biochemistry*, *100*, 110-117. https://doi.org/https://doi.org/10.1016/j.soilbio.2016.06.009

Zeng, X., Han, B., Xu, F., Huang, J., Cai, H., & Shi, L. (2012). Effects of modified fertilization technology on the grain yield and nitrogen use efficiency of midseason rice. *Field Crops Research*, *137*, 203-212. https://doi.org/https://doi.org/10.1016/j.fcr.2012.08.012

Zhang, A., Cui, L., Pan, G., Li, L., Hussain, Q., Zhang, X., Zheng, J., & Crowley, D. (2010). Effect of biochar amendment on yield and methane and nitrous oxide emissions from a rice paddy from Tai Lake plain, China. *Agriculture, Ecosystems & Environment*, *139*(4), 469-475. https://doi.org/https://doi.org/10.1016/j.agee.2010.09.003

Zhang, G., Xiao, X., Dong, J., Xin, F., Zhang, Y., Qin, Y., Doughty, R. B., & Moore, B. (2020). Fingerprint of rice paddies in spatial–temporal dynamics of atmospheric methane concentration in monsoon Asia. *Nature Communications*, *11*(1), 554. https://doi.org/10.1038/s41467-019-14155-5

Zhang, G., Yu, H., Fan, X., Yang, Y., Ma, J., & Xu, H. (2016). Drainage and tillage practices in the winter fallow season mitigate CH4 and N2O emissions from a double-rice field in China. *Atmos. Chem. Phys.*, *16*(18), 11853-11866. https://doi.org/10.5194/acp-16-11853-2016

Zhang, H.-L., Bai, X.-L., Xue, J.-F., Chen, Z.-D., Tang, H.-M., & Chen, F. (2013). Emissions of CH4 and N2O under Different Tillage Systems from Double-Cropped Paddy Fields in Southern China. *PLOS ONE*, *8*(6), e65277. https://doi.org/10.1371/journal.pone.0065277

Zhang, K., Peng, C., Wang, M., Zhou, X., Li, M., Wang, K., Ding, J., & Zhu, Q. (2017). Process-based TRIPLEX-GHG model for simulating N2O emissions from global forests and grasslands: Model development and evaluation. *Journal of Advances in Modeling Earth Systems*, *9*(5), 2079-2102. https://doi.org/https://doi.org/10.1002/2017MS000934

Zhang, K., Zhu, Q., Liu, J., Wang, M., Zhou, X., Li, M., Wang, K., Ding, J., & Peng, C. (2019). Spatial and temporal variations of N2O emissions from global forest and grassland ecosystems. *Agricultural and Forest Meteorology*, *266-267*, 129-139. https://doi.org/https://doi.org/10.1016/j.agrformet.2018.12.011

Zhao, X., Zhou, Y., Min, J., Wang, S., Shi, W., & Xing, G. (2012). Nitrogen runoff dominates water nitrogen pollution from rice-wheat rotation in the Taihu Lake region of China. *Agriculture, Ecosystems & Environment*, *156*, 1-11. https://doi.org/https://doi.org/10.1016/j.agee.2012.04.024

Zhou, M., Wang, X., Wang, Y., & Zhu, B. (2018). A three-year experiment of annual methane and nitrous oxide emissions from the subtropical permanently flooded rice paddy fields of China: Emission factor, temperature sensitivity and fertilizer nitrogen effect. *Agricultural and Forest Meteorology*, *250-251*, 299-307. https://doi.org/https://doi.org/10.1016/j.agrformet.2017.12.265

Zhou, M., Zhu, B., Brüggemann, N., Wang, X., Zheng, X., & Butterbach-Bahl, K. (2015). Nitrous oxide and methane emissions from a subtropical rice–rapeseed rotation system in China: A 3-year field case study. *Agriculture, Ecosystems & Environment*, *212*, 297-309. https://doi.org/https://doi.org/10.1016/j.agee.2015.07.010

Zhou, M., Zhu, B., Butterbach-Bahl, K., Wang, X., & Zheng, X. (2014). Nitrous oxide emissions during the non-rice growing seasons of two subtropical rice-based rotation systems in southwest China. *Plant and Soil*, *383*(1), 401-414. https://doi.org/10.1007/s11104-014-2174-x

Zhou, M., Zhu, B., Wang, X., & Wang, Y. (2017). Long-term field measurements of annual methane and nitrous oxide emissions from a Chinese subtropical wheat-rice rotation system. *Soil Biology and Biochemistry*, *115*, 21-34. https://doi.org/https://doi.org/10.1016/j.soilbio.2017.08.005

Zhou, S., Sakiyama, Y., Riya, S., Song, X., Terada, A., & Hosomi, M. (2012). Assessing nitrification and denitrification in a paddy soil with different water dynamics and applied liquid cattle waste using the 15N isotopic technique. *Science of The Total Environment*, *430*, 93-100. https://doi.org/https://doi.org/10.1016/j.scitotenv.2012.04.056

Zhou, W., Xia, L., & Yan, X. (2017). Vertical distribution of denitrification end-products in paddy soils. *Science of The Total Environment*, *576*, 462-471. https://doi.org/https://doi.org/10.1016/j.scitotenv.2016.10.135

Zhu, G., Wang, S., Wang, Y., Wang, C., Risgaard-Petersen, N., Jetten, M. S. M., & Yin, C. (2011). Anaerobic ammonia oxidation in a fertilized paddy soil. *The ISME Journal*, *5*(12), 1905-1912. https://doi.org/10.1038/ismej.2011.63

Zhu, Q., Liu, J., Peng, C., Chen, H., Fang, X., Jiang, H., Yang, G., Zhu, D., Wang, W., & Zhou, X. (2014). Modelling methane emissions from natural wetlands by development and application of the TRIPLEX-GHG model. *Geosci. Model Dev.*, *7*(3), 981-999. https://doi.org/10.5194/gmd-7-981-2014

Zhu, Q., Peng, C., Ciais, P., Jiang, H., Liu, J., Bousquet, P., Li, S., Chang, J., Fang, X., Zhou, X., Chen, H., Liu, S., Lin, G., Gong, P., Wang, M., Wang, H., Xiang, W., & Chen, J. (2017). Interannual variation in methane emissions from tropical wetlands triggered by repeated El Niño Southern Oscillation. *Global change biology*, *23*(11), 4706-4716. https://doi.org/https://doi.org/10.1111/gcb.13726

Zou, J., Huang, Y., Qin, Y., Liu, S., Shen, Q., Pan, G., Lu, Y., & Liu, Q. (2009). Changes in fertilizer-induced direct N2O emissions from paddy fields during rice-growing season in China between 1950s and 1990s. *Global change biology*, *15*(1), 229-242. https://doi.org/https://doi.org/10.1111/j.1365-2486.2008.01775.x

Zou, J., Huang, Y., Zheng, X., & Wang, Y. (2007). Quantifying direct N2O emissions in paddy fields during rice growing season in mainland China: Dependence on water regime. *Atmospheric Environment*, *41*(37), 8030-8042. https://doi.org/https://doi.org/10.1016/j.atmosenv.2007.06.049

Chapter V:

Projection of nitrous oxide emissions from global agricultural ecosystems under future climate change and management practices

Hanxiong Song and Changhui Peng

To be submitted to *Earth's Future*

5.1 Résumé

Une prévision fiable des émissions futures de protoxyde d'azote (N_2O) est essentielle pour les politiques d'atténuation du climat. Cependant, notre compréhension actuelle de l'ampleur des émissions mondiales de N_2O face aux changements futurs du climat et des pratiques de gestion reste insuffisante. Dans cette étude, nous avons étudié l'évolution des schémas spatio-temporels des émissions de N_2O des sols agricoles mondiaux de 2015 à 2100 et quantifié la contribution des changements climatiques sous trois scénarios de Voies Socioéconomiques Partagées (SSP), pour la première fois en utilisant un modèle biogéochimique basé sur les processus, TRIPLEX-GHG v2.0, à une résolution spatiale de 0.25°. Nos simulations suggèrent des tendances à la hausse des émissions des émissions de N_2O agricoles, qui devraient atteindre 8.61 à 11.42 Tg N an^{-1}, soit une augmentation de 27.0 à 71.0 % par rapport à la période de référence entre 2015 et 2100, avec les émissions les plus importantes potentiellement sous le scénario intermédiaire (SSP2-4.5). Les terres cultivées en milieu sec sont identifiées comme la principale source d'émissions agricoles de N_2O à l'échelle mondiale, en particulier pour les nations en développement. Bien que les engrais azotés restent le facteur clé contrôlant les variations des émissions de N_2O agricoles, les futurs changements climatiques devraient contribuer à une augmentation globale de 0.41 Tg N an^{-1}. De plus, les effets du changement climatique devraient varier selon les différents écosystèmes, qui atténuent les émissions de N_2O dans les sols intensivement gérés mais tendent à présenter des effets négatifs pour les prairies. Cette projection souligne l'importance de la gestion agricole et du changement climatique dans la détermination des schémas futurs d'émissions de N_2O. La redistribution mondiale des apports en azote agricole, en fonction des changements climatiques locaux, jouerait un rôle essentiel dans la réduction des émissions de N_2O des écosystèmes agricoles mondiaux.

5.2 Abstract

Reliable prediction of future nitrous oxide (N_2O) emissions is crucial for climate mitigation policies. However, our current understanding of the magnitude of global N_2O emissions with future changes in both climate and management is still lacking. In this study, we investigated the evolution of spatiotemporal patterns of global agricultural soil N_2O emissions from 2015 to 2100 and quantified the contribution of climate changes under three Shared Socioeconomic Pathway (SSP) scenarios, for the first time using a process-based biogeochemical model, TRIPLEX-GHGv2.0 at 0.25° spatial resolution. Our simulations suggest increasing trends of agricultural N_2O emissions, which are projected to rise to 8.61 – 11.42 Tg N yr^{-1} by 27.0 – 71.0% relative to reference period during 2015 – 2100, with the largest emissions potentially occurring under intermediate pathway (SSP2-4.5). Upland croplands are identified as the dominant source of agricultural N_2O emissions globally, in particular for developing nations. Although N fertilizer remains for the key factor controlling variations in agricultural N_2O emissions, future changing climates would contribute an overall increase of 0.41 Tg N yr^{-1}. In addition, climate change effects are projected to vary across different ecosystems which buffer N_2O emissions with intensive managed soils but tend to present negative effects for rangelands. This projection highlights the importance of agricultural management and climate change in determining future N_2O emission patterns. Global redistribution of agricultural N inputs, depending on local climate changes, would play an essential role in mitigating N_2O emissions from global agricultural ecosystems.

5.3 Introduction

Nitrous oxide (N_2O) is the third largest greenhouse gases (GHGs) source of anthropogenic warming, with a global warming potential 265 – 298 times larger than that of CO_2 in 100-year horizon (IPCC, 2021). The atmospheric concentration of N_2O has increased significantly by ~20 % since the industrial revolution (i.e., 270 parts per billion, ppb in 1800 to 331 ppb in 2018) (Tian et al., 2020). As a by-product of the nitrogen cycle in the biosphere (e.g., nitrification and denitrification), terrestrial ecosystem soils are the primary source of N_2O emissions, with agricultural soils contributing ~ 45% of total in the early 21st century and likely to increase until the end of this century (Davidson & Kanter, 2014; Gong et al., 2024; Tian et al., 2020). Growing N_2O emission could pose a substantial threat to meeting the 1.5 – 2 °C climate target, maintaining stratospheric ozone, and thus human health in the future (Lawrence et al., 2021; Portmann et al., 2012).

Mitigating N_2O emissions is challenging due to global climate, environmental and management changes. Previous in-situ continuous monitoring and inverse modelling in extensively managed agricultural regions have shown a strong sensitivity of soil N_2O production and emission to changing climate, which tend to be significantly stimulated under warmer and wetter conditions (Griffis et al., 2017; Gu et al., 2023). However, inconsistent responses of soil N_2O have also been reported in several regions and ecosystems, indicating strong spatial heterogeneity of effect of climate change on N_2O emissions (Li et al., 2020; Ren et al., 2023). For instance, negative effects of warming to soil N_2O fluxes have been widely observed across Qinghai-Tibetan Plateau (Zhang et al., 2022). Negative to insignificant differences in N_2O emissions under larger precipitation regimes were recorded in semiarid and arid soils (Li et al., 2022; Shi et al., 2021). In addition, elevated atmospheric CO_2 concentrations also present divergent impacts on N_2O emissions across different biome and climate types, although most experiment results in croplands indicate enhanced N_2O emissions across the globe (Cui et al., 2023; Wang et al., 2021; Yao et al., 2021).

As a hotspot of soil N_2O emissions, N_2O fluxes in agricultural ecosystems are not only controlled by local climates, soil properties, and vegetation, but nowadays more importantly being driven by expanded agricultural lands and associated management practices (Butterbach-Bahl et al., 2013; Liao et al., 2022). As a N-trace gas, variations in total soil N_2O emissions are dominated by shifts in N inputs, particularly in managed ecosystems (Thompson et al., 2019). Increases in N fertilizer, manure application, and agricultural land area is likely to pose larger challenges to global N_2O mitigation in response to the constantly growing global population (Jones & O'Neill, 2016; Mueller et al., 2012; Reay et al., 2012). Soil N enrichment in less-managed soils caused by higher atmospheric N deposition rates also significantly enhances N_2O emissions (Shen & Zhu, 2022). In the future, these major transitions in soil nutrient and biogeochemical status are likely to interact with changing climate (e.g., warming), buffering the N induced stimulation of N_2O production and emissions at a global scale (Reay et al., 2012; Thompson et al., 2019).

In the past decade, policy circles began recognizing the significance of explicitly addressing N_2O mitigation to achieve sustainable development (Kanter et al., 2020). Various management strategies have been proposed and tested at sites to country levels to reduce reactive N, especially N_2O emissions from agriculture, achieving early-stage progress in some cases (Cui et al., 2022; Pan et al., 2022). Effective natural-based solution of mitigation for N_2O emissions requires quantitative understanding of the sources and how they may change in future. The overall magnitudes of effects of these management need careful assessment or comparison on a large scale (Ma et al., 2023). However, recent efforts have not drove enough attention to evaluating potential global N_2O emission scenarios under the projected future climate change (Kanter et al., 2020; Zhang et al., 2024). Since the CMIP6 provides a value opportunity by integrating both management and environmental changes (O'Neill et al., 2016), this study aims to project future global agricultural N_2O emissions at a spatial resolution of 0.25° under multiple scenarios utilizing a process-based biogeochemical model, TRIPLEX-GHGv2.0. We first provide an estimated range of N_2O emissions from global agricultural ecosystems in the future under different climate and management change scenarios. Next, we explicitly evaluate and compare the contribution of climate change and management effects. This study offers opportunities to systematically understand possible responses and mitigation potential of N_2O emission from global agricultural ecosystems to meet the 2 °C target and sustainable development goals.

5.4 Data and Methods

5.4.1 Climate, soil, and environment datasets

Daily meteorological data during the period from 1950 to 2100 at 0.25° spatial resolutions across the globe, were obtained from the NASA Earth Exchange Global Daily Downscaled Projections (NEX-GDDP-CMIP6) (Thrasher et al., 2022). This dataset has undergone bias-correction based on climate data (1901-2020) from the Climate Research Unit-National Center for Environmental Prediction 6-hourly climate data sets (Viovy, 2018; https://rda.ucar.edu/datasets/ds314.3/). Two CMIP6 Global Climate Models (GCMs, including ACCESS-CM2 and GFDL-ESM4) under three Shared Socio-economic Pathways-Representative Concentration Pathways (SSP-RCPs) were included at current stage. Because these two model products provide complete dataset covering the whole study period, which is required for forcing TRIPLEX-GHGv2.0, including daily maximum, minimum air temperature, mean surface temperature (K), precipitation (mm s^{-1}), specific humidity (g g^{-1}), and wind speed (m s^{-1}).

Regarding three SSP-RCPs (hereafter SSPs for consistency), SSP1-2.6, SSP2-4.5, and SSP5-8.5

were selected to represent the sustainable, the intermediate, and the most extreme pathway, respectively. SSP1-2.6 projects a future under a green growth paradigm which combines high economic growth, improvements in technologies and agriculture, and climate mitigation policies, constraining radiative forcing at 2.6 W m^{-2} (~ 2 °C warming) before 2100 (van Vuuren et al., 2017). SSP2-4.5, the 'middle of the road' scenario, describes a future where the world has relatively modest outcomes in mitigating climate change (Riahi et al., 2017). SSP2 envisions trends in social, economic, and technological development do not deviate significantly from historical patterns and RCP4.5 implies a stabilization of radiative forcing at 4.5 W m^{-2} by 2100. Finally, the scenario SSP5-8.5 projects a radiative forcing close to RCP8.5 due to high levels of fossil fuel use over the course of the century. Meanwhile, SSP5 denotes a rapid development in economic, technological, and agricultural progress to meet demand of up to doubling population (Kriegler et al., 2017).

Soil physical and chemical properties of different layers were extracted from Harmonized World Soils Database version 2.0 (https://gaez.fao.org/pages/hwsd). Major variables include soil sand, clay content, pH, soil organic carbon content (SOC), and C:N ratio.

Global monthly atmospheric NHx and NOy deposition during both historical and future periods were downloaded from the Inter-Sectoral Impact Model Intercomparison Project (ISIMIP) Repository generated by International Global Atmospheric Chemistry (IGAC)/Stratospheric Processes and Their Role in Climate (SPARC) Chemistry–Climate Model Initiative (CCMI) N deposition fields. We used monthly gridded atmospheric CO_2 concentration data to better assess the possible spatial, seasonal and interannual variations in effects of nonuniform distributed rising CO_2 (Cheng et al., 2022). The historical part of this dataset was reconstructed based on AGAGE and NOAA networks, firn and ice core data, and Carbon Dioxide Information Analysis Centre (CDIAC). The CMIP6 future scenarios are interpolated temporally and spatially based on the features of CO_2 distributions and the seasonal cycle of current monthly atmospheric CO_2 concentrations distributions from 2015 to 2100.

5.4.2 Agricultural management input datasets

For land use data, model initialization used vegetation cover data from the Global Land Cover Map for 2009 (GlobCover2009) with the ecoregions framework from the World Wildlife Fund (WWF). Both historical and future land use data (i.e., croplands and pasturelands fractions etc.) were obtained from Land-Use Harmonization 2 (LUH2) (Hurtt et al., 2020). Specifically, across all three scenarios, global cropland area exhibit general increasing trends while total area of pastures, rangelands, and rice-paddies present decreasing trends, during 2015 – 2100 (Figure 5. S1).

Agricultural managements, especially anthropogenic N inputs, are vital for simulating soil N_2O emissions. Historical chemical N fertilizer applications on croplands were extracted by combining International Fertilizer Agency (IFA) country-level inventory, IFA crop-specific N fertilizer use rate, and crop type distribution map. N fertilizer applied on pasturelands were based on country level proportion of total fertilizer allocated to grasslands (FAOSTAT 2018).

Future gridded annual N fertilizer application rates on croplands were based on LUH2 outputs (i.e., weighted mean by combining national fertilizer application rates in kgN ha^{-1} yr^{-1} per crop functional type and grid fraction of different crop function types) and a fixed cropping intensity map (1 to 3 times yr^{-1}). Cropping intensity represents the annual number of crops harvested on cropland relying on MIRCA2000 method which is based on the ratio of harvested area to total cropland area (Portmann et al., 2010). The outcome is generally consistent with existing global datasets (Franke et al., 2020; Zhang et al., 2021). Despite changing climate, policies, and management, the probability of maintaining original cropping intensity is much greater than transiting to different patterns, particularly in major agriculture regions (e.g., China and India) for the future (Yibin Wang et al., 2024). This approach allows for defining spatialized fertilizer application dates based on specific crop calendars, cropping area and intensity (i.e., one basal fertilizer application and one topdressing for each cropping season, accounting 60% and 40% of total N rate, respectively) (Nishina et al., 2017). Notably, this study specifically considered managements associated with winter wheat growth which has a distinct phenology compared with other vegetation (not just cereal crops, following GGCMI phase 2 experiment). For future N fertilizer use in pasturelands, the mean historical fertilization of croplands to pasturelands ratios in different continents was applied with future fertilizer rates on C3/C4 crops provided by LUH2 (Lassaletta et al., 2014). The fertilization timing for global pasturelands is consistent with the previous study by Song et al. (2023). Specifically, we differentiated chemical N fertilizer into ammonium N (NH_4^+-N) and nitrate N (NO_3^--N) based on country-level fertilizer NH_4^+ fraction provided by Nishina et al. (2017). Due to lacking in this dataset, this study assumed the NH_4^+/ NO_3^- ratios stay at constant level of 2014 during projections.

For both historical and future fertilizer usage, we differentiated ammonium N (NH_4^+-N) and nitrate N (NO_3^--N) fertilizer applications based on country-level fertilizer NH_4^+ fraction provided by Nishina et al. (2017) and we assume the NH_4^+/ NO_3^- ratios stay constant after 2015.

Regarding another important external N inputs, global spatialized manure N applied on croplands and pasturelands, historical datasets (prior to 2015) were generated on the basis of N production from manure in six livestock and poultry groups and FAOSTAT (Xu et al., 2019; B. Zhang et al., 2017). To construct future manure application rates (post 2015), we simply assumed that they follow the same trends of annual synthetic N fertilizer application changes during 2015—2100 across different continents. Livestock deposited manure N on grazing lands (pasturelands and rangelands) is an important soil nutrient supply for those ecosystems. Historical manure N depositions on grazing lands (1850—2015) was extracted from Xu et al. (2019). Given the significant correlation between world population (https://ourworldindata.org/population-growth) and livestock counts (https://ourworldindata.org/grapher/livestock-counts; $r = 0.25$, $p < 0.0001$), we build the projected livestock manure N deposition by applying the variation trends of human population in each continent to historical data under respective SSPs scenarios (Jones & O'Neill, 2016).

All input datasets used in this study were transformed into a spatial resolution of 0.25° conducted by R (v.4.3; R Core Team 2023)

5.4.3 The TRIPLEX-GHG model v2.0

The TRIPLEX-GHGv2.0 was used to simulate the dynamics of N_2O emissions and impacts of climate changes. TRIPLEX-GHGv2.0 is a process-based global ecosystem model which couples the major land natural processes (heat, energy, and hydrology of land surface, plant phenology and physiology, soil biogeochemistry, long-term vegetation dynamics) and management practices (e.g., fertilization, harvesting, and irrigation) (Song et al., 2022; K. Zhang et al., 2017). TRIPLEX-GHGv2.0 describes soil N_2O production and emissions with different processes, including nitrification, denitrification, nitrifier denitrification, and anaerobic ammonium oxidation. The coupled C-N flows ensure the capability of model to reasonably reflect the dynamics of soil N_2O fluxes in various ecosystems under different environmental and management conditions, which has been extensively calibrated and validated against observation results globally.

Global simulations were conducted at a spatial resolution of 0.25 × 0.25° latitude/longitude from 1840 – 2100 using a high-performance computer system. The model simulations underwent an initial 300-year spin-up to obtain a relative equilibrium in soil carbon and nitrogen. For the period 1840 –

1950, the multi-year average meteorological data (1900 – 1920) were used. Simulations for subsequently years (post 1950) are driven by datasets described in above sections. In addition, the present study addressed the complexity of global agricultural ecosystems with four types: (upland) croplands, pastures (intensively managed grasslands), rangelands (extensively managed grasslands), and rice-paddies. The vegetation in our model was represented by plant functional types (PFTs) and three types of crops (C3, C4, and N-fixing crops), two types of grass (C3 and C4 grass), and rice were specifically included for croplands, grazing lands, and rice-based ecosystems, respectively.

5.5 Results

5.5.1 Temporal variations in projected N_2O emissions from 1950 to 2100

Between 1950 and 2014, global agricultural ecosystems contributed 5.09 ± 1.03 (mean ± 50%SD) Tg N_2O-N yr^{-1}. In general, modeled N_2O emission from global agricultural soils exhibit a growing trend but a shift was detected in 1991, suggesting a slight decrease and plateau during the early 2010s. This trend shows divergent changes under different SSPs scenarios (Figure 5.1).

From 2015 to 2100, the general increasing trends of global N_2O emission from agricultural ecosystems slow down and even reverse after the 2050s (9.44 ± 0.05) under the SSP5-8.5 scenario. This trajectory would result in a relatively low N_2O emissions from agricultural ecosystems globally at the end of this century (8.36 ± 0.11 Tg N yr^{-1}). However, under the SSP2-4.5 scenario, emissions are projected to continuously increase to 12.90 ± 0.23 Tg N yr^{-1} between 2060 and 2100 (a ~150% increase compared to the reference period), with a growth rate of 0.066 Tg N yr^{-2} ($p < 0.001$). In contrast, under the SSP1-2.6 scenario, global N_2O emissions from agricultural soils would present a moderate increasing trend (0.0062 Tg N yr^{-2}, $p < 0.001$) which leads to a generally smallest emission rate among scenarios (8.62 ± 0.15 Tg N yr^{-1}) during the projected future.

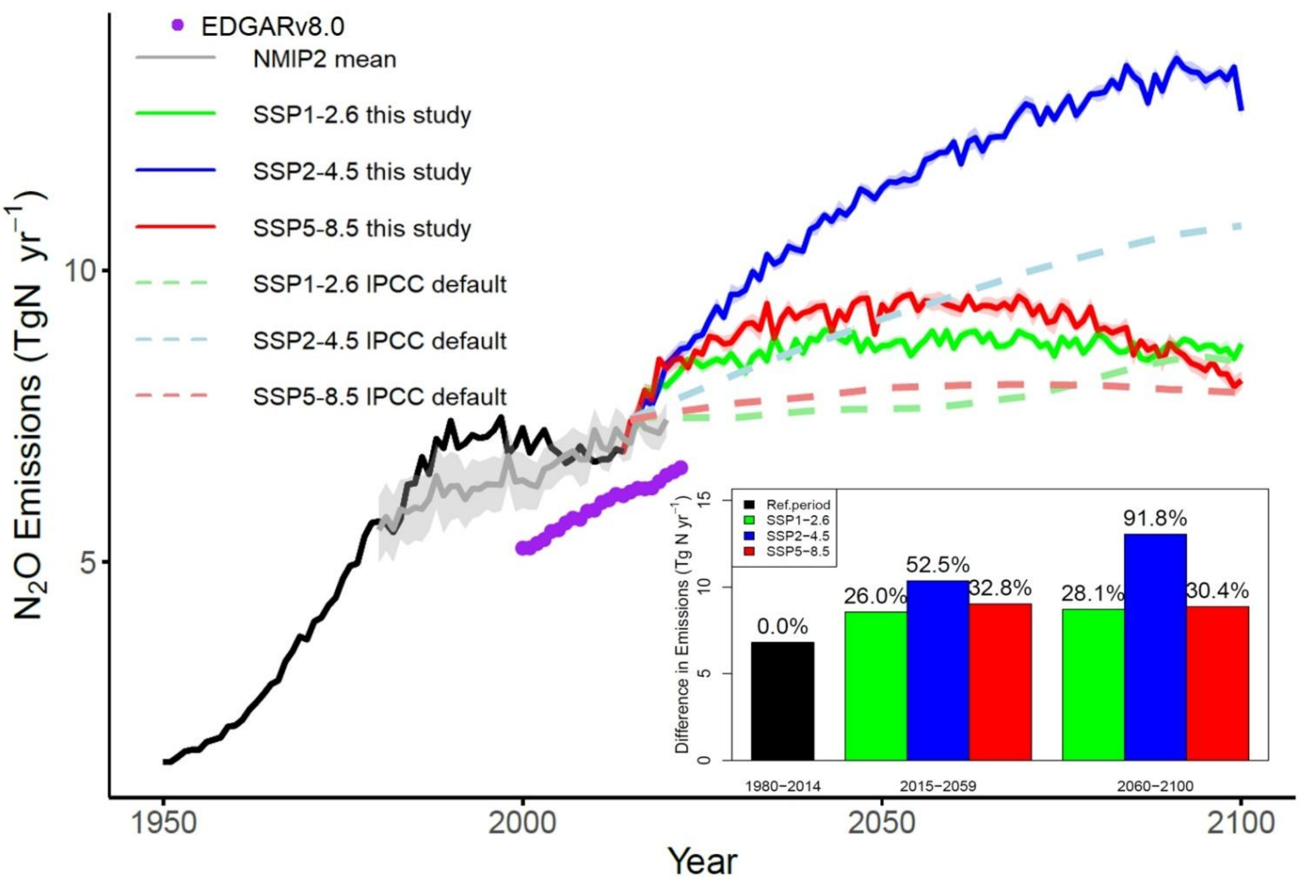

Figure 5.1 Temporal variation in N_2O emissions from global agricultural ecosystems during 1950 – 2100 under different SSP scenarios. The inset bar chart indicates the changes of projected N_2O emissions relative to reference period. The sloid grey line represents the ensemble mean of participating models of NIMP2; EDGARv8.0, the purple dots, are the most updated outcome of new Emissions Database for Global Atmospheric Research community GHG emissions database based on FAO statistics; dashed lines show the results estimated by IPCC default model (EF) with the same N management data used in our model simulations.

Upland croplands account for the largest source of annual agricultural N_2O emissions which are projected to increase across all three scenarios in the projected future (Figure 5.2a). They would slightly increase from 2.8 ± 0.77 Tg N yr^{-1} in the reference period to 6.31 ± 0.05 and 6.00 ± 0.13 Tg N yr^{-1} between 2060 and 2100 under scenarios SSP1-2.6 and SSP5-8.5, respectively. However, for SSP2-4.5, global cropland N_2O emission would drastically increase by 2-folds to 9.83 ± 0.28 Tg N yr^{-1} in 2015-2100 compared with reference period.

Conversely, since 2015, the predicted N_2O emissions from global grazing lands (pasture and rangeland) present consistent decreasing trends across all three projected scenarios. Under the sustainable pathway, modeled future grazing-lands N_2O emissions show the largest decrease at a rate of -0.012 Tg N yr-2 (1.78 Tg N yr^{-1} during 2015-2100, ~85% of the reference period). Therefore, emissions from both pasture and rangeland would rapidly return to the level of the 1970s at the middle of this century (~ 0.46 and 1.23 Tg N yr^{-1}, respectively). Under the intermediate and the most extreme pathways, estimated grazing-lands N_2O emissions only exhibit a slight or moderate reduction after 2015 (~ -0.005 and -0.004 Tg N yr-2 for SSP2-4.5 and SSP5-8.5, $p < 0.001$; Figure 5.2 b and c). Regarding global rice-based ecosystems, estimated future N_2O emissions are projected to reach 0.85 ± 0.05, 0.78 ± 0.06, and 0.77 ± 0.05 Tg N yr^{-1} for SSP1-2.6, 2-4.5, and 5-8.5 respectively, with insignificant difference among scenarios (Figure 5.2d).

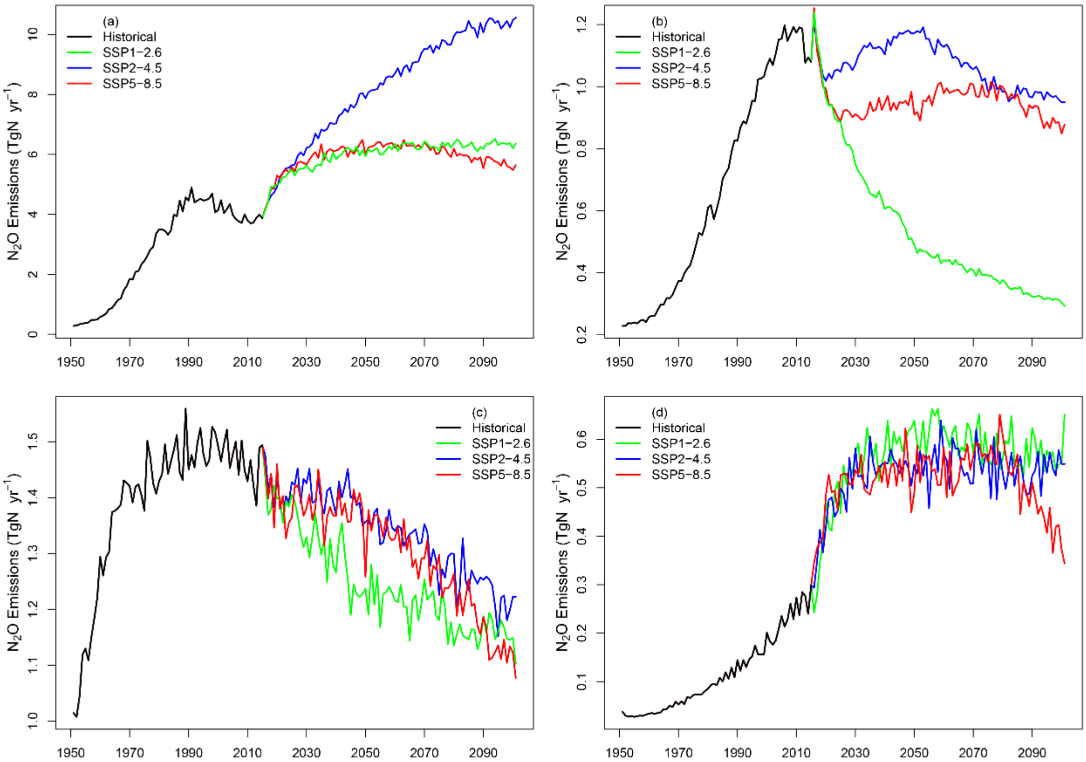

Figure 5.2 Temporal variation in annual N_2O emissions from upland croplands (a), pasture (b), rangelands (c), and rice-paddies (d) during 1950 – 2100.

5.5.2 Spatial variation patterns of projected N_2O emissions

Modeled N_2O emission from agroecosystems during the projected future exhibit strong spatial variations on a global scale and the variation patterns differ significantly among SSP scenarios. Between 2060 and 2100, our results suggest that eastern China, northeast India, and mid North America are consistent hotspot of N_2O emission from agricultural soils across three scenarios (i.e., >3 kg N ha^{-1} yr^{-1}, Figure 5.3.a,c,d). Moderate modeled N_2O fluxes would be observed in western Europe, south Brazil and Argentina for most of scenarios. Notably, under SSP2-4.5, an important character is that eastern Europe, including Ukraine, Turkey, and Russia, may become major N_2O emission hotspots after 2060 (Figure 5.3 c).

In comparison with the reference period (1980 – 2014), constant reductions in N_2O emissions would be identified in the Great Lake region in North America, western Europe and Xinjiang, China, under all three SSP scenarios (Figure 5.3 b,d,f). However, for most of the agricultural-intensive regions, modeled results suggested increases in projected N_2O emissions across SSPs, especially for mid-Canada, Argentina, northern India, Turkey, and Australia. Notably, agricultural N_2O emissions are predicted to decrease in Eastern Europe for both SSP1-2.6 and SSP5-8.5 whereas this region might be responsible for a large increase in predicted N_2O fluxes under SSP2-4.5 probably because the significantly enhanced N_2O fluxes in Ukraine and Russia (Fig.5.2 d).

Different agroecosystems types would present varying trends and play diverse roles in determining regional N_2O emissions in projected future. In general, N_2O emission from croplands are predicted to increase for most of the world under all three scenarios, especially for developing nations or regions (e.g., India, South America, southern Aisa, and Africa) (Figure 5.4 and Figure 5. S2). And this is responsible for the overall growing trend of total agricultural N_2O emissions in the projected future. For example, south Asia, South America and Africa may experience significant growth in both N_2O fluxes and total emissions under all SSPs (Figure 5.4 f, h, i). While the opposite trends may occur in Europe (Figure 5.4 d) where regional cropland N_2O emissions decrease by ~0.42 and 0.54 Tg N yr^{-1} for SSP1-2.6 and SSP5-8.5, respectively. The significant N_2O increase in croplands across the globe, ranging from 0.25 (India) to 1.99 (South America) Tg N yr^{-1} in the late 21st century, dominate the rapid increase in N_2O emissions under SSP2-4.5 scenarios (Figure 5.4).

In contrast, grazing lands, including both pastures and rangelands, tend to show smaller N_2O emissions than that of prior 2014 in the projected future. Globally, difference of pastures and rangelands N_2O emissions between 2060 – 2100 and 1980 – 2014 are -0.58 and -0.29, 0.05 and -0.20, -0.01 and -0.25 TgN yr^{-1} for SSP1-2.6, SSP2-4.5, and SSP5-8.5, respectively. Europe, North America and China would have substantial contribution to the declined trend of N_2O emission from global grazing lands which might be challenged by Africa where pasture N_2O emissions may increase by ~ 0.23 Tg N yr^{-1}under SSP5-8.5 (Figure 5.4 i). As for rice-based ecosystem, modeled results suggest increases in rice-based N_2O emissions globally are expected under climate changes in the 21st century which range from 0.40 to 0.52 TgN yr^{-1}. In particular, south Asia such as Vietnam and Thailand, is identified as the largest source for increasing rice- N_2O in the projected future, followed by India and China (Figure 5.4 b,c,f).

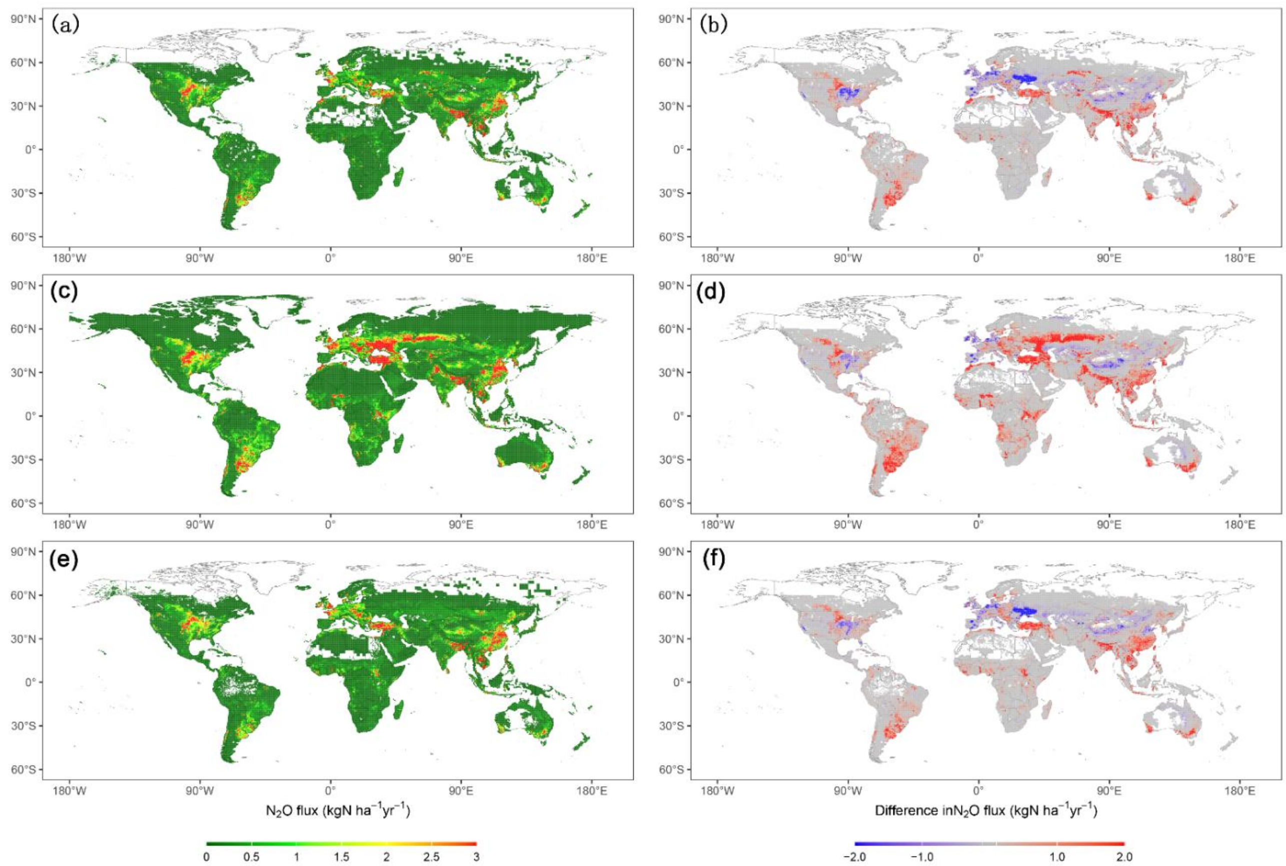

Figure 5.3 Spatial distribution of weighted mean N_2O emissions from agricultural soils globally from 2060 – 2100 under three SSPs (a, c, e for SSP1-2.6, SSP2-4.5, and SSP5-8.5, respectively) and their corresponding changes (b, d, f) relative to the reference period (1980 – 2014).

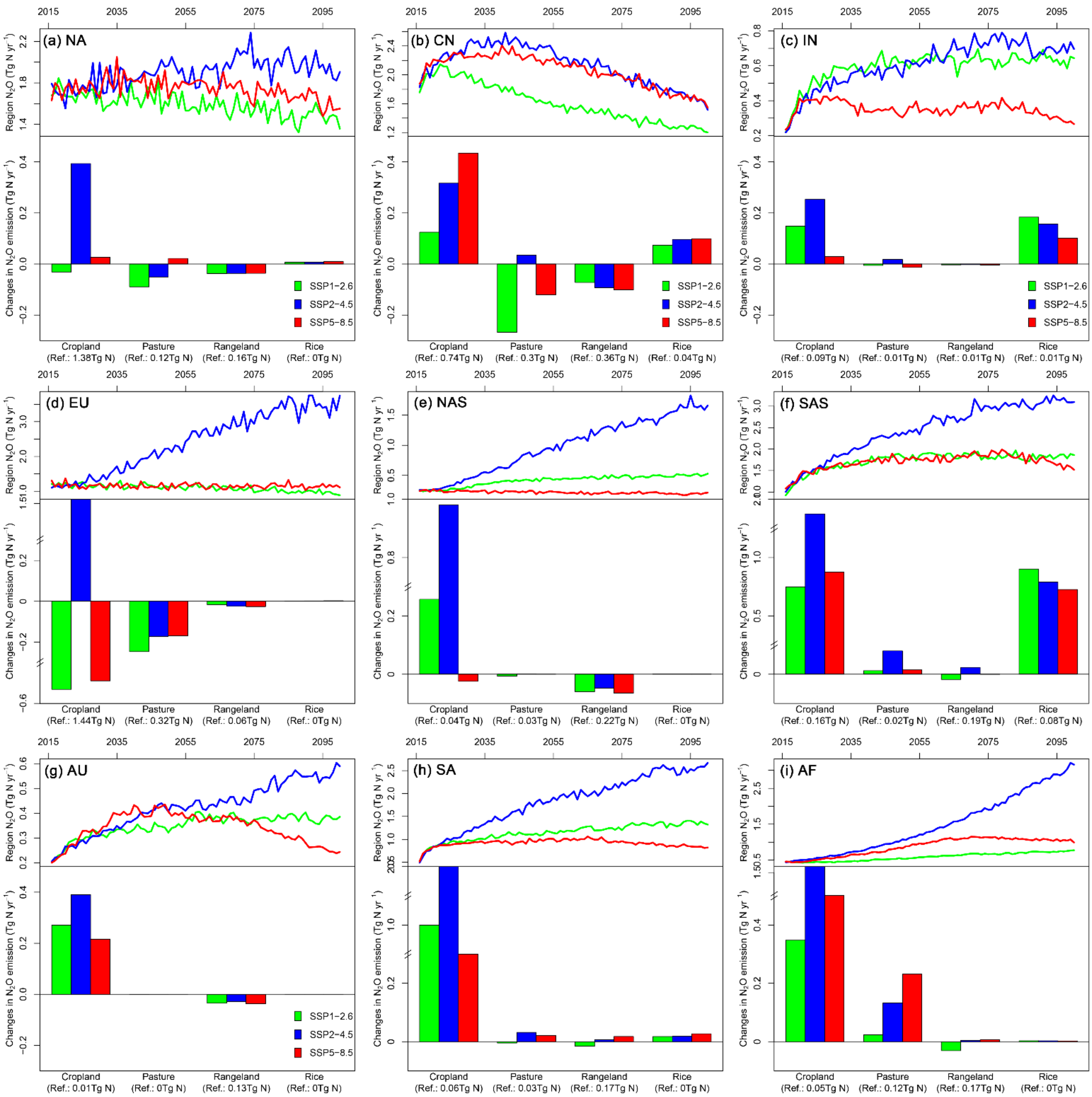

Figure 5.4 Regional total N_2O emissions from agricultural ecosystems during 2015 – 2100 (above line plot) and the changes in N_2O emission of different agroecosystem types in late 21st century (2060 – 2100) relative to mean of reference period (Ref.: 1980 – 2014). NA: North America, CN: China, IN: India, EU: Europe, NAS: North Asia (Mongolia and Siberia etc.), SAS: South Asia (Japan, Southeast Asia etc.), AU: Australia (include New Zealand), SA: South America, and AF: Africa.

5.5.3 Effect of climate change on N_2O emissions from agricultural ecosystems

By setting climate forcing data consistent since 2015, we quantified the climate change effects on agricultural soil N_2O emissions under the sustainable pathway (SSP1-2.6) and the extreme pathway, (SSP5-8.5). In general, changing climate is projected to enhance N_2O emissions from global agricultural ecosystems, increasing total emission by ~ 0.32 (± 0.09) and 0.50 (± 0.14) TgN yr^{-1} under SSP1-2.6 and SSP5-8.5, respectively (Fig. 5.4a). However, modeled N_2O emissions show varying responses to projected climate change for different ecosystems. Croplands are projected to have strong sensitivities to changing climate which result in ~ 0.44 (SSP1-2.6: 0.35, SSP5-8.5: 0.53) TgN yr^{-1} and ~ 0.25 (SSP1-2.6: 0.22, SSP5-8.5: 0.30) kg N ha^{-1} yr^{-1} increases in total emission and mean flux (Fig. 5.4 b, Fig. 5. S5 b). However, a negative effect of projected climate change on modeled N_2O emissions are found for rangelands, which are suggested to decrease by ~ 0.046 and 0.13 Tg N yr^{-1} globally during 2015 – 2100 under SSP1-2.6 and SSP5-8.5 scenarios (Fig. 5.4 b). The weighted mean flux may decrease by ~4.0 % and ~10.8 % due to projected changing climate (Fig. 5. S5). Regarding pasture and rice-paddy ecosystems, the magnitudes of the total climate change effect on N_2O emissions are milder because of the smaller total area (Fig. 5. S6). Meanwhile, N_2O fluxes from pasture and rice ecosystems are also projected to show positive response to climate changes with 2.0 – 10.9 % and 6.3 – 8.1 % increase respectively (Fig. 5. S5). The general positive climate change effects exhibit great spatial variation globally, while the intensive agricultural regions are projected to have more rapidly increased N_2O fluxes (e.g., > 1 kg N ha^{-1} yr^{-1}) due to future climate change, such as the Great Lakes region in North America and mid Europe (Fig. 5.4 c).

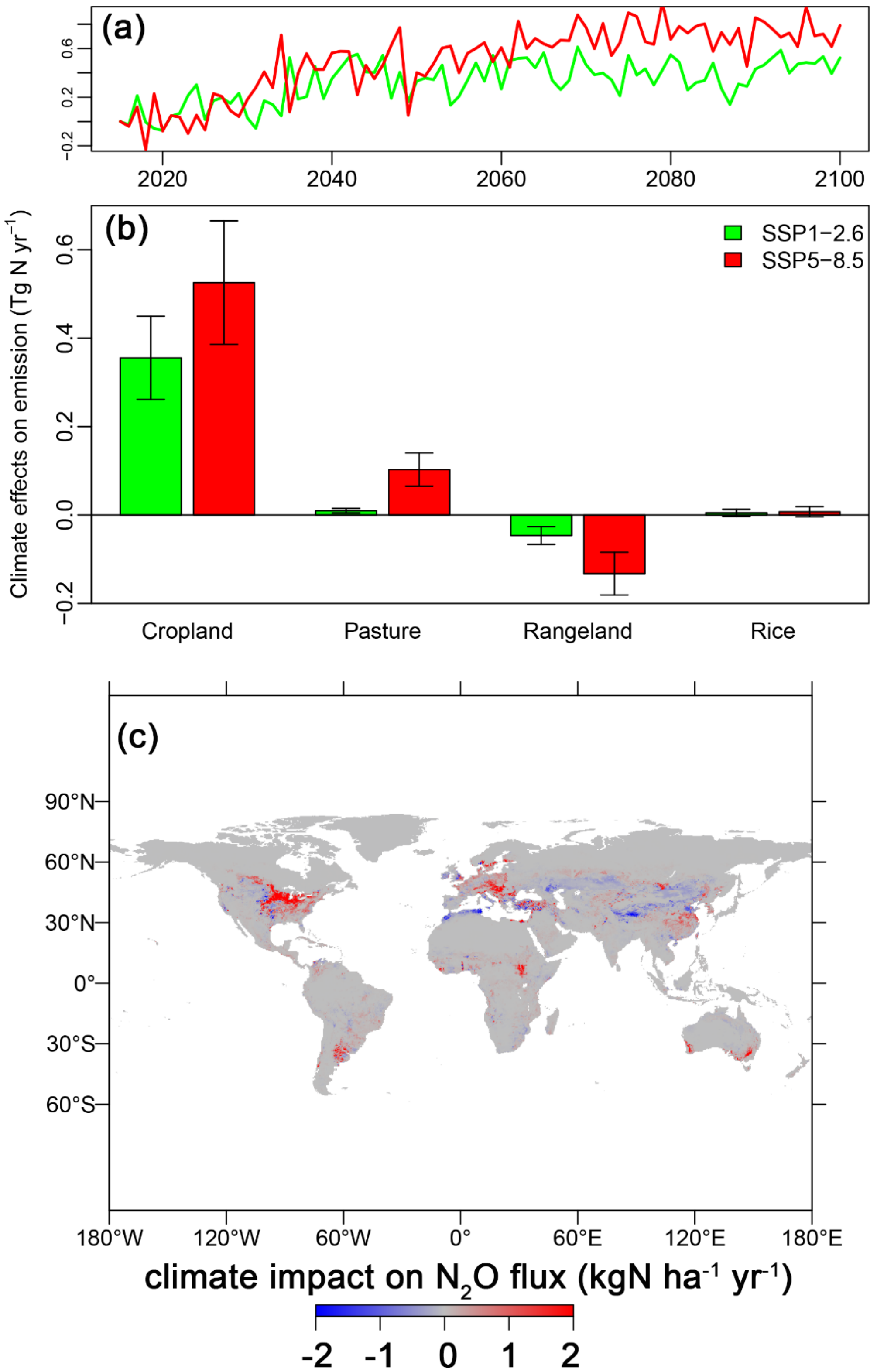

Figure 5.5 Modeled climate-induced changes in N_2O emissions from global croplands, pastures, rangelands, and rice fields under SSP1-2.6 and SSP5-8.5 scenarios. (a) Temporal variations in the climate change effect of total N_2O emissions; (b) Mean climate change effects on projected N_2O emission from different agricultural ecosystems; (c) spatial variations of projected climate

change impacts on agricultural soil N_2O flux during 2015 – 2100 (mean of SSP1-2.6 and SSP5-8.5).

5.6 Discussion

5.6.1 Comparison with other studies

Between 1950 and 2015, our study found that N_2O emissions from global agricultural ecosystems presented a general increasing trend but such increases slow down and turn into slightly decreasing to plateau since the 2000s. Overall estimated N_2O emission from global agroecosystems (6.92 ± 0.08 Tg N yr^{-1}) account for ~43.2% of global N_2O budget in the 21st century (Tian et al., 2020). This result aligns with the range of 9 participating process-based models of NMIP-2 (ensemble mean 6.93 ± 0.17 Tg N yr^{-1}) (Tian et al., 2024).

A few modeling studies using projected climate forcing data have estimated the dynamics of soil N_2O fluxes, but only covering site to regional scales. In a wheat-maize-soybean rotation cropland in Ontario, Canada, the DNDC model reported N_2O emissions ranging from 2.3 to 5.8 kg N ha^{-1} driven RCP4.5 and RCP8.5 forcing data, which is in line with our simulated results (4.3 and 2.4 kgN ha^{-1} yr^{-1} for SSP2-4.5 and 5-8.5, respectively) (He et al., 2018). Similarly, at a wheat field in northwest China, our model also obtained a good agreement with DNDC output (1.4 – 2.1 kg N ha^{-1} yr^{-1}) (Chen et al., 2019). Roelandt et al. (2007) provided an estimate of cropland and grassland N_2O emission in Belgium until 2050. Their modeled results (3 – 6 and 1 –2 kg N ha^{-1} yr^{-1} for croplands and grasslands) are within the range of our estimations (i.e., 4.5 – 8.2 kgN ha^{-1} yr^{-1} under SSP5-8.5, Figure 5.3). Zhang et al. (2023) reported N_2O emission from croplands in China may increase up to ~ 0.87 Tg N yr^{-1} (mean of RCP2.6, RCP6.0, and RCP8.5; mean emission rate is ~7.59 kgN ha^{-1} yr^{-1}) between 2061 to 2090 which is close to our simulated SSP1-2.6 results (~0.84 Tg N yr^{-1}; Figure 5.4). Their apparent underestimation likely results from their assumption that agricultural management and land use change remain constant during 2015 – 2100.

However, our modeled result is larger than data reported by other bottom-up models, mostly EF-based models, for both historical period and projected future. For instance, the most updated EDGARv8.0 (Emissions Database for Global Atmospheric Research) suggested global agricultural emission is ~ 5.94 Tg N yr^{-1} from 2000 – 2022 (EDGAR 2023). Reay et al. (2012) estimated that agricultural N_2O emissions may reach up to 7.6 Tg N yr^{-1} by 2030, which is smaller than any projected trajectories of our results (8.56, 9.54, and 8.76 Tg N yr^{-1} in 2030 for SSP1-2.6, SSP2-4.5, and SSP5-8.5, respectively). The difference stems from the different inclusion of agricultural soils and the EF-based model they applied. A number of global atmospheric inversion and meta-analysis studies also pointed out the risk of underestimated agricultural N_2O emissions by ~ 60 – 400 % using current EF models (including the IPCC refined EF), especially under global change backgrounds (Harris et al., 2022; Shcherbak et al., 2014; Thompson et al., 2019).

Discrepancy between EF-based estimation and field measurements have been widely documented in various agroecosystems globally (Cui et al., 2021; Mancia et al., 2022; Song, Zhu, et al., 2023). A major challenge for EF-based empirical models (i.e., both default and 2019 refinement), is that they treat N_2O emissions induced by external N additions independent from soil emissions. This separation causes significant underestimation because it not only neglect the legacy effect of external N additions in previous years, but also fails to account the stimulatory effect of fertilizer N on priming grass N mineralization, thus N_2O produced by N from native soils (Frick et al., 2023; Liu et al., 2010; Xu et al., 2023). EF values have been proved to be affected by input N doses (Harris et al., 2022; Shcherbak et al., 2014). Additionally, oversimplified quantification of background emissions and omitted emissions during non-growing seasons also causes incomplete estimated total N_2O fluxes by EF methods on varying scales. Instead of a constant (e.g., 1 kgN ha^{-1} yr^{-1}, IPCC 2006 default), background N_2O emissions vary significantly with local climates, soil physical and chemical properties, and vegetation types (Aliyu et al., 2018; Yin et al., 2022). Built on measured data in growing seasons mostly, EF-based models underrate the contribution of non-growing (or fallow) season N_2O emissions, which could constitute up to 50% of annual N_2O budget (Shang et al., 2024).

5.6.2 Climate changes and management control agricultural N_2O emissions

Compared to the reference period, modeled results suggest substantial changes in the spatiotemporal variation patterns of N_2O emissions from global agricultural ecosystems in the future. Upland croplands accounts for the most important driver to the magnitude of soil N_2O emissions which is responsible for ~ 50.3 and 68.9 % in historical period and projected future respectively. Consistent with previous studies, developing worlds would make more contribution to total cropland N_2O emissions in the future because of the increases in both cropland area and projected mean N_2O fluxes (e.g., southern Asia, south America, and Africa) (Hurtt et al., 2020; Reay et al., 2012). The largest projected cropland N_2O emissions is obtained under SSP2-4.5 suggesting that anthropogenic N additions serve as the predominant role in determining soil N_2O fluxes because the projected global mean N fertilizer application rates under SSP2-4.5 (95.37 kgN ha^{-1} yr^{-1}) is ~ 7.0 and 48.2 % larger than those of SSP1-2.6 and SSP5-8.5, respectively (Figure 5.S1) (Tian et al., 2024). The non-linear response of N_2O emission to N inputs further cause excessive emission rates under high N addition levels (Shcherbak et al., 2014). As the 'middle of the road' pathway, SSP2-4.5's larger N fertilizer application rate results from moderate economic and technological progress, lack of strong sustainability measures, and significant agricultural expansion and intensification (Hurtt et al., 2020; O'Neill et al., 2016). Regarding SSP5-8.5, the 'business as usual' pathway underscores the fossil-fuel-based economic development but it assumes high technological advancements that improve agricultural productivity with less fertilizer use (Figure 5.S1). While a common feature of three scenarios is that a large portion of this increased N fertilizer use is attributed to developing nations, thus N_2O emissions (Martre et al., 2024). Our projection suggests that developed world should take more international responsibilities by reducing domestic N fertilizer applications and exporting improved agro-technologies to minimize the risk of excessively increased agricultural N_2O emissions elsewhere (Bonilla-Cedrez et al., 2021; van Wesenbeeck et al., 2021). Our study estimated that the projected N_2O emissions from grazing lands probably would not increase in the future (Fig. 5. S3, S4) although both pastures and rangelands might receive increasing amount of manure due to increasing dairy and meat requirement (Pelletier & Tyedmers, 2010). Previous studies on grazing-lands already demonstrated the stimulatory effect of deposited manure to soil N_2O emissions is less significant without chemical N fertilizers (Flechard et al., 2007; Song, Peng, et al., 2023; Tang et al., 2019; van der Weerden et al., 2021). The significant correlation between N_2O emissions and the reduced N fertilizer application rates for pastures in our estimation further support this. Therefore, the reduction of projected pasture N_2O emissions in Europe, China, and North America are probably caused by decreased N fertilizer use as in croplands and shrink in pasture area in these regions (Figure 5.4, Fig 5. S6). In the meantime, projected increasing pasture N_2O emissions in South America and Africa pointed out the challenge in mitigation measures due to imbalanced economic development.

Our projections of N_2O emissions suggest a major impact of climate changes on N_2O emissions from global agricultural soils. As the two most important characters, previous long-term observations and control experiments highlighted that warming and increasing precipitations tend to enhance soil

N_2O emissions across large scale (Griffis et al., 2017; Li et al., 2020). Warming and wetting promote soil microbes with more substrates (e.g., NH_4^+ and NO_3^-), elevates activity of key enzymes, and accelerate soil wet-aeration cycles, which create favorable conditions for denitrification (Bai et al., 2013; Gao et al., 2022; Tu et al., 2024). The IPCC addressed the determinant role of climate to sensitivity of N_2O emissions by improving EF values under moist climate regions (Hergoualc'h et al., 2021). Our projected magnitude of croplands N_2O emission further suggests that the mid North America and the Great Lake region in particular, would be greatly affected by climate change, becoming emission hotspots (Griffis et al., 2017; Lu et al., 2022). There is a growing trend for global cropland area to experience higher temperature and more rainfall (Zhou et al., 2021). Therefore, wise management are recommended to mitigate such positive feedback, including precise fertilizer application and alternative tillage (Gao et al., 2022; Harris et al., 2022).

However, climate change effects present a clear spatial explicit pattern, as our modeled N_2O emissions from pasture and rangelands exhibit opposite responses. Pasture receives external N fertilizer inputs but the intensity is smaller than that of cropland, leading to less pronounced responses of N_2O emission patterns to climate change (Figure 5.4, 5. S3). In mid Aisa specifically, where rangeland is widely distributed with cold and dry local weather, projected climate change tends to reduce soil N_2O emissions under both scenarios. In support of this study, negative responses of grassland soil N_2O fluxes to increasing temperature were reported in relatively cool or semiarid regions (Barneze et al., 2022). This is probably because: 1) increased temperature in winter reduce the freeze-thaw induced N_2O emission pulses in early spring (Wolf et al., 2010) and 2) improved growth of vegetation favors uptake mineral N from soils, reducing N supplies for N_2O production (Dijkstra et al., 2013). In consistency, Chang et al. (2021) reported a decrease in estimated N_2O emission from global sparsely grazed grasslands but an increase for managed grasslands during historical warming. Such difference demonstrates that climate change impacts on soil N_2O emissions are probably stronger buffer for ecosystems with intensive management such as reactive N supplies (Feigenwinter et al., 2023). Therefore, climate and environment specific management strategies are mandatory to mitigate direct N_2O emissions from global agricultural ecosystems, such as redistributing fertilizer and manure N inputs to prevent excessive soil N surplus under climate changes (Harris et al., 2022).

5.6.3 Uncertainties and research needs

Despite applying more GCMs product to drive the model for better reflect the improvement in estimation quality of present study is expected by addressing the following uncertainty sources.

First and foremost, the TRIPLEX-GHGv2.0 model is not equipped with a land-use change module which simulates the changes in soil C and N flows after transition. However, the expansion of agroecosystems, especially croplands, significantly alters local biogeochemical cycles and N_2O dynamics. In the current study, transformation from pasture to cropland is projected to be the dominant land conversion type which are found to have limited influence on soil N dynamics without tillage and N fertilizations (Hurtt et al., 2020; Mielenz et al., 2017). But other types of transformation are found as important N_2O source. For instance, draining peatland for cropping could increase N_2O emissions by a degree of four driven by the interaction between accelerated peat decomposition and external N fertilizers (Prananto et al., 2020; Yuqiao Wang et al., 2024). Moreover, conversions from tropical forest to agricultural lands (e.g., croplands or pasture) cause drastic N_2O emissions in short term (McDaniel et al., 2019; van Lent et al., 2015) but inconsistent results are also recorded, like a synthetic study which reported no effect on soil N_2O efflux after deforestation due to varying legacy effects (Han & Zhu, 2020). Therefore, improved model functions are vital to fill this research gap.

In addition, several agricultural practices effectively mitigate soil N_2O emissions while the lacking in these gridded management data limit the current estimated results. For example, inhibitors (e.g., nitrification inhibitors and urease inhibitors) have promising impacts on reducing soil N_2O emissions without jeopardizing vegetation productivity (Adhikari et al., 2021; Fan et al., 2022). Similarly, growing biochar amendment in agricultural lands is conceivable to improve soil quality and mitigate soil N_2O world-wide (Cayuela et al., 2014; Schmidt et al., 2021). At least national statistics of the amounts of inhibitors and biochar used are needed for large scale modeling. It is possible that, by considering these practices, this study only provides the upper limit of N_2O emission from agricultural soils under the projected future.

Another important factor influencing agricultural N_2O emissions is regional conflicts and political changes in pivotal fertilizer producing or major agriculture nations. Our study well reflects the negative effect of dissolution of Soviet Union on agricultural N_2O emission because of the significant decline in N fertilizer in this largest production unit globally (Fig. 5.1, Fig. 5. S1) (Nishina et al., 2017). Similarly, Ukraine-Russia conflict have impact on global fertilizer price and food security (Alexander et al., 2023). This event is likely to affect the N_2O emission hotspot in east Europe but the projected N fertilizer data does not incorporate such information in this study and should be considered in the future research.

Finally, the interaction between agricultural decisions and changing environmental conditions are crucial challenges for the quality of projections. For instance, individual farmers would conduct early transplanting or seedling to cope with potential yield penalty due to warming climate and the decisions are highly variable and unpredictable without a clear spatial pattern. However, current study only employed a fixed crop calendar rather than climate-specific approach which is widely adopted in current practices.

5.7 Conclusion

To the best of our knowledge, we provided the first comprehensive projection of possible trajectories of global N_2O emissions from agricultural ecosystems using a process-based model of TRIPLEX-GHGv2.0, which incorporates both future climate, environmental, and management changes at a fine spatial resolution. Our findings reveal that under all Shared Socioeconomic Pathway (SSP) scenarios, future N_2O emissions are likely to increase significantly by 21.0 – 71.0% compared to the reference period (1980 – 2014). Upland croplands account for the largest source (> 65%) of projected agricultural N_2O emissions across three scenarios, particularly in developing world because of growing N fertilizer applications in those regions. Such global increases offset the projected reduction in emissions from current leading countries of agricultural N_2O emissions due to imbalance development, which emphasizes need of international collaboration. Importantly, while nitrogen fertilizer use remains a critical factor, future climate changes also have major influence in emission patterns, with varying effects across different ecosystems. Our projections highlight that agricultural N_2O emissions may have larger contribution to global warming under intermediate pathways (SSP2-4.5), which implies the importance of integrating agricultural management into climate policies. This integration is crucial for achieving effective and comprehensive GHG mitigation and adaptation measures to ensure the future fate of agricultural ecosystems.

5.8 Supplementary Information

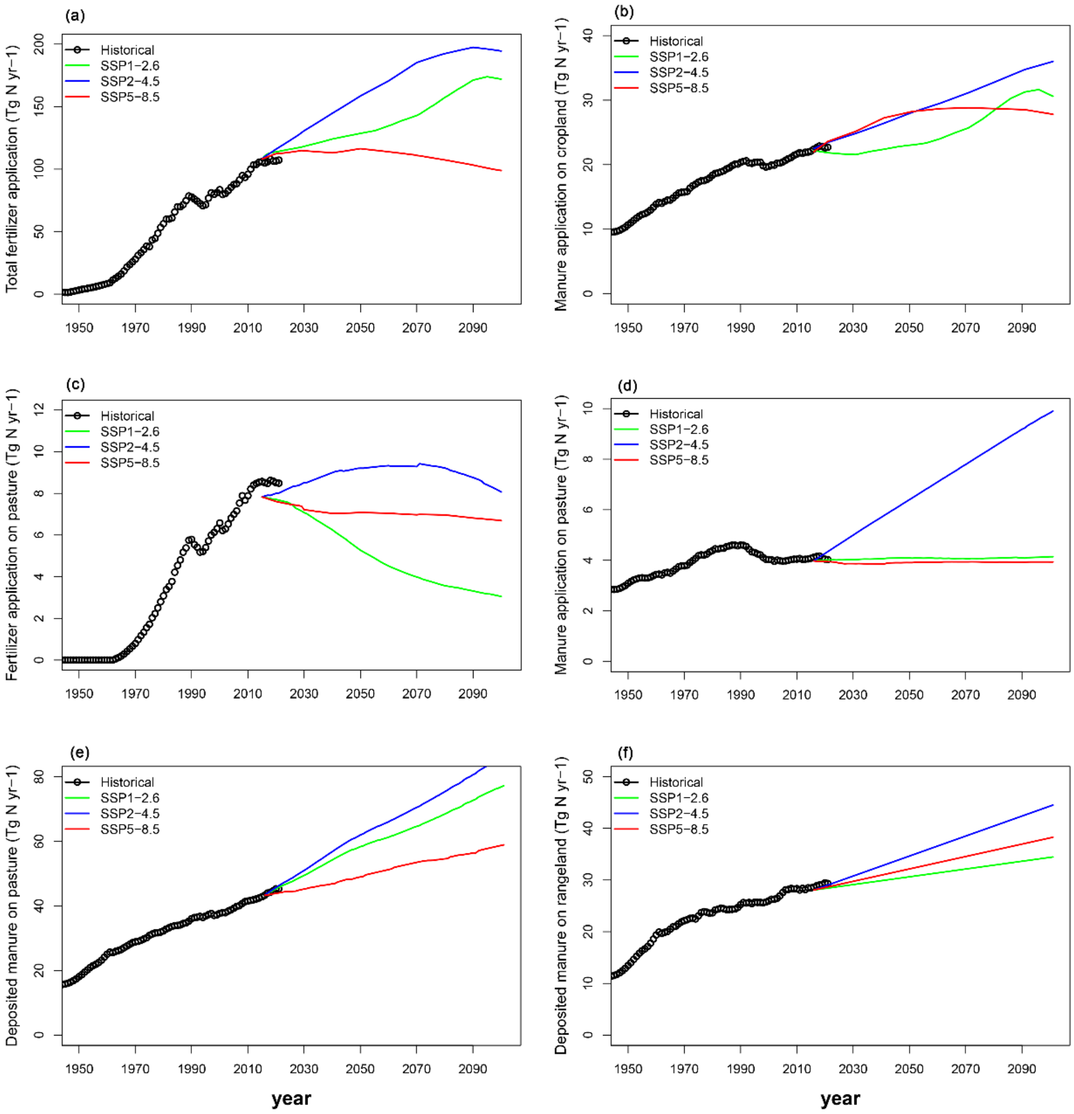

Figure 5.S1 Temporal variations of different external N inputs during study period. (a) chemical N fertilizer used for croplands, (b) manure applied on cropping area, (c) chemical N fertilizer applied on pasture, (d) manure applied on pastures, (e) deposited livestock excreta N on pasture, (f) deposited livestock excreta N on rangelands, and (g) atmospheric N deposition.

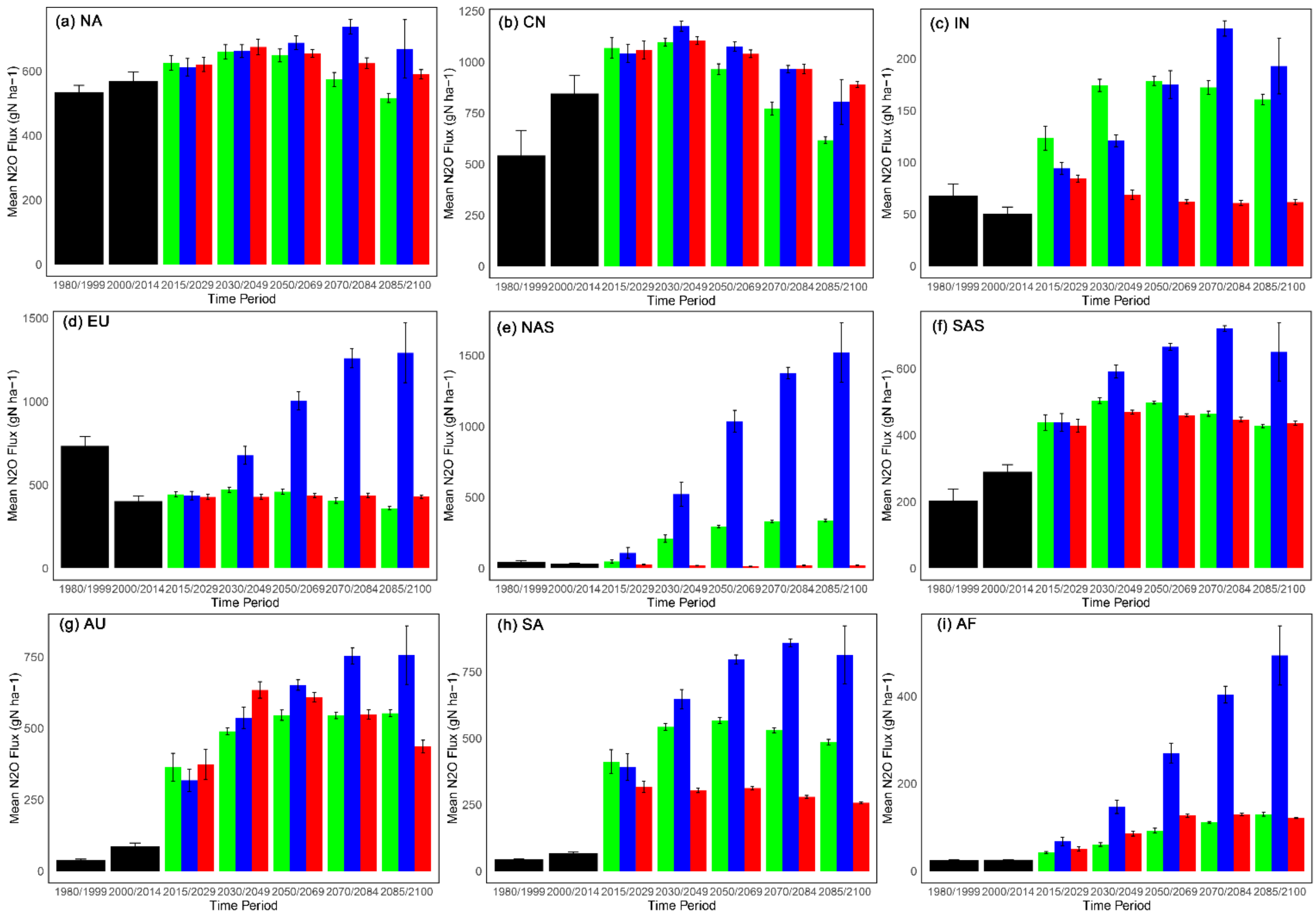

Figure 5. S2 Temporal variation in historical and projected N_2O fluxes from cropland soils in different regions.

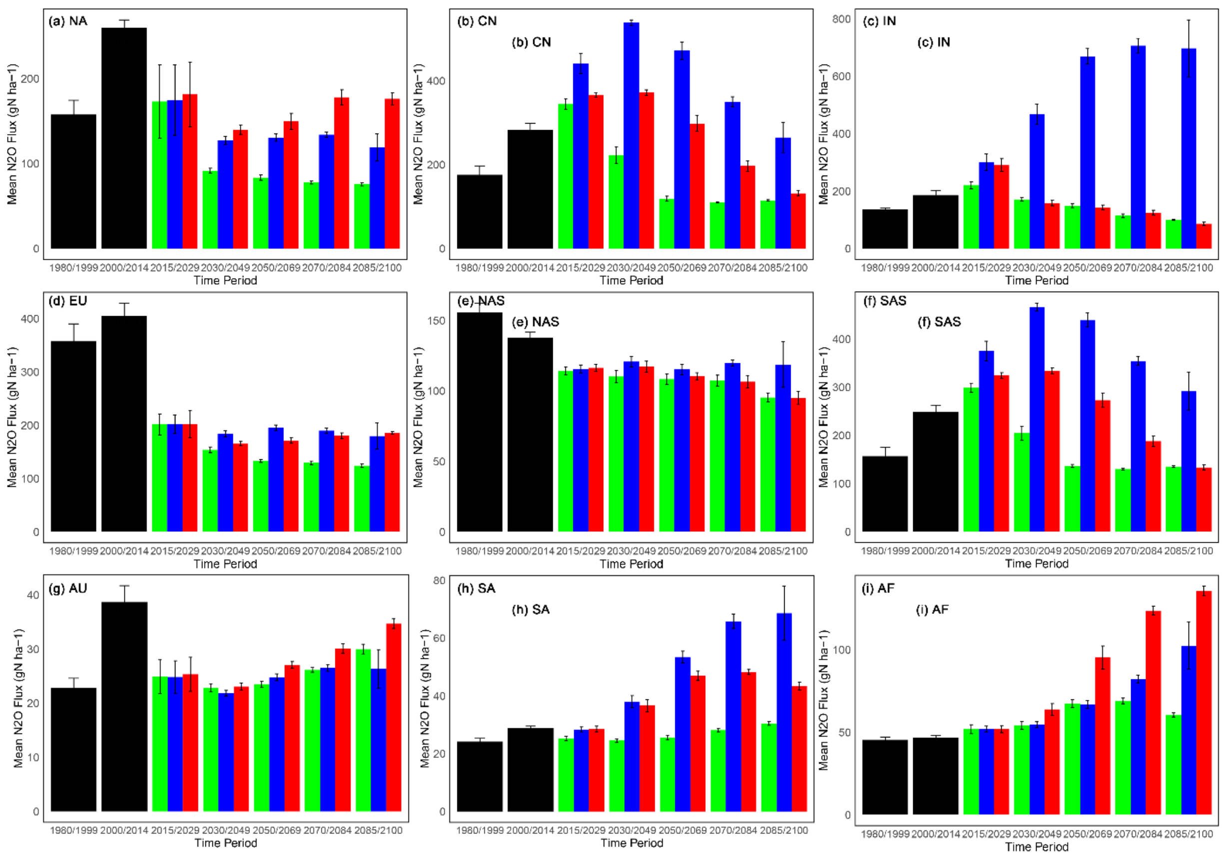

Figure 5. S3 Temporal variation in historical and projected N_2O fluxes from pasture soils in different regions.

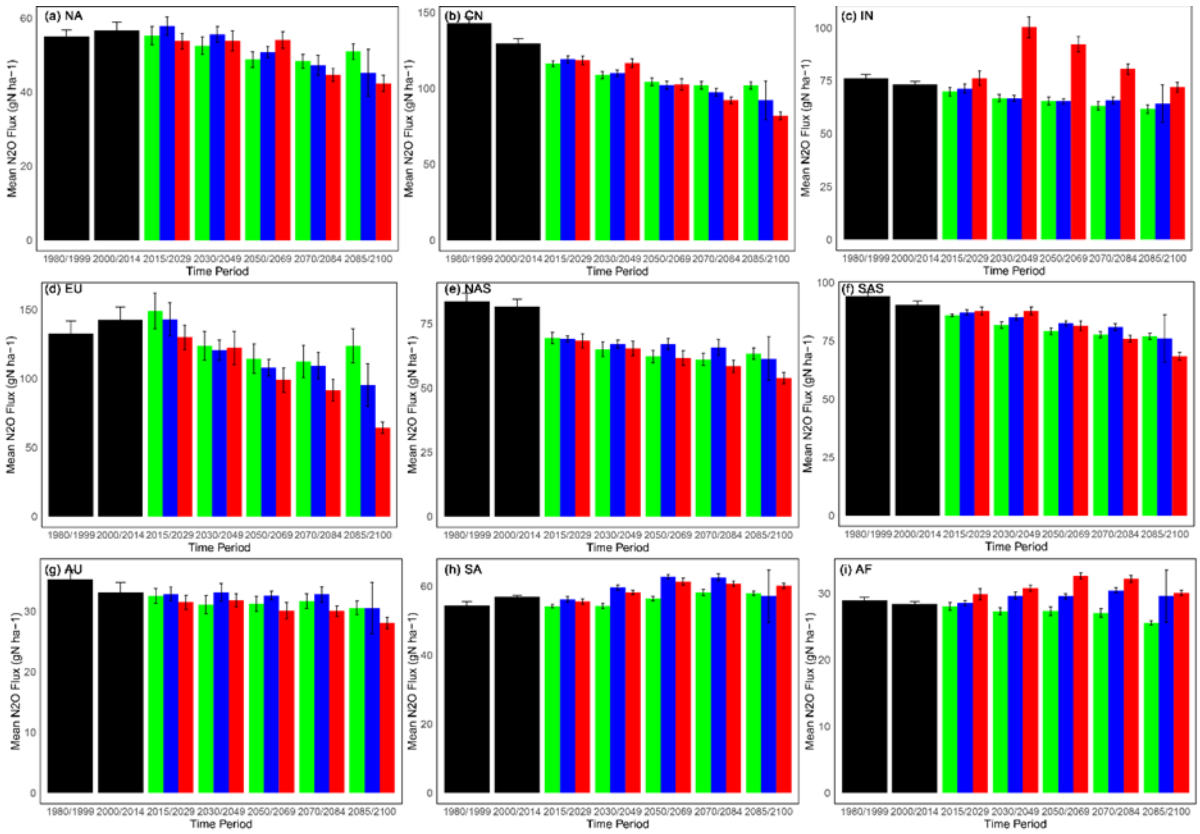

Figure 5. S4 Temporal variation in historical and projected N_2O fluxes from rangeland soils in different regions.

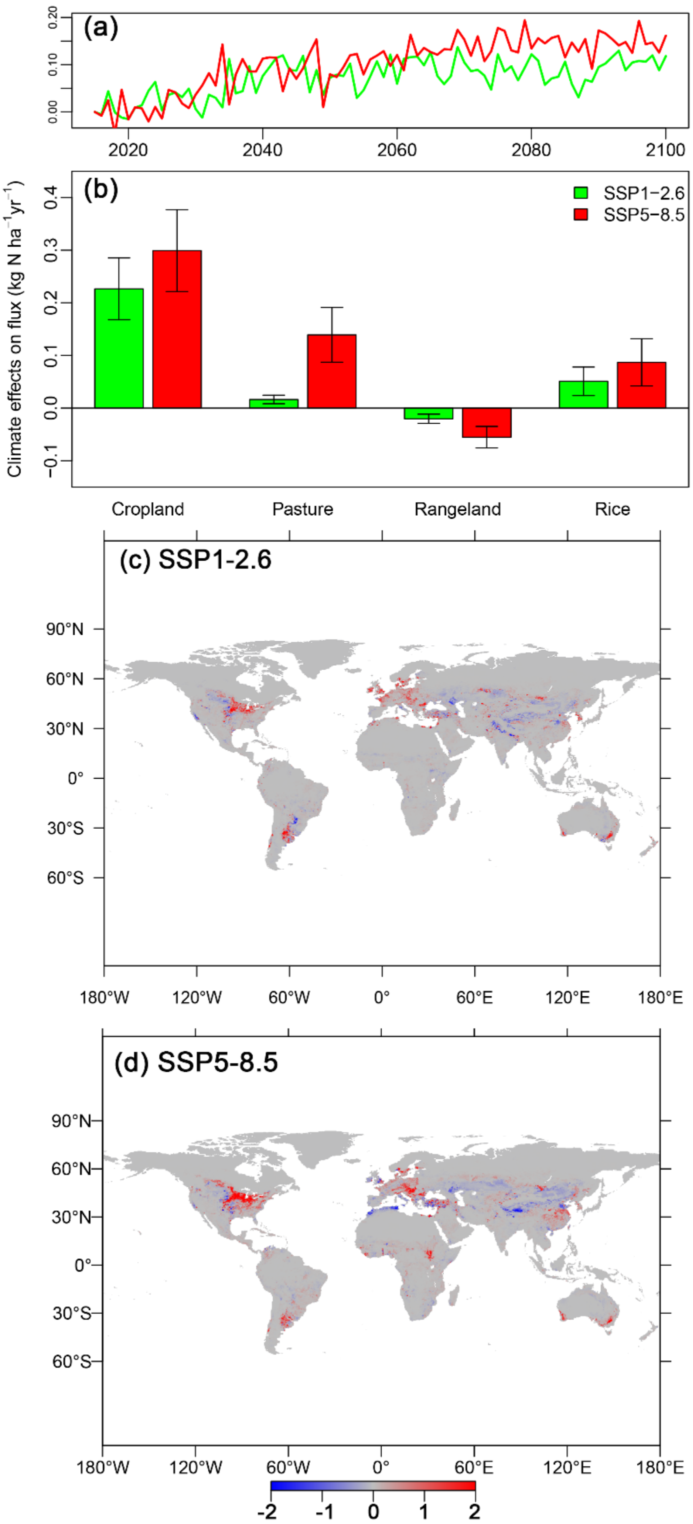

Figure 5. S5 Modeled climate-induced changes in N_2O emissions from global croplands, pastures, rangelands, and rice fields under SSP1-2.6 and SSP5-8.5 scenarios. (a) Temporal variations in the climate change effect of total N_2O emissions; (b) Mean climate change effects on projected N_2O emission from different agricultural ecosystems; (c) and (d) spatial variations of projected climate change impacts on agricultural soil N_2O flux during 2015 – 2100 under SSP1-2.6 and SSP5-8.5, respectively.

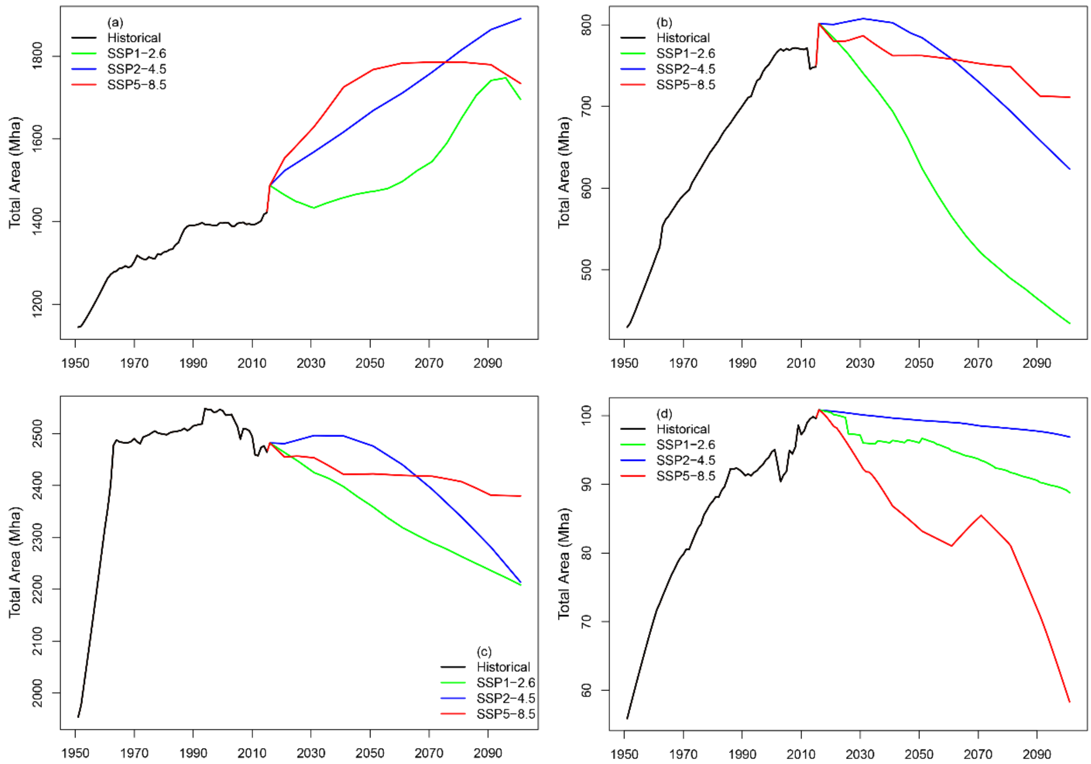

Figure 5. S6 Changes in total area of different agroecosystems during study period under three scenarios.

5.9 References

Alexander, P., Arneth, A., Henry, R., Maire, J., Rabin, S., & Rounsevell, M. D. A. (2023). High energy and fertilizer prices are more damaging than food export curtailment from Ukraine and Russia for food prices, health and the environment. *Nature Food*, *4*(1), 84-95. https://doi.org/10.1038/s43016-022-00659-9

Aliyu, G., Sanz-Cobena, A., Mueller, C., Zaman, M., Luo, J., Liu, D., Yuan, J., Chen, Z., Niu, Y., Arowolo, A., & Ding, W. (2018). A meta-analysis of soil background N2O emissions from croplands in China shows variation among climatic zones. *Agriculture Ecosystems & Environment*, *267*, 63-73. https://doi.org/10.1016/j.agee.2018.08.003

Bai, E., Li, S., Xu, W., Li, W., Dai, W., & Jiang, P. (2013). A meta-analysis of experimental warming effects on terrestrial nitrogen pools and dynamics. *New Phytologist*, *199*(2), 441-451. https://doi.org/https://doi.org/10.1111/nph.12252

Barneze, A. S., Whitaker, J., McNamara, N. P., & Ostle, N. J. (2022). Interactions between climate warming and land management regulate greenhouse gas fluxes in a temperate grassland ecosystem. *Science of The Total Environment*, *833*, 155212. https://doi.org/https://doi.org/10.1016/j.scitotenv.2022.155212

Bonilla-Cedrez, C., Chamberlin, J., & Hijmans, R. J. (2021). Fertilizer and grain prices constrain food production in sub-Saharan Africa. *Nature Food*, *2*(10), 766-772. https://doi.org/10.1038/s43016-021-00370-1

Butterbach-Bahl, K., Baggs, E. M., Dannenmann, M., Kiese, R., & Zechmeister-Boltenstern, S. (2013). Nitrous oxide emissions from soils: how well do we understand the processes and their controls? *Philosophical Transactions of the Royal Society B: Biological Sciences*, *368*(1621), 20130122. https://doi.org/10.1098/rstb.2013.0122

Cayuela, M. L., van Zwieten, L., Singh, B. P., Jeffery, S., Roig, A., & Sánchez-Monedero, M. A. (2014). Biochar's role in mitigating soil nitrous oxide emissions: A review and meta-analysis. *Agriculture, Ecosystems & Environment*, *191*, 5-16. https://doi.org/https://doi.org/10.1016/j.agee.2013.10.009

Chen, H., Li, L., Luo, X., Li, Y., Liu, D. L., Zhao, Y., Feng, H., & Deng, J. (2019). Modeling impacts of mulching and climate change on crop production and N2O emission in the Loess Plateau of China. *Agricultural and Forest Meteorology*, *268*, 86-97. https://doi.org/https://doi.org/10.1016/j.agrformet.2019.01.002

Cheng, W., Dan, L., Deng, X., Feng, J., Wang, Y., Peng, J., Tian, J., Qi, W., Liu, Z., Zheng, X., Zhou, D., Jiang, S., Zhao, H., & Wang, X. (2022). Global monthly gridded atmospheric carbon dioxide concentrations under the historical and future scenarios. *Scientific Data*, *9*(1), 83. https://doi.org/10.1038/s41597-022-01196-7

Cui, J., Zhang, X., Reis, S., Wang, C., Wang, S., He, P., Chen, H., van Grinsven, H. J. M., & Gu, B. (2023). Nitrogen cycles in global croplands altered by elevated CO2. *Nature Sustainability*, *6*(10), 1166-1176. https://doi.org/10.1038/s41893-023-01154-0

Cui, X., Shang, Z., Xia, L., Xu, R., Adalibieke, W., Zhan, X., Smith, P., & Zhou, F. (2022). Deceleration of Cropland-N2O Emissions in China and Future Mitigation Potentials. *Environmental Science & Technology*, *56*(7), 4665-4675. https://doi.org/10.1021/acs.est.1c07276

Cui, X., Zhou, F., Ciais, P., Davidson, E. A., Tubiello, F. N., Niu, X., Ju, X., Canadell, J. G., Bouwman, A. F., Jackson, R. B., Mueller, N. D., Zheng, X., Kanter, D. R., Tian, H., Adalibieke, W., Bo, Y., Wang, Q., Zhan, X., & Zhu, D. (2021). Global mapping of crop-specific emission factors highlights hotspots of nitrous oxide mitigation. *Nature Food*, *2*(11), 886-893. https://doi.org/10.1038/s43016-021-00384-9

Davidson, E. A., & Kanter, D. (2014). Inventories and scenarios of nitrous oxide emissions. *Environmental Research Letters*, *9*(10), 105012. https://doi.org/10.1088/1748-9326/9/10/105012

Dijkstra, F. A., Morgan, J. A., Follett, R. F., & LeCain, D. R. (2013). Climate change reduces the net sink of and in a semiarid grassland. *Global Change Biology*, *19*(6), 1816-1826. https://doi.org/https://doi.org/10.1111/gcb.12182

Feigenwinter, I., Hörtnagl, L., & Buchmann, N. (2023). N2O and CH4 fluxes from intensively managed grassland: The importance of biological and environmental drivers vs. management. *Science of The Total Environment*, *903*, 166389. https://doi.org/https://doi.org/10.1016/j.scitotenv.2023.166389

Flechard, C. R., Ambus, P., Skiba, U., Rees, R. M., Hensen, A., van Amstel, A., Dasselaar, A. v. d. P.-v., Soussana, J. F., Jones, M., Clifton-Brown, J., Raschi, A., Horvath, L., Neftel, A., Jocher, M., Ammann, C., Leifeld, J., Fuhrer, J., Calanca, P., Thalman, E., . . . Grosz, B. (2007). Effects of climate and management intensity on nitrous oxide emissions in grassland systems across Europe. *Agriculture, Ecosystems & Environment*, *121*(1), 135-152. https://doi.org/https://doi.org/10.1016/j.agee.2006.12.024

Franke, J. A., Müller, C., Elliott, J., Ruane, A. C., Jägermeyr, J., Balkovic, J., Ciais, P., Dury, M., Falloon, P. D., Folberth, C., François, L., Hank, T., Hoffmann, M., Izaurralde, R. C., Jacquemin, I., Jones, C., Khabarov, N., Koch, M., Li, M., . . . Moyer, E. J. (2020). The GGCMI Phase 2 experiment: global gridded crop model simulations under uniform changes in CO2, temperature, water, and nitrogen levels (protocol version 1.0). *Geosci. Model Dev.*, *13*(5), 2315-2336. https://doi.org/10.5194/gmd-13-2315-2020

Frick, H., Oberson, A., Cormann, M., Wettstein, H.-R., Frossard, E., & Bünemann, E. K. (2023). Similar distribution of 15N labeled cattle slurry and mineral fertilizer in soil after one year. *Nutrient Cycling in Agroecosystems*, *125*(2), 153-169. https://doi.org/10.1007/s10705-022-10205-5

Gao, H., Tian, H., Zhang, Z., & Xia, X. (2022). Warming-induced greenhouse gas fluxes from global croplands modified by agricultural practices: A meta-analysis. *Science of The Total Environment*, *820*, 153288. https://doi.org/https://doi.org/10.1016/j.scitotenv.2022.153288

Gong, C., Tian, H., Liao, H., Pan, N., Pan, S., Ito, A., Jain, A. K., Kou-Giesbrecht, S., Joos, F., Sun, Q., Shi, H., Vuichard, N., Zhu, Q., Peng, C., Maggi, F., Tang, F. H. M., & Zaehle, S. (2024). Global net climate effects of anthropogenic reactive nitrogen. *Nature*. https://doi.org/10.1038/s41586-024-07714-4

Griffis, T. J., Chen, Z., Baker, J. M., Wood, J. D., Millet, D. B., Lee, X., Venterea, R. T., & Turner, P. A. (2017). Nitrous oxide emissions are enhanced in a warmer and wetter world. *Proceedings of the National Academy of Sciences*, *114*(45), 12081-12085. https://doi.org/doi:10.1073/pnas.1704552114

Gu, B., Zhang, X., Lam, S. K., Yu, Y., van Grinsven, H. J. M., Zhang, S., Wang, X., Bodirsky, B. L., Wang, S., Duan, J., Ren, C., Bouwman, L., de Vries, W., Xu, J., Sutton, M. A., & Chen, D. (2023). Cost-effective mitigation of nitrogen pollution from global croplands. *Nature*, *613*(7942), 77-84. https://doi.org/10.1038/s41586-022-05481-8

Han, M., & Zhu, B. (2020). Changes in soil greenhouse gas fluxes by land use change from primary forest. *Global Change Biology*, *26*(4), 2656-2667. https://doi.org/https://doi.org/10.1111/gcb.14993

Harris, E., Yu, L., Wang, Y. P., Mohn, J., Henne, S., Bai, E., Barthel, M., Bauters, M., Boeckx, P., Dorich, C., Farrell, M., Krummel, P. B., Loh, Z. M., Reichstein, M., Six, J., Steinbacher, M., Wells, N. S., Bahn, M., & Rayner, P. (2022). Warming and redistribution of nitrogen inputs drive an increase in terrestrial nitrous oxide emission factor. *Nature Communications*, *13*(1), 4310. https://doi.org/10.1038/s41467-022-32001-z

He, W., Yang, J. Y., Drury, C. F., Smith, W. N., Grant, B. B., He, P., Qian, B., Zhou, W., & Hoogenboom, G. (2018). Estimating the impacts of climate change on crop yields and N2O emissions for conventional and no-tillage in Southwestern Ontario, Canada. *Agricultural Systems*, *159*, 187-198. https://doi.org/https://doi.org/10.1016/j.agsy.2017.01.025

Hergoualc'h, K., Mueller, N., Bernoux, M., Kasimir, Ä., van der Weerden, T. J., & Ogle, S. M. (2021). Improved accuracy and reduced uncertainty in greenhouse gas inventories by refining the IPCC emission factor for direct N2O emissions from nitrogen inputs to managed soils. *Global Change Biology*, *27*(24), 6536-6550. https://doi.org/https://doi.org/10.1111/gcb.15884

Hurtt, G. C., Chini, L., Sahajpal, R., Frolking, S., Bodirsky, B. L., Calvin, K., Doelman, J. C., Fisk, J., Fujimori, S., Klein Goldewijk, K., Hasegawa, T., Havlik, P., Heinimann, A., Humpenöder, F., Jungclaus, J., Kaplan, J. O., Kennedy, J., Krisztin, T., Lawrence, D., . . . Zhang, X. (2020). Harmonization of global land use change and management for the period 850–2100 (LUH2) for CMIP6. *Geosci. Model Dev.*, *13*(11), 5425-5464.

https://doi.org/10.5194/gmd-13-5425-2020

IPCC. (2021). *Climate Change 2021: The Physical Science Basis. Contribution of Working Group I to the Sixth Assessment Report of the Intergovernmental Panel on Climate Change* (Vol. In Press). Cambridge University Press. https://doi.org/10.1017/9781009157896

Jones, B., & O'Neill, B. C. (2016). Spatially explicit global population scenarios consistent with the Shared Socioeconomic Pathways. *Environmental Research Letters*, *11*(8), 084003. https://doi.org/10.1088/1748-9326/11/8/084003

Kanter, D. R., Ogle, S. M., & Winiwarter, W. (2020). Building on Paris: integrating nitrous oxide mitigation into future climate policy. *Current Opinion in Environmental Sustainability*, *47*, 7-12. https://doi.org/https://doi.org/10.1016/j.cosust.2020.04.005

Kriegler, E., Bauer, N., Popp, A., Humpenöder, F., Leimbach, M., Strefler, J., Baumstark, L., Bodirsky, B. L., Hilaire, J., Klein, D., Mouratiadou, I., Weindl, I., Bertram, C., Dietrich, J.-P., Luderer, G., Pehl, M., Pietzcker, R., Piontek, F., Lotze-Campen, H., . . . Edenhofer, O. (2017). Fossil-fueled development (SSP5): An energy and resource intensive scenario for the 21st century. *Global Environmental Change*, *42*, 297-315. https://doi.org/https://doi.org/10.1016/j.gloenvcha.2016.05.015

Lassaletta, L., Billen, G., Grizzetti, B., Anglade, J., & Garnier, J. (2014). 50 year trends in nitrogen use efficiency of world cropping systems: the relationship between yield and nitrogen input to cropland. *Environmental Research Letters*, *9*(10), 105011. https://doi.org/10.1088/1748-9326/9/10/105011

Lawrence, N. C., Tenesaca, C. G., VanLoocke, A., & Hall, S. J. (2021). Nitrous oxide emissions from agricultural soils challenge climate sustainability in the US Corn Belt. *Proceedings of the National Academy of Sciences*, *118*(46), e2112108118. https://doi.org/doi:10.1073/pnas.2112108118

Li, L., Zheng, Z., Wang, W., Biederman, J. A., Xu, X., Ran, Q., Qian, R., Xu, C., Zhang, B., Wang, F., Zhou, S., Cui, L., Che, R., Hao, Y., Cui, X., Xu, Z., & Wang, Y. (2020). Terrestrial N2O emissions and related functional genes under climate change: A global meta-analysis. *Global Change Biology*, *26*(2), 931-943. https://doi.org/https://doi.org/10.1111/gcb.14847

Li, Z., Zeng, Z., Song, Z., Tian, D., Huang, X., Nie, S., Wang, J., Jiang, L., Luo, Y., Cui, J., & Niu, S. (2022). Variance and main drivers of field nitrous oxide emissions: A global synthesis. *Journal of Cleaner Production*, *353*, 131686. https://doi.org/https://doi.org/10.1016/j.jclepro.2022.131686

Liao, J., Luo, Q., Hu, A., Wan, W., Tian, D., Ma, J., Ma, T., Luo, H., & Lu, S. (2022). Soil moisture–atmosphere feedback dominates land N2O nitrification emissions and denitrification reduction. *Global Change Biology*, *28*(21), 6404-6418. https://doi.org/https://doi.org/10.1111/gcb.16365

Liu, J., You, L., Amini, M., Obersteiner, M., Herrero, M., Zehnder, A. J. B., & Yang, H. (2010). A high-resolution assessment on global nitrogen flows in cropland. *Proceedings of the National Academy of Sciences*, *107*(17), 8035-8040. https://doi.org/10.1073/pnas.0913658107

Lu, C., Yu, Z., Zhang, J., Cao, P., Tian, H., & Nevison, C. (2022). Century-long changes and drivers of soil nitrous oxide (N2O) emissions across the contiguous United States. *Global Change Biology*, *28*(7), 2505-2524. https://doi.org/https://doi.org/10.1111/gcb.16061

Ma, H., Jia, X., Yang, J., Liu, J., Shangguan, Z., & Yan, W. (2023). Inhibitors mitigate N2O emissions more effectively than biochar: A global perspective. *Science of The Total Environment*, *859*, 160416. https://doi.org/https://doi.org/10.1016/j.scitotenv.2022.160416

Mancia, A., Chadwick, D. R., Waters, S. M., & Krol, D. J. (2022). Uncertainties in direct N2O emissions from grazing ruminant excreta (EF3PRP) in national greenhouse gas inventories. *Science of The Total Environment*, *803*, 149935. https://doi.org/https://doi.org/10.1016/j.scitotenv.2021.149935

Martre, P., Dueri, S., Guarin, J. R., Ewert, F., Webber, H., Calderini, D., Molero, G., Reynolds, M., Miralles, D., Garcia, G., Brown, H., George, M., Craigie, R., Cohan, J.-P., Deswarte, J.-C., Slafer, G., Giunta, F., Cammarano, D., Ferrise, R., . . . Asseng, S. (2024). Global needs for nitrogen fertilizer to improve wheat yield under climate change. *Nature Plants*, *10*(7), 1081-1090. https://doi.org/10.1038/s41477-024-01739-3

McDaniel, M. D., Saha, D., Dumont, M. G., Hernández, M., & Adams, M. A. (2019). The Effect of Land-Use Change on Soil CH4 and N2O Fluxes: A Global Meta-Analysis. *Ecosystems*, *22*(6), 1424-1443. https://doi.org/10.1007/s10021-019-00347-z

Mielenz, H., Thorburn, P. J., Harris, R. H., Grace, P. R., & Officer, S. J. (2017). Mitigating N2O emissions from cropping systems after conversion from pasture − a modelling approach. *European Journal of Agronomy*, *82*, 254-267. https://doi.org/https://doi.org/10.1016/j.eja.2016.06.007

Mueller, N. D., Gerber, J. S., Johnston, M., Ray, D. K., Ramankutty, N., & Foley, J. A. (2012). Closing yield gaps through nutrient and water management. *Nature*, *490*(7419), 254-257. https://doi.org/10.1038/nature11420

Nishina, K., Ito, A., Hanasaki, N., & Hayashi, S. (2017). Reconstruction of spatially detailed global map of NH4+ and NO3− application in synthetic nitrogen fertilizer. *Earth Syst. Sci. Data*, *9*(1), 149-162. https://doi.org/10.5194/essd-9-149-2017

O'Neill, B. C., Tebaldi, C., van Vuuren, D. P., Eyring, V., Friedlingstein, P., Hurtt, G., Knutti, R., Kriegler, E., Lamarque, J. F., Lowe, J., Meehl, G. A., Moss, R., Riahi, K., & Sanderson, B. M. (2016). The Scenario Model Intercomparison Project (ScenarioMIP) for CMIP6. *Geosci. Model Dev.*, *9*(9), 3461-3482. https://doi.org/10.5194/gmd-9-3461-2016

Pan, S.-Y., He, K.-H., Lin, K.-T., Fan, C., & Chang, C.-T. (2022). Addressing nitrogenous gases from croplands toward low-emission agriculture. *npj Climate and Atmospheric Science*, *5*(1), 43. https://doi.org/10.1038/s41612-022-00265-3

Pelletier, N., & Tyedmers, P. (2010). Forecasting potential global environmental costs of livestock production 2000–2050. *Proceedings of the National Academy of Sciences*, *107*(43), 18371-18374. https://doi.org/doi:10.1073/pnas.1004659107

Portmann, F. T., Siebert, S., & Döll, P. (2010). MIRCA2000—Global monthly irrigated and rainfed crop areas around the year 2000: A new high-resolution data set for agricultural and hydrological modeling. *Global Biogeochemical Cycles*, *24*(1). https://doi.org/https://doi.org/10.1029/2008GB003435

Portmann, R. W., Daniel, J. S., & Ravishankara, A. R. (2012). Stratospheric ozone depletion due to nitrous oxide: influences of other gases. *Philosophical Transactions of the Royal Society B: Biological Sciences*, *367*(1593), 1256-1264. https://doi.org/10.1098/rstb.2011.0377

Prananto, J. A., Minasny, B., Comeau, L.-P., Rudiyanto, R., & Grace, P. (2020). Drainage increases CO2 and N2O emissions from tropical peat soils. *Global Change Biology*, *26*(8), 4583-4600. https://doi.org/https://doi.org/10.1111/gcb.15147

Reay, D. S., Davidson, E. A., Smith, K. A., Smith, P., Melillo, J. M., Dentener, F., & Crutzen, P. J. (2012). Global agriculture and nitrous oxide emissions. *Nature Climate Change*, *2*(6), 410-416. https://doi.org/10.1038/nclimate1458

Ren, C., Zhang, X., Reis, S., Wang, S., Jin, J., Xu, J., & Gu, B. (2023). Climate change unequally affects nitrogen use and losses in global croplands. *Nature Food*, *4*(4), 294-304. https://doi.org/10.1038/s43016-023-00730-z

Riahi, K., van Vuuren, D. P., Kriegler, E., Edmonds, J., O'Neill, B. C., Fujimori, S., Bauer, N., Calvin, K., Dellink, R., Fricko, O., Lutz, W., Popp, A., Cuaresma, J. C., Kc, S., Leimbach, M., Jiang, L., Kram, T., Rao, S., Emmerling, J., . . . Tavoni, M. (2017). The Shared Socioeconomic Pathways and their energy, land use, and greenhouse gas emissions implications: An overview. *Global Environmental Change*, *42*, 153-168. https://doi.org/https://doi.org/10.1016/j.gloenvcha.2016.05.009

Schmidt, H.-P., Kammann, C., Hagemann, N., Leifeld, J., Bucheli, T. D., Sánchez Monedero, M. A., & Cayuela, M. L. (2021). Biochar in agriculture – A systematic review of 26 global meta-analyses. *GCB Bioenergy*, *13*(11), 1708-1730. https://doi.org/https://doi.org/10.1111/gcbb.12889

Shang, Z., Cui, X., van Groenigen, K. J., Kuhnert, M., Abdalla, M., Luo, J., Zhang, W., Song, Z., Jiang, Y., Smith, P., & Zhou, F. (2024). Global cropland nitrous oxide emissions in fallow period are comparable to growing-season emissions. *Global Change Biology*, *30*(2), e17165. https://doi.org/https://doi.org/10.1111/gcb.17165

Shcherbak, I., Millar, N., & Robertson, G. P. (2014). Global metaanalysis of the nonlinear response of soil nitrous oxide (N2O) emissions to fertilizer nitrogen. *Proceedings of the National Academy of Sciences*, *111*(25), 9199-9204. https://doi.org/10.1073/pnas.1322434111

Shen, Y., & Zhu, B. (2022). Effects of nitrogen and phosphorus enrichment on soil N2O emission from natural ecosystems: A global meta-analysis. *Environmental Pollution*, *301*, 118993. https://doi.org/https://doi.org/10.1016/j.envpol.2022.118993

Shi, Y., Wang, J., Ao, Y., Han, J., Guo, Z., Liu, X., Zhang, J., Mu, C., & Le Roux, X. (2021). Responses of soil N2O emissions and their abiotic and biotic drivers to altered rainfall regimes and co-occurring wet N deposition in a semi-arid grassland. *Global Change Biology*, *27*(19), 4894-4908. https://doi.org/https://doi.org/10.1111/gcb.15792

Song, H., Peng, C., Zhang, K., Li, T., Yang, M., Liu, Q., & Zhu, Q. (2023). Quantifying patterns, sources and uncertainty of nitrous oxide emissions from global grazing lands: Nitrogen forms are the determinant factors for estimation and mitigation. *Global and Planetary Change*, *223*, 104080. https://doi.org/https://doi.org/10.1016/j.gloplacha.2023.104080

Song, H., Peng, C., Zhang, K., & Zhu, Q. (2022). Integrating major agricultural practices into the TRIPLEX-GHG model v2.0 for simulating global cropland nitrous oxide emissions: Development, sensitivity analysis and site evaluation. *Science of The Total Environment*, *843*, 156945. https://doi.org/https://doi.org/10.1016/j.scitotenv.2022.156945

Song, H., Zhu, Q., Blanchet, J.-P., Chen, Z., Zhang, K., Li, T., Zhou, F., & Peng, C. (2023). Central Role of Nitrogen Fertilizer Relative to Water Management in Determining Direct Nitrous Oxide Emissions From Global Rice-Based Ecosystems. *Global Biogeochemical Cycles*, *37*(11), e2023GB007744. https://doi.org/https://doi.org/10.1029/2023GB007744

Tang, S., Wang, K., Xiang, Y., Tian, D., Wang, J., Liu, Y., Cao, B., Guo, D., & Niu, S. (2019). Heavy grazing reduces grassland soil greenhouse gas fluxes: A global meta-analysis. *Science of The Total Environment*, *654*, 1218-1224. https://doi.org/https://doi.org/10.1016/j.scitotenv.2018.11.082

Thompson, R. L., Lassaletta, L., Patra, P. K., Wilson, C., Wells, K. C., Gressent, A., Koffi, E. N., Chipperfield, M. P., Winiwarter, W., Davidson, E. A., Tian, H., & Canadell, J. G. (2019). Acceleration of global N2O emissions seen from two decades of atmospheric inversion. *Nature Climate Change*, *9*(12), 993-998. https://doi.org/10.1038/s41558-019-0613-7

Thrasher, B., Wang, W., Michaelis, A., Melton, F., Lee, T., & Nemani, R. (2022). NASA Global Daily Downscaled Projections, CMIP6. *Scientific Data*, *9*(1), 262. https://doi.org/10.1038/s41597-022-01393-4

Tian, H., Pan, N., Thompson, R. L., Canadell, J. G., Suntharalingam, P., Regnier, P., Davidson, E. A., Prather, M., Ciais, P., Muntean, M., Pan, S., Winiwarter, W., Zaehle, S., Zhou, F., Jackson, R. B., Bange, H. W., Berthet, S., Bian, Z., Bianchi, D., . . . Zhu, Q. (2024). Global nitrous oxide budget (1980–2020). *Earth Syst. Sci. Data*, *16*(6), 2543-2604. https://doi.org/10.5194/essd-16-2543-2024

Tian, H., Xu, R., Canadell, J. G., Thompson, R. L., Winiwarter, W., Suntharalingam, P., Davidson, E. A., Ciais, P., Jackson, R. B., Janssens-Maenhout, G., Prather, M. J., Regnier, P., Pan, N., Pan, S., Peters, G. P., Shi, H., Tubiello, F. N., Zaehle, S., Zhou, F., . . . Yao, Y. (2020). A comprehensive quantification of global nitrous oxide sources and sinks. *Nature*, *586*(7828), 248-256. https://doi.org/10.1038/s41586-020-2780-0

Tu, X., Wang, J., Liu, X., Liu, Y., Zhang, Y., Uwiragiye, Y., Elrys, A. S., Zhang, J., Cai, Z., Cheng, Y., & Müller, C. (2024). Warming-Induced Stimulation of Soil N2O Emissions Counteracted by Elevated CO2 from Nine-Year Agroecosystem Temperature and Free Air Carbon Dioxide Enrichment. *Environmental Science & Technology*, *58*(14), 6215-6225. https://doi.org/10.1021/acs.est.3c10775

van der Weerden, T. J., Noble, A., de Klein, C. A. M., Hutchings, N., Thorman, R. E., Alfaro, M. A., Amon, B., Beltran, I., Grace, P., Hassouna, M., Krol, D. J., Leytem, A. B., Salazar, F., & Velthof, G. L. (2021). Ammonia and nitrous oxide emission factors for excreta deposited by livestock and land-applied manure. *Journal of Environmental Quality*, *50*(5), 1005-1023. https://doi.org/https://doi.org/10.1002/jeq2.20259

van Lent, J., Hergoualc'h, K., & Verchot, L. V. (2015). Reviews and syntheses: Soil N₂O and NO emissions from land use and land-use change in the tropics and subtropics: a meta-analysis. *Biogeosciences*, *12*(23), 7299-7313. https://doi.org/10.5194/bg-12-7299-2015

van Vuuren, D. P., Stehfest, E., Gernaat, D. E. H. J., Doelman, J. C., van den Berg, M., Harmsen, M., de Boer, H. S., Bouwman, L. F., Daioglou, V., Edelenbosch, O. Y., Girod, B., Kram, T., Lassaletta, L., Lucas, P. L., van Meijl, H., Müller, C., van Ruijven, B. J., van der Sluis, S., & Tabeau, A. (2017). Energy, land-use and greenhouse gas emissions trajectories under a green growth paradigm. *Global Environmental Change*, *42*, 237-250. https://doi.org/https://doi.org/10.1016/j.gloenvcha.2016.05.008

van Wesenbeeck, C. F. A., Keyzer, M. A., van Veen, W. C. M., & Qiu, H. (2021). Can China's overuse of fertilizer be reduced without threatening food security and farm incomes? *Agricultural Systems*, *190*, 103093. https://doi.org/https://doi.org/10.1016/j.agsy.2021.103093

Wang, X., Li, Y. e., Waqas, M. A., Wang, B., Hassan, W., & Qin, X. (2021). Divergent terrestrial responses of soil N2O emissions to different levels of elevated CO2 and temperature. *Oikos*, *130*(9), 1440-1449. https://doi.org/https://doi.org/10.1111/oik.07738

Wang, Y., Calanca, P., & Leifeld, J. (2024). Sources of nitrous oxide emissions from agriculturally managed peatlands. *Global Change Biology*, *30*(1), e17144. https://doi.org/https://doi.org/10.1111/gcb.17144

Wang, Y., Wang, J., Li, F., Liu, X., & Zhao, D. (2024). Can the transition of multiple cropping systems affect the cropland change? *Agricultural Systems*, *214*, 103815. https://doi.org/https://doi.org/10.1016/j.agsy.2023.103815

Wolf, B., Zheng, X., Brüggemann, N., Chen, W., Dannenmann, M., Han, X., Sutton, M. A., Wu, H., Yao, Z., & Butterbach-Bahl, K. (2010). Grazing-induced reduction of natural nitrous oxide release from continental steppe. *Nature*, *464*(7290), 881-884. https://doi.org/10.1038/nature08931

Xu, C., Zhu, H., Wang, J., Ji, C., Liu, Y., Chen, D., Zhang, H., Wang, J., & Zhang, Y. (2023). Fertilizer N triggers native soil N-derived N2O emissions by priming gross N mineralization. *Soil Biology and Biochemistry*, *178*, 108961. https://doi.org/https://doi.org/10.1016/j.soilbio.2023.108961

Xu, R., Tian, H., Pan, S., Dangal, S. R. S., Chen, J., Chang, J., Lu, Y., Skiba, U. M., Tubiello, F. N., & Zhang, B. (2019). Increased nitrogen enrichment and shifted patterns in the world's grassland: 1860–2016. *Earth Syst. Sci. Data*, *11*(1), 175-187. https://doi.org/10.5194/essd-11-175-2019

Yao, Z., Wang, R., Zheng, X., Mei, B., Zhou, Z., Xie, B., Dong, H., Liu, C., Han, S., Xu, Z., Butterbach-Bahl, K., & Zhu, J. (2021). Elevated atmospheric CO2 reduces yield-scaled N2O fluxes from subtropical rice systems: Six site-years field experiments. *Global Change Biology*, *27*(2), 327-339. https://doi.org/https://doi.org/10.1111/gcb.15410

Yin, Y., Wang, Z., Tian, X., Wang, Y., Cong, J., & Cui, Z. (2022). Evaluation of variation in background nitrous oxide emissions: A new global synthesis integrating the impacts of climate, soil, and management conditions. *Global Change Biology*, *28*(2), 480-492. https://doi.org/https://doi.org/10.1111/gcb.15860

Zhang, B., Tian, H., Lu, C., Dangal, S. R. S., Yang, J., & Pan, S. (2017). Global manure nitrogen production and application in cropland during 1860–2014: a 5 arcmin gridded global dataset for Earth system modeling. *Earth Syst. Sci. Data*, *9*(2), 667-678. https://doi.org/10.5194/essd-9-667-2017

Zhang, B., Yu, L., Wang, J., Tang, H., Qu, Z., & Zhu, T. (2022). Effects of warming and nitrogen input on soil N2O emission from Qinghai-Tibetan Plateau: a synthesis. *Agricultural and Forest Meteorology*, *326*, 109167.

https://doi.org/https://doi.org/10.1016/j.agrformet.2022.109167

Zhang, J., Tian, H., Li, X., Qin, X., Fang, S., Zhang, J., Zhang, W., Wang, S., & Pan, S. (2024). A Warmer and Wetter World Would Aggravate GHG Emissions Intensity in China's Cropland. *Earth's Future*, *12*(2), e2023EF003614. https://doi.org/https://doi.org/10.1029/2023EF003614

Zhang, K., Peng, C., Wang, M., Zhou, X., Li, M., Wang, K., Ding, J., & Zhu, Q. (2017). Process-based TRIPLEX-GHG model for simulating N2O emissions from global forests and grasslands: Model development and evaluation. *Journal of Advances in Modeling Earth Systems*, *9*(5), 2079-2102. https://doi.org/https://doi.org/10.1002/2017MS000934

Zhang, M., Wu, B., Zeng, H., He, G., Liu, C., Tao, S., Zhang, Q., Nabil, M., Tian, F., Bofana, J., Beyene, A. N., Elnashar, A., Yan, N., Wang, Z., & Liu, Y. (2021). GCI30: a global dataset of 30 m cropping intensity using multisource remote sensing imagery. *Earth Syst. Sci. Data*, *13*(10), 4799-4817. https://doi.org/10.5194/essd-13-4799-2021

Zhou, D., Xiao, J., Frolking, S., Liu, S., Zhang, L., Cui, Y., & Zhou, G. (2021). Croplands intensify regional and global warming according to satellite observations. *Remote Sensing of Environment*, *264*, 112585. https://doi.org/https://doi.org/10.1016/j.rse.2021.112585

Chapter VI: GENERAL CONCLUSIONS AND FUTURE DIRECTIONS

6.1 General conclusions

Given the significant role of nitrous oxide (N_2O) emission in climate change and sustainable development, this dissertation has provided a comprehensive analysis of the patterns, drivers, and future trajectories of N_2O emissions from global agricultural ecosystems. By improving and utilizing the state-of-the-art process-based model, TRIPLEX-GHGv2.0, the research reveals a general increase in global agricultural N_2O during historical period (before 2020) but switch to a slightly decline trend in the 21st century. Projection suggest agricultural N_2O emission would continuously increase across all scenarios by at least 25% through 21st century. Spatially, Europe accounts for the largest source of historical emissions but also contributes to the recent decrease and would play a dominant role in determining the direction of changes in future agricultural N_2O emission. Chemical N fertilizer is primarily responsible for the overall trends (decreasing and sometimes slightly decreasing) for both historical and future emissions. The contribution of manure, livestock excreta and water regime managements to N_2O emissions are likely to be overestimated by previous oversimplified models for upland croplands, grazing lands, and rice-paddies on a global scale, respectively. Overall, this work offers quantitative and evidence-based understanding of the complex interactions between agricultural practices, environmental and climate changes which align well observations and synthetic studies. The results lay a robust foundation for agriculture managers and policy-makers to maintain the sustainability of agricultural resources and reduce the potential risk of N_2O emissions from global agricultural ecosystems under a changing world.

6.1.1 Model development and application for N_2O emission from croplands

The TRIPLEX-GHG model v2.0 was improved by integrating key biogeochemical processes and major agricultural practices to accurately simulate the dynamics of N_2O fluxes from croplands on a global scale as demonstrated by model calibration and validation. From 1960 to 2016, global cropland N_2O emissions increased significantly by ~ 2.5 Tg N yr^{-1}. Western Europe and North America were consistent hotspots for cropland N_2O emissions during this period with a decreasing trend in recent decade. In contrast, eastern China and south America have seen a rise in cropland N_2O emissions since the 1990s. N fertilizer accounted for the larger source of cropland N_2O emissions while manure was found to show both positive and negative effects on N_2O emissions depending on local soil properties and atmospheric N deposition rates. Our study implies a potential of focusing on quality of N inputs instead of quantity only for upland cropland N_2O mitigation.

6.1.2 Model development and application for N_2O emissions from grazing lands

Pastures were responsible for the increase in global grazing land N_2O emissions due to growing N fertilizer applications, while the rangeland emissions remained relatively stable from 1960 to 2016. Deposited excreta were identified as the largest contributor to total grazing land N_2O emissions, but existing estimations probably overestimated such effect. Modeled results suggested chemical forms of external N inputs, such as nitrate fraction of fertilizer and urine (i.e., inorganic N) fraction of excreta, are crucial for estimating spatial temporal variation patterns of N_2O emissions from grazing lands. This chapter implies the exclusive effect of grazing activity may not a major concern for emitting N_2O globally.

6.1.3 Model development and application for N_2O emissions from rice-based ecosystems

By integrating detailed management practices related to fertilizer application and water regimes based on the rice crop calendar, the TRIPLEX-GHGv2.0 model suggest that N_2O emissions from global rice-based ecosystems are almost doubled during 1960 – 2020, reaching 0.18 Tg N yr^{-1} dominated by irrigated rice ecosystems. For the first time, this study quantitively evaluated that N fertilizer plays a determinant role over water regime changes in controlling rice N_2O emissions globally, clarifying the long-time debate. We addressed the importance of co-management of water and fertilizer for N_2O mitigation in rice-based ecosystems.

6.1.4 Projection of future N_2O emissions from global agricultural ecosystems

Under three SSP-RCP scenarios (SSP1-2.6, SSP2-4.5, and SSP5-8.5), projections revealed that N_2O emissions from global agricultural ecosystems would increase to 8.61 – 11.42 Tg N yr^{-1} during 2015 – 2100. Croplands are projected to remain the largest source of N_2O emissions, with their share increasing consistently across all scenarios. Our projection suggested future agricultural N_2O

emissions would not algin with changes in CO_2 concentrations, underscoring the importance of management practices over climate change in regulating emission patterns and sources. Subsequently, developing nations are projected to present increasing contributions to global agricultural N_2O emissions, potentially offsetting the reduction efforts in developed world. International collaborations are mandatory and helpful to address this imbalance and achieve global climate change mitigation goals.

6.2 Limitations and Future Work

My Ph.D. study has led to the new development of a process-based model of TRIPLEX-GHGv2.0 for simulating and predicting N_2O emissions from global agricultural ecosystems under climate change and management practices. However, uncertainties and limitations remain. First and foremost, parameter uncertainties and incomplete descriptions of several biogeochemical processes should be address to improve model performance and capability. For example, continent-mean values for the COE_{dNO3} parameter may cause the overestimation of N_2O emission pulses and emission factors, particularly due to variations in local soil properties (Abdalla et al., 2020). Secondly, N_2O emissions from ecosystems dominated by fruits or nuts trees is an uncertainty source of global agricultural N_2O budget given the similar N management they received as cereal crops (Li et al., 2024; Xu et al., 2022). The major challenge is identifying the spatial distribution of these orchards from other forests, which might need machine-learning driven remote sensing approach (Underwood et al., 2016; Zhao et al., 2022). In addition, current TRIPLEX-GHGv2.0 lacks a dedicated land-use change module, which limits its ability to simulate the effects of agroecosystem expansion and land-use transitions on N_2O emissions. This limitation may lead to underestimated agricultural contribution to global N_2O budget (Tian et al., 2019; van Lent et al., 2015). Moreover, the absence of detailed data on agricultural practices, such as the use of nitrification inhibitors or biochar amendments, affect the quality of current estimations. These practices are already involved in various agroecosystems across large area (e.g., North China Plain and western Europe) since the 1990s, which causes overestimated historical N_2O emissions in those regions, and restricts the model's capacity to account for potential mitigation strategies in the projected future (Fan et al., 2022; Ma et al., 2023).

Building on the findings and limitations of this work, several avenues for future research are proposed:

1. **Model Enhancement and Data Integration**: The TRIPLEX-GHGv2.0 model could benefit from further refinement, particularly in incorporating land-use change dynamics and addressing key parameter values by Bayesian calibration or linking with environmental factors through machine learning approaches (Couvreux et al., 2021; Myrgiotis et al., 2018). Additionally, current models primarily focus on direct soil emissions of N_2O. To fully account for N_2O emissions from agroecosystems, future work should aim to develop and integrate submodules that estimate indirect N_2O emissions, such as those resulting from nitrogen leaching and runoff into aquatic systems which may have comparable contribution to direct N_2O emissions (Griffis et al., 2017; Wang et al., 2022). This would provide a more holistic assessment of the total N_2O budget associated with agricultural practices (Tian et al., 2024).
2. **Multi-GCMs Scenarios and Impact of Extreme Climate Events**: To better understand the range of potential future N_2O emissions, future studies should apply a multi-set of General Circulation Models (GCMs) and scenarios using ensemble approach. This would provide a more comprehensive estimate of future emissions under various climate change trajectories and enhance the robustness of projections across different regions and agricultural systems (Zhang et al., 2024). Moreover, future research should explore the impacts of extreme climate events, such as droughts and floods, on N_2O emissions (Gelfand et al., 2015; Li et al., 2023). These events are likely to become more frequent and intense under future climate scenarios, and understanding their effects on agricultural N_2O emissions is crucial for developing sustainable mitigation strategies.
3. **Testing of Mitigation Practices with Policy and Economic Analysis**: Future research should evaluate the effectiveness of various N_2O mitigation policies or practices, such as optimized N fertilizer use, biochar incorporations, under different SSP scenarios. This includes conducting scenario analyses to assess the mitigation potential of these practices across diverse climate, economic, and land use in future (Kanter et al., 2016). Such studies also need evaluate economic implications of different mitigation strategies and their feasibility within existing policy frameworks which would provide critical insights in balancing the reduction of global N_2O emissions and economic development (Kanter et al., 2020).
4. **Coupling with Earth System Models (ESMs)**: Currently, the interaction between climate and

agricultural N_2O emission as well as associated management have not been incorporated. Such limitation may cause underrated climate changes, especially warming trend given the strong radiative forcing capacity of N_2O. Consequently, coupling the improved TRIPLEX-GHG v2.0 with ESMs address this critical gap in climate-management feedback to improve the quality of the projections.

By addressing these aspects, future research will enhance the predictive power of N_2O emission models and provide actionable insights for mitigating emissions from global agroecosystems. This work will contribute to a more comprehensive and accurate understanding of N_2O emissions and support and inform policy decisions aimed at mitigating global climate change.

6.3 References

Abdalla, M., Song, X., Ju, X., Topp, C. F. E., & Smith, P. (2020). Calibration and validation of the DNDC model to estimate nitrous oxide emissions and crop productivity for a summer maize-winter wheat double cropping system in Hebei, China. *Environmental Pollution*, *262*, 114199. https://doi.org/https://doi.org/10.1016/j.envpol.2020.114199

Couvreux, F., Hourdin, F., Williamson, D., Roehrig, R., Volodina, V., Villefranque, N., Rio, C., Audouin, O., Salter, J., Bazile, E., Brient, F., Favot, F., Honnert, R., Lefebvre, M.-P., Madeleine, J.-B., Rodier, Q., & Xu, W. (2021). Process-Based Climate Model Development Harnessing Machine Learning: I. A Calibration Tool for Parameterization Improvement. *Journal of Advances in Modeling Earth Systems*, *13*(3), e2020MS002217. https://doi.org/https://doi.org/10.1029/2020MS002217

Fan, D., He, W., Smith, W. N., Drury, C. F., Jiang, R., Grant, B. B., Shi, Y., Song, D., Chen, Y., Wang, X., He, P., & Zou, G. (2022). Global evaluation of inhibitor impacts on ammonia and nitrous oxide emissions from agricultural soils: A meta-analysis. *Global Change Biology*, *28*(17), 5121-5141. https://doi.org/https://doi.org/10.1111/gcb.16294

Gelfand, I., Cui, M., Tang, J., & Robertson, G. P. (2015). Short-term drought response of N2O and CO2 emissions from mesic agricultural soils in the US Midwest. *Agriculture, Ecosystems & Environment*, *212*, 127-133. https://doi.org/https://doi.org/10.1016/j.agee.2015.07.005

Griffis, T. J., Chen, Z., Baker, J. M., Wood, J. D., Millet, D. B., Lee, X., Venterea, R. T., & Turner, P. A. (2017). Nitrous oxide emissions are enhanced in a warmer and wetter world. *Proceedings of the National Academy of Sciences*, *114*(45), 12081-12085. https://doi.org/doi:10.1073/pnas.1704552114

Kanter, D. R., Ogle, S. M., & Winiwarter, W. (2020). Building on Paris: integrating nitrous oxide mitigation into future climate policy. *Current Opinion in Environmental Sustainability*, *47*, 7-12. https://doi.org/https://doi.org/10.1016/j.cosust.2020.04.005

Kanter, D. R., Zhang, X., Mauzerall, D. L., Malyshev, S., & Shevliakova, E. (2016). The importance of climate change and nitrogen use efficiency for future nitrous oxide emissions from agriculture. *Environmental Research Letters*, *11*(9), 094003. https://doi.org/10.1088/1748-9326/11/9/094003

Li, L., Hao, Y., Wang, W., Biederman, J. A., Zheng, Z., Wang, Y., Tudi, M., Qian, R., Zhang, B., Che, R., Song, X., Cui, X., & Xu, Z. (2023). Effects of extra-extreme precipitation variability on multi-year cumulative nitrous oxide emission in a semiarid grassland. *Agricultural and Forest Meteorology*, *343*, 109761. https://doi.org/https://doi.org/10.1016/j.agrformet.2023.109761

Li, L., Hong, M., Zhang, Y., & Paustian, K. (2024). Soil N2O emissions from specialty crop systems: A global estimation and meta-analysis. *Global Change Biology*, *30*(3), e17233.

Ma, H., Jia, X., Yang, J., Liu, J., Shangguan, Z., & Yan, W. (2023). Inhibitors mitigate N2O emissions more effectively than biochar: A global perspective. *Science of The Total Environment*, *859*, 160416. https://doi.org/https://doi.org/10.1016/j.scitotenv.2022.160416

Myrgiotis, V., Williams, M., Topp, C. F. E., & Rees, R. M. (2018). Improving model prediction of soil N2O emissions through Bayesian calibration. *Science of The Total Environment*, *624*, 1467-1477. https://doi.org/https://doi.org/10.1016/j.scitotenv.2017.12.202

Tian, H., Pan, N., Thompson, R. L., Canadell, J. G., Suntharalingam, P., Regnier, P., Davidson, E. A., Prather, M., Ciais, P., Muntean, M., Pan, S., Winiwarter, W., Zaehle, S., Zhou, F., Jackson, R. B., Bange, H. W., Berthet, S., Bian, Z., Bianchi, D., . . . Zhu, Q. (2024). Global nitrous oxide budget (1980–2020). *Earth Syst. Sci. Data*, *16*(6), 2543-2604. https://doi.org/10.5194/essd-16-2543-2024

Tian, H., Yang, J., Xu, R., Lu, C., Canadell, J. G., Davidson, E. A., Jackson, R. B., Arneth, A., Chang, J., Ciais, P., Gerber, S., Ito, A., Joos, F., Lienert, S., Messina, P., Olin, S., Pan, S., Peng, C., Saikawa, E., . . . Zhang, B. (2019). Global soil nitrous oxide emissions since the preindustrial era estimated by an ensemble of terrestrial biosphere models:

Magnitude, attribution, and uncertainty. *Global Change Biology*, *25*(2), 640-659. https://doi.org/https://doi.org/10.1111/gcb.14514

Underwood, J. P., Hung, C., Whelan, B., & Sukkarieh, S. (2016). Mapping almond orchard canopy volume, flowers, fruit and yield using lidar and vision sensors. *Computers and Electronics in Agriculture*, *130*, 83-96. https://doi.org/https://doi.org/10.1016/j.compag.2016.09.014

van Lent, J., Hergoualc'h, K., & Verchot, L. V. (2015). Reviews and syntheses: Soil N₂O and NO emissions from land use and land-use change in the tropics and subtropics: a meta-analysis. *Biogeosciences*, *12*(23), 7299-7313. https://doi.org/10.5194/bg-12-7299-2015

Wang, J., Wang, G., Zhang, S., Xin, Y., Jiang, C., Liu, S., He, X., McDowell, W. H., & Xia, X. (2022). Indirect nitrous oxide emission factors of fluvial networks can be predicted by dissolved organic carbon and nitrate from local to global scales. *Global Change Biology*, *28*(24), 7270-7285. https://doi.org/https://doi.org/10.1111/gcb.16458

Xu, P., Li, Z., Wang, J., & Zou, J. (2022). Fertilizer-induced nitrous oxide emissions from global orchards and its estimate of China. *Agriculture, Ecosystems & Environment*, *328*, 107854. https://doi.org/https://doi.org/10.1016/j.agee.2022.107854

Zhang, J., Tian, H., Li, X., Qin, X., Fang, S., Zhang, J., Zhang, W., Wang, S., & Pan, S. (2024). A Warmer and Wetter World Would Aggravate GHG Emissions Intensity in China's Cropland. *Earth's Future*, *12*(2), e2023EF003614. https://doi.org/https://doi.org/10.1029/2023EF003614

Zhao, H., Lakshmanan, P., Wang, X., Xiong, H., Yang, L., Liu, B., Shi, X., Chen, X., Wang, J., Zhang, Y., & Zhang, F. (2022). Global reactive nitrogen loss in orchard systems: A review. *Science of The Total Environment*, *821*, 153462. https://doi.org/https://doi.org/10.1016/j.scitotenv.2022.153462